AD-769 576

COMBUSTION OF POWDERED METALS IN
ACTIVE MEDIA

P. F. Pokhil, et al

Foreign Technology Division
Wright-Patterson Air Force Base, Ohio

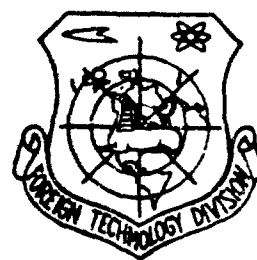18 October 1973

FTD-MT-24-551-73

FOREIGN TECHNOLOGY DIVISION

COMBUSTION OF POWDERED METALS IN ACTIVE MEDIA

by

P. F. Pokhil, A. F. Belyayev,
Yu. V. Frolov, V. S. Logachev,
A. I. Korotkov

D D C

NOV 26 1973

E

Unclassified
Security Classification

DOCUMENT CONTROL DATA - R & D

(Security classification of title, body of abstract and indexing annotation must be entered when the overall report is classified)

1. ORIGINATING ACTIVITY (Corporate author)	2a. REPORT SECURITY CLASSIFICATION
Foreign Technology Division Air Force Systems Division U. S. Air Force	Unclassified
	2b. GROUP

3. REPORT TITLE

COMBUSTION OF POWDERED METALS IN ACTIVE MEDIA

4. DESCRIPTIVE NOTES (Type of report and inclusive dates)

Translation

5. AUTHOR(S) (First name, middle initial, last name)

P. F. Pokhil, A. F. Belyayev, Yu. V. Frolov, V. S. Logachev,
A. I. Korotkov

6. REPORT DATE	7a. TOTAL NO. OF PAGES	7b. NO. OF REFS
1972	395 409	356

8a. CONTRACT OR GRANT NO.	9a. ORIGINATOR'S REPORT NUMBER(S)
b. PROJECT NO.	FTD-MT-24-551-73
c.	9b. OTHER REPORT NO(S) (Any other numbers that may be assigned this report)
d.	

10. DISTRIBUTION STATEMENT

Approved for public release;
distribution unlimited.

11. SUPPLEMENTARY NOTES	12. SPONSORING MILITARY ACTIVITY
	Foreign Technology Division Wright-Patterson AFB, Ohio

13. ABSTRACT

11

DD FORM 1473
1 NOV 65

Unclassified
Security Classification

FTD-MT- 24-551-73

EDITED MACHINE TRANSLATION

Approved for public release;
distribution unlimited.

PREPARED BY:

TRANSLATION DIVISION
FOREIGN TECHNOLOGY DIVISION
WP-AFB, OHIO.

FTD-MT- 24-551-73   Date 18 Oct 19 73

ib

TABLE OF CONTENTS

U. S. BOARD ON GEOGRAPHIC NAMES TRANSLITERATION SYSTEM

Block		Italic		Transliteration	Block		Italic		Transliteration
А	а	*А*	*а*	A, a	Р	р	*Р*	*р*	R, r
Б	б	*Б*	*б*	B, b	С	с	*С*	*с*	S, s
В	в	*В*	*в*	V, v	Т	т	*Т*	*т*	T, t
Г	г	*Г*	*г*	G, g	У	у	*У*	*у*	U, u
Д	д	*Д*	*д*	D, d	Ф	ф	*Ф*	*ф*	F, f
Е	е	*Е*	*е*	Ye, ye; E, e*	Х	х	*Х*	*х*	Kh, kh
Ж	ж	*Ж*	*ж*	Zh, zh	Ц	ц	*Ц*	*ц*	Ts, ts
З	з	*З*	*з*	Z, z	Ч	ч	*Ч*	*ч*	Ch, ch
И	и	*И*	*и*	I, i	Ш	ш	*Ш*	*ш*	Sh, sh
Й	й	*Й*	*й*	Y, y	Щ	щ	*Щ*	*щ*	Shch, shch
К	к	*К*	*к*	K, k	Ъ	ъ	*Ъ*	*ъ*	"
Л	л	*Л*	*л*	L, l	Ы	ы	*Ы*	*ы*	Y, y
М	м	*М*	*м*	M, m	Ь	ь	*Ь*	*ь*	'
Н	н	*Н*	*н*	N, n	Э	э	*Э*	*э*	E, e
О	о	*О*	*о*	O, o	Ю	ю	*Ю*	*ю*	Yu, yu
П	п	*П*	*п*	P, p	Я	я	*Я*	*я*	Ya, ya

* ye initially, after vowels, and after ъ, ь; e elsewhere.
When written as ё in Russian, transliterate as yё or ё.
The use of diacritical marks is preferred, but such marks
may be omitted when expediency dictates.

FOLLOWING ARE THE CORRESPONDING RUSSIAN AND ENGLISH

DESIGNATIONS OF THE TRIGONOMETRIC FUNCTIONS

Russian	English
sin	sin
cos	cos
tg	tan
ctg	cot
sec	sec
cosec	csc
sh	sinh
ch	cosh
th	tanh
cth	coth
sch	sech
csch	csch
arc sin	$\sin^{-1}$
arc cos	$\cos^{-1}$
arc tg	$\tan^{-1}$
arc ctg	$\cot^{-1}$
arc sec	$\sec^{-1}$
arc cosec	$\csc^{-1}$
arc sh	$\sinh^{-1}$
arc ch	$\cosh^{-1}$
arc th	$\tanh^{-1}$
arc cth	$\coth^{-1}$
arc sch	sech^{-1}
arc csch	csch^{-1}

---

rot	curl
lg	log

Combustion of powdered metals in active media. Pokhil, P. F., Belyayev, A. F., Frolov, Yu. V., Logachev, V. S., Korotkov, A. I., "Nauka" ["Science"], 1972, 294 pages.

This book deals with the subject of important contemporary problems in igniting and ourning such metals as aluminum, beryllium, magnesium, boron, lithium and others which are widely used in the new technology. They make it possible, for example, to considerably improve the physical and chemical characteristics of rocket propellants. Extensive experimental and theoretical material obtained by Soviet and foreign authors during the last 10-15 years is presented and generalized. Contemporary research methods and the basic rules of metal ignition and burning are also discussed. We also deal with the effect of metal additives on physical and energy parameters of powders and explosives.

The book is intended for scientific technicians and engineers working in the field of combustion and also for the use of students specializing in this field

Tables 51. Illustrations 148. References 356.

Editor-in-chief
Academician M. A. Sadovskiy

PREFACE

The use of powdered metals in active and corrosive media,
which are encountered in the new technology, has stimulated the
investigation of the characteristic peculiarities and regularities
found in the ignition and self-ignition of metal particles under
conditions of industrial production, exploitation, and storage.

Along with this, in the last two decades, in connection with
the tremendous development of rocket technology and astronautics,
there has appeared a no less interesting and important trend
toward using light metals - additives of high-energy metals in
developing highly effective rocket propellants with a higher spe-
cific impulse and improved physical and chemical characteristics.

The use of light metals and their compounds for fuels in
liquid rocket engines was first discussed by the Soviet scientists
Yu. V. Kondratyuk and F. A. Tsander.

At the present time such metals as aluminum, boron, and
magnesium are some of the basic components of solid rocket
propellants and pyrotechnical compositions.

However, the use of metal-containing propellants has
complicated the process of burning in combustion chambers and
has lead to the appearance of a unique and, at the same time,

widespread type of burning – heterogeneous burning of condensed
particles in an active high-temperature flow.

In connection with this, the problem has been posed
concerning a detailed comprehensive study of the ignition and
burning mechanism of powdered metals in high-temperature oxidized
media and the combustion products of heterogeneous condensed
systems and powders. This has stimulated scientific research
covering a wide range of problems touching upon the basic
regularities in the ignition and burning processes and the use
of metals (aluminum, magnesium, boron, etc.) and metallized
propellants. However, in spite of the increasing interest in
this problem, which has become considerably complex at the present
time, the concepts cannot be considered completely established.

This book is a first attempt to unite and systematize
the results of many years of work by the authors in this direction
and also the results of studies of Soviet and foreign scientists.
These include the works of V. A. Fedoseyev, L. A. Klyachko,
M. A. Gurevich, Ye. S. Ozerov, R. Friedman, A. Macek, T. Brzustowski,
I. Glassman, and D. Kuehl.

Chapters I and II deal with the basic properties of metals
which are most widely used or promising from the point of view
of use in rocketry and the contemporary methods of studying
processes of metal ignition and burning. Also examined are
methods of recording burning time and the nature of the induction
of individual particles, methods of sampling and analyzing the
combustion products of metals, and methods of processing the
results.

Chapter III deals with a study of the basic rules of ignition
for metal particles in an active oxidized medium. The close
relationship between the nature of induction and the parameters
of the ambient medium, as well as the properties of the metal,
is shown.

Chapter IV presents extensive data on the burning of high-energy metals in active gas media and the combustion products of solid propellants. Based on an analysis of experimental and theoretical material, the physical picture of metal particle combustion is given.

Chapter V examines the phenomenon of enlargement (agglomeration) of particles of finely dispersed powdered metals on the burning surface of powders and heterogeneous condensed systems. The basic regularities of this phenomenon are traced and a possible mechanism of agglomeration is proposed.

The effect of additives of powdered metals on basic physical and energy parameters of the burning of powders and mixed systems is discussed in Chapters VI and VII. The effect of the disperaity, concentration, and properties of the metallic ingredient on combustion rate, its dependence on pressure, specific impulse, and the completeness of the combustion of mixed systems on a base of organic fuel and oxidizer is studied. Also examined are the peculiarities of metal behavior in the initial combustion stage of ballistic and mixed powders.

Chapter VIII briefly discusses the effect of additives of powdered metal on the basic detonation parameters of an explosive.

The authors hope that this book will be a useful aid to engineers, technicians, and students specializing in the physics of combustion and explosion.

CHAPTER I

PROPERTIES OF METALS

§ 1. General Characterization of Metals

In evaluating substances whose use as propellants is most
probable, the most important characteristics are the quantity
of heat released as a result of chemical reaction, the temperature
of the flame, and also the nature of the combustion products
since the specific impulse of the engine depends on the momentum
of the flow of exhaust gas. The heat released during the
combustion of the propellant is the measure of the greatest
energy which can be imparted to the working medium. The achievement
of high temperatures and high momentum depends on the quantity of
heat released in an exothermal reaction, as well as the thermal
stability of the combustion products.

Figure 1 [1] presents the dependence of the specific impulse
on the heat content of the burning gases; specific heat capacity
is taken as the parameter. The curves are plotted for a pressure
in the chamber of 22 atm; the pressure on a section of the Laval
nozzle is equal to atmospheric pressure. The molecular weight
of the combustion products must be as little as possible. The
necessity for a low molecular weight is brought about by the fact
that although the specific impulse depends only on the velocity of
the molecules, temperature however is proportional to the mass of
the molecules multiplied by the square of velocity. Therefore,

for a given specific pulse, if the molecular weight is doubled
the gas temperature doubles.
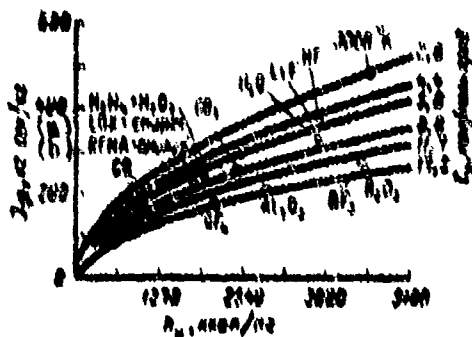
Fig. 1. Dependence of specific impulse
($J_{yд}$) on the heat content of burning
gases.
KEY: (a) Alcohol; (b) aniline.
Designations: кг·сек/кг = kg·s/kg;
кал/моль·град = cal/mole·deg;
ккал/кг = kcal/kg.

Thus, the best propellant for a rocket is the one during
whose combustion gases are formed with low specific heat capacity,
high heat of formation, and low molecular weight. These circum-
stances limit the selection of propellants only to those which
contain atoms with low atomic weight. Thus, as oxidizers, it
is best to select fluorine and oxygen, and as fuels - hydrogen,
lithium, beryllium, boron, carbon, sodium, magnesium, aluminum,
and silicon.

In order that specific heat capacity be sufficiently low,
diatomic combustion products should be preferred over polyatomic
gases. Therefore, HF, HCl, LiF, NaF, Be, MgO, CO, OH and NO
will be more effective during isentropic expansion than more
complex molecules. HF, LiF, H_2O, B_2O_3, BF_3, AlF_3, Al_2O_3, have the
highest heat of formation.

The use of some metals as fuel is generally connected
with their high combustion heat values. The following 15 elements
give the greatest amount of heat during combustion from both air
oxygen and oxidizer oxygen: metals - lithium, beryllium,
magnesium, calcium, aluminum, titanium, zirconium, yttrium,
vanadium, scandium; nonmetals - hydrogen, boron, carbon, silicon,
phosphorus. As is apparent from Table 1, the metals in groups II,
III, and IV have the highest heat of combustion [2, 3].

Table 1. Estimated values for heat of combustion.

Heat of combustion, kcal/g	Elements
>2	H, B, C, Li, Be, Al, Si, P, Mg, Ca, V
2.0—1.0	Na, Mn, Cr, Fe, Zn, Ga, Ge, As, S, Mo
1.0—0.4	K, Rb, Se, Cd, In, Sn, Sb, Tl, Ba
<0.4	Cu, Ag, Au, Hg, Tl, Pb, Bi, Po

To evaluate the possibility of using metals as the fuel in a propellant, we can use the following quantities: Q_1, the heat released during combustion of one gram of the element; Q_2, the amount of heat released during the formation of one gram of oxide; and Q_3, the amount of heat obtained from dividing the gram-molecular heat of formation of oxide ΔH by the number of atoms in the oxide molecule. Q_1 is calculated by dividing the gram-molecular heat of formation of oxide ΔH by quantity nA:

$$Q_1 = \frac{\Delta H}{nA},\qquad\qquad (I.1)$$

where A is the atomic weight; n is the number of atoms of the element in the oxide molecule.

The quantity of heat Q_1 can serve as the measure of caloricity of the fuel (metal) under the condition that its combustion is due to the oxygen of air (Fig. 2). The quantity of heat Q_2 can be, to some extent, the effectiveness standard of the combustion of the metal in the propellant composition due to the oxygen of the oxidizer (Fig. 3). The quantity of heat Q_3 enables us to judge, to a certain extent, the burning temperature of the element since, in the first approximation, the burning temperature is proportional to the quantity of heat which occurs in 1 g-atom, i.e., is proportional to Q_3. Metals such as zirconium, beryllium, aluminum, magnesium, and calcium give the highest temperature during burning in oxygen (p = 1 atm), as is apparent from Fig. 4.
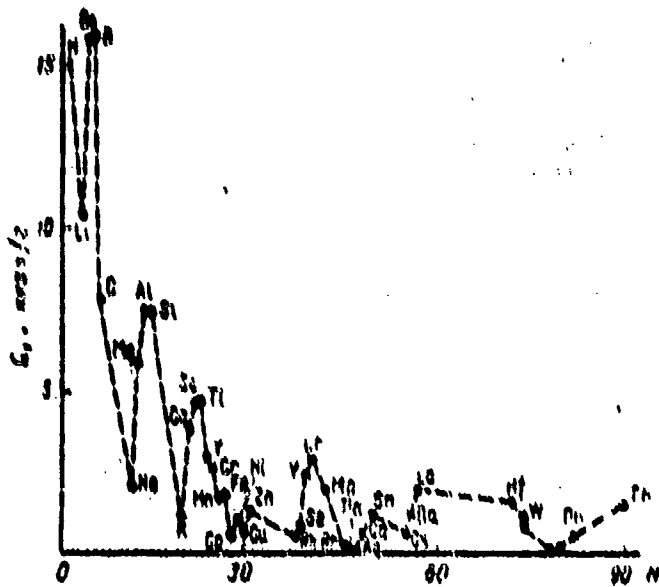
Fig. 2. Heat released during the combustion of one gram of an element with atomic number N.

Designation: ккал/г = kcal/g.
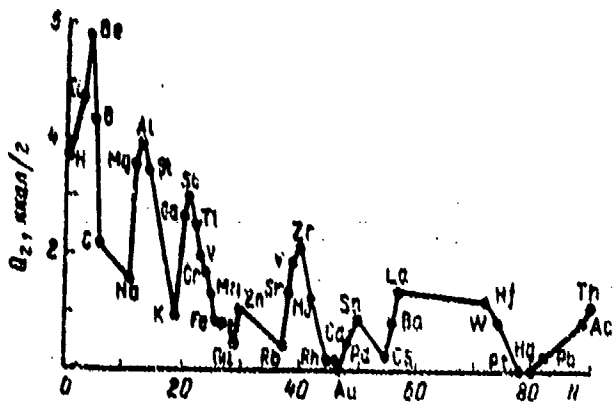
Fig. 3. Quantity of heat released during the formation of one gram of oxide of an element with atomic number N.
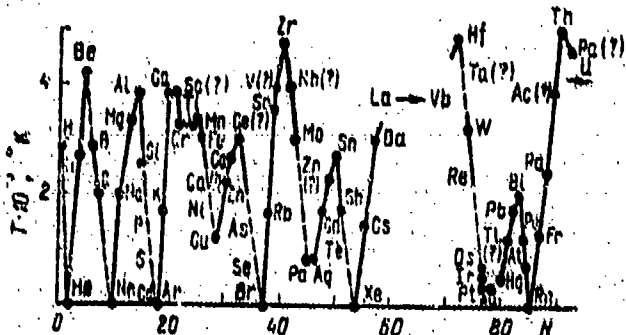
Fig. 4. Dependence of element burning temperature in oxygen on atomic number N (estimated value).

4

On the basis of the above data, we can conclude that the best elements for use as fuels are hydrogen, lithium, beryllium, and boron. After these elements are magnesium, aluminum, silicon, and calcium. All these elements form a rather compact group in a relatively narrow region of the periodic system of elements. At the present time, only aluminum and magnesium are widely used.

Along with the caloricity of the metal,[1] related to unit weight, the quantity of heat released in the burning of a unit volume of fuel (metal) Q_4 (kcal/cm^3) is, in many cases, of considerable importance. Hence in rocket engines not only the quantity of heat per unit weight of propellant but also the volume occupied by the propellant is important. As shown by Leonard [1], the final velocity of the rocket can be increased by using propellant with variable density and heat of combustion. At the beginning of burning, mixtures of propellants with high density should be used, and at the end, combinations of propellants with high heating capacity. From Fig. 5 it is apparent that with respect to per-volume caloricity, boron is at the top of the list, while such metals as zinc, molybdenum, thorium, and tungsten have per-volume caloricity comparable to aluminum and considerably higher than magnesium.

Table 2 presents the physical and chemical properties of metals and their oxides, which are presently used as fuel in solid propellants. Table 3, for comparison, contains similar data for several fluorides [1].

Compounds of elements presented in Tables 2 and 3 are distributed in the order of increasing atomic weight. As is seen

---

[1] Henceforth metals will arbitrarily include boron, silicon, and other metalloids which can be included in the composition of a propellant.

Table 2. Physical and chemical properties of metals and their oxides.

Element	Molecular weight	Density at 18°C, g/cm³	Тпл, °C [Melting point]	Ткип [Boiling point] at 1 atm, °C	Heat of fusion, cal/g	Heat of evaporation, cal/g	Heat capacity, cal/g·deg	Heat of formation, kcal/mole
Al	27	2,7	660	2050	96	2100—3050	0,22—0,26	—
Be	9	1,85	1283	2970	341	5340	0,5	—
B	11	2,33	2100	2550	480	8250	0,3—0,37	—
Li	7	0,53	180	1370	405	4600	0,81	—
Mg	24	1,74	651	1105	90	1320	0,24—0,27	—
Cd	112	8,65	321	765	13,1	213	0,055	—
W	184	19,35	3360	5660	46	1150	0,032	—
Zn	65	7,13	419	906	17	424	0,09—0,14	—
Zr	91	6,52	1835	(1750)	(68)	—	0,112	—
Ti	48	4,5	1710	3260	91	2100	0,112	—
Al₂O₃	102	4,0	2050	2980	255	1130	0,304	400,3
BeO	25	3,0	2530	4240	681	4680		143,1
B₂O₃	70	1,8	423	2200	79	1000		305,4
Li₂O	30	2,02	Subl.(1430)	—	780	—		142,6
MgO	40	3,2	2900	(3600)	463	—	0,3—0,4	143,7
CdO	128	7,2—8,2	1500	1770	—	—		61,0
WO₃	232	7,23	1453	2200	60	—		200,8
ZnO	91	5,5	1973	Субл.	155	—	0,8	83,2
ZrO₂	123	5,5—6,0	2660	4290	169	—	0,12—0,144 / 0,108	261,5
TiO₂	80	4,1	1833	2983	194	—	0,19	225,6

from the tables, the values for the heat of compound formation usually decrease with an increase in atomic weight.

Table 3. Physical and chemical properties of several inorganic fluorides.

Chemical formula	Molecular weight	T°C [Melting point]	[Boiling point] at 1 atm °C	Heat of fusion, cal/g	Heat of evapor-ation, cal/g	Heat of formation, 10^3·cal/mole
HF	20	—92	19	—	—	71.7
AlF₃	84	Subl. 1255	—	Subl. 920	—	323.0
BeF₂	47	780	(1300)	(130)	(850)	(227)
BF₃	68	—127	—101	7.0	68.0	273.5
LiF	26	870	1676	9.1	1960	146.3
MgF₂	62	1246	2240	224	1050	263.5
CaF₂	150	1095	1733	36	346	167.0
ZnF₂	103	855	1475	68	427	176.0
ZrF₄	167	1510	(4300)	87	—	230.0
TiF₃	105	(1200)	(1400)	(114)	(470)	315.0

In comparing the effective heat of compound formation, we see that for certain elements at the beginning of the tables the corresponding values for oxides are approximately equal to the values for fluoride compounds. In contrast to this, for elements with high atomic weight, fluorine is preferable over oxygen as an oxidizer.

If, however, we set up similar tables for sulfides, selenides, tellurides, chlorides, bromides, and iodides, it will be apparent that for them the heat of formation is considerably lower than for a corresponding fluoride compound. In a compound with heavier elements this ratio is approximately half. All other oxidizers give values less than chlorine. Although the density of heavier oxidizers and their compounds is somewhat greater than the density of oxygen and fluorine, this does not compensate for the difference of values in the heat of compound formation. Hence it follows that for propellants containing elements with low atomic weight the oxidizer must be rich in oxygen and fluorine. For elements with high atomic weight we can use only those oxidizers which are rich in fluorine.

As we know from literature [1, 4, 5], oxygen is far from the best oxidizer; the best oxidizers are fluorine monoxide, fluorine, nitrogen trifluoride, ozone and oxygen.

The best fuels, as noted above, are hydrogen, lithium, beryllium, and boron. After them, are aluminum, magnesium, and calcium.

Boron hydrides, liquid lithium, and hydrazine can obviously be considered the most effective liquid fuel. Combinations of propellants characterized by significantly greater density and giving the greatest exhaust velocity are fluorine monoxide in a mixture with beryllium and hydrazine or with boron hydrides.

The high values of propellant performance, which, in principle, can be obtained using metals as fuels, also have negative consequences. The high heat of formation for combustion products of metals during an exothermal reaction indicates that these products must exist in condensed phase in the form of extremely stable compounds.

As established by Gerstein and Coffin [6], the evaporation of solid propellants and, particularly, metals before the burning process can be disregarded in many cases. For this reason, the first stages of the reactions leading to ignition will depend on the mechanism and weight of surface reaction. The vapor pressure of various metals and their oxides is presented in Fig. 6.

Many works on the oxidation of metals have been performed at low temperatures. Gulbransen and colleagues [7] studied the growth of oxide films of aluminum, beryllium, tungsten, magnesium, titanium, zirconium, and iron at low pressures and temperatures below ignition temperature. Teresh [8] studied the oxidation of aluminum, magnesium, beryllium, and nickel in an atmosphere of
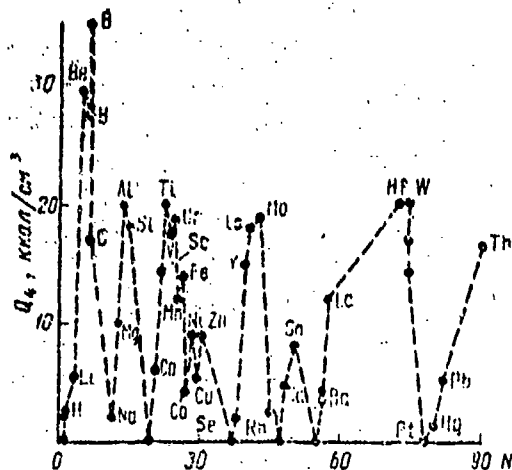
Fig. 5. Quantity of heat
released during the burning
of a unit volume of an element
with atomic number N.

Designation: ккал/см3 = kcal/cm³.
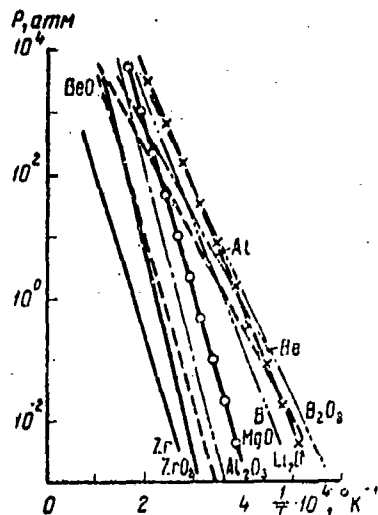
Fig. 6. Vapor pressure
of various metals and
their oxides as a function
of 1/T.

Designation: атм = atm.

air and oxygen near ignition temperature at atmospheric pressure.
On the basis of these works, we can generalize conclusions
relative to the effect of temperature on the oxidation of metals.
The dependence of the oxide formation rate constant on temperature
is exponential and conforms, within the range of experimental
error, to either the Arrhenius equation:

$$K = A \exp(-E/RT),$$ (I.2)

or the theory of transient state:

9

$$\frac{K}{T} = C \exp(-E/RT),$$

(I.3)

where $C = a \exp(\Delta S/R)$.

Several values for activation energy and the temperature range within which they are valid are presented in Table 4 [7, 9-11].

Table 4. Activation energy of several metals.

Metal	$T, °C$	Activation energy, kcal/mole	Metal	$T, °C$	Activation energy, kcal/mole
Al	350—475	22,8	Zr	200—425	18,3
Be	350—950	50,3	Cu	50—400	37,8
Ti	350—600	26,0			

The intensity of the course of the reactions on the surface of metal particles, to a considerable degree, depends on the properties of the oxide layer which is formed during oxidation.

According to the rule of Pilling and Bedworth [12, 13], if the volume of the oxide being formed is less than the volume of the metal from which this oxide is formed, the oxide film has a loose cell structure and cannot reliably protect the metal from further oxidation. If, however, the volume of the oxide exceeds the volume of the metal, then a protective layer is formed which hinders the process of metal oxidation under the condition that the boiling temperature of the oxide is sufficiently high.

The coefficient β of Pilling and Bedworth is calculated from the formula

$$\beta = \frac{M \rho_M}{n A \rho_{OK}},$$

(I.4)

where M is the molecular weight of the oxide; ρ_{OK} is the density of the oxide; ρ_M is the density of the metal; A is the atomic weight of the metal; n is the atomic number of the metal in the oxide molecule.

Table 5 presents the values of β for various metals. As is apparent from Table 5, for light metals – alkali metals, alkali-earth metals, and magnesium – β < 1, while for heavy metals and aluminum β > 1.

Table 5. Ratio β of oxide volume to metal volume.[1]

Oxide	β	Oxide	β	Oxide	β
Li_2O	0,58	ZrO_2	1,56	ZnO	1,55
Li_2O_2	0,83	VO	1,51	CdO	1,21
Na_2O	0,55	V_2O_3	1,82	$Al_2O_3 (\alpha)$	1,28
Na_2O_2	0,67	V_2O_5	3,19	$Al_2O_3 (\beta)$	1,54
K_2O	0,45	Cr_2O_3	2,07	SnO_2	1,32
K_2O_2	0,73	CrO_3	5,1	PbO	1,31
BeO	1,68	WO_2	2,08	Pb_3O_4	1,4
MgO	0,81	WO_3	3,35	MnO	1,79
CaO	0,64	Fe_2O_3	2,14	Mn_3O_4	2,15
Ti_2O_3	1,46	Cu_2O	1,64	B_2O_3	2,46
TiO	1,20	CuO	1,72		

[1]Data concerning the volume ratio are presented for 20°C. For other temperatures tabular data must be corrected, which is easy to do if we know the value of the coefficient of thermal expansion.

As Pilling and Bedworth have found, the value of β determines the behavior of metals during high-temperature corrosion: if β < 1, the metal corrodes easily and rapidly. Obviously, the low value of β for magnesium, alkali metals, and alkali-earth metals is one of the reasons for their high burning rate.

At very high values for β the oxide layer obtains considerable internal stresses, cracks, and loses its protective properties; therefore, layers in which β does not greatly exceed one have the highest protective properties [14]. This includes aluminum to the fullest extent.

The basic characteristic of compound ability, which serves as a measure of the energy of the interatomic bond, is the isobaric thermodyanmic potential or the free energy of their formation, defined by the Hibbs-Helmhold equation:

$$\Delta Z = \Delta H - T \Delta S.$$ <div align="right">(I.5)</div>

However, more complete data are available on the heats of formation, which differ comparatively little from the values of free energy. Therefore, it is natural in comparing the strength of the chemical bond of compounds to use data on the standard heats of their formation [15- *] [Translator's Note: This number is illegible in the original document].

The thermochemical constants for inorganic compounds are the largest fundamental quantitative characteristics since the heat and free energy of the formation of oxides, fluorides, chlorides, and other metal compounds are the foundation for calculating burning processes. The corresponding periodic curve for oxides is presented in Fig. 7. Heat of formation is referred to one atom of oxygen, i.e., for the convenience of comparison it is calculated for one bond. As is apparent from Fig. 7, the heat of formation of metals widely used as additives to propellants lies in the upper portion of the curve. The maximum heats of formation are those for the oxides of alkali-earth metals BeO, CaO, MgO.

Fig. 7. Heat of oxide formation for elements with atomic number N, referred to one atom of oxygen.

Designation: ккал/моль.атом = kcal/mole·atom.

12

However, more complete data are available on the heats of formation, which differ comparatively little from the values of free energy. Therefore, it is natural in comparing the strength of the chemical bond of compounds to use data on the standard heats of their formation [15- *] [Translator's Note: This number is illegible in the original document].

The thermochemical constants for inorganic compounds are the largest fundamental quantitative characteristics since the heat and free energy of the formation of oxides, fluorides, chlorides, and other metal compounds are the foundation for calculating burning processes. The corresponding periodic curve for oxides is presented in Fig. 7. Heat of formation is referred to one atom of oxygen, i.e., for the convenience of comparison it is calculated for one bond. As is apparent from Fig. 7, the heat of formation of metals widely used as additives to propellants lies in the upper portion of the curve. The maximum heats of formation are those for the oxides of alkali-earth metals BeO, CaO, MgO.

Fig. 7. Heat of oxide formation for elements with atomic number N, referred to one atom of oxygen.

Designation: ккал/моль.атом = kcal/mole·atom.

For comparison, the periodic curve showing the heats of fluoride formation is illustrated in Fig. 8. As is apparent, the maximum heats of formation are those for the fluorides of oxygen and lithium; the fluorides of metals of interest to us also lie in the upper portion of the graph.

Fig. 8. Heat of fluoride formation for elements with atomic number N, referred to one atom of fluorine.

We should note that all six elements to which the maximum points on the curve correspond are found in the third and fourth groups of the periodic system of elements. This indicates the possible connection between the position occupied by the element in the periodic system and its properties as a rocket propellant.

Since shells of such high-melting oxides as Al_2O_3, MgO, BeO, which are formed in the process of burning on the surface of metal particles (or near it), have a considerable effect on the burning process itself, it is necessary to examine, in a general outline, the physical and chemical properties of these oxides. The most stable compounds are those which have the maximum negative value of free energy of their formation from elements.

13

The comparative thermal stability of high-melting oxides is presented in Fig. 9 [18]. The solid lines connect the oxides having identical values for heat of formation, calculated in g-eq (at 25°C). The widely spaced cross hatching indicates comparatively low thermal stability of the oxides. The denser cross hatching indicates the region of greatest stability.

Fig. 9. Comparative thermal stability of high-melting oxides.

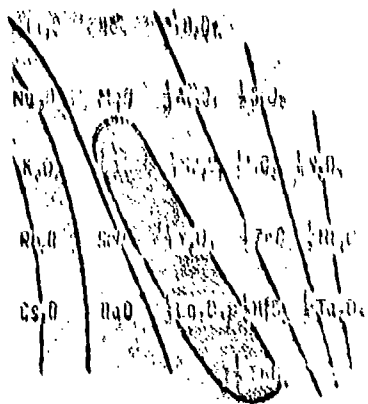Oxides can interact with the ambient atmosphere and with other oxides. Usually, high-melting oxides are stable to the effect of various atmospheres. In dry air and in oxidized atmospheres they, as a rule, are stable up to the melting point. With reduced atmospheres, as well as with atmospheres containing carbon and sulfur, oxides can enter into a reaction [19-29].

Aluminum oxide is inert with respect to air, water vapor, hydrogen, argon, carbon dioxide and monoxide, and nitrogen up to 1700°C. At higher temperatures aluminum oxide reacts with water and reducing atmospheres with the formation of Al_2O [19, 20]. Although aluminum oxide is one of the most stable oxides, it reacts, to a certain extent, with hydrogen sulfide at high temperatures, becoming saturated with sulfur. Al_2O_3 enters into a reaction with hydrogen fluoride, while at the same time being stable with respect to HCl.

14

Aluminum oxide interacts with carbon only if oxide of a carbide-forming element is added to the composition. The reaction of aluminum carbide formation occurs even when an oxide is added which is thermodynamically more stable than Al_2O_3 (for example, ThO_2, BeO, ZrO_2):

$$V_2O_3 + 7C = 2VC + 5CO,$$
$$2Al_2O_3 + VC + 7C = Al_4C_3 + VO + 5CO. \tag{I.6}$$
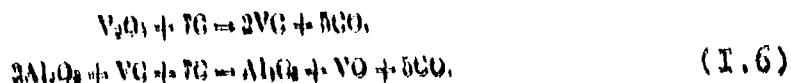
This process takes place at approximately 2100°C. The oxide of the carbide-forming element is probably surface-active.

Graphite-forming oxides include SiO_2, TiO_2, ZrO_2, Be_2O_2, Cr_2O_3, Nb_2O_5, Fe_2O_3, V_2O_5, GeO_2, BeO, ThO_2.

Beryllium oxide is also stable in air, hydrogen, carbon monoxide, and nitrogen up to temperatures not exceeding 1700°C. Although BeO has low vapor tension [21, 22], it evaporates rapidly in the presence of water vapor at high temperatures due to the formation of $Be(OH)_2$ in vapor form. In atmospheres containing halogens and sulfur, beryllium oxide also is unstable.

Magnesium oxide is stable in air, nitrogen, carbon monoxide, hydrogen, and ammonia to a temperature on the order of 1700°C. Atmospheres containing halogens and sulfur interact with MgO; carbon-containing media reduce magnesium oxide at high temperatures. At temperatures above 1800°C magnesium oxide intensely dissociates and evaporates [23]; in a vacuum the rapid evaporation begins at temperatures above 1900°C.

Between pure oxides at temperatures much lower than the melting point of any of the components, reactions with the formation of liquid eutectics begin to occur, which, in a number of cases, will promote the destruction of the oxide film during the

burning of metal particles. Liquidus temperature for various
binary systems is indicated in Table 6 [11].

Table 6. Liquidus temperature for various
oxide combinations.

Oxide	Temperature, °C						
	Al₂O₃	BeO	CaO	MgO	TiO₂	ZrO₂	SiO₂
Al₂O₃	—	1900	1400	1930	1720	1700	1545
BeO	1900	—	1450	1800	1700	2000	1670
CaO	1400	1450	—	2300	1420	2200	1410
MgO	1930	1800	2300	—	1600	1500	1540
TiO₂	1720	1700	1420	1600	—	1750	1540
ZrO₂	1700	2000	2200	1500	1750	—	1675
SiO₂	1545	1670	1410	1540	1540	1675	—

As is apparent from Table 6, in a number of cases, combina-
tions of basic oxides, for example Al_2O_3, MgO, or CaO, with
acids, for example SiO_2, are the best in this respect.

High-melting oxides are usually stable in contact with
carbides; however, at sufficiently high temperatures they react
with them. This reaction occurs most easily in a vacuum where,
as a result of the reduction of various compounds, free oxygen
is formed. In contact with graphite, BeO is the most stable of
the oxides in question. Below are presented the temperatures
(°C) for the beginning of the reactions of various oxides with
graphite in vacuum [30, 31]:

| Oxide	Al₂O₃	BeO	MgO	SiO₂	ThO₂	ZrO₂
T, °C	1500	2300	1800	1400	1950	1800

The basic thermal properties of oxides at high temperatures
are the following: melting point, coefficient of thermal expansion,
heat capacity, thermal radiating power, and thermal conductivity.

The melting point, as shown in Fig. 10, depends on crystal structure and the strength of the molecular linking.

The coefficient of thermal expansion (α), in the general case, is approximately proportional to absolute melting point, as seen in Fig. 11 in the example of a number of oxides and halogens. Similarly, the heat capacity and the coefficient of thermal expansion grow rapidly at low temperatures, approaching a certain limit or increasing very slowly at temperatures above the Debye temperature. In this region the heat capacity agrees rather accurately with the law of Dulong and Petit, on the basis of which it is approximately 6 cal/deg·g-atom. In certain compounds expansion occurs in one direction of the crystal and contraction in another, due to which the total expansion during heating is very little. $CaCO_3$, Al_2TiO_5 and a number of lithium alumosilicates have such properties.

The effect of temperature on the thermal expansion coefficient and the heat capacity of aluminum oxide is presented in Fig. 12. Data on thermal conductivity (λ) of some oxides in a wide temperature range for various structural forms are presented in Fig. 13. The difference between a good powdered heat-insulating material, such as finely pulverized magnesium oxide MgO, and the best heat conductor of the BeO oxides is more than four orders in magnitude [30-32].

The heat radiating capacity of oxides is an important characteristic when examining the burning processes of flames in which there are condensed particles of, for example, MgO, Al_2O_3, BeO, etc. Detailed studies of the radiating capacity of many metals and their oxides can be found in various books and articles [33-44].
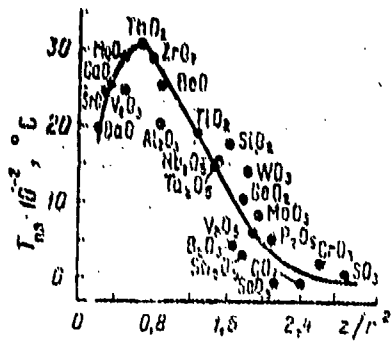
Ionic bond← →Covalent bond

Fig. 10. Melting point of oxides.
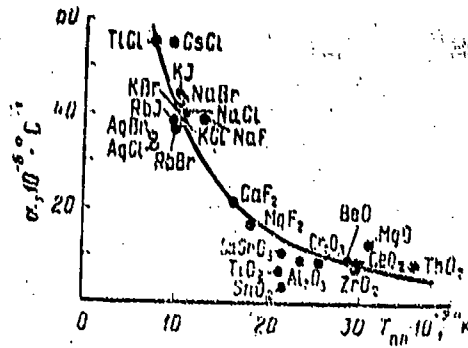
Fig. 11. Thermal expansion coefficient (α) versus T.
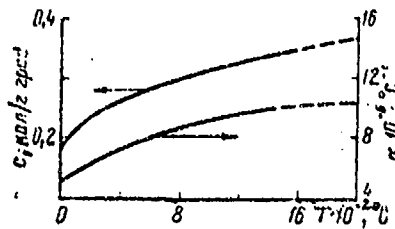
Fig. 12. Effect of temperature on thermal expansion coefficient and heat capacity of aluminum oxide.

Designation: кал/г град = = cal/g deg.

Fig. 13. Heat conductivity λ of oxides versus temperature. 1 – Platinum; 2 – graphite; 3 – pure dense BeO; 4 – SiC with binding; 5 – pure dense MgO; 6 – fireclay; 7 – pure dense Al_2O_3; 8 –

fused quartz glass; 9 – pure dense ZrO_2; 10 – powdered MgO.

Designation: кал/см·сек.°C = cal/cm.s.°C.

As a rule, the amount of radiating capacity of polycrystalline oxides is generally determined by the quantity and distribution of the pores in them. The reflection factor of a porous surface differs greatly from its value for a smooth surface since the pores act as scatte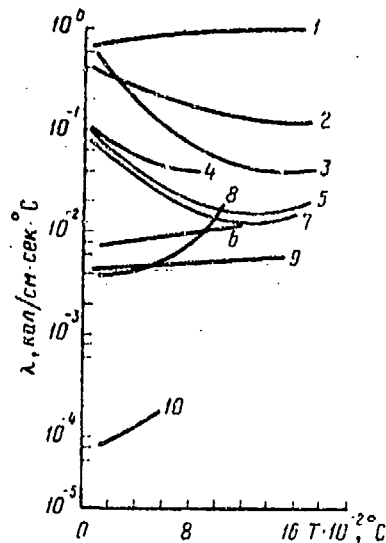ring centers and their effectiveness, in this respect, depends on the dimensions and concentration of the pores. With high scattering effectiveness (and, consequently, low absorption) the reflecting capacity can be very high while the radiating capacity is accordingly very low. Pores of larger dimensions and the presence of impurities can bring about a significant increase in radiating capacity.

Reference [41] presents the dependence of integral radiating capacity of aluminum oxide on temperature (Fig. 14).
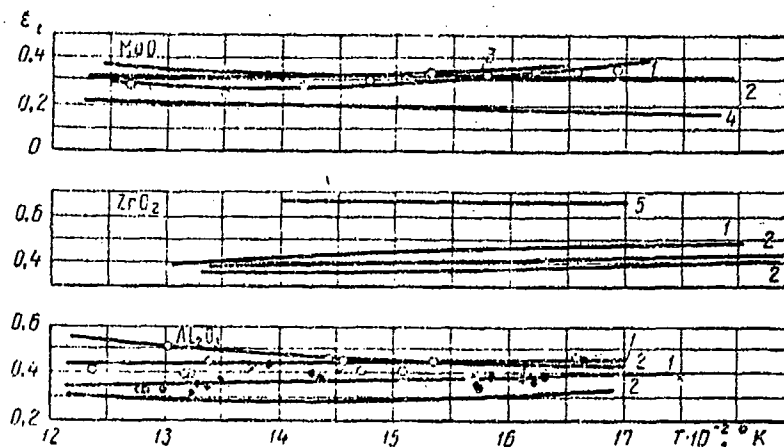
Fig. 14. Dependence of integral radiating capacity for a number of oxides on temperature, according to the given authors. 1 - Petrov [41]; 2 - Olson and Morris [45]; 3 - Bronlow [45]; 4 - Feri [45]; 5 - Lemmon and Buda [45].

For two specimens of aluminum oxide different results are obtained. Petrov [41] explains this difference by the character of pores and cracks since one specimen had many more cracks; their number increased after the specimen was ground to a thickness of 2 mm. With respect to radiating capacity, there is much more data available in the range of comparatively low temperatures for aluminum oxide than there is for other oxides.

19

Data from Olson and Morris [45] for two different specimens
of aluminum oxide differ much more than the results obtained by
Petrov (by approximately 0.2). These authors indicate the brand
of material, but do not present information about it. Patison's
results [45] fall between the values of Olson and Morris for
two specimens of aluminum oxide.

Figure 14 illustrates the dependence of integral radiating
capacity of magnesium oxide on temperature. In the range
approximately up to 1300°K, there is observed a decrease in the
radiating capacity, and then an increase. The maximum disagreement
between the results obtained in reference [41] and the results
of Olson and Morris [45] is 10%; the disagreement between the
results obtained in [41] and the results from reference [39] is
14%.

Full radiating capacity of BeO is studied in reference [46].
For $\lambda = 0.65$ µm the spectral emittance at 900-1600°C is approxi-
mately 0.22.

For quantitative evaluations of burning rates and especially
oxidation of metal particles at relatively low temperatures, it
is frequently necessary to know the value of the rates of
diffusion through the oxide shells. At the present time there
are data for a rather large number of alloys, metals and their
oxides.

The temperature dependence of the diffusion rate is defined
by an exponential expression just as the chemical reaction rate
is defined by the Arrhenius equation

$$D = D_0 \exp(-Q/RT),$$

where D_0 and Q are constant.

20

If the logarithms of the coefficients of chemical diffusion
are plotted on a graph as a function of a quantity inverse to
temperature, the inter-relationship can be characterized by
two intersecting lines, according to the expression

$$D = D_0' \exp(-Q'/RT) + D'' \exp(-Q''/RT). \tag{I.7}$$

From this equation it follows that diffusion rates at low
and high temperatures are determined by two different mechanisms.
In ionic crystals this can be brought about by the diffusion
of atoms of one sort possessing a different activation energy
than atoms of another sort although their diffusion rates have
approximately the same order of magnitude [47].

An equation in the form of (I.7) can also characterize the
situation when the rate of the process at low temperatures is
determined by the rate of diffusion along the intergrain boundaries,
and at high temperatures the rate of diffusion through the grains
themselves. In alloys the transition temperature is comparatively
low; however, in the case of oxides, which are frequently more
refractory than the metals themselves, diffusion along the inter-
grain boundaries can predominate even at comparatively high
temperatures [48].

The values of the coefficients of diffusion for a number
of oxides are presented in Table 7.

Table 7. Data on diffusion rate of ions in
metals and oxides.

Metal of compound	Diffusing element	Temperature range, $^\circ C$	D_0, cm^2/s	q, kcal/g-atom
Fe (γ).	Fe	905—1401	5.8	74.2
Fe (α)	C	from —40 to +800	0.02	20.1
	N	from —23 to +37	0.03	18.2
Cu	Zn	550—900	0.0024	30.2
	Cd	500—800	0.0035	29.2
Al	Be	500—630	52	39.0
α-Zr	O (ion)	400—585	5.2	51.0
V	O (ion)	70—180	0.011	29.0
MgO	Mg (ion)	1400—1600	0.25	79.0
	O (ion)	1300—1750	$2.5 \cdot 10^{-4}$	62.4

21

Table 7 Cont'd.

CaO	Ca (ion)	900—1640	0,4	81,0
Cr₂O₃	Cr	1000—1350	$4 \cdot 10^3$	100,0
Fe₂O₃	Fe	930—1270	$4 \cdot 10^1$	112,0
	O	1150—1250	10^{11}	146
Cu₂O	Cu	800—1050	0,12	36,1
	O	—	0,0065	39,3
ZnO	Zn	950—1370	1,3	73,5
	O	1100—1300	$6,5 \cdot 10^{11}$	165
Al₂O₃	O	1200—1600	$6,3 \cdot 10^{-8}$	57,6
PbO	Pb	490—600	10^5	66

§ 2. Aluminum

Aluminum is crystallized in a face-centered lattice with parameter a = 4.04 Å; atomic radius 1.43 Å. Aluminum does not have allotropic modifications. The basic physical properties of aluminum are presented below:

Atomic weight	26.98
Density, g/cm^3	2.7 (20°C)
	2.35(1000°C)
$T_{пл}$, °C [Melting point]	660
$T_{кип}$, °C [Boiling point]	2050 (1 atm)
Specific heat capacity, cal/g·deg	0.214(20°C)
Latent heat of fusion, cal/g	96
Latent heat of evaporation, cal/g	3050
Heat conductivity, cal/cm·s·deg	0.503(20°C)
Coefficient of linear expansion, $10^{-6} \cdot deg^{-1}$	23.8 (20–100°C)

The modulus of elasticity for aluminum, according to the data from various studies, lies within 6670–7300 kgf/mm^2 [49–50]. The viscosity of melted aluminum, as a function of temperature, changes from 0.0635 poise at 670° to 0.01392 poise at 800°C [51].

The value of the surface tension of aluminum in the range 700-820°C is 520 dyne/cm [52].

The vapor pressure of aluminum at various temperatures (expressed in mm Hg) is as follows: at 0°C, $1 \cdot 10^{-43}$; at the melting point, $5.25 \cdot 10^{-7}$; and at 1880°C, 1 mm Hg. In vacuum (evacuation 1 mm Hg) the boiling temperature of aluminum drops to 1603°C [16].

The electric conductivity of aluminum, as a function of temperature, changes from $156 \cdot 10^4 \ \Omega^{-1} \cdot cm^{-1}$ (-189°C) to $12.5 \cdot 10^4$ $\Omega^{-1} \cdot cm^{-1}$ (+400°C). The electric conductivity of aluminum depends on the degree of purity of the metal and drops with an increase in impurity content. Thus, if the electric conductivity of aluminum with a purity of 99.997% is 65.45% of the electric conductivity of copper, then for aluminum with a purity of 99.5% this figure drops to 62.5%. The specific resistance of high-purity aluminum at 20°C is $2.620 \cdot 10^{-6} \ \Omega \cdot cm$.

In the periodic system of elements aluminum is located below boron; therefore, its metallic properties are more strongly pronounced while it is inferior to boron with respect to chemical activity.

Aluminum reduces the majority of metal oxides to metal, joins vigorously with halogens, and at high temperatures with sulfur, nitrogen, phosphorus, and carbon. Traces of the formation of aluminum carbide Al_4C_3 are detected even at 650°C and the reaction reaches full development at 1400°C [28]. Aluminum carbide above 2100°C dissociates and the aluminum thus released is capable of dissolving in carbide. With cooling, this solution decomposes and there occurs a reverse formation of metallic aluminum In vacuum, in the range 400-1400°C, aluminum carbide is stable and no changes are detected. At 2200°C aluminum carbide sublimates without changing to liquid state. The vapor tension of aluminum

carbide which is in equilibrium with graphite and aluminum saturated with graphite is 400 mm Hg at this temperature. The density of aluminum carbide is 2.36 g/cm^3, while the heat of formation with respect to the $4Al + 3C \rightarrow Al_4C_3$ reaction is 63.2 kcal/mole. At high temperature aluminum carbide is a rather stable compound but is oxidized by all compounds capable of giving off oxygen. Therefore, Al_4C_3 reduces metal oxides; the course of the reactions depend on temperature conditions, can be rather complex and lead either to a reduction of the oxide to metal with the formation of aluminum oxide or, from the aluminum carbide, aluminum can be partially separated in parallel and give an alloy with reduced metal.

From rather numerous works (including [53, 54]), we know that the very first film forming on aluminum when air at room temperature acts on it is amorphous in the sense that its crystal nature cannot be distinguished by either electron diffraction or X-ray diffraction. This in no way excludes the possibility of the existence of very small crystalline formations consisting, for example, of two Al_2O_3 molecules [54]. Holding aluminum at 400°C in air or under partial oxygen pressure 10^{-8} mm Hg [55] enables us to distinguish the crystal nature of the oxide on the metal-oxide interface. At temperatures above 500°C in air, due to chaotic generation, there is formed a continuous layer of oxide crystals with a maximum of 0.1-0.2 µm in diameter. As it appeared, the films forming on the melted aluminum in air atmosphere are amorphous at 650-700°C, while at 700-710°C crystalline films of γ-Al_2O_3 occur [54].

For aluminum oxide Al_2O_3 two crystal modifications are known: α-Al_2O_3 (corundum) with a rhombohedral lattice and γ-Al_2O_3 (aluminum oxide) which has a cubic face-centered lattice [57]. Lower oxides (monoxide) AlO and Al_2O can also form during the oxidation of aluminum. The heat of dissociation for monoxide AlO is -97 kcal/mole.

The density of Al_2O_3 in the form of corundum is 3.96 g/cm^3 and in the form of aluminum oxide is 3.42 g/cm^3. The average specific heat capacity of commercial aluminum oxide in the range 20-1000°C is defined as equal to 0.304 cal/g [16]. The average thermal expansion of Al_2O_3 in the range 20-1000°C is taken as $8.5 \cdot 10^{-6}$ deg^{-1}. The heat conductivity of aluminum oxide is 0.025 cal/cm·s·deg.

According to a number of determinations from various studies, the melting point of Al_2O_3 can be taken as lying within 2010-2050 °C, and the latent heat of fusion and evaporation is 58.5 and 115.7 cal/g, respectively [16].

The vapor tension of Al_2O_3 at various temperatures is presented below:

T, °C	2360	2490	2580	2980
Vapor tension, mm Hg	6	22	53	760

The heat of formation for Al_2O_3 is 400.5 kcal/mole. The change in weight of pure aluminum during its oxidation in an oxygen atmosphere at temperatures above 350°C was determined by Gulbrasen and Wyson [7], Aylmore, Gregg, and Jepson [58]. It was found that the degree to which the studied specimens were polished and degassed strongly affected the experimental results. The increase in the amount of absorbed oxygen with time, observed at temperatures of ∿400°C, is subject to parobolic law. In the range 450-600°C the curves $\Delta m = f(t)$ agree best with the rules of paralinear oxidation [58]. At 600°C the asymptotic character of the oxidation is brought about by the transformation of the amorphous structure of Al_2O_3 to crvstalline, which can be detected by electron diffraction.

In spite of the high heat of formation for aluminum oxide, it is difficult to oxidize aluminum even at high temperature in pure oxygen and in a finely ground state. This fact is due to the presence in aluminum of a dense film of Al_2O_3, completely impenetrable for gases; the approximate thickness of this film is 0.0002 mm; its weight per 1 cm^2 of aluminum surface is approximately 0.1 mg. This thin film is a protection against the propagation of the oxidation into the depth of the metal.

At room temperature, aluminum ceases to oxidize after approximately one hour [59]. According to Dankov [52, 60], when storing aluminum at room temperature, the oxide film on its surface after seven days reaches a thickness of 50–100 Å. With an increase in storing temperature up to the melting point, film thickness can reach 2000 Å.

As a result of a three-month storage of aluminum, an oxide film approximately 70 Å thick forms on it, which, in the course of time, increases at a rate of 2–3 Å per month. The film on remelted aluminum consists of crystal $\gamma-Al_2O_3$. The same film is formed on aluminum during long heating in the range 400–500°C. With rapid heating, however, up to a temperature of 500°C, an amorphous film of Al_2O_3 is formed on it and, with heating up to 700°C, a mixture of amorphous Al_2O_3 and $\gamma-Al_2O_3$ is formed.

On electron-diffraction patterns of oxide films, taken from liquid aluminum and its alloys not containing magnesium, in addition to the diffraction rings of $\gamma-Al_2O_3$, there are rings which belong to the structure of metallic aluminum with the characteristic grain-oriented packing [60]. This phenomenon is connected with the presence of very fine aluminum dendrites in the composition of the oxide film, which is also seen when examining the structure of the oxide film in an electron microscope with magnification on the order of 5000–6000.

The tendency of oxide film toward penetration by very fine aluminum dendrites with a definite orientation can apparently be explained by the crystal-chemical and dimensional correspondence of the crystal lattices of aluminum and its oxide.

With an increase in temperature the grain-oriented rings of aluminum disappear and on the electron-diffraction pattern there remain only rings of pure aluminum oxide γ-Al_2O_3.

Aluminum-magnesium alloys with a magnesium content from 4-12% have become widely used. Aluminum with magnesium forms intermetallic compounds Al_3Mg_2, Al_3Mg_4, Al_2Mg_3. The compound Al_3Mg_4 has a heat of formation of 49 kcal/mole; its density is 2.15 g/cm^3 and boiling point 463°C. This alloy differs favorably from corresponding mixtures of aluminum with magnesium by its lower corrosion capacity; it is very brittle, which makes it possible to pulverize it easily. We know that intermetallic compounds are generally characterized by considerable brittleness and hardness which is much greater than the hardness of their components.

Considerable attention has been given to the properties of aluminum alloys with magnesium in an atmosphere of air and water vapor. An electron-diffraction study of aluminum alloys with 2.4-8% magnesium, heated in an atmosphere of dry air, was undertaken by De Brouckere [53], whose expanded and confirmed experimental data was obtained earlier by Preston and Biroumshaw [61], as well as Dobinski [62].

The composition of films forming on these alloys depends considerably on temperature. At high temperatures (above 350°C) magnesium oxide (with an impurity of some amount of Mg_3N_2) is mainly formed during the oxidation of liquid alloys in an air atmosphere [63], while aluminum oxide is completely absent. The films are yellow or brown. The thick black films observed under practical conditions consist of MgO. Heating the alloys

to 120-300°C is accompanied by the formation of a crystal
γ-modification of aluminum oxide [60]. The successive heating
of alloys to 400°C (for example, holding at 250°C for 12 hours
and then final heating up to 400°C) leads to the formation of
double films consisting of magnesium oxide over aluminum oxide.
It is assumed that the formation of the upper layer of magnesium
oxide is explained by the diffusion of magnesium ions through
a film of aluminum oxide and oxidation along the oxide-air
interface (more accurately along the interface between Al_2O_3
and MgO).

Smeltzer [64] determined the oxidation rate of an aluminum
alloy with 2.9% Mg at 200-550°C and an oxygen pressure of 76 mm Hg
by the weight method. The rate of its oxidation was clearly
subject to parabolic law; the transition from parabolic
oxidation to linear set in when the thickness of the film
reached approximately 1000 Å. The two constants of the oxidation
rates are expressed by the following equations:

$$K_{парабол} = 2 \cdot 10^{-3} \exp(-33000/RT), \quad g^2/cm^4 \cdot s,$$
[parabolic]

$$\qquad\qquad\qquad\qquad (I.8)$$

$$K_{лин} = 0.2 \exp(20000/RT), \quad g/cm^2 \cdot s.$$
[linear]

Hirashima [63] rather thoroughly studied the selective
oxidation of an aluminum alloy with 2.5% Mg. At a partial
pressure of water vapor from 0.007 to 0.06 mm Hg the alloy
oxidizes according to parabolic law; its oxidation rate apparently
is determined by the rate of the diffusion of Mg^{2+} or O^{2-} ions
through a film of MgO. However, when the partial pressure of
water vapor is 1 mm Hg, oxidation, from parabolic in the initial
state, soon becomes linear. A broader study of the oxidation of
aluminum-magnesium alloys by water vapor is presented in
reference [65].

§ 3. Beryllium

Beryllium is a bright-gray refractory brittle metal. The structure of the low-temperature modification of beryllium is characterized by a hexagonal lattice [66-69]: $a_0 = 2.2854$ Å, $a_0 = 3.5829$ Å, $c/a = 1.5677$.

Below 1200°C no polymorphic transformations of beryllium are observed. The phase transition of α-Be to cubic form β-Be ($a_0 = 2.54$ Å), occurs at 1254°C [70]. Beryllium has the following physical properties [68]:

Density, g/cm^3	1.847
$T_{пл}$, °C [Melting point]	1283
$T_{кип}$, °C [Boiling point]	2970
Heat of formation, kcal/g·atom	2.8 ± 0.5
Electric conductivity, $\Omega^{-1} \cdot cm^{-1}$	$38.0-43.1 \cdot 10^4$
Brinell hardness, kgf/mm^2	97-114
Modulus of elasticity, kgf/mm^2	29,280-30,000

Gulbransen and Endrew [7] studied the evaporation of beryllium below the melting point. Data from these authors are expressed by equation

$$\ln P \, (\text{atm}) = 6.186 + 1.454 \cdot 10^{-4} T - (16734 \pm 80) T^{-1}, \qquad (\text{I.9})$$

From this equation it follows that the graph of ln P as an inverse function of temperature does not differ noticeably from a straight line.

The evaporation rate of beryllium, as noted by Gulbransen, noticeably decreases when there is an oxide or nitride film on the surface of the specimen. With an average oxide film thickness of 600 Å, vapor pressure decreases by one order, but when thickness is 5000 Å, it decreases by a factor of 60. A nitride film 2000 Å thick reduces evaporation rate by a factor of 4. The effect of

surface films on evaporation rate is greater the lower the temperature. According to observations of Popirov and Tikhinskiy [67], the oxide film noticeably reduces evaporation rate only below 1100-1150 °C; in the range of higher temperatures the film scales off the surface and during sufficiently long tests has little effect on evaporation rate.

According to Holden [71], the latent heat of sublimation for beryllium is 76500 ± 370 cal/mole.

Bauer and Brunner (cited in [68]) have shown that vapor pressure (mm Hg) in the range 1577-2058°C can be expressed by equation

$$\ln P = 6.404 - 11710 T^{-1},$$ (I.10)

Their extrapolation of the vapor pressure curve up to a value of 1 atm gives 2970°C for the boiling point of beryllium.

The enthalpy of beryllium grows almost linearly from 42.6 cal/g at 94° to 571 cal/g at 896°C [72].

Thermal conductivity of beryllium at 0°C is 0.3847 cal/cm·s·deg. In the range from -176° to +190.4°C the thermal conductivity of beryllium increases from 0.232 to 0.508 cal/cm·s·deg.

Gulbransen and Endrew [7] studied the oxidation of sufficiently pure beryllium in oxygen and nitrogen by determining the weight variation of ground and polished specimens on sensitive thermal scales. At a pressure of 76 mm Hg the results of two-hour tests were expressed by the following equations:

in an atmosphere of O_2:

$$\text{for } T = 350\text{-}700°C$$
$$K_n = 1.8 \cdot 10^{-12} \exp(-8500/RT), \ g^2/cm^4 \cdot s;$$

in an atmosphere of O_2:

$$\text{for } T = 750\text{-}900°C$$
$$K_n = 3.5 \cdot 10^{-3} \exp(-50,300/RT), \ g^2/cm^4 \cdot s;$$

$$(I.11)$$

in an atmosphere of N_2:

$$\text{for } T = 725\text{-}925°C$$
$$K_n = 23.6 \exp(-75,000/RT), \ g^2/cm^4 \cdot s.$$

These equations do not take into account the initial accelerated weight increase. In these short tests the oxygen-time dependence had an almost parabolic nature.

However, Aylmore, Gregg, and Jepson [73], after increasing the length of the tests to 300 hours, could not confirm this observation for the range 500-700°C. The beryllium which they used was purer and contained 0.3% BeO and 0.16% other metals. At temperatures below 650°C the oxidation rate, according to observations, continuously decreased with time, achieving after 300 hours the level 0.02-0.04 $\mu g/cm^2 \cdot g$; the oxidation rate was not subject to parabolic law. Nevertheless, as the authors note, oxidation was most likely determined by the diffusion of Be^{2+} ions, and the deviation from parabolic law was probably due to the variation in impurity content in the scale.

Beryllium oxide crystallizes in the form of colorless (polycrystalline mass has a white color) hexagonal crystals and is one of the most stable chemical compounds [74]. The crystal lattice constants of beryllium oxide at 18°C are a = 2.698 Å and c = 4.377 Å; density is 3.025 g/cm^3.

The melting point of beryllium oxide is $2570 \pm 25°C$ [18, 31, 75]. Erway and Seifert [76] have established that the boiling point of beryllium oxide must be on the order of 4100°C, although a value of approximately 4300°C is frequently found in literature. It was further established that the high volatility observed for beryllium oxide is due to water vapor impurities and that in dry atmosphere the pressure of its vapor is not great. In reference [76] the following equation relating the vapor pressure of beryllium oxide to temperature was found experimentally:

$$\lg P = (18,50 \pm 0,23) - \frac{(34\,230 \pm 530)}{T} - 2 \lg T, \qquad (I.12)$$

where P is expressed in millimeters of mercury.

Based on the melting point and the calculated values for the entropy of fusion, Erway and Seifert established the value of the latent heat of fusion, equal to 17.0 ± 1.4 kcal/mole·deg. They also found that the value of the latent heat of evaporation of beryllium oxide is 117.0 ± 40.5 kcal/mole, which corresponds to the entropy of evaporation at the boiling point, equal to 25.6 ± 2.7 cal/mole·deg.

Grossweiner and Seifert [77] studied the volatility of beryllium oxide in the presence of water vapor and established that the weight loss of beryllium oxide is a linear function of the value of the partial pressure of water vapor and corresponds to the reaction

$$BeO_{TB} + H_2O \rightarrow BeO \cdot H_2O_{TB}.$$
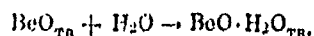
They calculated the heat and free energy of this reaction, which at 1400°C was 41.5 and 29 kcal/mole, respectively. The results of works [76, 77] on vapor pressure made it possible to calculate the following values for the reaction occurring in vapor phase: $\Delta H^0 = -108.5$ kcal/mole; $\Delta F^0 = -57.5$ kcal/mole.

32

The variation in the amount of free energy for this reaction is much more favorable than for the reaction with solid beryllium oxide. If we examine this reaction as a simple association of molecules, the heat of the reaction is too great and corresponds more nearly to the reaction

$$BeO_{TB} + H_2O \rightarrow Be(OH)_{2\,TB}.$$
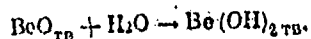
$$[TB = solid]$$

Hence it follows that although solid hydroxide $Be(OH)_2$ is unstable at temperatures above 240-300°C and atmospheric pressure [78-81, 83], at high temperatures it becomes stable in a gaseous state. To confirm this, Grossweiner and Seifert [77] calculated the binding energy of Be—OH for the gaseous phase of $Be(OH)_2$, which was 109 kcal/mole. Consequently, we can conclude from this that the product of beryllium oxide interaction with watervapor is beryllium hydroxide in a stable gaseous phase.

§ 4.   Boron

Boron is known in two modifications: a fine-crystal form, the so-called amorphous boron, which is a brown powder, and crystalline boron with a dark gray color. According to data from Laubengayer [82], the minimum elementary cell of the latter modification of boron contains approximately 50 atoms and has the following parameters: a = 8.93 Å, c = 5.06 Å; the orientation of the axis agrees with the axis of an acicular crystal.

The physical and chemical properties of elementary boron, to a considerable extent, are determined by the purity of the product, which is connected with the method of obtaining it. The basic physical and chemical properties of boron are presented below [84-88]:

Density, g/cm^3

    crystalline   2.33 ± 0.2

    amorphous   2.3

$T_{пл}$, °C   2075 ± 50

$T_{кип}$, °C   2550

Heat capacity, cal/g·atom·deg   1.54 + 0.0044

Heat of evaporation, kcal/g-atom   90

Heat conductivity, cal/s·cm·deg   0.003

Heat of combustion, kcal/g-atom   306 ± 1

Entropy, kcal/g-atom·deg   1.408(cryst. boron)

                                          1.564(amorph. boron)

Heat of transformation
$B_{аморф}$[amorphous] − $B_{крист}$[crystalline],
kcal/g-atom   0.4

Coefficient of thermal expansion, deg^{-1} $8.3 \cdot 10^{-8}$ ± 3%

Boron acquires a considerable vapor pressure beginning at 1200°C and noticeably evaporates at 1600°C. The vapor pressure of boron at 1600° is 10^{-5} atm, at 1750° is 10^{-4} atm, and at 2150°C 10^{-2} atm [87].

The partial oxidizability of the surface of particles of even the purest specimens of amorphous boron causes the considerable hydrophily of its powder [88]. As concerns particle dimensions for boron powder, this, of course, depends on the method of obtaining the powder. According to data from Markovskiy and colleagues [88], Moissan boron, obtained by adsorption methods, has an average particle size on the order of 0.3 µm and a specific surface of approximately 6 m^2/g.

Boron has a negative temperature coefficient of resistance, and its electric conductivity with a temperature increase from 200°C to 1000°C grows by a factor of approximately $2 \cdot 10^8$ [89].

The reaction capacity of elementary boron depends substantially on the purity of the product, as well as on the degree of its crystallinity. Thus, although amorphous boron oxidizes slowly in air even at room temperature, upon heating to 800°C it ignites and burns with a blinding white light. Large crystals of boron, on the other hand, are sufficiently stable even at rather high temperatures. This difference between amorphous and crystalline boron is apparently connected with the fact that the film of B_2O_3 being formed protects the latter from further oxidation.

During the combustion of boron in air, boron anhydride is always formed. In addition to B_2O_3, as oxygen compounds of boron we know of several other oxides including B_2O_2 and B_4O_5, as well as BO.

On the basis of experimental data from references [90, 91], the thermodynamic stability of various oxides forming in gaseous phase during the evaporation of liquid B_2O_3 below 2400°K was evaluated. According to these data, ~95% of the volume of gas consists of B_2O_3 and only 5% of the suboxides B_2O_2 and BO or gaseous elements.

The spectral data for molecules of gaseous BO are presented in Hertzberg's work [93].

From the data presented below we can see that the oxide B_2O_2 is more stable than the oxide BO:

Molecule	ΔH (at 0°K), kcal/mole	Dissociation energy (at 0°K), kcal/mole
BO (gas)	+5.3	189.5
B_2O_2 (gas)	-110.9 ± 7	500.5 ± 10
B_2O_3 (gas)	-214.4 ± 5	662.9 ± 6

At high temperatures boron anhydride is reduced by many metals, particularly Al and Mg, with the formation of elementary boron and its alloys [88]. Carbon reduces B_2O_3 with the formation of boron carbide at a temperature on the order of 2100-2400°C.

Crystals of boron anhydride have a rhombohedral shape and give a characteristic X-ray pattern, which can be identified as hexagonal with a = 4.325 $\overset{o}{A}$ and c = 8.317 $\overset{o}{A}$ [92].

Zintl and colleagues (cited in [88]) established that during the heating of a mixture of Al_2O_3 with elementary boron at 1300°C the following reaction occurs

$$Al_2O_3 + 3B \rightleftarrows 2Al + 3BO.$$
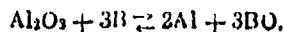
This reaction can lead to the formation of a number of suboxides of boron.

Boron easily combines with fluorine, chloride, bromine, and iodine [87]. Pure boron does not interact with chloride at temperatures below 500°C, but combines rapidly with it at 550°C, forming boron trichloride. Certain properties of boron were discovered and studied by Culilleron [94]. A mixture of boron with potassium permanganate, minium, antimony trioxide, or lead nitrate ignites upon impact or friction, but without explosion. The reaction of boron with hydrogen iodide occurs with explosion.

As was noted earlier, Leonard [1, 95] studied the possibility of using boron hydrides as rocket propellant. The highest specific impulse is achieved when using elements with low atomic weight as propellants.

Although the theoretically most contemporary propellant for engines is, of course, hydrogen, nevertheless because of practical considerations it must be used in a compound with other elements, for example, boron or lithium. It is usually assumed that for many reasons boron suits this purpose better. In the case of rocket propellant, we should expect very high specific impulses during the interaction of boron hydride with fluorine oxide or water. Since boron hydride is a propellant which reacts with water, it is particularly explosive upon contact with moist air or traces of moisture [96].

It is interesting to compare the energy released by boron with the energy released by other propellants. In the burning of 1 m^3 of boron 32,075,475 kcal is given off; in the burning of the same amount of kerosene 8,419,400 kcal is released, and with the burning of the same amount of gasoline this figure is 7,031,000 kcal [96]. Boron-containing propellants have a heat release per 1 kg which is twice as great as the best hydrocarbon propellant. These propellants usually are obtained as a result of the reaction of lithium hydride with boron trifluoride or boron trichloride. As a result of such reactions, modified in any manner, we can obtain diborane B_2H_6, pentaborane B_5H_9, and decaborane $B_{10}H_{14}$.

§ 5. Lithium

Lithium is a silver-white metal and, like sodium and potassium, very soft. The physical properties of lithium are presented in Table 8. For comparison, the properties of other alkali metals - sodium, potassium, rubidium, cesium - are also presented [12, 52, 96, 97].

Table 8. Basic physical properties of alkali metals.

Parameter	Li	Na	K	Rb	Cs
Atomic number	3	11	19	37	55
Atomic weight	6.939	22.99	39.096	85.47	132.905
Atomic radius, Å	1.56	1.86	2.23	2.43	2.62
Ionic radius, Å	0.60	0.95	1.33	1.48	1.69
$T_{пл}$, °C	179.0	97.9	63.7	38.5	28.5
$T_{кип}$, °C	1317	883	760	688	705
Specific heat capacity, cal/g·deg at 20°C	0.84	0.288	0.177	0.0913	0.060
Latent heat of fusion, cal/g	158	27.05	14.6	6.1	3.766
Latent heat of evaporation, cal/g	4680	1005	496	212	146
Density at 20°C, g/cm^3	0.534	0.971	0.862	1.532	1.903
Coefficient of linear expansion from 0 to 100°C, $10^{-6} \cdot deg^{-1}$	56.0	71.0	84.0	90.0	97.0

Lithium belongs to the group of metals which are most active chemically. The chemical activity of alkali metals increases from lithium to cesium. During combustion lithium gives the oxide LiO_2, which is a stable compound. However, it easily reacts with water and carbon dioxide. Only one lithium peroxide is known, that having the composition Li_2O_2. Below are presented the physical properties of lithium oxides:

	Li_2O	Li_2O_2
Density, g/cm^3	2.013	2.297
$T_{пл}$, $°C$	1427	425
$T_{кип}$, $°C$	1427	–
Heat of formation, kcal/mole	–142.4	–151.7
Heat capacity, kcal/mole	0.024	–

As an extremely active metal, lithium decomposes water and is capable of forming chemical compounds with nitrogen, carbon, sulfur, phosphorus, hydrogen, etc. The hydrogen compound of lithium – LiH hydride – is a solid white crystalline mass which forms with a flash and has a density of 0.775 g/cm^3. This compound melts at $688°C$ and at this temperature has a vapor pressure of 27 mm Hg. The formation of crystalline LiH occurs with heat release (21.59 kcal/mole).

Lithium hydride is very reactive. It easily reduces oxides, chlorides, and sulfides.

Deal and Svec [98] studied the manometric method of oxidation under the effect of water vapor at a pressure of 22-25 mm Hg in the temperature range 45-75°C. The oxide layer consisted of LiOH. Oxidation rate was subject to logarithmetic law:

$$\Delta x = k \log (1 + 0.43t),$$ (I.13)

where t is time, hours; k is the oxidation rate constant.

In the studied range the rate constant remained independent
of the water vapor pressure. The activation energy of the
reaction was ~6 kcal/mole. An X-ray study did not clarify the
crystalline nature of LiOH forming in the initial stage of the
interaction.

According to the data of Asman (cited in [99]), in the
formation of solid solution of Li-Al the solubility of lithium
in aluminum is 3.5% at the melting point of aluminum and 2.2%
at room temperature. The effect of small amounts of lithium
on the physical properties of aluminum or alloys enriched with
it is very similar to that which occurs with magnesium. However,
in view of the lower equivalent weight of lithium for achieving
the same effect with respect to the physical properties of the
alloy, lithium is added in smaller quantities than magnesium.
Lithium with aluminum forms the compound Li_2Al_3, which melts
at 598°C [99, 100].

§ 6. Magnesium

Magnesium crystallizes in a hexagonal lattice (a = 3.2 $\overset{o}{A}$,
c = 5.2 $\overset{o}{A}$); there are no allotropic transformations. The
principal physical constants of magnesium are presented below:

Atomic weight	24.312
Density, g/cm^3	1.74(20°C)
$T_{пл}$, °C	651
$T_{кип}$, °C	1103
Latent heat of fusion, cal/g	82.2
Latent heat of evaporation, cal/g	1337
Specific heat capacity, $cal \cdot g^{-1} \cdot deg^{-1}$	0.25(20°C)
Heat conductivity, $cal \cdot cm^{-1} \cdot s^{-1} \cdot deg^{-1}$	0.376(0-100°C)
	0.35(101-250°C)
Coefficient of linear expansion, $10^{-6} \cdot deg^{-1}$	27.3(0-160°C)
	39.6(455-600°C)

The boiling point of magnesium in vacuum (1 mm Hg) is 604°C. Noticeable evaporation of magnesium begins around 600°C; for the variation in vapor pressure of solid magnesium with temperature the following relation is found:

$$\log p = -\frac{7400}{T} + 2.5 \log T + 3.27. \tag{1.14}$$

The vapor pressure of magnesium above its melting point has the following value [16, 101]:

T, °C	750	800	850	900	950	1000
Vapor pressure of magnesium, mm Hg	12	26	49	94	166	280

The electric conductivity of magnesium is 38.6% of the electric conductivity of copper. With recalculation, taking into account density, it is found that with the same weight magnesium has an electric conductivity which is almost twice as great as the electric conductivity of copper (197%). The electric conductivity of magnesium is $23.2 \cdot 10^4 \ \Omega^{-1} \cdot cm^{-1}$ at 0°C and $8.41 \cdot 10^4 \ \Omega^{-1} \cdot cm^{-1}$ at 400°C.

The oxidation of magnesium to MgO occurs with the release of a considerable amount of heat (145.76 kcal/mole), which is the reason for the high strength of this compound which is very stable during heating to high temperatures. The variation in density of magnesium oxide as a function of the annealing temperature indicates the complex phenomena of polymerization which occur at this time. The density of magnesium oxide after annealing at 350°C is 3.1932 g/cm^3, and after melting in an electric furnace is 3.654 g/cm^3, while ordinary commercial magnesium oxide has a density of 3.07-3.2 g/cm^3.

The melting point of MgO is 2800°C; above this temperature severe evaporation of magnesium oxide is observed. The boiling point of MgO, determined in inert gas [16], lies around 3600°C. The heat of fusion for MgO is 300 kcal/mole.

41

At 1900°C magnesium in vacuum dissociates with the sublimation of metallic magnesium.

With respect to the problem of reducing magnesium oxide with carbon, we can take the following three assumptions as a basis:

1) the reaction $MgO + C \rightleftarrows Mg + CO$ at very high temperatures moves to the right, and at low temperatures in the opposite direction;

2) the reduction of magnesium oxide with carbon at 1950°C occurs very slowly and becomes noticeable at 2030°C;

3) magnesium oxide is reduced more vigorously by carbides than by pure carbon [52].

At 2200°C in a finely pulverized mixture of magnesium oxide with carbon, mixed in a stoichiometric ratio, up to 80% of the oxide is reduced to magnesium which evaporates.

In dry air or oxygen there is formed on the magnesium the ordinary oxide MgO with a cubic lattice (a = 4.2 Å). The thickness of the oxide film forming in the first stage can reach 70 Å [102], but the presence of mineral oil reduces the oxidation rate.

At high temperatures not exceeding 450°C, in dry oxygen and at temperatures below 380°C in moist oxygen the oxide film preserves for a long time (at least up to 300 hours) its protective capacity, ensuring an approximately parabolic oxidation rate [7, 103]. The thickening of the film at high temperatures leads to a loss of its protective capacity, due to which the oxidation proceeds according to linear law. As established

42

by Leontis and Rhines [104], in the range 475-575°C the constants
of the linear oxidation of magnesium and oxygen (p = 1 atm)
are characterized by the following equation

$$N = 1.7 \cdot 10^{6} \exp(-36\,500/RT), \quad g/cm^{2} \cdot s, \qquad (I.15)$$

For oxidation in air at 400-600°C Nakolkin [105] obtained the
following equation also:

$$N = 0.11 \exp(-23\,700/RT), \quad g/cm^{2} \cdot s. \qquad (I.16)$$

Although the empirical values of activation energy differ
considerably, the actual oxidation rate remains almost constant
in the temperature range covered.

The effect of such elements as nickel, bismuth, zinc, silver,
copper, tin, lead, antimony, indium, aluminum and cobalt on the
ignition of solid magnesium in dry oxygen was studied by Fassell,
Gulbransen, Lewis, and Hamilton [106]. In a concentration up
to several percent all these metals reduce the ignition temperature.
For example, aluminum (16.7%) lowers the ignition temperature
from 623° to 503°C at atmospheric oxygen pressure. On the basis
of their experiments, the authors have made the assumption that
the ignition temperature must be inversely proportional to the
(linear) oxidation rate of magnesium alloys.

Beryllium in small concentrations (0.002%) quite effectively
increases the ignition temperature of magnesium in air [107, 108].
This effect is due to the formation of a protective film. As
shown on the basis of spectrographic studies by Keil [109],
at first the beryllium is largely oxidized and because of this
the volume ratio increases. Furthermore, very small additions
of beryllium reduce the oxidation rate very effectively for
magnesium alloys with aluminum [110, 111].

43

The oxidation of magnesium under the effect of water vapor at a pressure of 31-208 mm Hg and temperatures of 425-575°C was studied by Svec and Gib's [112]. It was found that the oxidation rate changes linearly and that under all conditions the only oxide which forms is MgO. These peculiarities are determined by the high vapor pressure of magnesium at temperatures above 500°C and the porosity of magnesium oxide. At 425-500°C in the entire pressure range studied, the reaction develops on the metal surface itself or directly by it.

It is interesting to note that the oxidation rate of magnesium in moist oxygen, as established by Teresh [8], is less by a factor of 2 than in an air atmosphere. This can be attributed to the formation of hydroxide which has a large volume ratio as compared with magnesium oxide MgO although Gibbs and Svec [112] do not name magnesium hydroxide among the products of oxidation under the action of water vapor.

The critical magnesium ignition temperature remains approximately the same (∿625°C) both in water vapor and in hydrogen peroxide. The same thing applies to magnesium with various aluminum additives [110].

CHAPTER II

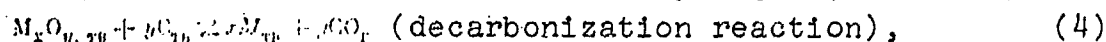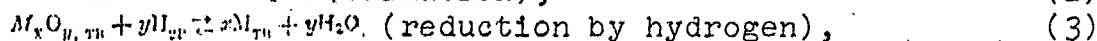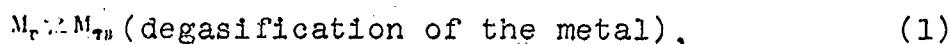## METHODS OF STUDYING THE BURNING AND IGNITION OF METALS

To study the burning and ignition of metals a wide range of physical and chemical methods are used: determining the brightness of the particle track using photographic or photoelectric instruments; performing spectroscopic analysis of the flame; effecting mass spectrometric, chemical, and X-ray analysis of the combustion products; determining the degree of burn-up according to the electrical resistance of strips and rods; making visual observations; filming the burning process with ordinary and shadow photography; using rapid extinguishment; performing studies with optical or electron microscopes; etc. Because of the high exothermicity and, consequently, the high burning temperature of metals, the considerable burning rate (up to several tens of centimeters per second), the accumulation of condensed combustion products on the burning surface, conditions are very unfavorable for an experiment in which elements of the burning process itself are studied.

Since powdered metals have become widely used in modern rocketry, from the practical and theoretical point of view, the best information can be obtained by studying the burning of metal products. At the present time, a number of experimental methods have been developed which enable us to determine the effect of the metal particle size, the heating rate of the particles,

and the composition of the ambient medium on the ignition delay time and the burning rate of the metal particles.

§ 1.   Methods for Studying the Low-Temperature Oxidation of Metals

For metals used in solid propellants, high reactivity is characteristic. Under normal conditions, the surface of the metal is protected by a layer of oxide. The combustibility of the metals and the conditions which lead to ignition, to a considerable extent, are determined by the nature of this oxide. The most comprehensive research in this area has been performed by Gulbransen [7]. Five reactions are basic in a study of the low-temperature oxidation of metal.

$$M_\Gamma \rightleftarrows M_{TB} \text{ (degasification of the metal)}, \tag{1}$$
$$xM_{TB} + yO_\Gamma \rightleftarrows M_xO_y{}_{TB} \text{ (oxidation)}, \tag{2}$$
$$M_xO_{y,TB} + yH_{2\Gamma} \rightleftarrows xM_{TB} + yH_2O \text{ (reduction by hydrogen)}, \tag{3}$$
$$M_xO_{y,TB} + yC_{\Gamma} \rightleftarrows xM_{TB} + yCO_\Gamma \text{ (decarbonization reaction)}, \tag{4}$$
$$M_xO_{y,TB} \rightleftarrows M_xO_{y,\Gamma} \text{ (evaporation)}. \tag{5}$$

In the above equations M is metal; M_{TB} and M_Γ are the solid and gaseous states of the substance. The formation rate of the oxide film is generally determined by the reaction (2). The presence or absence of gas in the metal can not only affect the oxidation rate but can also be a problem during measurement. This gas can be removed by heating the metal in a high vacuum according to reaction (1). The oxidation of metals or alloys free of oxide film can be studied if the metal oxides can be reduced in reaction (3) with hydrogen or removed by decarbonization (reaction 4). Reaction (5) makes it possible to judge the volatility of the oxide.

Generally the three methods which are the most useful in studying the kinetic regularities of the formation of the thin oxide film are the following: the polarimetric method, the

46

differential pressure method developed by Cambell and Thomas [113], and the method of measuring the weight of the specimen during oxidation on sensitive quartz microscales placed in the vacuum system. The last method enables us to carry out a continuous study of the process of metal oxidation in a wide temperature and pressure range. The diagram of the installation presented in reference [7] is shown on Fig. 15. Variation in specimen weight during oxidation is recorded with a micrometric optical tube. Preparation for the test includes the creation of a pressure of 10^{-6} mm Hg, degasification of the system, and the reduction of the initial oxide film by hydrogen or carbon. The scales, along with a heater in the form of a tube, are placed in a closed glass vessel. The accuracy of weight measurement is 0.3×10^{-6} g with very low sensitivity to pressure and temperature variation.

The instrument can be filled with any gas at a pressure below 1 atm. The heating coil must be noninductive; the inner part of the heater was made in the form of a heavy block of stainless steel fully covering the lower part of the experimental tube. All operations, for example, degasification and reduction of the initial oxide film, were performed directly on the scales. Specimens were prepared from thin metal plates approximately 0.13 mm thick for substances with a density of 7-9 g/cm^3 and 0.26 mm thick for lighter materials. The plates weighing 0.684 g had a surface within 10-12 cm^2. Using this method, Gulbransen studied the oxidation of molybdenum, tungsten, iron, aluminum, and magnesium at 400°C. The oxygen pressure in the experiment was usually 76 mm Hg, except for the experiments with magnesium where oxygen pressure was 20 mm Hg. A detailed description of the installation, operation, and preparation of the high-sensitivity scale can be found in the monograph [114].
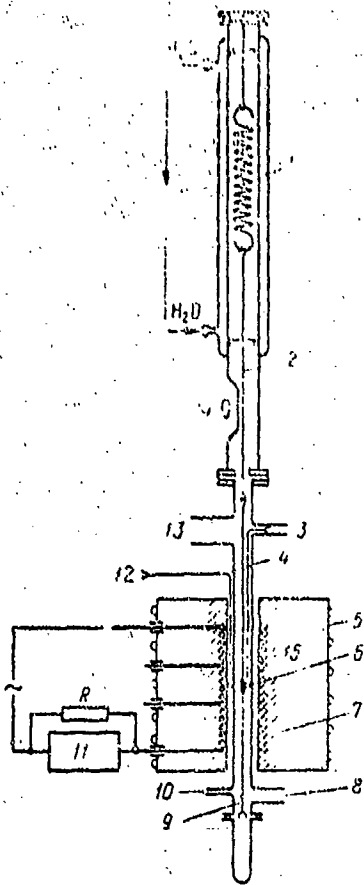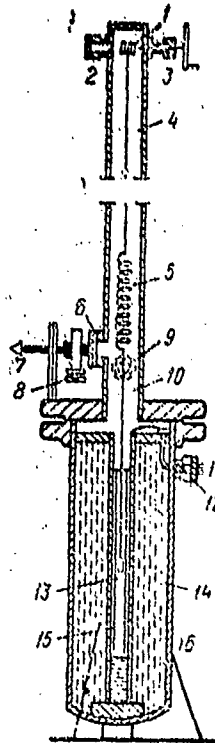
7

Fig. 15.   Fig. 16.

Fig. 15. Installation for studying the oxidation of metals by the weight method. 1 - Quartz spring; 2 - quartz filament; 3 - thermocouple contacts; 4 - platinum filament; 5 - water cooling; 6 - specimen; 7 - electric heater; 8 - inlet for oxidizing reagents; 9 - platinum filaments; 10 - inlet for neutral gases; 11 - specimen heat regulator; 12 - thermocouple contacts; 13 - outlet to diffusion pump; 14 - cathetometer; 15 - insulator of pressed MgO powder.

Fig. 16. Installation for a per-weight determination of oxidation rate at an oxygen pressure below 40 atm. 1 - Drum; 2 - opening for installing and moving drum; 3 - lift mechanism; 4 - gold chain; 5 - quartz spring; 6 - observation port; 7 - microscope; 8 - cathetometer; 9 - opening for introducing the specimen to the heater; 10 - platinum-rhodium wire; 11 - electric and thermocouple contacts; 12 - gland; 13 - specimen; 14 - heat insulation; 15 - heater; 16 - steel hermetically sealed casing.

Dignam and colleagues [115] studied the growth of the
amorphous oxidized film in the 454-601°C range for a specimen of
ultrapure aluminum whose surface was obtained by electrolytic
polishing with the aid of a microbalance (see Fig. 15). The
installation generally consists of a vacuum microbalance with
automatic recording and a heating of quartz tubing attached to
the basic system with metal rings. The specimen, suspended in
the balance with platinum wire, can be introduced to the heater zone
at any moment. The vacuum system consisting of three pumps - an
oil pump, diffusion pump, and rotation pump - enabled us to
obtain a pressure of 10^{-6} mm Hg. Temperature was measured by
a thermocouple within 0.1°C. The reading of the sensitive
scale of the balance $100 \cdot 10^{-6}$ could be performed within 10^{-6} g.
A difference in weight up to 5 mg between the two arms of the
balance could be compensated by changing the tension of the
torsion wire on which the rocker of the balance was suspended.
This made it possible to take measurements according to the
most sensitive scale during the entire experiment. Gas of the
necessary composition was introduced through a system of valves.
For a low-temperature study of metal oxidation at high pressures
the installation of Mac Kuen and Fassell [116, 117] can be used
(Fig. 16) for a per-weight determination of oxidation rate at
oxygen pressure up to 40 atm. A heater with a michrome winding
is mounted inside a steel hermetically sealed casing with a
flange at the top. Contact for the thermocouple and the electric
current is made through gland 12. The specimen 13 is suspended
on a quartz hook attacked to a suspension of platinum-rhodium
wire, which is connected with a quartz spring 5 and a gold chain 4.
The specimen is raised and lowered with a hand wheel. On the
shaft of this wheel, which passes through gland 3, inside the
installation is mounted a drum of stainless steel 1, on which
a gold chain is wound. If the step of the winding on the drum
is identical to the step of the screw at the end of the gland,
during the lifting and lowering of the specimen and the suspension
there will be no horizontal displacement. The specimen is

49

introduced to the heater and removed from it through opening 9.
The extension of the quartz spring during specimen oxidation is
determined with the microscope 7 and the cathetometer 8, which
are rigidly mounted on the casing of the heater, through observa-
tion port 6. The heater is connected with a vacuum pump and
a source of oxygen supply, which was dried by activated aluminum
oxide. Pressure below atmospheric was measured by a mercury
pressure gauge; pressure above atmospheric was measured by a
pressure gauge with an arrow.

In the latter version of this installation the heater was
charged from below and the leads for the thermocouple and the
power supply were connected to special small fixtures.

At a pressure somewhat above 20 atm serious difficulties
are encountered with the heat insulation, apparently because of
the increasing thermal conductivity of the oxygen. At a pressure
around 40 atm it is important to provide external water cooling
for the heater casing.

Boggio and Plumb [118] used the method of measuring the
rate of increase in the aluminum oxide film at room temperature,
based on the relationship between film thickness and the
reflectivity of the surface. Aluminum films were obtained by
evaporating aluminum in a high-vacuum system at a pressure of
10^{-8} mm Hg, which had an optical window for observing the
scattering of rays at 80°. This method made it possible to
obtain a film of aluminum with minimum porosity and roughness.
The ellipticity and slope of the ellipsoid during the reflection
of linearly polarized light with a wavelength of 5461 Å from the
metal film were measured. The optical constants of pure aluminum
at a pressure of 10^{-9} torr were determined beforehand. Oxidation
occurred in a dry air atmosphere in the pressure range

50

6×10^{-6} – 337 torr. The thickness and optical properties of the film can be calculated from the ellipticity of the deviation of reflected light [119] on the assumption that the film which is forming has a uniform structure. Optical methods for the high-temperature oxidation of metals were used in references [120, 121]. Smeltzer [112] studied the oxidation of aluminum in the range 400-600°C using Gulbransen's method [7]. The specimens before testing were carefully degased in a vacuum of 10^{-6} torr at room temperature for 5 hours and then at 500°C for 30 minutes. Aluminum containing only about 0.002% impurities can be obtained with this method. The formation of a film of aluminum oxide was studied as a function of time and temperature at an oxygen pressure of 76 mm Hg. This pressure was selected because the oxidation rate, in this case, does not depend on pressure [7].

In the first series of tests, before the oxygen was fed to the system, the specimens were hardened in vacuum for 3 minutes at 500°C; in the second series of tests this was done at 600°C for an hour.

Cochran and Sleppy [123] studied the oxidation of chemically polished high-purity aluminum and aluminum-magnesium alloy (97.5/2.5) in dry oxygen, water vapor, and moist air in the range 450-640°C. The following two methods were used; the first – a recording of the weight variation in the sample on the self-recording microbalance [123]; the second – the recording of the oxygen pressure variation during the oxidation of the metal with constant volume [113]. The microbalance method is the same, in principle, as the above method if we do not take into account the automatic recording of the measurement process. We shall pause briefly on the second method.
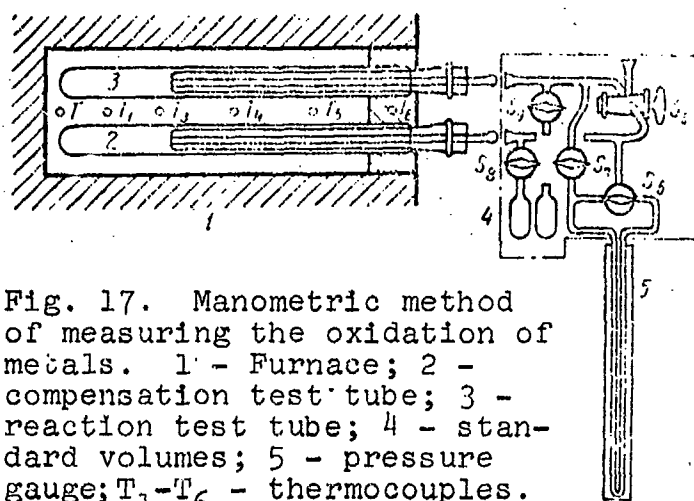
Fig. 17. Manometric method
of measuring the oxidation of
metals. 1 - Furnace; 2 -
compensation test tube; 3 -
reaction test tube; 4 - stan-
dard volumes; 5 - pressure
gauge; T_1-T_6 - thermocouples.

The manometric apparatus is presented in Fig. 17. Two
identical quartz test tubes were mounted inside an electric
furnace. One of the tubes contained a sample of the metal;
the other was used to compensate the pressure variation which
resulted from the temperature variation of the furnace. An
oil pressure gauge located at a 60° angle to horizontal was
used to measure pressure. In the test tube, after air removal
and degasification, 200 mm^3 of dry oxygen was fed through the
valve S_5; then the valve was rapidly shut off. The test lasted
100 minutes. During the experiment the temperature of the
furnace was kept constant within ±1°C. The nonuniformity in
specimen heating, which was due to the fact that part of the
test tube projected from the furnace, did not exceed ±7°C.
The system has the capability of measuring gas pressure by a
mercury pressure gauge at the moment of oxygen admission since
it can be assumed that it is exactly in this initial period
that vigorous oxidation of the exposed surface of aluminum or
its alloy occurs. However, the first tests indicated that this
was not so. In our opinion, the latter method is considerably
inferior in sensitivity to the method of the vacuum microbalance,
but has enviable simplicity and the possibility of performing
studies at high temperatures (up to 1500°C). In reference [58]

Sleppy studied the oxidation of melted aluminum at 660-850°C in a dry oxygen atmosphere, using the method described above but introducing certain variations of his own.

The essential change was to add standard volumes with a capacity of 8.3 ml. Before a test the standard volumes were filled with dry oxygen at atmospheric pressure, while the remaining system underwent degasification for several hours. After the furnace was heated to a certain temperature and thermal equilibrium was achieved, valves S_7 and S_9 were closed and S_8 was opened, as a result of which the oxygen filled the control (compensation) test tube and both arms of the differential oil pressure gauge. Then valve S_6 was turned so as to disconnect the reaction and control volumes and the corresponding arms of the pressure gauge from each other. The beginning of the oxidation reaction was considered to be the moment that valve S_7 opened, when the oxygen from the second standard volume was fed to the reaction test tube. The recording of differences in the levels in the arms of the pressure gauge was done by periodically opening the valve S_5. It is recommended that this procedure be accomplished with the maximum possible speed.

It was rather simple to process the obtained results. The amount of oxygen which had reacted with the metal is proportional to the change in specimen weight due to the formation of the oxide film and can be found from the following equation:

$$\Delta W = K_1 h (1 + K_2),$$

(II.1)

where

$$K_1 = 37,7 \left[\sum_i \frac{V_i}{T_i} \right] \rho,$$

$$K_2 = \frac{1,36 \cdot r^2 P_0}{T_1 \left[\sum_i \frac{V_i}{T_i} \right] \rho};$$

53

here ρ is the oil density of the pressure gauge, g/ml; P_0 is the gas pressure, mm Hg; r is the radius of the capillary of the pressure gauge, cm; ΔW is the weight of the reacted oxygen, µg; h is the reading of the difference in the oil levels in the pressure gauge, mm Hg; T_i is the temperature of the furnace, °K; V_i is the volume of the test tube when (ml) at temperature T_i; T_1 is the temperature of the supply pipe outside the electric furnace.

The first term in equation (II.1) takes into account the oxygen pressure variation during the formation of the oxide film; the second introduces the corrections which occur due to the rising and lowering of the oil in the arms of the pressure gauge and the nonuniformities of the change in volume of the test tubes themselves during a temperature increase.

The sum $\sum_i (V_i/T_i)$ was evaluated by two methods: the volumes were directly measured as a function of temperature along the test tubes or the pressure P_0 was measured and the sum $\sum_i (V_i/T_i)$ was found from expression

$$ R N_0 = \frac{P_c V_c}{T_1} = P_0 \sum \frac{V_i}{T_i}, \qquad (II.2) $$

where N_0 is the initial number of moles of oxygen in the standard volume; V_c is the volume of the standard vessel (ml) connected with the reaction test tubes; P_c is the pressure of N_0 moles of oxygen (mm Hg) enclosed in the volume of the reaction test tube and the standard vessel; R is the gas constant.

Usually at a temperature of 600°C, $K_1 = 2.03$ and $K_2 = 0.746$. In developing a method for studying low-temperature oxidation of metals by recording the variation in oxygen content in a closed volume, the reaction test tube should usually be connected with a large tank. The pressure variation in the installation is recorded better with a capillary tube into which a drop of mercury or diethyl phthalate is introduced [124]. All equipment

must be thermostatic. This method is preferred when studying the reaction of metals with pure gases.

The reaction capacity of the specimens can also be judged by determining, with the use of gas chromatography, the oxygen content before and after a test. In this version it is not necessary to use a pressure gauge because it will introduce error into the measurement because of the change in volume during the test [125].

If reaction products form in a gaseous state, the kinetics of the reaction rate are determined by the change in the diameter of the metal specimen with the use of a cathetometer. This method was used successfully in a study of the oxidation of tungsten up to 3000°C [126, 127].

The following methods can also be used in studying high-temperature oxidation of metals: measurement of the decrease in electric conductivity due to the change in the cross section of the metal during oxidation; measurement of the electric potential of the oxide film; chemical analysis of the specimen after tests; etc. [128].

Quartz or ceramic tubes are usually used as the reaction vessels. Quartz is used up to 1500-1600°C; corundum is used up to 1800-1900°C under the condition that heating and cooling of the reaction vessels are performed gradually. Materials from the oxides of magnesium, zirconium, and thorium can be used up to very high temperatures, 2500-3000°C, but should be carefully protected from abrupt variations in temperature. At low pressures and high temperatures, from the walls of the tubes there occurs an evaporation of oxides, for example, SiO and AlO, which leads to contamination of the studied specimens, and the presence of water vapor intensifies this process.

High-temperature furnaces can be heated by electric current, by the induction method, or by hot gases. A furnace whose heating element is a wire of nickel-chromium-aluminum (tantalum) alloy can be used in an air atmosphere up to 1300°C. If a platinum-rhodium (40% rhodium) wire is used, the temperature range can be expanded to 1800°C [11], although at high temperatures such furnaces operate for a limited period of time because of the evaporatio of the heating element. A wire of $MoSi_2$ can be used in oxidizing atmospheres up to 1700°C.
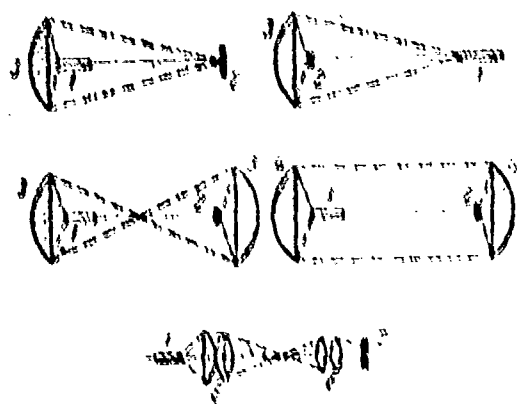

Fig. 18. Reverberatory arc furnaces. 1 - Arc; 2 - specimen; 3 - elliptical mirror; 4 - parabolic mirror; 5 - lenses.

Molybdenum or tungsten wire can be wound directly on a tube of Al_2O_3 and, under the condition that the heating element is protected from the oxygen atmosphere (usually they are placed in high vacuum or an inert atmosphere), such a heating device can be used up to 1800-1900°K. The same precautions should be taken if tantalum tubes or rods are used as heating elements because of tantalum's high affinity to oxygen [11].

High heating temperature can also be achieved using reverberatory arc furnaces [18, 116, 117]. In a reverberatory arc furnace the image of the sources, usually a carbon arc, is focused on the surface of the specimen, as shown in Fig. 18. With this method temperatures of 1400-1600°C are achieved, and the maximum possible temperatures which can be obtained lie in the range 3200-3700°C [22, 23].

Any reactions or contaminations of the metal specimen during the heating period (several milliseconds) can be disregarded since the reaction chamber itself does not become significantly heated. There is only one substantial disadvantage in these systems - the impossibility of accurate temperature control. Metal specimens can also be heated to very high temperatures 3000-4000°C by passing them through an electric current, but it is difficult to combine this method with thermogravimetric methods of measuring reaction rates.

In the above measurements, difficulties can arise in finding an inert material to which the specimen can be attached. The high-melting oxides Al_2O_3, AgO, ThO_2, ZrO_2, etc., can usually be used with success for this purpose. Sometimes a wire suspension device from the same material as the specimen is used, but, in this case, it is necessary to make corrections in the measurements.

At very high temperatures it can also be a problem to measure the temperature itself. Iridium-rhodium thermocouples can be used in an oxidizing atmosphere at higher temperatures than platinum-rhodium thermocouples. Thermocouples of heat-resistant metals or alloys, for example, tungsten-rhenium, can be used up to 3000-3500°C [11, 35].

Of the optical methods for measuring temperature, the most frequently used is the color method, which makes it possible to avoid, in the measurements during the test, errors connected with the change in the emission factor $\varepsilon_{\lambda, T}$ of the metal specimen, the vapor condensation on the walls of the reaction chamber, etc., [33, 34].

§ 2. Gas Burners

Friedman and Macek [129] studied the ignition and burning of single particles of aluminum with a diameter of 15-67 μm in a burning mixture with a known gas composition and maximum temperature. The flame at atmospheric pressure was stabilized in the form of a plane burning front with the use of a burner designed by Bota and Spaulding [130], the advantage of which is the water-cooled bronze disk with openings of approximately 5-10 μm. This burner makes it possible to obtain two-dimensional flames of burning mixtures with high burning rates. It was designed to measure burning rates but can also be used in spectroscopic flame studies. The advantage this burner has over others includes a narrow reaction zone (on the order of fractions of a millimeter at atmospheric pressure), which makes it possible to obtain a rather extended zone of several centimeters with constant gas composition and temperature. The installation diagram for studying the burning of metal particles in a gas burner is presented in Fig. 19. Aluminum particles of different dimensions were introduced into the two-dimensional flame along the central axis of the tongue, with the use of tubes, 250 μm in diameter, located in the center of the disk. In the central chamber the metal particles were moved with nitrogen or helium, which was used as the particle carrier. With the proper regulation of the gas flow it could be arranged that only single particles entered the tongue of the flame. Depending on the desired final temperature, propane was burned with an excess or deficiency of oxygen and was also diluted with nitrogen or helium (the test results, as the authors indicate, do not depend on the nature of the inert gas). The gas rate was controlled in such a manner that the chemical reactions of the gaseous propellant were completed several millimeters from the burner outlet. This was completely acceptable since the particles, depending on diameter, ignited at a distance of 10-150 mm. The burning rate was on the order of 10 m/s and was determined either according to the known gas flow

58

rate or by photographing the trajectories of the periodically
exposed particles. In the latter case, the particles must be
so small that they can move along with the gas flow, but then
the intensity of the light reflected by them will be a complex
function of particle size and position with respect to the light
source and the optical system. It is best to place the light source
approximately opposite the camera. In this case, the intensity
of the scattered light, controlled by the camera, will be maximum.
The best light source is either a flash of magnesium in conjunction
with a rapidly rotating sector or a controlled spark system.
As particles, it is recommended to use magnesium oxide particles
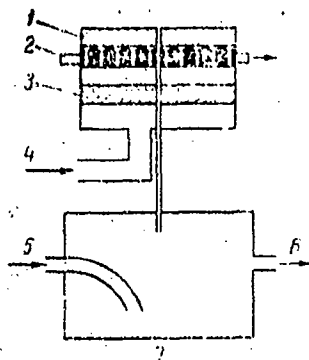[131, 132].

Fig. 19. Installation for studying the
burning of metal particles in a gas
burner. 1 - Two-dimensional flame;
2 - water cooling; 3 - arrestor to
prevent passage of flames; 4 - burning
mixture; 5, 6 - inlet and outlet for
the gas which creates a cloud of metal
particles in the chamber; 7 - chamber.

The adiabatic temperature of the flame of a propane-oxygen-
hydrogen mixture at atmospheric pressure and an initial temper-
ature of 300°C was calculated on an electronic computer taking
into account all possible dissociative processes of the combus-
tion products. The adiabatic temperature as a function of
composition is presented in Fig. 20. As is apparent from this
figure, in the installation developed by Friedman and Macek [133],
the temperature and composition of the gas can be changed within
a relatively wide range. We should also note that the actual
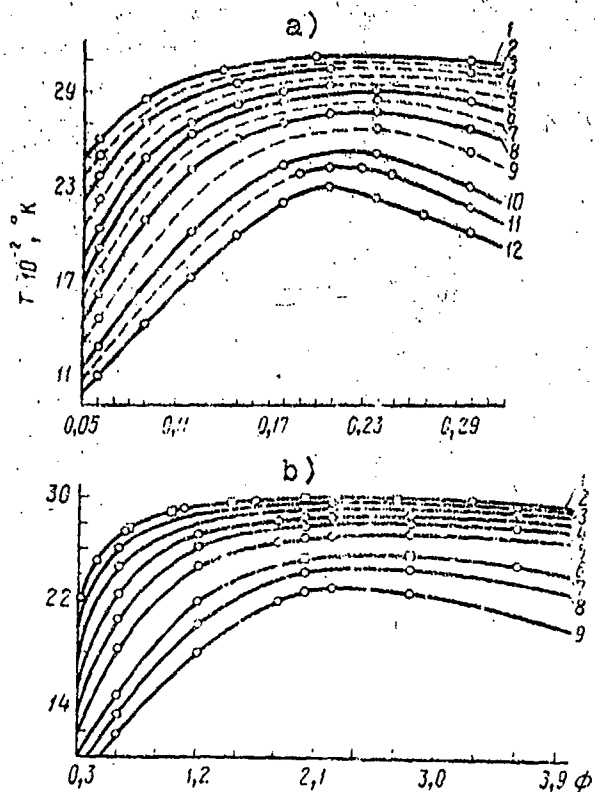temperature was 30-40°C lower.

Fig. 20. Flame temperature as a function of component ratio for the following mixtures. a) Propane-oxygen-hydrogen: 1 - x = 1.00; 2 - 0.87; 3 - 0.77; 4 - 0.67; 5 - 0.57; 6 - 0.51; 7 - 0.45; 8 - 0.39; 9 - 0.33; 10 - 0.27; 11 - 0.24; 12 - 0.21; b) oxygen-carbon monoxide: 1 - 1.00; 2 - 0.85; 3 - 0.70; 4 - 0.56; 5 - 0.46; 6 - 0.36; 7 - 0.26; 8 - 0.22; 9 - 0.18; $x = O_2/N_2 + O_2$ - the degree of mixture dilution $\Phi = C_3H_8(CO)/O_2$ - ratio between fuel and oxidizer.

The combustion products of a propane-oxygen-nitrogen mixture contain a relative large amount (18%) of water vapor; this percentage can vary only within 14-18% depending on the ratio of components. For the purpose of evaluating the effect of water vapor on the burning of aluminum particles, a burning mixture of CO_2-O_2-N_2 was used [133-135]. To stabilize the two-dimensional flame a certain amount of oxygen had to be added to this mixture, and this led to the appearance of ∿0.5% water vapor in the combustion products. The adiabatic temperature of a flame of carbon monoxide as a function of the component ratio is presented in Fig. 20.

60

Table 9. Physical and chemical characteristics of propellant-air flames.

Propellant	Molec-ular weight	Density, kg/m³	Mole fraction during stoi-chiometry with atmospheric oxygen	Adiabatic burning temperature, °K
Acetone	58	0.782	0.0497	2122
Acetylene	26	0.621	0.0772	-
Ammonia	17	0.817	0.2181	-
Benzene	78	0.885	0.0271	2306
Butane	58	0.584	0.0312	2.56
Carbon monoxide	28	-	0.2950	-
Ethylene	28	-	0.0652	2375
Methane	16	-	0.0947	2236
Propane	44	0.508	0.0402	2250
Propylene	42	0.522	0.0444	2339
Propylene oxide	58	0.831	0.0497	2317
Toluene	92	0.872	-	2344

In most cases, the temperature which can be achieved in the combustion products of a burning mixture is determined by calculation on the basis of thermochemical data. The theoretical flame temperature can be achieved if there is no heat removal due to thermal conductivity and radiation. As indicated by temperature measurements according to the height of the flame's tongue, using optical methods and thermocouples, maximum temperature is reached only in the center of rather large homogeneous flames. Certain characteristic values for calculated (adiabatic) temperatures and the composition of the gases for frequently encountered flames are presented in Table 9.

To determine the ignition temperature of particles of aluminum, magnesium, and a 50/50 aluminum-magnesium alloy, Cassel and Leibman [136] used a heater 65 cm long with an inner diameter of 2.7 cm and a zone 35 cm long which could be uniformly heated

to 1700°K. The temperature inside the heater was measured by a platinum-platinum-rhodium thermocouple within ±2.5°. The size of the particles introduced into the hot zone of a vertically arranged heater with the use of a water-cooled tube was measured by the change in the flow rate of the gas (measured by a rotameter) which was used as the carrier. The separation of particles according to their diameters could be done with this method within ±15%. The metal particles were kept almost motionless in the hot zone of the heater by a flow of dry air or oxygen, heated beforehand, which was used as the oxidizer. To determine particle size and concentration, microscope slides were introduced into the flow leaving the heater. Ignition was observed through a port in the bottom of the heater.

In the work of Fassell and colleagues [137], burners of various types (Fig. 21) were used for burning alloy and metal powders. A burner of the first type A was used to determine the burning time with a high-speed movie camera capable of a frame speed of 3000-8000 frames/s. Metal particles were introduced into the flame by the movement of a piston and the flow of oxygen fed through the tube.

In the burner of the second type B, methane enriched with oxygen was used as the particle carrier. This burner was used for collecting the combustion products with glass or brass microscope slides located at different heights along the tongue of the flame in order to sample partially or completely burned particles.

Gordon [138] studied the burning of particles of magnesium, titanium, and aluminum on a burner of type C. A small amount of metal powder with a given particle size was introduced into a gas flow which carried the powder through a tube to the carrier flame. When the flame was ring-shaped, the particles ignited on the boundary of the carrier gas-flame and the burner generally
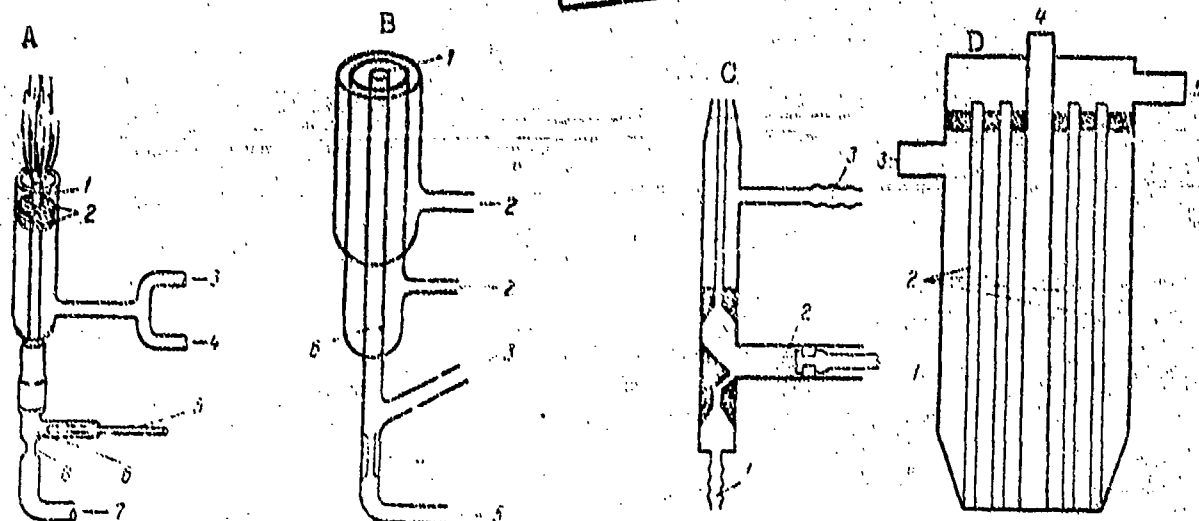
Fig. 21. Diagram of burners for studying the burning of powdered metals.

A. 1 - Stainless steel tube; 2 - reflector screens; 3 - gas; 4 - air; 5 - piston; 6 - metal powder; 7 - oxygen; 8 - capillary restriction to increase speed.

B. 1 - Zirconium tube; 2 - oxygen; 3 - metal powder feed; 4 - capillary; 5 - gas; 6 - connection of zirconium with glass.

C. 1 - Carrier gas; 2 - metal particles; 3 - burning mixture.

D. 1 - Burner housing; 2 - tubes for feeding oxidizers; 3 - propellant feed; 4 - tubes for introducing metal particles; 5 - oxidizer feed.

in an atmosphere of the carrier gas with a temperature of several hundred degrees. In the case of a continuous carrier flame (the so-called "closed center"), the burning of particles occurred in a medium with a temperature and composition identical to that of the flame. The change in the composition and temperature of the burning medium was regulated by the selection of the composition of the carrier gas and the dimensions and composition of the flame. Particles were classified using standard screens with the following approximate mesh dimensions: 420, 250, 150, 105, 62 and 44 μm. Also studied, but less extensively than pure metals and alloys, were boron, graphite, and several compounds of metals with nonmetals (carbides, nitrides, hydrides, borides).

Although the conditions of the experiment were far from definite, as the author notes, however, the visually observed character and duration of burning do not depend on the working parameters of the apparatus (dimensions of flame, carrier gas rate, particle concentration, purity and method of preparing powder) in a wide range of variations. For the most part, oxygen was used as the particle carrier in the study and the minimum ring-shaped methane-air carrier flame necessary for igniting the particles was used; the medium in which burning occurred was enriched with oxygen to a considerable extent.

The appearance on the photograph of ill-defined, indistinct tracks of burning metal particles was explained by Gordon as burning in vapor phase (diffusion flame), while the appearance of distinct tracks of considerable lengths (low burning rate) was attributed to surface reaction. However, in the work there is no mention made of the magnification or the depth of focus, which is important in interpreting the results.

We should mention two essential deficiencies of the above methods: the nonuniformity of the supply of metal particles and the impossibility of controlling their entry into the tongue of the flame.

We can consider the burner developed by Drew and colleagues [139] free of these disadvantages to a certain extent. This burner (D) consists of a set of closely spaced tubes through which oxygen is fed; the space between the tubes is occupied by the flow of fuel. As a result of the mixing, a flame is formed on the surface, whereupon the danger of its slippage is eliminated. The burner has a central tube for obtaining a small flame of previously mixed components whose entry is controlled separately. Spherical metal particles, 70 and 150 μm in diameter, are introduced through this same tube. Two mixtures of gas H_2/O_2 and CO/O_2 were used. Solid combustion products were collected in a cup located

under the flame of a burner turned downward. This burner position considerably facilitates the introduction of metal particles in the flame. Particles entered from a vibrating tray into a small funnel which directed them to the central tube and fell into the flame, while having a certain initial speed acquired during their fall downward aloɪ ⌐ the cylinder of the burner. Since this system does not depend on a gas flow for particle transfer, the flame can be regulated without affecting the flow rate of the particle as would otherwise occur. This circumstance proved to be especially favorable for studying the burning of large particles.
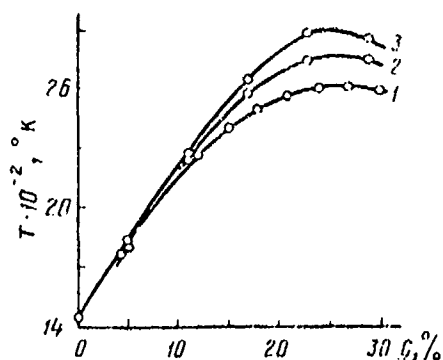

Fig. 22. The adiabatic temperature of the flame for the propellant APC-polyformaldehyde as a function of fuel content (C, %). 1 - 1 atm; 2 - 10 atm; 3 - 300 atm.

In a sufficiently hot and steady oxygen-hydrogen flame, spherical particles with a diameter up to 100 μm could be ignited without giving them significant additional velocity because of the gases of the flame; however, to ignite large particles a stronger flame was required.

Flames of gaseous propellant generally enable us to study the burning of metal particles only at atmospheric pressure since the stabilization of the flame at lower and, particularly, at higher pressure involves considerable difficulties. Therefore, at pressures above atmospheric, most authors use flames of solid propellant with oxidizers of potassium perchlorate or ammonium perchlorate and any fuel with a small amount 0.05-0.1% of the

powder of the studied metal added to this mixture. Figure 22 gives the calculated maximum adiabatic burning temperature as a function of the percentage ratio between the components of the ammonium perchlorate-polyformaldehyde mixture. As a rule, the powdered oxidizer-fuel components are carefully mixed and pressed in the form of a column 5-10 mm in diameter and 15-30 mm high. The specimen is burned in a constant-pressure bomb, which is a thick-walled steel cylinder with supplementary equalizing volumes and windows for various optical and spectral studies.

The authors of reference [129] put together a mixture of ammonium perchlorate, organic fuel, and approximately 0.1% aluminum powder of a certain size. Then the composition was pressed in the form of a cylinder 6.5 mm in diameter which surrounded the propellant without the addition of metal. A column 17 mm in diameter and 25 mm high was obtained. Trihydroxymethylene or a plastisol type of polyvinyl chloride was used as the fuel. All components of the propellant were in the form of a powder.

The combustion products of these mixtures contained approximately 40% water vapor, CO and CO_2 and partially oxygen in free form, whose maximum content, depending on the component ratio, could be reduced to approximately 9%.

§ 5. Methods of Studying the Burning
of Metal Strips and Rods

In view of the fact that it is not possible with contemporary methods to follow all stages of the burning of a metal particle with its relatively rapid motion in the tongue of the flame, much useful information can be obtained by studying the burning of strips, wires, or rods of metal in various gaseous media.

Garrison and Joffe [140] studied the burning of thin wires of aluminum, magnesium, iron, molybdenum, titanium, and zirconium.

In most cases, the wires were suspended within a brass chamber 23 cm in diameter and 38 cm high and ignited at the bottom so that the burning extended upward. Observations were made through side ports located along the length of the chamber. Burning was studied in an atmosphere of pure oxygen at various pressures or in an oxygen-nitrogen mixture at a pressure of 760 mm Hg. The burning rate was determined by photorecording. The color temperature was measured in the tests with two photoresistors which recorded the luminous radiation from the burning zone in wavelengths of 0.87 and 0.53 µm, respectively. The system was calibrated with a standard tungsten lamp and the tungsten radiation factor was taken from the work of DeVos [141].

Oxygen distribution in the burning zone was determined by the rapid hardening of the reaction products. For this purpose, thin wires were burned in a small chamber with a volume of 400 ml, which, at a certain moment, was connected with a vessel in which a vacuum of approximately 10^{-3} mm Hg was created. The diameter of the thin wires, depending on the metal studied, was taken within 0.1-1.5 mm.

It is usually a difficult task to ignite aluminum because of the presence of a stable oxide film Al_2O_3 on its surface. In several works, tungsten spirals wound around the lower end of a vertically positioned wire have been used for this purpose. A temperature reaching ~2500°C can be created in the local volume by passing current along this spiral.

To record the flame propagation rate along thin aluminum wires or rods, photoelectric sensors, sensitive to infrared radiation, can be successfully used since the flame from aluminum gives a considerable luminous flux in the long-wave region of the spectrum, which is only slightly absorbed by the rather dense cloud of submicron particles of Al_2O_3.
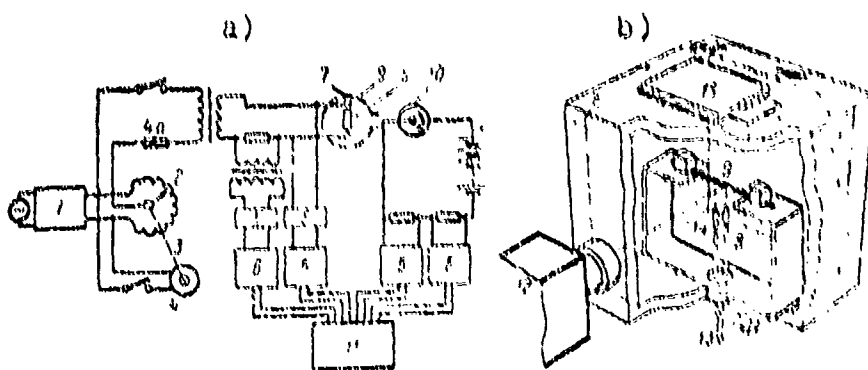
67

Fig. 23. Installation for studying the burning of metal strips.
a) Electric circuit; b) design of installation.
1 - Voltage regulator; 2 - continuously adjustable autotransformer;
3 - reducer; 4 - electric motor; 5 - rectifier; 6 - dc amplifier;
7 - experimental chamber; 8 - electrodes; 9 - specimen; 10 -
photocell; 11 - oscillograph; 12 - movie camera; 13 - gas inlet
tube; 14 - igniter; 15 - cover.

Coffin [142] studied the burning of magnesium strips for
the purpose of finding the general physical and chemical regular-
ities in the burning of magnesium. Tests were performed in a
transparent chamber (Fig. 23) in an atmosphere containing from
17 to 100% oxygen, where argon, nitrogen, helium, and argon-water
vapor were used as diluting agents. A magnesium strip 4.6 cm
long, 0.015-0.31 cm thick, and weighing 0.0074 g/cm was clamped
horizontally to a special support. No special methods for
removing magnesium oxide from the surface of the strips were used.
The magnesium was ignited in the middle of a strip from the
nichrome spiral. The burning process was monitored by a movie
camera with a frame speed of 16 frames per second.

Brzustowski and Glassman [143], to some extent, continued
the work of Coffin, whose purpose was to find the conditions
under which the vapor-phase mechanism of burning occurs. Experi-
ments were planned so that a more detailed study of the processes
occurring in flames could be conducted.

Under static conditions, aluminum and magnesium strips were burned in a closed chamber. The chamber was a vertical steel cylindrical vessel 300 mm high with an inner diameter of 250 mm. Four ports 25 mm in diameter were located uniformly along the radius at midheight of the combustion chamber. Two brass rods hermetically sealed into the base of the chamber served, at the same time, as holders for the specimen and the electrodes. A centimeter of magnesium strips 0.29 cm wide weighed 7.7 mg. Traces of sodium and manganese impurities were seen on the spectrograms obtained in the test. Aluminum was used in the form of a wire 0.89 mm in diameter, 1 cm of which weighed 17 mg. The aluminum was sufficiently pure and contained noticeable traces of only helium, copper, and sodium. The experimental specimens, as a rule, were from 8 to 10 cm long. Mixtures of oxygen and argon were used as the oxidizer. Experiments were performed with pressures below 32 atm and various mixture compositions from pure oxygen to pure argon.

During the experiment the gas in the chamber was motionless except for free convection current, caused at the beginning by the wire being heated and later by the flame. Pressure during the test increased by only 1-2%. Oxygen content in the chamber during all experiments was greater than necessary for complete combustion of the specimen.

The flames were photographed on a plate and spectrograms were taken at the same time with a 1.5-meter spectrograph with a diffraction grating. The range of first-order dispersion extended from 3700 to 7400 Å with a linear dispersion of approximately 15 Å in 1 mm. Exposures were made with a 60 μm slot for a duration of 1 to 5 s. The spectrograms were analyzed on an automatic photomicrodensitometer.

As Brzustowski and Glassman indicated, ignition is the first and a very important stage of the burning process. Effects connected with ignition have a substantial influence on the pattern of burning observed in the test, which also depends on the following characteristics of this experiment: attachment of the metal strip on the ends; burning, with the use of an internal heat source by the passage of an electric current, and cooling from the surface by convection and radiation; heat transfer to the electrodes on which the specimen is attached; temperature of the surrounding gas, which is approximately equal to room temperature during the entire burning period. All these factors must be taken into consideration when interpreting the results of observations. The specimens were ignited by electric current. To regulate voltage on the electrodes, a step-down transformer and a continuously adjustable autotransformer were used. Reproducible ignition was accomplished by slowly increasing voltage from zero while turning the knobs of the continuously adjustable autotransformer.

In the experiments with magnesium the rate of voltage increase was approximately 0.046 V/s. This rate was doubled in experiments with aluminum. In both cases, the middle of the specimen in a section approximately 1-1.5 cm long had uniform temperature. The specimen almost always ignited in approximately the middle between the electrodes.

At the moment of ignition there is a rather high current strength in the electric power supply: from 17 to 40 A for magnesium strips and from 37 to 72 A for aluminum wires. The power applied during ignition to the magnesium strip was 40 W; losses from thermal conductivity were approximately 16 W. This fact indicates that the thermal conductivity to the electrodes plays an important role in the experiment.

Tally [144] studied the burning of high-purity boron so that the effect of contamination on the burning rate could be evaluated in the simplest manner.

For this purpose, cylindrical rods of boron were prepared, which were brought by electric heating to a temperature above the melting point of boron in various gaseous media. These rods were prepared by the chemical deposition of boron on incandescent metal wire 25 μm in diameter, near whose hot surface the following reaction occurred:

$$2BBr_3 + 3H_2 \rightarrow 2B + 6HBr$$
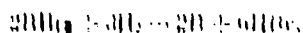
If the conditions are exactly fulfilled, a dense coating approximately 1 mm thick is obtained. Such rods of boron with a purity above 99% and an internal conductor to supply current for heating were used for studying burning at temperature above the melting point of boron (2300°K). Conditions were developed for depositing polycrystalline and glass-like boron.

Two basic experimental methods were used. The experiments using the first method measured the absorption of cold oxygen as a function of time, at various temperatures of the hard boron surface and pressure. The rod temperature varied between 1000-1900°K and gas pressure between 0.1-1.0 atm.

In the other method, the linear propagation rate of the flame was measured with a rod of boron burning from one end in a flow of oxygen at various pressures and a temperature of 2500°K.

From the results of these experiments, which are examined while taking into account the thermodynamic and physical properties of boron and its oxide, and the observations, in a microscope, of the moving incandencent burning surface, it was possible to judge the burning mechanism.

§ 4.   Methods of Studying the Ignition
and Burning of Single Metal Particles
and Clouds of Metal Particles
in Aggressive Gaseous Media

For the purpose of creating high-temperature sources of light radiation, Gross and Conway [145] performed extensive studies on the burning of various metals in both powder form and rod form.

The burning of large quantities of metal is difficult to study because of the problems connected with the ignition and position of the studied specimen. Gross and Conway managed to perform such a study with aluminum, using water-cooled steel reactors lined with aluminum oxide for this purpose. By controlling the rate of the oxygen supply, significant changes in burning intensity could be achieved. With low oxygen flow rates, no aluminum oxide smoke particles were formed, and burning extended along the surface of the liquid aluminum. At higher oxygen flow rates, a large amount of aluminum oxide smoke was formed.
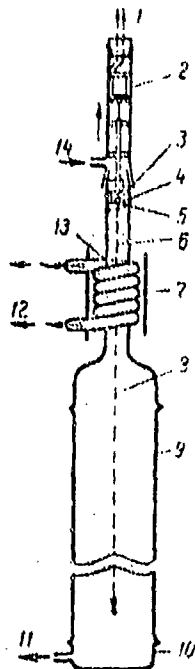
Fig. 24.   Transit time installation for studying the burning of metal particles.
1 - Solenoid contacts; 2 - solenoid;
3 - magnet; 4 - metal particle holder;
5 - opening direction of holder site;
6 - path of metal particles before ignition;
7 - reflector; 8 - track of burning particles;
9 - glass tube; 10 - viewing glass or cup for collecting combustion products; 11 - gas outlet;
12 - leads to capacitor bank; 13 - discharge tube; 14 - gas inlet.

An important method which makes it possible to measure accurately the time of particle existence before its full combustion or separation or separation as a result of explosion, at a certain composition, pressure, and ambient gas temperature, is the method of igniting metals by heating through radiation from the flash of a pulsed xenon lamp [146-151]. In this method, an intense light pulse (whose brightness temperature reaches 10^4°K [152]) heats the tested specimen to several thousand degrees in several milliseconds [11, 18, 39]. Since the heat source itself is not in contact with the atmosphere in which the test specimen is placed, this technique makes it possible to study the burning of particles or strips of metal in gaseous media whose composition and pressure can vary over a wide range. The study was performed in a chamber (Fig. 24) made of glass tubing, consisting of four detachable se ons. The first section contained the specimen holder; at the instant the electromagnet was switched on the specimen was released and began to fall freely. The pulsed lamp was placed in the second section. The length of the third section could be changed from several centimeters to several meters depending on the required length of the experiment. The lower end of this section was joined with the fourth section, which was a cup in which the combustion products were collected. A flat piece of glass was sometimes inserted instead of the fourth section in order to photograph vertically.

The pressure in the chamber could vary from 10^{-3} mm Hg to atmospheric pressure; the metal particle itself could burn either in a motionless gas medium of the necessary composition or in a flow of gas.

The pulsed lamp in the form of a spiral with an inner diameter of 30 mm and a height of 50 mm, made from quartz tubing 8 mm in diameter, was filled with xenon.

Upon discharge of the capacitor bank, around 3600 J of energy was released in the pulsed lamp; approximately half of this energy was expended in 1.2 ms. During the entire discharge time, more than 27.6 J was received per unit surface of the specimen in the middle of the spiral of this lamp [153].

During the melting of metal foil, metal droplets are formed, whose diameter is determined by the size of the piece taken. Usually, these foil pieces had a thickness of 10-15 μm and an area of $250 \times 1500 \ \mu m^2$.

The burning process was photographed with a high-speed movie camera, frame speed 3000-5000 frames per second. When required, the burning particle could be rapidly cooled in any stage of combustion by placing a Dewar vessel with liquid argon in the second section at various heights. The combustion products were usually analyzed after evaporation of the liquid argon.

The burning of Zr, Ta, Ti, Mo, W, Pu, Sm, Re and Al particles in oxygen and various oxygen-nitrogen and oxygen-argon mixtures was studied with this experimental installation.

An end-burning fractional horsepower motor was used in reference [154] to study the regularities of the ignition and burning of metal particles included in a propellant as energy admixtures.

There were two versions of this installation made. In the first version, optical instruments were used as the main method of recording the burning and ignition of particles. In the second version, the unit impulse of the propellant and its dependence on the concentration and combustion efficiency of the metal was the main parameter characterizing the burning of the metal (Fig. 25).
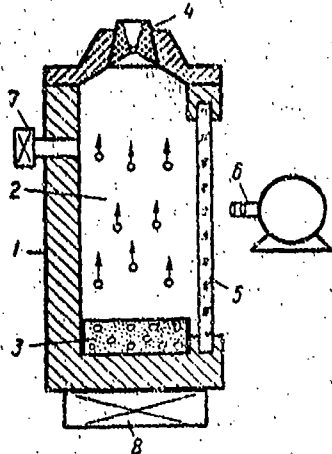
Fig. 25. Installation for studying the burning of metal particles in a composition of solid fuel.
1 - Chamber; 2 - flow of gas with metal particles; 3 - propellant charge; 4 - nozzle; 5 - Plexiglas; 6 - SKS-I movie camera; 7, 8 - pressure and thrust sensors.

Along one entire side of the motor there was a 13×300 mm window 5 for optical observations. Plexiglas walls to prevent rapid contamination and burnout were equipped with interchangeable Plexiglas plates on the channel side of the motor.

A standard high-speed SKS-IM movie camera [155] and a photo-recorder produced by IKhF [Institute of Chemical Physics] of the Academy of Sciences, USSR, [156] were used as the optical instruments necessary for the visual observations of the motion of the burning aluminum particles and the surface of the propellant. Photography was usually performed at speed of 4500-5000 frames per second with reduction by a factor of 1.5-2.

The installation illustrated in Fig. 25 was used to measure the unit impulse of the propellant. This installation consists of a fractional horsepower motor, a thrust sensor, a pressure gauge, a calorimeter, an amplifier, a MPO-2 oscillograph, and a power supply unit. The fractional horsepower motor differs from the one mentioned above only in that it has no window for optical observation or device for feeding additional charge and, instead of the "point" nozzle a standard Laval nozzle with the ratio $d_0/d_\text{H} = 2.3-2.45$ was used.
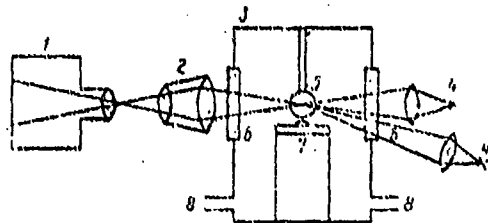
Fig. 26. Installation for high-
speed photomicrography of the
burning of metal particles.
1 - SKS-I movie camera; 2 -
microscope; 3 - chamber; 4 -
illuminating lamp; 5 - metal
particles; 6 - chamber windows;
7 - igniter; 8 - openings for
feeding gas to chamber.

An experimental study using still photography and movie
photography of the burning of metal particles in a moving flow
has a number of disadvantages which make it impossible to study
the important characteristics of the burning mechanism of
separately taken particles under prescribed conditions (the
character of the burning, the structure and geometric characteris-
tics of the burning zone surrounding the particle, the dynamics
of the burning process, etc).

These characteristics can be rather fully studied only in
a study of the burning process of motionless particles using
various methods of photomicrography [157].

Kashporov [158] developed an installation which has made
it possible to study the burning process of single motionless
metal particles in various gaseous oxidizing media using high-
speed movie photomicrography. The basic units of the installation
are shown in Fig. 26.

The necessary oxidizing medium is created by blowing the
previously prepared gaseous oxidizer (water vapor, carbon dioxide,
or an oxygen-argon mixture, etc.) for a long time through the
working volume of the chamber.

The test particle is ignited in the oxidizing medium by a miniature element heated by electric current (silicon carbide, or graphite rods, as well as nichrome or molybdenum plates, etc., can be used as heating elements). However, it should be remembered, as mentioned above, that the presence of carbon can lead to the reduction of aluminum oxide, which always covers pure aluminum, and can thus affect the ignition process.

The processes of symmetric and asymmetric burning of particles can be studied on this installation, which is necessary in order to obtain the correct representation of the kinetics of the burning of particles which are located in a flow of an oxidizing medium in a suspended state or on the interface of the condensed phase of the propellant and the flame.

The optical system of the installation makes it possible to obtain a high-quality negative image on the film with eleven-fold magnification and a resolution of 20 lines per 1 mm.

Great care should be taken, however, in interpreting the results obtained on the film, during the burning of the metal particles, in the form of tracks or diffusion halos. The fact is that even with low magnification, let us say 5, the depth of focus is only fractions of a millimeter. Actually, the range of definition Δ is determined by expression [157]

$$\Delta = \pm (2 N . A'^{2} \beta^{2})^{-1}, \qquad (II.3)$$

where $A' = \sin \frac{\alpha}{2}$ is the aperture number in the exit pupil of the system (α is the angle formed by the rays from the edge of the exit pupil of the lens to the center of the image); N is the resolution of the photographic layer, line/mm; β is the magnification of the photomicrographic installation.

If we take even a somewhat lower resolution for the photographic layer N = 50 line/mm, and the average value of the aperture A' = 0.2 [159], then when β = 5 we find that the depth of focus is only approximately Δ = 5 μm. Therefore, the sharp, clear track of metal particle burning, which indicates heterogeneous (surface) burning, can appear diffused and ill-defined in photomicrography (because of the small depth of focus) and, on the basis of this evidence, the burning could be interpreted as diffused (occurring in vapor phase).

The ignition of metal particles depends on many factors: the composition of the ambient medium, the surface condition and size of the particles, the reaction rate, the concentration of particles per unit volume, the natural intensity of the ignition source itself [160], etc. The process of oxidation occurs at temperatures rarely exceeding 800-1000°C, and for many metals ignition takes place at significantly lower temperatures; however, active burning takes place at temperatures above 2500°C. Although there are many works on oxidation performed at a temperature near the ignition point of metals, the relationship between slow oxidation and the rate of actual burning is still unclear.

Boyle and Lewellyn [161] measured the ignition energy of aluminum and magnesium using a spark in a particulate cloud of metal in air. They found that ignition energy changes with a change in resistance, which determines the discharge time, i.e., there is an optimal discharge time for ignition. The ignition energy of the particulate cloud is a function of particle size; the smaller the particle the less energy will be required. The energy values for aluminum and magnesium are presented in Table 10.

Table 10. Ignition energy (in J) for aluminum and magnesium.

Resistance, Ω	Mg			Al	Al—Mg 50 : 50
	90 мк	70 мк	40 мк	40 мк	90 мк 10 мк
$50 \cdot 10^3$	0,20	0,033	0,025	0,055	0,060
10^4	1,20	0,14	0,09	0,55	0,80

[мк = μm]

The ignitability of the particulate cloud containing particles of various sizes will be determined by the smallest particles since they will ignite more easily. Comparatively large particles of aluminum can be ignited only in a medium with a temperature exceeding 2000°C. Thermal flux with such a temperature cannot be obtained on particle-tracking installations [162-165]; therefore, in many studies [166-169] on aluminum particle burning, arc burners (plasmotron) (Fig. 27) have been used.
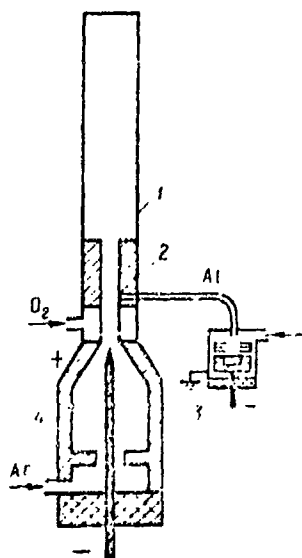

Fig. 27. Arc burner.
1 - Quartz tube; 2 - fireclay fitting; 3 - vibrator for feeding metal particles; 4 - argon-arc burner.

Any inert gas, most frequently argon, is used as the heat-transfer agent. An argon-arc burner gives a plasma stream of argon with a calculated temperature of 5000-15,000°K at a current strength of 100-500 A. The argon is heated in a ring-shaped arc discharge between a tungsten cathode and an internal copper nozzle-anode. A secondary gas (usually air) is used to press the stream of plasma into the ring-shaped gap between the outer and inner nozzles through the tube and the distributor ring.

The particles can be introduced into the gas flow with a feeder similar to the one used by Friedman and Macek [133]. This feeder is a cylindrical cavity whose bottom (a phosphor bronze membrane) can be vibrated by an electric vibrator. On top of the membrane is a thin vertical tube through which the gas in the cavity exits. Powder particles, poured on the membrane, during the vibration form a cloud from which part of the particles are carried by the flow through the vertical tube to the stream of hot gas. The frequency of particle feed to the flow is controlled by the amplitude of the membrane vibration, the flow rate of the gas through the chamber, and the height of the lower section of the vertical tube above the membrane.

The temperature of the flow can be controlled by changing the current of gas in the burner or by changing the total flow rate of the gas with a given current.

The composition of the medium is determined by the flow rate of the components measured with rheometers which are graduated by the displacement of gas by water from the measuring vessel. In control experiments the oxygen content can be checked by analyzing samples taken from the stream cooled by the gas-collecting tube. As a rule, the results of analyzing samples taken from the upper nozzle edge agree with the calculated results of measuring gas flow rate within the range of error.

Gurevich and colleagues [167-169] collected the combustion products at various heights over the exit section of the burner nozzle on cold glass lubricated with a thin layer of vaseline. The particles thus collected were examined and photographed under a biological microscope with a magnification of 60-600.

The ignition limit was determined as follows. The operating current through the burner and the flow rate of argon and oxygen were assigned. The flow rate of nitrogen was first selected so that the test particles would be reliably ignited. Tracks of two types were observed visually: long and bright, which were located rather far from the nozzle edge, and short and weak, which indicated the presence of very fine particles in the basic fraction. Then the nitrogen flow rate was increased until the particles of the basic fraction ceased to burn. This mode of the plasma burner was considered the ignition mode.

The gas temperature along the height of the gas plasma stream was measured by the method of turning spectral lines if it was above $1400^{\circ}C$ and by a thermocouple if it was below this figure.

To improve the feeding of metal particles into the gas flow, an electric charge was sometimes given to the particles. The method used was as follows.

A grounded diaphragm with a small opening was installed over the metal cup with the powder. A brief pulse was fed to the cup. Because of the action of the electric forces, particles were ejected from the cup and flew to the diaphragm. Some of them flew out through the hole. The possibility of the escape of adhering particles is substantially reduced since they are electrically charged.

Burning of metal particles in various gaseous media can be studied using plasma burners at higher pressures up to 20 atm on the installation (with slight changes) of Polak and Shchipachev [166], which was developed in order to obtain nitrogen oxides in a plasma stream. On this installation, a plasma stream with temperature up to 3100-3200°K can be obtained.

The design of the heater, which was developed by Klepeys and Roza in order to study a strong Hall effect [170], can also be used successfully for studying the burning of particles in gaseous media of various compositions (Fig. 28). The main heating element of inert gas (argon) was a device of graphite rods 9 mm in diameter and 59 cm long, arranged tightly in a cylindrical graphite chamber 40 cm in diameter and 59 cm high. At the beginning, with the aid of four dc welding generators (with the power of approximately 30 kW), the graphite rods were heated to 2000°K and then into the space between the rods was fed inert gas which acquired the temperature of the rods due to convective heat exchange. The introduction of metal particles and the desired gaseous medium, consisting of oxidizing agents CO_2, H_2O, O_2, into the heated flow can be accomplished through special quartz tubes located either in the channel which discharges the heated gas or at the exit from it.

Experiments with this heater were performed at a temperature of 1900-2000°K for the graphite rods with a gas flow rate of 100 g/s. The temperature drop during feed of gas for 15 seconds was less than 10°C.

The gas temperature at the outlet was measured only with a rod heating temperature of around 1000°C. Measurements indicated that the gas and the graphite rods have the same temperature.
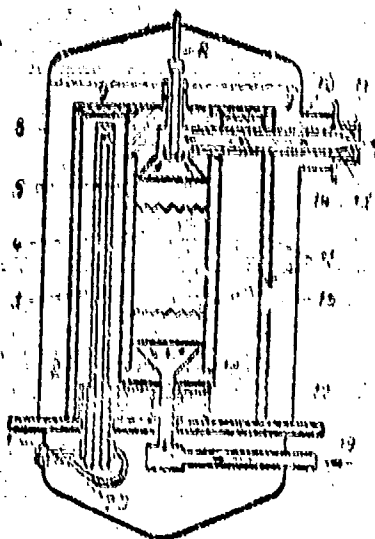
Fig. 29. Rod-type graphite electric gas heater. 1 - Water-cooled copper terminals; 2, 7, 9, 18 - insulation; 3 - heating element; 4 - adapter; 5 - adapter ring; 6 - outer steel casing; 8 - admixture inlet tube; 10 - corner wadding; 11 - cooled copper flange; 12 - exhaust; 13 - ceramic nozzle; 14 - graphite drain tube; 15 - grate for adapter holder; 16 - inner casing; 17 - steel support plate; 19 - gas supply; 20 - current conductors from welding unit.

§ 5. Method of Studying the Burning of Metallized Propellants

We know that the introduction of metals into the composition of a propellant substantially improves its characteristics [4, 6, 138, 171]. One of the interesting problems in the burning of such systems is the study of the surface structure of a propellant with the addition of aluminum, magnesium, and their alloys. This study makes it possible to clarify a number of problems: whether metal ignites on the burning surface of the propellant or not; whether there occurs an agglomeration of metal on the burning surface; how the initial size of the metal particles and the percentage content of the metal in the propellant affect the processes occurring on the burning surface.

In references [172-174] it was first shown that during the burning of ballistic powder with an aluminum admixture, on the surface of the charge there occurs an adhesion of metal particles with thermally stable decomposition products of nitrocellulose and the subsequent merging of them near the burning surface. In the case of the burning of a model APC fuel composition, adhesion and merging of aluminum particles occurs on the burning

surface of the propellant. A method was developed which made it possible to sample the k-phase of the smoke-gas mixture at various distances from the surface of the burning charge.

The selection of particles along the height of the flame's tongue was done on the installations illustrated in Fig. 29.
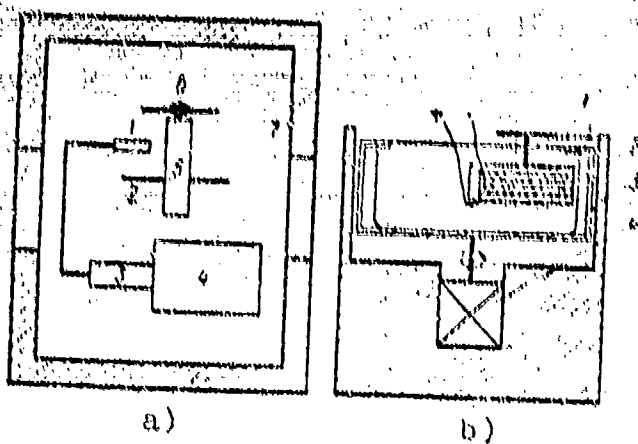

Fig. 29. Combustion product samplers.
a) Electromagnetic: 1 - metallic or glass plate; 2 - copper wire; 3 - core; 4 - solenoid; 5 - powder charge; 6 - igniter. b) Centrifugal: 1 - Slotted powder charge; 2 - rotating drum; 3 - alcohol; 4 - electric motor.

Particles were taken on metal or glass plates and then studied under an MBR-3 microscope, which made it possible to measure particles up to $3 \cdot 10^{-5}$ cm in size. An electromagnet 4 with a core 3 were used to intersect the flame's tongue with a plate at a certain distance from the surface of the burning charge. Before each test, plate 1 was installed at a certain distance, within ∿0.2 mm, from a copper wire 10 μm in diameter which passed through the core of the specimen and was used as a retainer of the burning surface of the charge relative to the plate. At the moment the copper wire 2 burned out, a current was automatically fed to the winding of the magnet and the core 3

84

moved the subject plate over the burning specimen. A check using movie photography with a magnification of 5 showed that the surface of the charge could be fixed within ~0.5 mm relative to the plate.

In order to verify that there are collected on the plate those particles of condensed products which are formed during the burning of metallized compositions, i.e., agglomeration of particles on the plate itself does not occur during sampling, it is necessary to fulfill the following conditions:

$$n v s t < 1, \tag{II.4}$$

where n is the number of aluminum particles in 1 cm^3 of the composition, cm^{-3}; v is the burning rate of the charge, cm/s; t is the time the object plate is in motion over the burning surface of the charge, s; s is the cross-sectional area of the metal particle, cm^2.

This expression is obtained on the assumption that the initial size of the metal particles does not change during the burning of the fuel-oxidizer composition.

Usually, the time of plate motion, for each specific composition, was selected so as to be 5-6 times shorter than the time obtained on expression (II.4). This clearly prevented the adhesion of the melted metal particles to the surface of the object plate, and also made it possible to obtain a relatively uniform concentration of sampled condensed products. The combustion products were sampled at three places along the height of the tongue of the specimen's flame: $h = 0.5$, $h = 5$, and $h = 10$ mm from the burning surface of the charge. Tests were made in a constant-pressure cylinder in a nitrogen atmosphere in the pressure range $P = 1-30$ atm.

The original methodology used in sampling the condensed combustion products of metallized propellants is described in reference [154] (see Fig. 29b).

Specimens consisting of two thin plane-parallel plates rigidly attached to a plastic housing were burned in a constant-pressure cylinder. The use of specimens with this shape made it possible to blast the burning surface with hot products moving at speeds of up to 200 m/s. A slotted specimen 7 was attached in front of the inner side surface of the drum 2, which was turned by a 1000 r/min motor 4. The alcohol poured into the drum spread out in a thin layer 3 along its side surface. Condensed combustion products, coming out of the slot in the charge and falling in the alcohol, were quenched. Such a sampling procedure made it possible to collect condensed combustion products up to 100 μm in size, no more than 1 μs after their escape from the burning surface without a change in their shape or structure.

Particles thus collected were then analyzed under a microscope with a magnification of 60-600. The results were formulated in the form of integral curves of volume distribution [175]. For the short-term distribution curve the dimensions $D_{50} =$ $= (\Sigma n_i d_i^3/n_i)^{1/3}$ and D_{90} were used (50 and 90%, respectively, of the particles, according to volume, are smaller than the size given). Both sizes are obtained directly from integral distributions.

Cassel and Liebman [176] collected particles on glass wadding by blowing through it a flow carrying these particles. They used this method in order to more precisely define the size of the particles under a microscope and determine their concentration in a heterogeneous flow. However, this method can also be used, of course, for collecting condensed solid products of the combustion of metal particles.

The method used by Cassel and Liebman differs favorably from the selection of particles by glass in that it makes it possible to trap all combustion products and to perform a quantitative determination of the insufficient burning of the metal at various stages of particle burning, for example, for particles of aluminum by the volumetric method based on the change in the volume of hydrogen released during the interaction of aluminum with alkali according to the following reaction:

$$2Al + 2NaOH + 6H_2O \rightarrow 2Na[Al(OH)_4] + 3H_2.$$
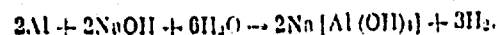
The accuracy of this method with an aluminum content of less than 5% is within ±1.5%. Since aluminum carbide can be present in some specimens, it is necessary to make a correction for the liberated methane (as we know, during the interaction of aluminum carbide with water methane is liberated). For this it is necessary to conduct parallel tests with water instead of the alkaline solution and to recalculate the liberated gas for aluminum, which must be deducted from the quantity of aluminum obtained with an alkaline solution.

Aluminum nitride can be determined by the ammonia distillation method [177].

During the interaction of ammonium nitride with water in the presence of alkali, ammonia is liberated and absorbed by sulfuric acid. The excess sulfuric acid is titrated by the alkaline solution.

The content of aluminum chloride can be determined by the argentometric method [178], based on the precipitation of a chlorine ion by silver nitrate and the back-titration of its surplus ammonium thiocyanate in the presence of the indicator — ferric ammonium alums. The determination is made in a water medium after processing the batch with water during heating.

The accuracy of the method, when the aluminum chloride content is below 2%, is ±0.15%.

In order to determine the content of soluble aluminum oxide in hydrochloric acid, the complexometric method was used, based on the ability of aluminum with trilon B to form complex compounds [179].

Since aluminum, aluminum chloride, aluminum nitride, and ferric oxide are dissolved in hydrochloric acid, they are titrated along with a soluble oxide; then their content, found by other methods, is recalculated for aluminum oxide and subtracted from the mound of soluble aluminum oxide obtained. When the aluminum oxide content is approximately 4% or more, the accuracy of the method is ±0.5%.

After the determination of soluble aluminum oxide in a batch, an insoluble residue can remain, which is insoluble aluminum oxide. It is analyzed by melting with potassium bisulfate (converted to a soluble salt), and the melt is dissolved in hydrochloric acid and filtered. The aluminum oxide content in the filtrate is determined by the complexometric method. With an aluminum oxide content of 90% the accuracy of the method is approximately ±1.0%.

Existing methods of determining the dispersity of highly dispersed powders, based on counting and establishing particle sizes by optical and electron microscopes, are tedious and require large expenditures of time. Methods which are more progressive in this respect are based on the measurement of light absorption. However, it should be noted that they can be used only for powders with particles of less than 50 µm. Dispersity is measured based on the intensity of the light passing through a layer of suspension of a certain thickness [40, 180-183]. Depending on whether instantaneous photometric measurement is performed or the suspension sedimentation is recorded over time, we can find the specific surface area and the distribution curve of particles according to size.

Gumprecht and Sliepcevich [184] gave the mathematical basis for obtaining the distribution curve of particles according to size in polydispersed systems by measuring the light transmission of suspensions in the process of sedimentation. Prop [185] created a semiautomatic instrument for analyzing powders with a dispersity from 1 to 40 µm. However, as Beigin and Butler [186] indicated, although optical determination during sedimentation is very convenient, the decoding of experimental data required rather long and complex computations. Pechkovskaya and colleagues [187] used the tubidimetric method for studying the dispersity of carbon black. They measured the optical density of a suspension in monochromatic beams of light with various wavelengths. The greater the dispersity of particles of the suspension, the greater the difference between the optical densities of the suspension and beams of light with various wavelengths and the **colorimetric number** which served as the criterion of dispersity.

Using the **turbidimetric** method, we can, by measuring the intensity of incident and passed light, calculate the specific surface area of a powder according to the formula proposed by Rose [188]

$$S_0 = \frac{4}{cl} \ln \frac{I_0}{I},$$

where c is the concentration of the suspension, g/cm^3; l is the thickness of the suspension layer, cm; I_0 and I are the intensities of incident and passed light, respectively.

With this method we can obtain reliable results when analyzing powder with a particle size below 1 µm. There are correction factors, introduced by Rose, which depend on the range of dispersity.

Aksencv and Kuchenogiy [189] developed a photoelectric device for the automatic computation and determination of particle size on a VDK-4 continuous-flow ultramicroscope. The device is assembled on semiconductors, which enables it to operate both in stationary conditions and in the field. Along with computing the total number of particles, this device sorts them according to size, using the principle of differential amplitude discrimination simultaneously along eight channels [190].

The results of tests wherein concentration was measured both visually and by the photoelectric device in the aerosol particle size range (according to data from microscopic analysis) from 0.3 to 2 µm in diameter (root-mean-cube diameter was 0.8 µm), showed that with a variation in particle concentration from $3 \cdot 10^2$ to $2 \cdot 10^6$ cm^{-3} the measurements from both methods agreed, on the average, within 20%. Within these limits, the results of measurements did not depend on the counting rate with a variation in the latter from 100 to 1000 pulse/min. The maximum rate of osteration through the container, at which there is still no noticeable distortion in the counting results, is ~ 150 cm$^3 \cdot$s. This instrument can be particularly useful in counting highly dispersed condensed particles sampled by various methods during the burning of metallized condensed systems.

A detailed analysis of various methods and instruments developed in the USA for determining dispersity (particle distribution according to size) and partial concentration is given in [191-192] and a detailed analysis of those developed in the Soviet Union is given in [193, 194].

It is known [195, 196] that the initial stage in the burning of condensed systems occurs in the reaction layer, in which total-exothermic processes of decomposition and dispersion of the larger part of the condensed substance take place.

At the present time there are many works [6, 197-201] dealing with studies of the structure of the burning surface in propellants both with and without the addition of aluminum. Watermeier and colleagues [202] made a photographic study of the burning surface of a propellant consisting of nitroglycerin, nitrocellulose, and ammonium perchlorate with the addition of aluminum with various dispersities and concentrations. The tests were performed in a constant-pressure bomb in the 12-55 atm range. During the burning the surface of the specimen was illuminated since the illumination of the burning surface by the tongue of the flame was insufficient for movie photography. Based on experimental data, the authors concluded that aluminum melts on the burning surface of the propellant at all pressures (however, the temperature of the burning surface was not measured). In certain cases, drops of metal on the surface began to burn or evaporate since a trace of flame in the form of smoke was observed coming from the metal drop and directed toward the high-temperature zone of the flame. The following phenomena were observed during the burning process.

1) Drops of aluminum grew in diameter as they moved along the burning surface and coagulated with other drops; then the metal agglomerates formed were carried to the flame zone.

2) Part of the drops remained in place for several milliseconds; the drops grew in diameter and then were carried to the tongue of the flame; the phenomena observed are proof of the process of adhesion (agglomeration) of aluminum on the burning surface of the propellant.

A study of the structure of the burning surface of a mixed propellant (on a base of APC and polybutadieneacrylic acid) with aluminum additive, made by Povinelly and Rosenstein [203], showed that in the pressure range 1-3.5 atm metal particles moved along the propellant surface, with an increase in the pressure the rate of their motion decreased. The phenomenon of metal particle agglomeration was observed.

91

According to the authors' hypothesis, there are two conditions which must be fulfilled for metal agglomeration to occur on the burning surface of a propellant: a) particle residence time on the burning surface must be greater than agglomeration time; b) agglomeration time must be less than burning time.

A deficiency of [203] is the absence of photography as well as an insufficient quantity of experimental data for the statistical evaluation of particle motion along the surface of the propellant. There is also an indication that the results with respect to the displacement of aluminum particles were obtained only at low pressures since at higher pressures soot shielded the burning surface of the propellant. For this reason, Povinelly and Rosenstein obviously could not see that agglomeration can occur even in the absence of particle motion along the burning surface, simply from the accumulation of metal on those sections where pyrolysis of the fuel bundle occurs [172, 173].

Using movie photography, Heath and Hirst [199] studied the burning surface of ballistite propellant (41% natural glycerin, 48% natural cellulose) under conditions of a Crawford bomb. Frame-by-frame filming showed that on the burning surface there was a number of bright spherical particles whose size reduced with an increase in pressure. In the burning process the observed particles periodically appeared and disappeared; however, on the average, their number on the burning surface was approximately constant and their residence time on the propellant surface decreased with an increase in pressure. In the opinion of the authors, the observed spherical particles are gas bubbles on the liquid-viscous burning surface of the powder.

Silhouette photography of the burning surface of a composition based on APC and polystyrene [6] showed that oxidizer particles emerge over the middle level of the burning surface. In this connection, the results obtained by Pokhil [204] and Vandenkerkhave [200] are of interest. Vandenkerkhave indicated that at low

pressures the oxidizer crystals emerge over the fuel. However, at increased pressures the opposite pattern was observed: APC crystals were found on the bottom of small grooves and the visible surface consisted generally of distinct peaks of protruding fuel. Studies of the structure of the burning surface of model propellant (on a base of APC and a number of fuels) extinguished during burning, performed by Pokhil and Romodanova [204], showed that at low pressures (in vacuum) the oxidizer crystals protrude beyond the middle level of the burning surface. Between the crystals there are depressions in which the fuel is located. It was found that the larger the initial crystals the more they protruded over the surface of the propellant. As pressure increased the protruding APC crystals decreased; with a pressure above 30 atm crater depressions were formed at the location of the oxidizer crystals. The authors explain this effect by the fact that at a pressure below 30 atm APC does not burn stably, while at pressures above 30 atm it is capable of burning independently and during the burning process the fuel disappears more rapidly, which leads to the appearance of craters. In connection with this, the study made by Hightower and Price [201] is of interest. They investigated the surface of single APC crystals in the 20-190 atm range. Depending on pressure, the burning surface is represented as a series of channels, troughs, and craters with heights of ~20 μm; the shape of the surface remains relatively constant while the burning surface moves for a distance on the order of 1 mm.
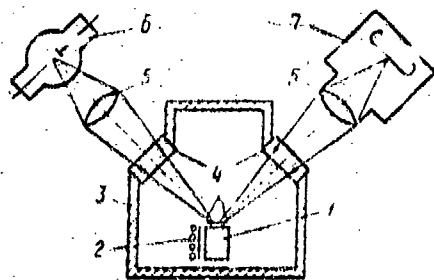

Fig. 30. Photographic method of studying a burning surface. 1 - Powder charge; 2 - electrically heated furnace; 3 - chamber; 4 - window; 5, 5' - lenses; 6 - xenon lamp; 7 - movie camera.

The original method for studying the structure of a burning surface was developed by Pokhil and colleagues [172] (Fig. 30).

The studied specimen of propellant 1 was placed in a constant-pressure bomb [cylinder] 3 inside which pressure could be created from 10^{-2} mm Hg to 40 atm. For observation during the burning process the bomb is equipped with plexiglas windows 4 installed at a 45° angle to the burning surface of the studied specimen. For preheating the specimen in vacuum conditions (where the heat released from the total-exothermic reactions of the decomposition of condensed phase is insufficient for self-propagation of the burning process), an electrically heated furnace 2 was used. The movie camera was attached to a special rail at a 45° angle. This allowed the geometric inhomogeneities of the burning surface to be revealed. Preliminary tests showed that filming the burning surface of a propellant without external lighting is ineffective since the illumination of the surface from its own radiation and the radiation of the flame alone is too weak. For this reason, powerful lighting achieved by a DKSSh-1000 xenon lamp 6 was used.

In [173, 206] a method was developed for measuring the temperature along the height of the tongue of flame from metallized solid propellant by the brightness-spectral method (Fig. 31).

The powder specimen 10 to be burned was placed in a constant-pressure bomb 1 (the design of the installation was developed at IKhF [Institute of Chemical Physics] of the Academy of Sciences, USSR),in a nitrogen atmosphere and was ignited from the end by a nichrome spiral. The surface of the specimen was armored in order to exclude the possibility of a flame flashback along the side surface. To monitor the burning of the propellant charge and to obtain a high-quality picture of the process a SKS-I movie camera was used.

94

The radiation from the tongue of the flame of a specimen of solid rocket propellant [TRT] was projected by the lens to the input slot of an ISP-51 spectrograph 2 in a 1:1 ratio. A glass lens with F = 210 mm was used. The spectrograph slot made it possible to vary the width of the defined section of the flame zone from 25 to 400 μm. In addition, on the slot of the spectrograph were attached two metal plates which limited the slot in length to a dimension equal to or less than the diameter of the specimen. Due to the high temperature gradients in the flame front, it is desirable, in this case, to work with as narrow a beam as possible for the best spatial resolution.
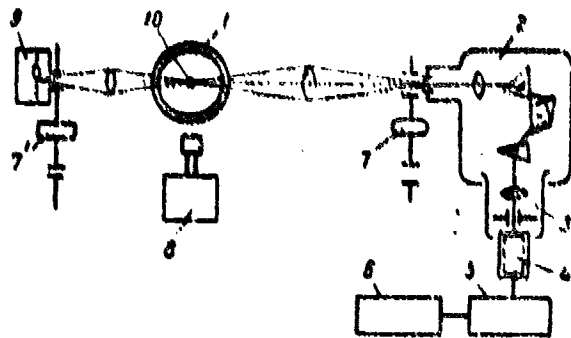

Fig. 31. An optical method of measuring the temperature of the flame from a solid propellant. 1 - Constant-pressure bomb; 2 - ISP-51 spectrograph; 3 - FEP-1 photoelectric device; 4 - photomultiplier; 5 - amplifier; 6 - loop oscillograph; 7, 7' - disk-baffles; 8 - SKS-1 movie camera; 9 - xenon or tungsten lamp; 10 - powder specimen.

The transillumination of the flame was done with a carbon arc, a standard ribbon-filament lamp, or a DKSSh-1000 xenon lamp 9. A RO-56 lens was used for intermediate focusing, in the plane of which was placed a disk-baffle 7 to cover the light signal from the lamp. Then the light flux from the comparison source 9 was projected onto the flame of the burning propellant specimen by a Jupiter-9 lens.

At the output of the spectograph there was an FEP-13 photoelectric attachment which was used in place of the FEU-42 photomultiplier which has good stability and low leakage current. The output slot of the FEP-I was selected so that the wavelength of interest could be isolated from the spectrum of the flame.

In measuring the temperature of flame from metallized powders the region of the sodium D-line was most frequently selected. For the following reasons: a) a very small amount of sodium provides intensive radiation (the sodium introduced during propellant preparation, due to so-called "contamination," is sufficient); b) the radiation of sodium atoms is usually in thermodyanmic equilibrium; c) the optimum sensitivity of the eye in the yellow part of the spectrum makes it convenient for focusing and adjusting the installation. The linear variance of the PEP-I is approximately 40 $\overset{o}{A}$ in 1 mm in the region of the yellow sodium doublet, which ensures a more accurate isolation of thin spectral line.

The above described installation makes it possible to measure temperature along the height of the tongue of flame from a burning charge of TRT both by the method of rotating the sodium spectral line (if desired, lithium, cesium, and other metals and compounds of them can be introduced into the flame and temperature can be measured according to their resonance lines) and by the brightness method (radiation-absorption) within the range 1200-4500°K. Temperature can be measured in a wide range of the spectrum 3800-6600 $\overset{o}{A}$.

A description of optical methods for measuring the temperature of the burning surface of powder can be found in [207-210].

In our book it is not possible to pause on such important problems in the creation of optical methods for temperature measurement as the dependence of measurement accuracy on the spectral region used, as the value of the radiative capacity of the flame, the spectral composition of the radiation, the heterogeneity of the flame of metalized propellants (it should be remembered that the radiative capacity of particles and flame can be different), the scattering of flame radiation by fine

96

particles, and the self-absorption of radiation in the outer
cold gas layer of the flame's tongue. Therefore, we shall only
reference the original work where these problems are discussed
in detail and undergo the necessary analysis [131, 179, 211-234].

To study the burning of metal particles in various aggressive
media, tracking methods were developed [162-165]. One of the
installations is presented in Fig. 32. Aggressive gases (oxygen,
chlorine, nitrous oxide) were fed from cylinders with the
appropriate compressed gas and steam was fed from a boiler with
an electric heater. Temperature was controlled with a platinum-
rhodium thermocouple within ±10°.

The reaction tracking tubes were made from pyrex glass or
transparent quartz. Metal powder was fed into the tracking tube
by a special slide through an opening in it near the inlet from the
nozzle of the tubular furnace. A thermocouple was introduced
into the same opening for measuring the temperature of the gas
flow. The combustion products were partially deposited on the
walls of the tracking tube; the particles which were not deposited
were removed by an electric filter. The tracks of the burning
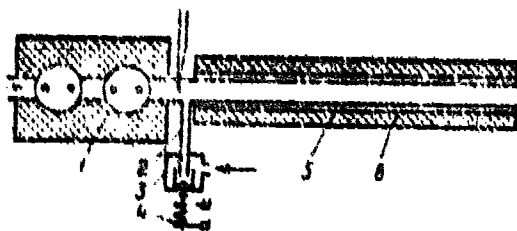particles were recorded on movie and photographic film.

Fig. 32. Tracking installation.
1 - Furnace; 2 - tube for introducing metal
particles; 3 - beaker with metal particles;
4 - vibrator; 5 - quartz tube; 6 - fireclay
jacket with electric heater.

Spectral methods, which make it possible to study the development of processes over time, have become more and more popular in recent years. Instruments have been constructed which record over short periods of time, in a selected wavelength range, the sequence of an object's spectra which reflects the kinetics of the process [235-237, 351, 352].

An SSU spectral scanning device based on an SF-4 spectrophotometer was developed by Logachev, Petukhov, and Zhuchkova in 1962 at the Institute of Chemical Physics of the Academy of Science, USSR, for spectral studies on the burning of aluminum and magnesium particles in the tongue of a flame from condensed systems in the high-temperature region (Fig. 33).

The radiation of a tongue of flame from TRT 1, passing through the quartz glass of a constant-pressure bomb 2, was focused on the input slot of an SF-4 spectrograph 5. Then the studied radiation hit the prism separating the light and was directed to the output slot of the instrument where an FEU-42 and an FEU-22 radiation receiver-photomultiplier 7 was located. The signal from the photomultipliers was amplified 10, 11 and recorded on an N-106 loop oscillograph 9. The frequency characteristics of the electronic circuit were determined by the natural frequency of the vibrators (loops).

The rotation angle of the prism 6, 8, the time marks from the GZ-IA audiofrequency oscillator 12, and the pressure in the bomb were recorded by a DD-10 induction gauge 14 and the burning process was monitored by a Konvas movie camera 15 simultaneously with the recording of the radiation spectrum along the height of the tongue of flame from TRT.

The prism of the SF-4 could be moved by the scanner 4 with a frequency of 8, 12, 24, and 40 Hz.
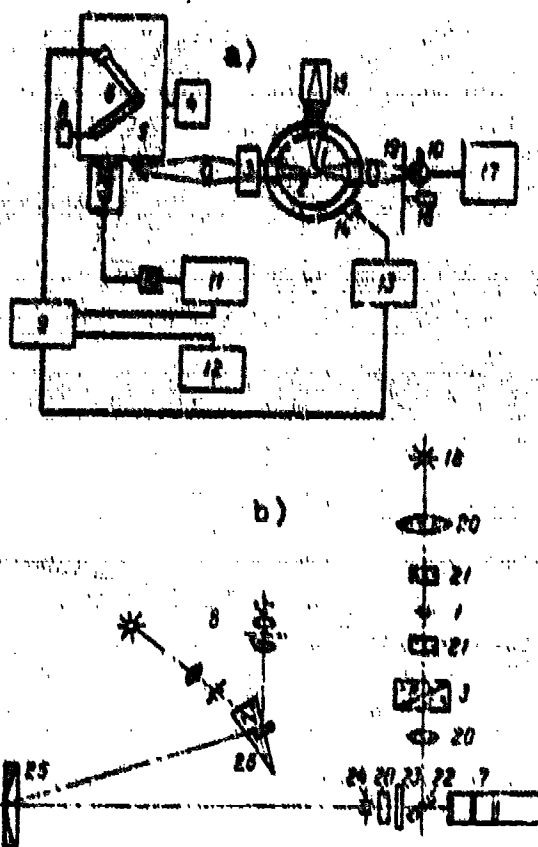
Fig. 33. Spectral installation.
a) Schematic diagram; b) optical
diagram. 1 - Powder charge; 2 -
constant-pressure bomb; 3 - rotary
prism; 4 - scanning device; 5 - SF-4
spectrograph; 6 - optical system of
the prism rotation-angle recorder;
7 - photomultiplier; 8 - current
source; 9 - oscillograph; 10 - cathode
follower; 11 - dc amplifier; 12 -
audiofrequency oscillator; 13 - ID-GI
amplifier; 14 - DD-10 pressure gauge;
15 - movie camera; 16 - electric
motor; 17 - power unit of mercury-
vapor lamp; 18 - mercury-vapor lamp;
19 - disk-baffle; 20 - quartz lenses;
21 - quartz glass of constant-pressure
bomb; 22 - rotary mirror; 23 - filter;
24 - input and output slot; 25 - mirror
lens; 26 - prism of the instrument.

The SSU made it possible to obtain 30-50 (depending on the burning time of the TRT specimen) spectrograms along the height of the tongue of flame from the TRT in one test.

The recording time for one spectrogram varied from 45 ms to 9 ms with prism swing frequencies of 8 and 40 Hz, respectively. The off-duty factor of the instrument (the ratio of the time interval between two successive recordings of the spectrum to the time required to record the spectrum) was 3-3.5.

CHAPTER III

IGNITION OF FINELY DISPERSED METAL

Metals can be conditionally broken down into two categories from the point of view of the characteristic features of the ignition and burning process. The first category consists of volatile metals (magnesium, etc.) which are in solid state before ignition and which do not form a solid protective oxide coating on the surface during oxidation.

The second category can include aluminum, beryllium, and others during whose oxidation a dense protective oxide layer is formed on the surface. For them the melting and boiling points of the oxide are above the melting and boiling points of the pure metal.

These groups of metals have different characteristic features and regularities during ignition and burning. These characteristics are manifested in a difference in the temperature and time regimes of the processes as well as in the overall pattern of metal behavior at any stage of oxidation.

In the general case, methods for studying the processes of metal ignition include the following.

1. Continuous high-speed microfilming of the studied object during the entire heating time up to the moment of transition to stationary burning. Preference is given to an experimental study of the ignition of fine wires since this makes it possible to localize the position of the observed object in time and space.

2. Visual observation of the studied object with high-resolution microscopes. In this case, preference is given to the study of separate particles selected and "extinguished" at various stages of heating and to the processes of low-temperature oxidation of metals in various active media.

With a combination of these methods very interesting details in the development of the ignition process of metal particles in active media have been revealed.

§ 1. Ignition of Aluminum

1. General Pattern of Ignition

Brzustowski, Glassman, and Mellor [235-238] studied the various stages in the ignition of fine aluminum wires (diameter 0.89 mm, length 8-11 mm) in a gaseous medium of oxygen, water vapor, carbon dioxide, and argon, used in different combinations and ratios. Straight or L-shaped anodized[1] and nonanodized wires of high purity were used in this study. The wires were heated by passing an electric current along them. Depending on the specific conditions, two types of ignition were noted.

The ignition of anodized aluminum in an atmosphere of carbon dioxide-argon, water vapor-argon, and carbon dioxide-water vapor, not containing oxygen in free state (P < 2 atm), is characterized by the appearance of a cylindrical vapor-phase flame (Fig. 34) at a certain distance from the surface of the wire, which lasted until the wire was destroyed.

---

[1] As a result of anodizing, an outer porous layer 500 Å thick and an inner thinner layer with protective properties are formed on the wire.
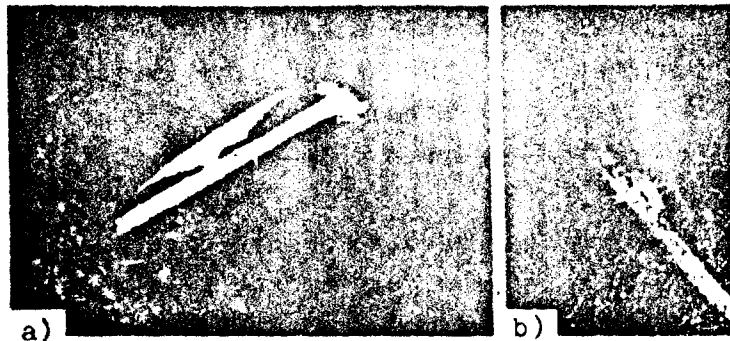
Fig. 34. Ignition of thin aluminum wires.
a) In a CO_2-Ar(50/50) medium, p = 50 mm Hg; b) in an H_2O-CO_2 medium.

In the case of an L-shaped configuration, the flame, as a rule, appeared on the vertical arm. Initially it occurred at spots where melted metal was concentrated, maintained by a solid or extremely viscous oxide film. The expansion and stretching of the oxide shell at these places apparently facilitated the diffusion of aluminum vapors outward and contributed to their ignition. Then the flame was rapidly propagated along the wire. The propagation rate along anodized wire was higher than along pure metal. Simultaneously, "streamers" of vaporous metal appeared on the surface (see Fig. 34). These were most frequently observed on anodized aluminum.

With the second type, aluminum ignites at the moment of direct contact between the active liquid metal and the oxidizing medium. The process has a predominately surface nature. However, vapor-phase ignition is not completely excluded. Its probability depends on the total pressure, the temperature of the medium, the oxygen concentration, and the aluminum vapor pressure at the moment of the wire's destruction. Ignition of this type is characteristic for aluminum wires heated in an atmosphere of pure oxygen or in a medium containing oxygen [239].

In all cases, regardless of pressure or oxygen concentration, ignition was established on the sudden appearance of a bright glow or flash on the surface of the wire (or very near it). If the oxygen concentration in the medium, by volume, did not exceed 50%, ignition coincided with the beginning of destruction and then changed to a stationary burning regime which developed at the location of the rupture.

With a higher oxygen concentration (50% by volume) ignition was very rapidly propagated from the initial point of origin to the ends of the wire. As a result of the melting of the oxide film, the specimen broke up into a series of independently burning drops of aluminum under the effect of surface tension forces. The initial coating of the aluminum by the amalgam facilitated ignition. If the coating was local, the ignition origin points always coincided with the amalgamation sites. It was characteristic that such treatment had virtually no effect on the burning process itself.

Thus, the experiments revealed the following.

1) If the main oxidizing reagent in the medium is oxygen, ignition of the wire, as a rule (at p - 1 atm), coincides with the moment of its destruction as a result of the direct contact between the pure aluminum and the oxygen.

2) If oxygen is present in the ambient medium in bound state (in the form of H_2O or CO_2) or if its concentration is low (at low pressure $p \leq$ _ atm), ignition of the aluminum begins in gas phase as a result of the diffusion of metal vapor through the oxide film. The wire does not lose its integrity at the moment of ignition.

The pattern of development of the process does not depend qualitatively on the degree of activity of the medium (concentration of the inert diluent) or the type of gas-oxidizer (H_2O, CO_2, etc.).

104

Ignition of finely dispersed powdered aluminum is also characterized by the sudden appearance and sharp increase in the intensity of particle glow.

The particles of aluminum collected directly before ignition are always spherical regardless of the shape of the initial particles of powder. At the moment of ignition they are in a molten state and coated with a solid protective oxide film.

Figure 35 is a photograph of aluminum particles collected with a heat-transfer plate from a flame of H_2-O_2 directly from the ignition zone. During the period of particle selection and cooling, a group of fine (~ 5 μm) oxide drops separated from the particle and formed a peculiar trail along the path of particle motion. Larger particles (150-200 μm) fragmented at the moment of impact with the sampling plate; the fragmentation was accompanied by the formation of radial tracks (Fig. 36) [139].
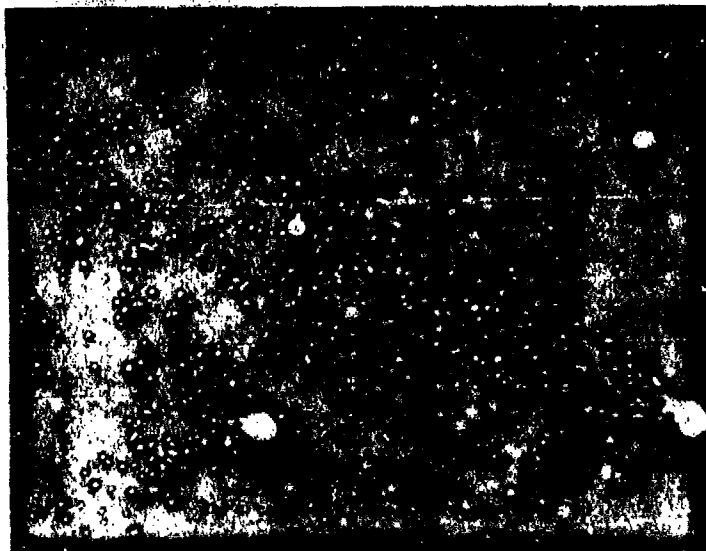
Fig. 35. Aluminum particles collected from the ignition zone.
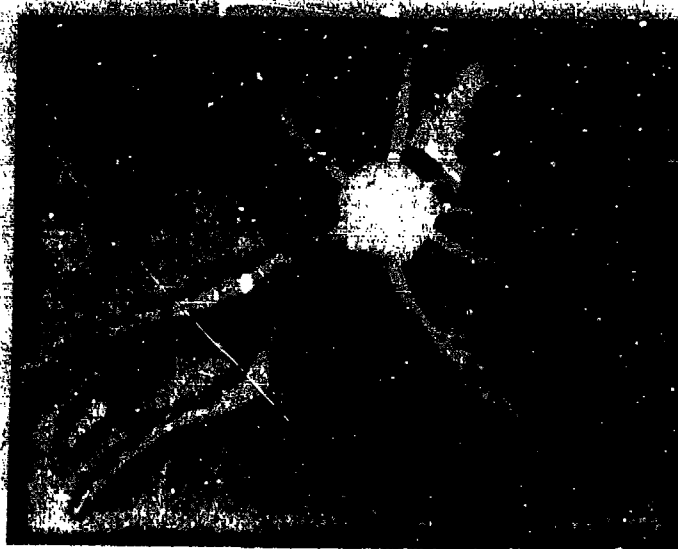
Fig. 36. Fragmentation of an Al
particle (d = 150 μm) on the sampler
plate.

Visual observations (microfilming) of the flight of the
particles revealed the fact that on the aluminum surface directly
before the flash individual bright spots appear. It can be
assumed that the appearance of these spots is connected either
with the surface glow of the pure metal which has been suddenly
freed of the oxide film or with phase changes (for example,
melting) which occur in the oxide layer coating the particle.
This has a local character.

The glow of the particle, which increases slightly with
time during the warm-up period, ends with a sharp flash and
with the formation around it of a uniform brightly glowing
spherical zone. The diameter of this zone exceeds the diameter
of the original aluminum by a factor of 1.5-3. The dynamics
of the process has, qualitatively, much in common with the process
of aluminum wire ignition. The transition from a weak glow to
a flash is completed in less than 0.1-0.15 ms.

Very interesting information [240] has been obtained in a study of particles subjected to intensified cooling at various stages of heating.

The surface of these particles (Fig. 37), just as that of initial particles, is coated with a dense solid oxide film. However, it differs in structure from the smooth and comparatively even surface of the initial particles: it is speckled with small shallow and randomly arranged creases and folds.

Such a surface is formed during a change in the temperature conditions (cooling) of a body coated with a thin layer of material having a low (with respect to the body) coefficient (volumetric) of thermal expansion β. The layer of aluminum-aluminum oxide, from this point of view, satisfies the above requirements: $\beta_{Al} \approx 3\beta_{Al_2O_3}$, $\beta_{Al} = 33.5 \cdot 10^{-6}$ deg^{-1} in the range $T = 20 - 1000$ C. $\beta_{Al_2O_3} = 8.6 \cdot 10^{-6}$ deg^{-1} in the range $T = 500-600°C$.
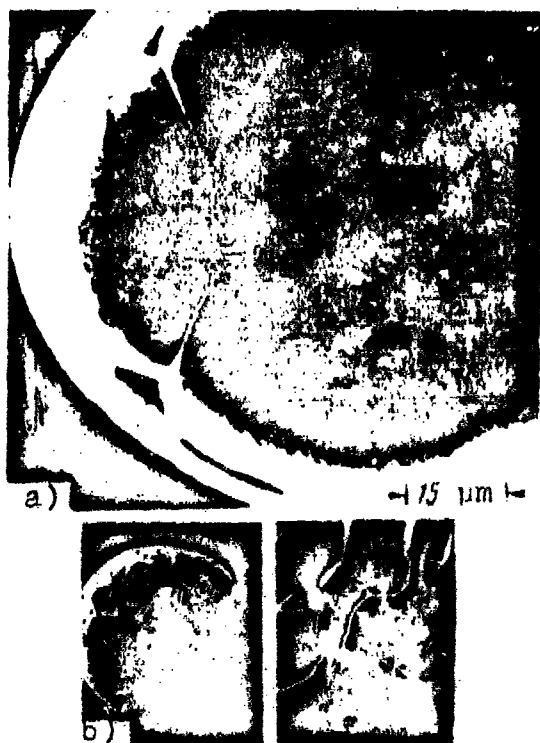

Fig. 37. Surface of initial spherical particle before heating (a) and after passing through the flame zone without ignition (b).

$\dashv$ 15 µm $\vdash$

During heating, the thermal expansion of metal (when particles are heated from 300 to 2300°K, volume increases by approximately 30%) is accompanied by reactions of surface oxidation which restore the continuity of the oxide coating. If, for any reason, heating is stopped, the aluminum while cooling can deform the thin oxide film which coats it, as indicated above.

More specific data on the change in aluminum particle shape with an increase in temperature up to 1400°C are presented in reference [241]. The following three methods and particle heating regime in an air medium are used:

1) heating at a rate of 500°C per minute, on the stage of a microscope, to a temperature of 600 (below the melting point of metal), 690 (above the melting point of aluminum), 854, 1040, and 1200°C;

2) heating at a rate of 1000°C per minute, on a sapphire disk, up to a temperature of 1400°C;

3) heating by the radiation of a CO_2 laser; heating rate 10,000°C per minute.

The surface of the initial particle (d = 100-125 μm) was similar in shape and structure to the surface of a leather ball (see Fig. 37). With heating up to 600°C (regardless of heating rate) the particle undergoes no changes; above 690°C, i.e., above the melting point of the metal, slight individual disturbances begin to appear on the surface. The joining (fusion) of touching particles was being observed (Fig. 38).

Fig. 38. Fusion of Al particles
during high-temperature heating.

Heating particles to 845°C leads to the cracking of the
surface and the formation of wrinkles on it after cooling. A
further increase in temperature up to 1040°C causes more abrupt
changes. Many of the cooled particles are broken, "rumpled"
(Fig. 39a), or hollow. The thin oxide shell peels from the
metal. The inner surface of the shell is even and smooth; the
outer is rougher. The shape of the hollow shells remains spherical;
no folds or creases are present.

At 1200-1400°C the pattern in general is repeated; however,
the thickness of the walls of the oxide shells increases somewhat
and their surface becomes more grooved and rougher (see Fig. 39c).

Increasing the heating rate to 1000°C per minute at 1400°C
causes a sharp decrease in the wall thickness of the shells;
they are now coated with numerous nodes, seams, and cracks
(Fig. 40). Such a structure can be formed if during high-speed
heating the protective film on the particle cracks; in the cracks
pure metal appears, which upon contact with the air oxides rapidly
with the formation of seams and bulges.

Fig. 39. Surface of particles (a) and oxide shell (b, c) after the high-temperature heating of Al in air to 1040°C (a, b) and 1200°C (c).

Designation: мк = μm.

The presence of connections between touching particles is noted [241]. Their appearance is apparently the result of the thermal cracking of the oxide film, which makes possible direct contact between the molten metal of neighboring particles.

An increase in heating rate with the use of a laser technique did not reveal any additional details except for a decrease in the total number of cases of particle fusion at high temperatures (1400°C).

Fig. 40. Outer (a, b) and inner (c, d)
surfaces of oxide shells; T = 1400°C.

The hollow spheres, the complex structures of the shells and
oxide films, the fusion of separate aluminum particles, and, finally,
the existence of a fine subdispersed condensate, which is character-
istic for the burning of aluminum in vapor phase, can be considered
confirmation of the postulate concerning the probability of a
process of active oxidation and evaporation of aluminum at tempera-
tures below boiling point of the metal.

The protective oxide film which coats the surface of particles
during heating can undergo substantial changes even below the
melting point of Al_2O_3. These changes affect the protective
functions of the film. With high heating regimes the surface of
the aluminum can be partially uncovered, thus facilitating evapora-
tion or direct contact between the metal and the oxidizing medium.
The latter is inseparably connected with the problem of aluminum
ignition.

111

2. Ignition Temperature

The first attempts to ignite single particles of aluminum in heated furnaces and tracking installations were not successful. Ignition took place only after the particles were heated to a certain - and very high - ignition temperature. Hill [242] could not ignite aluminum specimens in oxygen and nitrogen (p < 1 atm) at a temperature below 660°C. It is pointed out [145] that at the moment of ignition the temperature of aluminum exceeds the melting point of the metal - 973°K. Cassel and Liebman [136] could not observe the ignition of aluminum when the temperature of the oxidizing medium was below 1400°C.

In a flame of natural gas with air [138] (1500°C) isolated aluminum particles with a diameter of less than 44 μm ignited.

The ignition temperature of separate aluminum particles introduced into a gas flow (flame) with uniform temperature field, composition, and rate (∿10 m/s) was studied in greater detail by Friedman and Macek [133, 134]. A uniform gas flow was created by burning a propane-oxygen-nitrogen mixture or a carbon dioxide-oxygen mixture in a flat burner whose discharge opening was covered with a metal grid. The temperature of the flame was calculated according to the composition of the initial mixture and according to the program which assumes an adiabatically balanced state of the medium (see Fig. 20). The size of the aluminum particles did not exceed 100 μm; the time of their stay in the flame exceeded 20-35 ms. The moment of ignition was established by the abrupt appearance of a bright particle glow.

Figure 41 shows the critical temperature of a propane-oxygen-nitrogen flame, necessary for the ignition of particles 35 μm in diameter depending on their free-oxygen content. For a stoichiometric flame the critical temperature is 2270°K. With an increase in excess oxygen the aluminum ignition limit with

112

respect to temperature drops insignificantly (by 60°K) and does
not depend on the moisture content of the medium. In a medium
with negative oxygen balance the oxidation of aluminum occurs
not only because of the free oxygen but also as a result of inter-
action with water (vapor) and carbon dioxide. The growth of
critical temperature with a change in oxygen concentration in
such a medium occurs abruptly. Particle size has no effect on
ignition temperature.
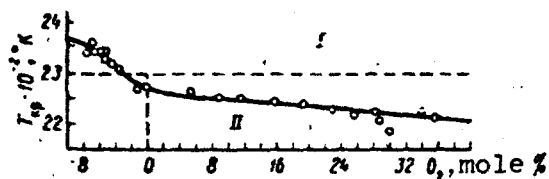
Fig. 41. Critical temperature of
the medium upon the ignition of
Al particles in a propane-oxygen-
nitrogen flame.

In region II there is no burning.
Melting point is 2300°K.

Similar results with respect to ignition of aluminum
particles 35-45 μm in diameter have been obtained in a constant-
pressure instrument at elevated pressure [135] (Fig. 42).

Thus, according to Friedman and Macek, the critical tempera-
ture of the oxidizing medium, necessary for the ignition of
individual aluminum particles (less than 100 μm in diameter),
turned out to be very near (±150°) the melting point of the oxide
Al_2O_3.
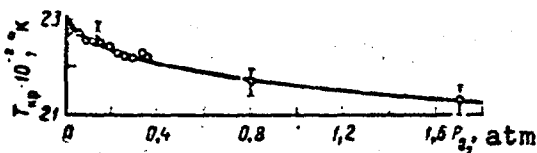
Fig. 42. Critical Al ignition
temperature versus P_{O_2}.

In spite of this assertion, it is noted in reference [243]
that if a drop of aluminum is previously heated in an inert
atmosphere and then the inert gas is abruptly replaced with oxygen,
ignition occurs at a temperature of ~1000°C. The ignition of

thin aluminum wires in water vapor takes place when the temperature of the medium is approximately 1700°K.

On the other hand, heated (by electric current) aluminum tubes 0.95-1.27 mm in diameter with a wall thickness of 0.25 mm and up to 16 cm long could not be ignited at all at a pressure of 1-20 atm in a CO_2-O_2 oxidizing medium [243]. After a temperature equal to the melting point of aluminum was achieved, the tube was destroyed without subsequent ignition.

Brzustowski and Glassman [237], with an optical pyrometer, measured the brightness temperature of thin aluminum wires slowly heated in an oxidizing medium containing pure oxygen. It was found that this temperature (Table 11) does not depend on the pressure of the ambient medium and the previous history of oxide layer formation. It has the same value both in the case of thin wires anodized by the industrial method and in the case where the oxide layer was formed as the wire was heated in the oxidizing medium.

Table 11. Highest values of brightness temperatures during the burning of thin aluminum wires in oxygen.

Pressure	Brightness temperature, °K		Pressure	Brightness temperature, °K	
	anodized wire[1]	pure wire		anodized wire[1]	pure wire
50 mm Hg	2000	1800[2]	4 atm	2025	2025[1]
100 mm Hg	2010	1890[2]	10 atm	2025	2025[1]
300 mm Hg	2010	2000	20 atm	2025	2025[1]
1 atm	2025	2025[1]			

[1]Ignition was observed in all experiments.
[2]No ignition.

Similar results have been obtained in heating anodized and nonanodized wires in a stationary oxidizing CO_2-Ar or O_2-Ar medium in the pressure range 50 mm Hg - 2 atm: regardless of the O_2 concentration in the medium, ignition temperature is also near the melting point of Al_2O_3. The moment of ignition coincides with the direct effect of the ambient atmosphere on the molten active metal during destruction of the wire. At the same time the brightness temperature of the wires (anodized and non anodized) at the moment of ignition in pure oxygen is lower by approximately 150°C than in a CO_2 medium.
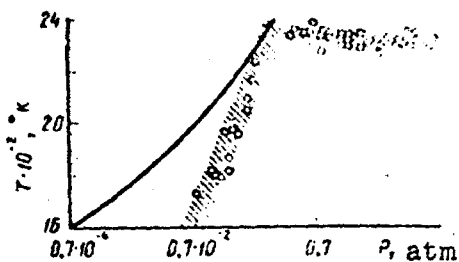
Fig. 43. Brightness temperature of thin aluminum wires at the moment of ignition.

Figure 43 presents data [239] on brightness temperatures of the ignition of thin aluminum wires (links 5-10 cm, diameter 0.25-1.0 mm) in an oxygen argon medium in a wider pressure range. The shaded area corresponds to the interval of experimental data. The solid line corresponds to the pressure of Al vapors.

In the region of pressures above 1 atm the values of brightness temperature for thin wires at the moment of ignition virtually coincide with the melting point of Al_2O_3 and do not depend on the partial pressure of oxygen in the ambient medium. Ignition is connected to the destruction of the wires. At p < 0.5 atm the brightness temperature of ignition drops substantially with a drop in pressure. There is a fully defined correlation between this temperature and the vapor pressure of aluminum. Ignition occurs in gas phase and is connected with the appearance of a flame located a certain distance from the surface of the wire.

115

Of considerable practical interest is the study of the ignition conditions of dispersed metals in the combustion products of solid propellants and powders.

With the use of high-speed color movie photography, Wood [244] performed a qualitative investigation of the burning (p = 35 atm) of thin plates of quick-burning mixed propellants with additives of magnesium and aluminum particles (0.01-10 wt. %). One of the objectives of the study was to determine the location of the ignition of aluminum particles relative to the surface of the propellant (Table 12).

Table 12. Ignition of metal particles in a plastisol propellant [244].

Average nominal diameter of metal particle, μm	Al, %	Ignition of metal
0.1	1	Ignition on the surface
5	1	" " " "
5	10	Ignition on the surface and in the gas flow
15-20	0.02	The same
40	0.15	" "
40	1	" "
40	10	" "
40 (at 7 atm)	10	" "
40 (at 70 atm)	10	" "
80	0.5	No ignition
80	1	" "
80	10	" "
80	8	Ignition directly above surface
5	2	Ignition on the surface
137	1	No ignition
137	1	" "

116

Particles less than 5 µm in diameter, as a rule, ignited on the surface of the propellant. The ignition of particles 40 µm in diameter occurred some distance from the burning surface. The location of ignition for particles of the intermediate fraction 5-20 µm was not constant: ignition occurred both on the surface of the propellant and far from it. Ignition of particles 80-137 µm in diameter could not be recorded within the field of observation (10 mm).

Since the surface temperature of modern condensed systems is usually 500-700°C, it follows that the temperature of the medium in which particles with a diameter of less than 5-10 µm ignite is near the upper limit of this temperature range.

In combustion products of pure ammonium perchlorate (1200°C) aluminum does not ignite at a pressure below 140 atm [134, 245]. The rise in flame temperature due to the mixing of fuel and APC increases the probability of aluminum ignition. However, here the minimum flame temperature at which the particles ignited was 2250-2300°K. In other words, the results of tests by Friedman and Macek [245] on the ignition of aluminum in the flame of gas burners and condensed mixture compositions agree.

Table 13. The fraction of particles which ignited in combustion products of the propellant composition APC-paraformaldehyde when (p = 70 atm) [246].

Propellant composition, %			Flame temperature, °K	Gas composition of flame					Ignition fraction particles
APC	para-formaldehyde	alu-minium		N_2	H_2O	HCl	O_2	CO_2	
99	0	1.0	1300	11.7	35.2	23.5	29.0	—	10^{-2}
90	10	0.1	2200	10.7	41.5	21.1	17.0	9.4	10^{-1}
85	15	0.04	2600	10.1	44.4	20.2	11.4	13.9	1
76	24	0.04	2600	9.1	50.0	18.2	—	22.7	1

117

It is interesting to estimate the probability of the ignition of finely dispersed (53-66 μm) particles of aluminum introduced in the amount 0.01-1.0% into the composition of a two-component mixed propellant (Table 13) [246]. As the specimen burned, metal particles fell into the tongue of a flame of decomposition products from a fuel and oxidizer of a certain composition and temperature.

The most probable temperature of combustion products of heterogeneous condensed systems, in which 100% ignition of individual aluminum particles occurs (in a given experiment), lies in the 2200-2600°K range. Unfortunantely, the geometric parameters of the flame and the dimensions of its high-temperature zone are not indicated in the work. Therefore, the question of the connection between the probability of particle ignition and the time of their stay in this zone, particularly at low temperatures, remains unanswered.

At the same time, excellent data are available for the maximum temperature of combustion products of mixed powders, necessary for the ignition of particles of finely dispersed aluminum. Using thinner spherical powders with an average particle size of 6-10 μm, Pokhil, Logachev, and Mal'tsev [172, 174, 247] found that the ignition temperature of aluminum particles in combustion products of condensed systems is ∼1300°K.

Belyayev, Frolov, and Korotkov [154, 248], having an extended and constant-temperature flow of combustion products from mixed systems in a semiclosed installation, observed similar results. Under these conditions, at a flow temperature of 1600°K, it was possible to observe the ignition of even larger aluminum (d = 70-100 μm). However, as will be shown below, the ignition delay time increased considerably.

118

On the basis of results obtained, it was concluded that the lower limit (temperature) of stable ignition for particles of finely dispersed aluminum in a high-temperature medium of combustion products from mixed condensed systems is a temperature of 1300°K. Apparently the main reason for the disagreement in the evaluation of the minimum temperature of the medium necessary for aluminum ignition is the difference in the dispersity of the experimental material and the time of particle stay in the high-temperature zone.

For example, the time of particle motion in the flow in a semiclosed installation exceeds, by one or more orders, the maximum possible stay time of the same particles in the tongue of a flame from specimens burned in an inert atmosphere in a constant-pressure instrument.

An analysis of the experimental results in determining the temperature limit for the ignition of thin wires and particles of finely dispersed aluminum in an oxidizing medium shows that the most favorable conditions for ignition are realized in a medium of combustion products of heterogeneous condensed systems and powders. The critical temperature of the medium, which ensures satisfactory ignition of aluminum under these conditions, is 1300°K [172, 173].

The critical ignition temperature in the tongue of a flame from gas burners and installations in which electrical heating of specimens was used, as a rule, is significantly higher and is near the melting point of aluminum oxide 2300°K. However, there is apparently no clear boundary between these two cases.

The size of particles and the concentration of active reagents in an oxidizing medium (concentration H_2O, CO_2, O_2) have virtually no noticeable effect (at least in the region of $d = 10-45$ μm) on the critical ignition temperature of aluminum. At the moment of ignition the temperature of the particles is near the melting point of aluminum oxide.

119

3. Ignition Delay Time
(Induction Period)

Most of the familiar quantitative measurements are made in connection with conditions in the flame of a gas burner (p = 1 atm). In determining the delay time of particle ignition, the distance along the trajectory of particle motion between the injection point and the spot where the glow appears and the gas flow rate are directly measured quantities. The ratio x/v_0 determines the so-called "apparent" or "conditional" induction period. In calculating it, we do not take into account the rate of injected particle delay with respect to the supporting flow.

The value of the "apparent" induction period for spherical aluminum particles in a propane-oxygen-nitrogen flame is presented in Fig. 44 and Table 14.

Table 14. Induction period $\tau'_{вп}$ of aluminum particles (T = 2510°K) [134].

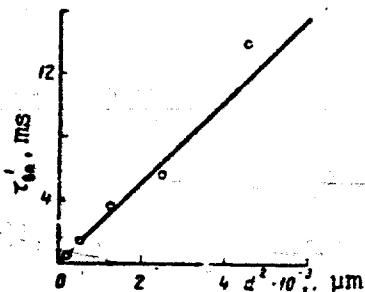| Average diameter of aluminum particles, μm	O_2 concentration, %	H_2O concentration, %	$\tau'_{вп}$, m/s
35	5.8	18.1	1.6 ± 0.4
49	5.8	18.1	11.7 ± 0.7
35	7.9	0.5	10.7 ± 1.0
49	7.9	0.5	16.5

Fig. 44. Ignition time ($\tau'_{вп}$) of aluminum particles as a function of d^2.

The main mass of the particles ignited 10-150 mm above the injection zone. With satisfactory accuracy $\tau'_{вп}$ (see Fig. 44) is subject to square law $\tau'_{вп} \sim d^2$ regardless of the moisture content of the medium.

Just as critical ignition temperature, $\tau'_{вп}$ is a very weak function of the concentration of active reagents in the medium. A change in the total concentration of $H_2O + O_2$ by a factor of 3 reduces $\tau_{вп}$ by no more than 40% (see Table 14); the greatest changes occur in the region of low concentration.

To calculate the actual value of $\tau_{вп}$, Friedman and Macek [133] proposed to introduce a correction for the velocity delay of the particles:

if the injection velocity is zero[1]

$$\tau_{вп} = \tau'_{вп} + \theta\,[1 - \exp\,(-\tau/\theta)]$$

and

$$\tau_{вп} = \tau'_{вп} + \theta\,[1 - \exp\,(-\tau/\theta)]\left(1 - \frac{V'}{V_0}\right). \qquad (III.1)$$

if the particles are introduced into a hot flow with a velocity of V'. Here

$$\theta = \frac{d^2 \rho}{18\eta}.$$

where d is the diameter of the particle; ρ is the density of the metal; η is the viscosity of the gas in the boundary layer of the particle; V_0 is the velocity of the gas.

_____

[1]From the ratio of Stokes and Newton forces the velocity of particle motion V(t) is given in the form of $V(t) = V_0 \exp\,(-t/\theta)$. The time is found from the solution to equation

$$z = V_0\tau' = \int_0^\tau [V_0 - V_0\exp\,(-t/\theta)]\,dt.$$

Since $\tau'_{вп}$ and θ are proportional to d^2, the induction period of the particles, with a correction for the lag behind flow, is also proportional to d^2. However, the size of this correction can be quite substantial. For particles with a diameter of 50 μm $\tau_{вп}/\tau'_{вп} = 1.9$, i.e., the "actual" ignition delay time must be 12.7 ms (when $\eta = 5 \cdot 10^{-4}$ poise) instead of 6.6 ms [133].

Along with a weak sensitivity to the moisture content and the concentration of the oxidizer in the medium, $\tau_{вп}$ virtually does not react to the degree of activity of the ambient atmosphere and, particularly, to the presence or absence of pure oxygen in the medium.

Presented below are the values of the induction period for aluminum particles of the 53-66 μm fraction in the flame of a gas burner with a temperature of 2610°K [246]:

Original gas mixture	Composition of medium (flame)	Induction period $\tau'_{вп}$, ms
CO + 1.5 O_2	CO_2 + O_2	10
CO + 0.5 O_2 + N_2	CO_2 + N_2	10

In spite of the fact that pure oxygen is present in the flame as the basic component in the first variant while a flame of the second type is diluted in half by nitrogen, the ignition delay time in both cases is identical and proportional to d^2. The temperature of the medium is another matter. Just as for drops of liquid hydrocarbons and solid carbon particles, this parameter is decisive in the ignition of metal particles (Fig. 45). A temperature increase of only 400° in the ambient medium (from 2500 to 2900°K), for example, increases the possibility of aluminum ignition by a factor of 2 [246].

This result is completely regular since the value of the induction period, in the first place, is determined by the heating of the particles from initial to critical ignition temperature. The main form of the heat exchange of a particle with the ambient medium, in this stage, is thermal conductivity in the laminar boundary layer (induced film) of the particle. Therefore, the heating rate is a function of the temperature level of the medium and the particle and the gradient dT/dR on the medium-particle boundary.

The nearness of the results presented in Table 14 and Figs. 44 and 45, taking into account the differences in the ambient temperature and initial particle size, underscores once more the decisive role of temperature and particle size as the main parameters in determining $\tau_{\text{вп}}$.

We should also note that the chemical composition of combustion products of heterogeneous systems, as we have already repeatedly emphasized, is quite complex. In combustion products of compositions based on an APC oxidizer, in addition to the basic oxidizing oxygen-containing reagents, HCl, N_2, and others are contained in considerable quantity. In an installation with a semiclosed volume, for the ignition delay time of the aluminum introduced into a condensed system (0.01-1.0% by weight), the authors of reference [154] took the time figured from the moment of particle escape from the surface of the specimen to the appearance of the flash. The time required for particle warm-up in the reaction layer of the powder and on the burning surface of the specimen, i.e. up to a temperature of 500-700°C, was not taken into account.

The greatest changes in the value of $\tau_{\text{вп}}$ are obtained during a variation in the temperature of the gas flow (Fig. 46).
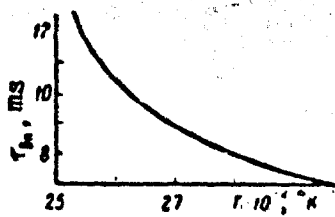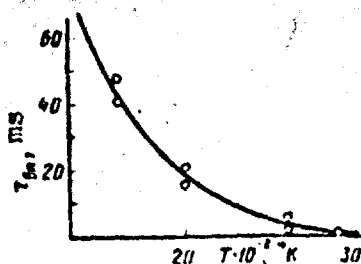
Fig. 45.   Fig. 46.

Fig. 45. Ignition time for Al particles (d = 53-56 μm, CO–O_2 medium) versus temperature.

Fig. 46. Ignition time for Al particles (d = 70 μm) in combustion products of condensed systems versus temperature.

As the temperature of the medium drops the ignition time for aluminum increases sharply and at a temperature of less than 2000°K begins to considerably exceed the combustion time ($\tau_r =$ = 9.5 ms). On the other hand, at high temperatures on the order of 3000°K, even with comparatively large particles (70 μm) the ignition time is brief and falls within 1-2 ms.

However, unlike temperature, the composition of the gas flow and the pressure (p > 10 atm) affect $\tau_{вп}$ only slightly. The differences observed in the experimental data fall within the range of measurement error. However, we can see nevertheless that with a sharp increase in H_2O and CO_2 concentration (up to 70%) the time of $\tau_{вп}$ decreases somewhat.

With a change to particles of another size (d < 200 μm), these regularities do not change qualitatively. In absolute value, however, $\tau_{вп}$ increases in proportion to the square of particle diameter.

In the general case, the ignition time of aluminum particles in combustion products of mixed compositions based on APC is satisfactorily described for d = 70 μm by an exponential function of the type $\tau_{вп} = 3.6 \cdot 10^{-6} \exp (32,000/RT)$, ms. These data are also presented below:

T, °K	1600	2000	2400	2800	3000
τ_{en} (exp), ms	60	18	6	2	1
τ_{en} (calc.) ms	72	18	5.0	1.8	1

Thus, the main parameter determining the ignition delay time of aluminum particles in combustion products of heterogeneous condensed systems is the temperature of the gas flow. The pressure and the gas composition of the medium, in this respect, is secondary. Just as in gas burners, τ_{en} is proportional to the square of the diameter of the initial particles.

At the present time there is no precise analytical solution to the problem of the ignition of metal particles having a dense protective oxide film.

Friedman and Macek [133] have proposed a formula for calculating the τ_{en} time based on the results of their experiments on the ignition of particles of finely dispersed aluminum in the flame of a gas burner in accordance with their assumption that the moment of ignition agrees with the phase transition of the oxide protective layer from solid state to liquid state, as a result of which the metal oxidation rate increases sharply.

The derivation of the formula is based on the assumption that particle warm-up from initial temperature T_0 to temperature $T_{кр}$ (near the melting point of aluminum oxide (see Fig. 41)) is accomplished by thermal conductivity from the medium with T_∞ in the thin boundary layer surrounding the particle. According to the conditions of the experiment for which this calculation is made, it is assumed that the Nu number = 2, the Re number = = 0.01-2 (for particles with d = 50 μm), and radiation (during ignition) can be disregarded. Finally, the expression for calculating the induction period is written in the form

$$\tau_{нп} = \frac{\rho d^2}{12\lambda}\left(c \ln \frac{T_\infty - T_0}{T_\infty - T_{кр}} + \frac{L}{T_\infty - T_{пл}}\right).$$ (III.2)

125

where ρ, c, L are the density, the specific heat capacity and the latent heat of fusion of the aluminum; λ is the coefficient of thermal conductivity of the gas (assumed to be independent of temperature).

Just as in the experiment, $\tau_{вн}$, according to (III.2), is proportional to d^2 and gives a fair agreement with the experiment.

At values of $\lambda = 2.1\cdot10^{-4}$ cal/cm·s·deg, $T_\infty = 2510°K$, $T_{пл} = 2230°K$ (see Fig. 41) and standard values for ρ, c, and L, the induction period $\tau_{вн}$ for particles with a diameter of 50 μm, calculated according to formula (III.2), is 16.1 ms. The experimental value for these same conditions (with correction for velocity lag) is 12.7 ms [133].

However, the region of application for formula (III.2) is apparently very limited. This is primarily related to the ignition of aluminum in the combustion products of the powders.

4. The Effect of the Concentration
of Metal Particles on the Ignition
Temperature and the Period of
Induction for Aluminum

The problem of the effect of metal concentration on the basic parameters of ignition - critical temperature and induction period - is solved unambiguously. In virtually all cases an increase in particle concentration reduces the temperature of the medium, during which particle ignition begins and $\tau_{вн}$ decreases.

The particles become easily ignitable even at a comparatively low temperature of the medium (or flame), in which single particles do not ignite at all.

In a CO_2 atmosphere, fine aluminum powder with an average particle size of 0.03 μm, placed in a test tube, begins to ignite at 360-420°C [249]. The aluminum powder which deposited

on the base in the form of a dust layer will ignite in air at a higher temperature, 585°C. If the same aluminum forms an air-suspension with air, the ignition temperature is 645°C [250]. In other words, thermal ignition of the deposited powder occurs at a lower temperature than the ignition of the same powder suspended in air.

If an electric discharge (spark) is the ignition source, the ignition energy of the aluminum air cloud is a function of particle size: for finer particles less energy is required [250]; this energy remains constant over a wide range of metal particle concentrations.

The ignition of a cloud containing a broad spectrum of particle sizes is generally determined by the smallest particles present. Figure 47 presents data on the ignition temperature of aluminum dust in an oxygen flow as a function of the average particle size [250].

The ignition of spherical powdered aluminum in combustion products of mixed compositions is also noticeably facilitated with an increase in particle concentration to 5-20% [173, 206, 251]. The aluminum becomes easily ignitable even at flame temperatures at which the ignition of single particles is not generally ovserved.

In a composition having a maximum burning temperature of 2400°K, the ignition delay time of particles with a diameter of 70 μm, only as a result of an increase in metal concentration to 10% (by weight), drops by more than 5: from 6 to ∿1 ms. Particles with a diameter of 15-20 μm and less, under these conditions, are ignited almost directly on the surface of the specimen.

The general tendencies of the change in τ_{BH} for aluminum particles, when the aluminum content in heterogeneous condensed systems is increased to 10%, become clear from a comparison of Fig. 46 and Fig. 48.
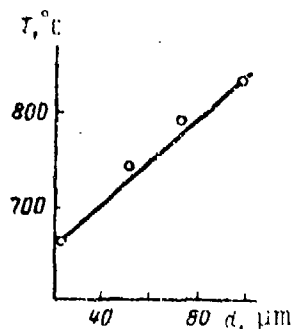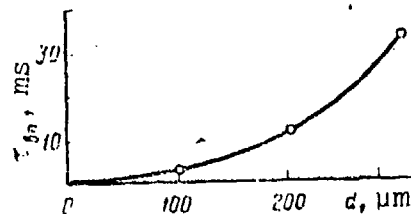
Fig. 47.   Fig. 48.

Fig. 47.   Ignition temperature for aluminum dust in oxygen.
Fig. 48. τ_{BH} of Al particles (d = 70 μm) in combustion products of condensed systems as a function of particle diameter (Al concentration is 10%).

A reduction in the induction period for large particles can be observed not only with an increase in their concentration. A similar effect can also be achieved if a small amount of finer particles of the same or more easily ignitable metal is mixed in.   Thus, for example, if 2% of the particles have a diameter of ~5 μm, the particles with a diameter of 80 μm are ignited at a considerably shorter distance from the surface of the specimen than is the case without the finer particles [244]. The decrease in the induction period of aluminum particles with an increase in their concentration in the gas flow or in the combustion products of heterogeneous condensed systems has a reasonable explanation within the framework of heat theory.

The ignition of particles is determined by the conditions of their heating in an ambient gaseous atmosphere up to ignition temperature.   These conditions, to a considerable degree, depend

on the temperature of the medium. For the total group of particles, heat released from their surface causes a general increase in ambient temperature, especially if additional self-heating occurs on the surface because of oxidation reactions. In addition, if particles are fed continuously into a gas flow (for example, during the burning of metallized powders) and the process develops into self-sustaining burning, then, because of the considerable thermal effect of the burning of a large amount of aluminum, the heating of newly arriving particles is determined not only by their heat exchange with the ambient medium but also by the additional heat supply (thermal conductivity and radiation) from the burning zone.

As a result of this, the heating rate of the particles increases and their $\tau_{вп}$ decreases.

5. The Physical Nature of Ignition
Processes in Aluminum Particles

Aluminum is a metal which has high reactivity in a high-temperature oxidizing medium. Under natural conditions, its surface is coated with a solid protective layer of oxide.

There is a direct connection between the kinetic reactions of surface oxidation and the properties of the oxide being formed [13]. If the volume of oxide is less than the volume of metal involved in the oxidation reaction V_{Me} (Pilling-Bedworth criterion $\beta = V_{ок}/V_{Me}$ less than one), a solid oxide film cannot form on the surface of the metal. Oxide, as a rule, is porous, as a result of which the surface of the metal is always open for oxidizer access. The rate of the oxidation reaction depends only slightly on the growth rate and character of the oxide coating on the metal surface and changes according to linear law.

If the Pilling-Bedworth criterion is more than one, then during oxidation on the surface of the metal a solid oxide layer builds up and the reaction continues only because of the diffusion of the oxide through this layer. The reaction rate is inversely proportional to the thickness of the oxide film; oxidation rate changes according to parabolic law.

The greatest density and, consequently, the best protective properties are found in oxide films of metals for which $1.0 < \beta < 1.5$. With large values for β the oxide layer, as it grows, experiences considerable internal stress and can crack. In this case, its protective functions drop sharply. For aluminum the value of the β criterion is near one ($\beta = 1.3$). Because of this, the surface layer of oxide on aluminum is very dense and has good protective properties. At room temperature in air, the thickness of the oxide layer grows to 50-100 Å in the first 5-10 days and then is virtually constant [252].

In the general case, the process of aluminum oxidation is an exothermic process whose rate increases with an increase in temperature.

In the 350-475°C range the oxidation rate constant conforms with satisfactory accuracy to the Arrhenius equation with activation energy $E = 22.8$ kcal/mole

$$k = A \exp(-E/RT).$$

According to established concepts, as the ignition temperature we take that minimum temperature of the particles or medium at which heat release from the oxidation reaction of the metal exceeds heat loss to the surrounding space and the temperature of the particle begins to rise with an increasing rate. The time required for the metal to warm up from the initial temperature to a temperature at which this condition begins to be fulfilled generally determines the ignition delay time.

130

At low particle temperatures the oxidation rate of the aluminum is quite low because of the presence of the solid protective oxide layer on its surface. Therefore, even in a high-temperature oxidizing medium, particle warm-up before a certain moment can be considered exclusively as a heat exchange process. This critical moment can be the phase for crystal-structure variations in the oxide film which are connected with temperature.

One of them is the melting of the oxide film, which abruptly increases the oxide flow to the surface of the metal. This increase is the result of a reduction in the diffusion resistance of the oxide film. According to this hypothesis, aluminum particles ignite when their temperature reaches the melting point of aluminum oxide, i.e., ~2300°K. The advantage of this is indicated by experimental data on determining the ignition temperature and induction periods of aluminum particles in the flames of gas burners and thin aluminum wires heated by electric current (see Sections 1, 2, 3).

The difference between the ignition temperature of particles and the melting point of Al_2O_3 is considered the measure of self-heating from the oxidation reaction. Under stationary conditions, based on the balance between the effect of the exothermic oxidation reaction and the heat-mass transfer in the gas, the connection between $T_{nn \cdot Al_2O_3}$ and $T_{\kappa p}$ is given by the expression [254]

$$T_{n\Lambda} - T_{\kappa p} = \frac{Q\lambda}{\eth \lambda} \, k\,(p_{O_2}/RT_{n\Lambda}) = kp_{O_2}^n,$$ (III.3)

[$n\Lambda$ = melting; p = critical]

where Q is the exothermic effect of the reaction; $k(p_{O_2}/RT_{n\Lambda})$ is the oxidation rate on the surface of the particle through a solid layer of Al_2O_3 at a temperature of 2300°K; n is the order of reaction with oxygen.

131

The processing of the experimental results presented in
Fig. 42 indicated that the numerical value of n is 0.41-0.5.
This shows a slight dependence of ignition temperature on oxygen
concentration in the atmosphere, i.e., the activity of the
medium.

Since the melting point of aluminum oxide changes only slightly
with pressure, the critical ignition temperature of particles
is virtually constant in a wide range of pressures (p > 1 atm)
and particles sizes. At the final stage of the transition of
the induction period to self-sustaining burning, the aluminum
ignition process is a heterogeneous process. The oxidation
reaction occurs on the surface of the particle along the
metal oxide interface. The exothermic effect of the reaction
ensures the subsequent self-heating of the particle to the boiling
point of aluminum and, as we shall see below, the transition of
the reaction to vapor phase.

The induction period, since it is generally determined by
heat exchange with the ambient medium, is proportional to the
square of particle diameter.

This method of aluminum ignition through the melting of
the oxide film is obviously not the only one. It does not
explain the ignition of aluminum particles at lower temperatures
in the combustion products of heterogeneous condensed systems
[172, 173, 206].

Significant in this respect also is the ignition of
electrically heated thin aluminum wires in an oxygen-containing
medium in the region of vacuum pressures. The ignition process
has a gas-phase nature and sets in at that moment when the
temperature of the wire is equal or exceeds the boiling point
of aluminum. Although at such temperatures the oxide shell is
still solid (Fig. 43), its physical integrity is impaired. This

is easily seen, for example, in Fig. 34, where separate streams coming from the surface of a wire coated with a porous layer of Al_2O_3 are revealed. The ignition of aluminum occurs because of the impairment of the oxide shell's structure; however, this is not because of phase transition (melting) but as a result of cracking and breaking of the oxide shell by the vapor of the metal and the diffusion of the latter into gas phase. The difference in the coefficients β of volume expansion for metal and oxide, to a certain extent, contributes to this.

If we assume that a spherical particle of aluminum is uniformly coated with a shell of Al_2O_3, then from strength considerations we can derive the following expression for evaluating the temperature at which a break occurs in the middle section of the shell:

$$\Delta t = \left[\frac{E(3 - \beta')R}{2\sigma\delta} - 3\beta' \right]^{-1} \simeq \frac{2\sigma\delta}{ER(3 - \beta')} \, ,$$

where $E = 0.7 \cdot 10^6$ kg/cm^2 is the modulus of elasticity for Al_2O_3; R is the radius of the particle, cm; $\sigma = 2.1 \cdot 10^3$ kg/cm^2 is the ultimate strength for Al_2O_3; δ is the thickness of the oxide film, cm.

If $R = 10^{-3}$ cm, $\delta = 10^{-4}$ cm, then $\Delta t \approx 30°C$.

In the combustion products of heterogeneous condensed systems and powders at atmospheric pressure and above, the minimum temperature of the medium at which aluminum particle ignition is observed is noticeably lower than the boiling point of the metal and almost 1000° less than the melting point of Al_2O_3. Therefore, under these conditions, the process of aluminum ignition cannot be limited either by the melting of the protective oxide film coating the particle or by its disruption by vapor-phase metal. At the same time, it is doubtful that, in this case, ignition is connected with a disturbance in the density of the diffusion barrier created by the oxide film.

133

An analysis of the pattern of variation in the surface structure of aluminum particles as a function of their heating mode in an oxidizing atmosphere provides a partial answer to the question of how this disruption occurs (see page 84)[1].

With low-speed heating (8-10 deg/s) the surface of the particle is coated with a dense "rough" oxide shell having inhomogeneities which are the result of the "healing" of cracks which occur in the shell during heating (to a temperature > 1040°C) because of the differences in the coefficients of thermal expansion for aluminum and its oxide. The cracks are not numerous and the active aluminum passing through them oxides rapidly and restores the protective functions of the oxide shell apparently without substantial self-heating of the particle. However, even under these conditions (at 1000°C), part of the aluminum manages to react.

With an increase in heating rate to 20 deg/s and more, the surface of the particle undergoes susbstantial changes, indicating a sharp intensification of the process of shell cracking and metal oxidation. The shell remains thin-walled; however, it is broken up with a dense network of fine seams and creases (see Fig. 40). Moreover, many shells turn out to be hollow. Among the final products of the heating are subdispersed particles of oxide whose presence is characteristic for the vapor-phase reaction. Under these conditions, the exothermic effect of the oxidation reaction must be more appreciable and the self-heating of the particles more powerful. This eases the requirements imposed on the minimum temperature of the medium which ensures particle ignition.

---

[1]This refers to page 84 of the original Russian document, the translation of which appears on pages 108, 109.- Translator's Note.

In the burning of powders, particles are in even more rigorous conditions of high-speed heating. If we assume that the surface temperature of a mixed composition on the average is 600-800°C, the coefficient of thermal diffusivity $\kappa = 1 \cdot 10^{-3}$ $cm^2.s^{-1}$, and the rate of normal burning u ± 5-10 mm/s, then the time required for particles to pass through the heated layer with a 700°C drop in temperature is, in order of magnitude, near

$$\tau \approx \frac{\kappa}{u^2} \approx 2 \cdot 10^{-4} \text{ s.}$$

Hence the heating rate for a substance and a particle in the reaction layer of the powder is, in order of magnitude, $\sim 10^5$ deg/s. Upon entering gas phase, a particle is subject to comparable heating modes.

For this reason, the hypothesis of oxide film destruction is apparently fully valid. Intensive self-heating of a particle and the reduction of the minimum temperature of the medium, at which heat release from the oxidation begins to exceed heat loss to the outside, finally becomes possible. According to experimental data [172, 173, 206, 247, 248], for mixed condensed systems this temperature is $\approx 1300°K$.

It should be mentioned that in a medium of decomposition products and the burning of mixed powders based on ammonium perchlorate there is a large amount of chlorine and its compounds. In the interaction of aluminum with chlorine, aluminum chloride is formed [143] which has a very low (450°K) temperature of vaporization (sublimation). The reaction $Al + 1.5 Cl_2 = AlCl_3 + 162$ kcal is accompanied by heat release which is, it is true, weaker than in the reaction of aluminum with O_2, H_2O, or CO_2. However, if such an interaction occurs, even partially, where the molten aluminum comes in direct contact with the ambient medium, this undoubtedly must facilitate ignition at lower temperatures of the medium.

Since the induction period, even in this case, is generally determined by the heat exchange of a particle with the medium (at least up to a temperature of 1300°K), its value is proportional to the square of particle diameter.

However, $\tau_{вп}$ is reduced quantitatively (as compared with gas burners and track installations) since particle self-heating from the oxidation reaction begins to play a substantial role when a temperature of 1300-1500°K is achieved, and the process is sharply accelerated.

If we maintain the condition that the main form of heat exchange between particle and medium in the induction period is thermal conductivity, i.e., time τ required for a particle to heat up to temperature $T_{кр}$ in a medium with temperature T_∞ is proportional to

$$\tau \sim \ln \frac{T_\infty - T_0}{T_\infty - T_{кр}},$$

then we can evaluate the relationship between the times required for particles to heat up to $T_{1кр} = 1300°K$ and $T_{2кр} = 2300°K$. For a medium with $T_\infty = 2500-3000°K$, it is 3.5-4.0.

From a comparison of experimental data it follows that the induction period of particles injected into a flame from a gas burner with a temperature of 2500-3000°K (Fig. 45) exceeds, by a factor of approximately 3, the $\tau_{вп}$ of particles introduced into a composition of heterogeneous condensed systems (see Fig. 46). Introducing a correction for particle velocity lag makes this difference even greater.

Such a correlation of results is obviously not accidental and indirectly confirms the soundness of the evaluation of the critical ignition temperature of aluminum particles in the above media and the reasons advanced to support them.

Thus, the minimum critical temperature for the medium, which ensures aluminum particle ignition, is determined by the intensity of the heat exchange with the ambient medium, the properties of the medium, and the nature of the impairment of the protective functions of the oxide coating.

In many respects, the latter also depends on the purity and method of obtaining the oxide. The presence of impurities, anodization, and amalgamation reduce its density and strength during heating, thereby facilitating the ignition of aluminum.

§ 2. Ignition of Beryllium

Beryllium (Be) is one of the most effective metals from the energy point of view. Just as aluminum, it belongs to the class of "volatile metals" [143]. The boiling point of beryllium ($T_{кип}$ = 2757°K) is below the boiling point of its stable oxide BeO ($T_{кип}$ = 4120°K) and below, though only slightly, its melting point ($T_{пл}$ = 2830°K).

Beryllium, just as aluminum, is an extremely reactive element. However, under ordinary conditions, its activity is surpressed by the presence of a protective oxide film on the surface.

For beryllium the ratio of the volume of oxide to the volume of the reacting metal – the Pilling-Bedworth criterion – is β = 1.68. This is an indication of the high density of the surface oxide layer and its protective properties.

At the present time, there is very little information on the ignition and burning of beryllium. The main obstacles to the development of experimental works in this direction and the barrier to wide practical use of Be in rocket propellants is the toxicity of its combustion products [69].

Therefore, the pattern of ignition examined below and the conclusions ensuing from it should be considered preliminary.

1. General Pattern of Beryllium Ignition

The ignition of beryllium particles is possible only in a chemically active medium at high temperatures. The ignition process is less clearly expressed in beryllium than in aluminum. Although with the latter the transition to stationary burning is accompanied by a sudden manifold increase in the brightness of the track or the glow of the particle, a beryllium particle begins to glow rather intensely long before the onset of the burning stage. In a medium with a low oxygen content (less than 16%) the transition from the induction period to burning has no clearly expressed boundary and is virtually indistinguishable. This imposes a certain uncertainty on the establishment of quantitative ignition parameters for Be particles.

Heating [241] small Be particles (on a sapphire disk) in an air atmosphere to 1570°K, which is above the melting point of the metal, and maintaining them at this temperature for 4 seconds did not lead to ignition. However, during heating, the particles gradually lost their initial spherical shape and did not regain it subsequently (Fig. 49).

After heating, some of the particles became transparent. However, the majority were coated with a rough nontransparent shell marked with deep cracks. This oxide shell consists of two layers. The upper, rather thick layer has a loose coarse structure and is connected rather weakly with the particle. It does not have good protective properties and, consequently, cannot protect the metal from further oxidation. The second dense layer of oxide, which has a dark color, is located under the first and tightly connected directly to the surface of the metal. In spite of its thinness, this layer is the main obstacle to oxidation of the active metal.

138
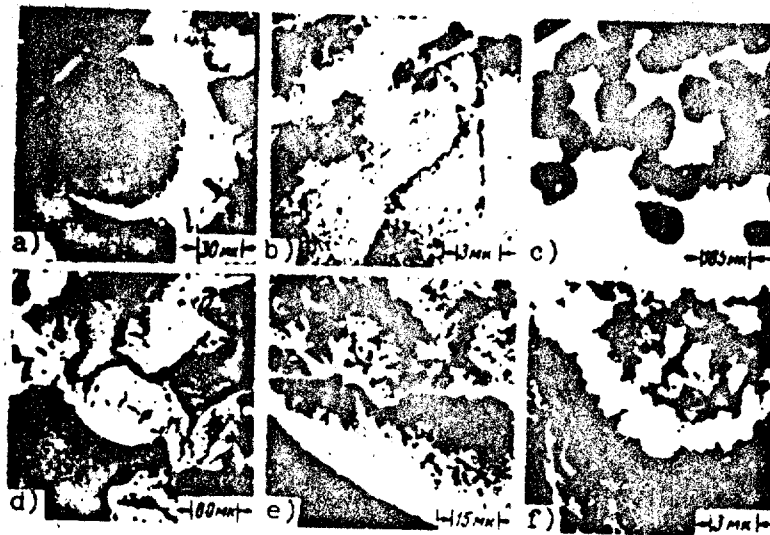
Fig. 49. Spherical particles of Be before
(a, b) and after heating in air to 1570°K
(c, d, e, f).

Designation: мк = μm.

The complex structure of the oxide film hinders the fusion
of touching particles during heating above the melting point of
the pure metal; however, it does not completely exclude this
phenomenon (Fig. 49). Interesting results were obtained in an
observation of the behavior of a thin beryllium foil heated by
a flash bulb [241] in an oxygen (20%)-argon medium (Fig. 50).
Separate holes appear in the foil at the first moment. The
reason for their appearance, apparently, is the presence in the
foil of active impurities which, with an increase in temperature,
become the localized centers of a chemical reaction. Then on
the backing around it appears a halo of subdispersed oxide,
which is usually the proof of a vapor-phase reaction. The
intensity of the formation of subdispersed particles and the
glow of the foil, particularly along the edges of the holes, are
even greater in this stage than in the subsequent stages of
burning. When the melting point is reached, a spherical particle

coated with an oxide layer is formed from the piece of foil.
If the ambient medium does not contain water vapor, the oxide is
very durable and has high reflectivity. The presence of moisture
in the medium leads to the appearance of the oxide shell consisting
of two layers which we discussed above. The fact of the existence
of subdispersed oxide at temperatures near, but not exceeding, the
melting point of the metal is quite significant. This means that
even in this state Be has very noticeable vapor pressure and the
protective properties of its oxide shell are more comparable with
aluminum. The density of the oxide coating is a function not
only of the composition of the medium in which Be oxidation occurs;
it depends greatly on the method of processing and the degree of
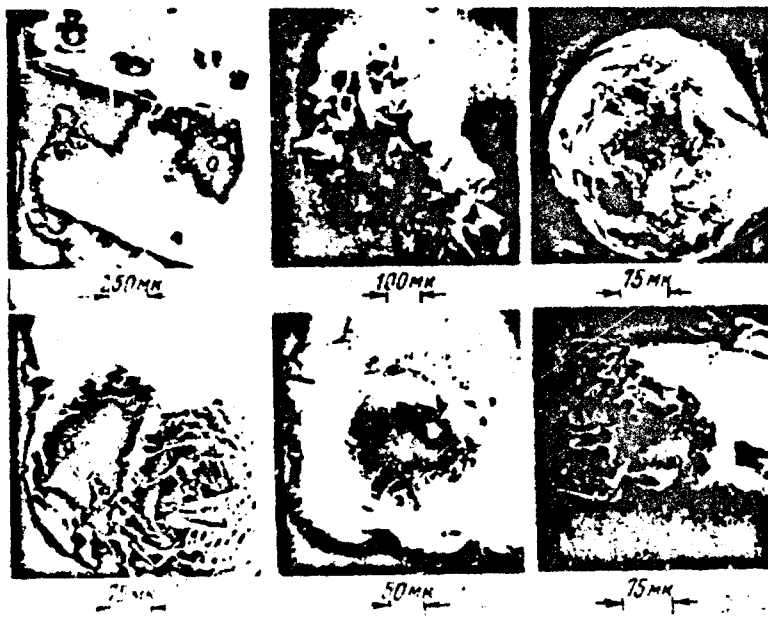surface purity of the initial material.

Fig. 50. Behavior of beryllium foil during
heating (P < 1 atm) in an O_2-Ar medium by a
flashbulb.

Designation: мн = μm.

Table 15 presents data on the degree of purity and the method of processing the surface of wires whose behavior was studied during heating in various gaseous media [253].

Table 15. Characteristics of beryllium wires [253].

Type	Processing technique	Degree of purity Be, %	Special processing
I	Drawing	96	
II	Drawing and annealing	96	
III	Drawing, annealing, etching	98	
IV	Drawing and annealing	98	Etching and coating of Fe
V	" " "	98	Etching and coating of Cu
VI	Drawing, annealing, etching	98	

The initial pressure (7 atm) and characteristic dimensions of the specimen (diameter 0.5 mm and length 50-100 mm) excluded the effect of these parameters on the heating and ignition of the wires.

Wires of types I and II were coated with an oxide layer (the weight of the oxide was 2% of the weight of the wire). During heating in an inert medium - argon, which prevents additional oxide formation - these wires elongate and sag when the melting point is reached. Further heating causes the wires to begin to stretch again between the electrodes (at a temperature 470-700°C below the melting point of BeO) and then to break. Rupture usually occurs at the melting point of BeO.

Wires of types V and VI, which, unlike the preceding type, were coated with a thinner layer of oxide (1%), broke in argon at a temperature 500°C below the melting point of BeO. The application of a coating of iron or chromium on the surface of etched beryllium did not change the strength of the oxide shell.

141

Experimental data indicates that in the behavior during heating there is much in common with aluminum. However, at the same time, there are certain differences.

In the first place, there is the structure of the oxide film and its properties, the process of transition to the stage of self-sustaining burning, and the strength of the oxide coating.

2. Particle Ignition Temperature

One of the determining factors in the ignition of Be is the strength of its oxide coating.

Type I wires (see Table 15), whose surface after drawing is coated with a thin layer of lubricant which is difficult to remove, broke in an oxygen atmosphere at 1940°K. Ignition did not occur. After preliminary annealing (type II), the wires ignited in the 2400-2820°K range without breaking. Before ignition, separate bright areas with higher temperature, near the melting point of BeO, appeared on the surface of the wire. The application of a thin film of iron on the surface of the wires (type IV) did not change the pattern of oxidation and ignition in Be. Chrome-plating has a different effect. Wires began to break at temperatures only approximately 100° above the melting point of Be. The process had a local character. However, ignition did not occur even in a medium of pure oxygen (P = 7 atm). The reason for such variation lies in the fact that chrome-plating prevents the oxidation of beryllium during heating and thus eliminates the growth of the oxide film on the surface of the metal. Actually, the preliminary oxidation of the etched wires in an air atmosphere (type V) increased their breaking temperature by almost 500°C (100°C above melting point). The breaking process ended with ignition.

With respect to ignition temperature, type III wires occupy an intermediate position between types II and VI.

The composition of the oxidizing medium is no less important than the state of the surface for the ignition of Be (Fig. 51).

The effect of oxidizer concentration on the temperature of the medium at which the ignition of finally dispersed beryllium particles is ensured, in the first approximation, is experimentally traced in reference [135]. If the temperature of a hydrogen-oxygen flame (O_2 < 20%) did not exceed 2600°K, particles with a diameter of 30-35 μm virtually did not ignite. For a flame with a lower concentration of free oxygen, this critical level for the temperature of the medium increased, gradually approaching $T_{кип}$ = = 2750°K. However, even in the case of a high oxygen concentration in a flame (O_2 > 20%), we cannot speak strictly of the existence of a maximum critical temperature for the medium, as we did with aluminum. In the 2600-2800°K range the number of igniting particles did not exceed 30%. In dry atmosphere, other conditions being equal, the total percent of ignition was higher than it was in the presence of H_2O [254]. At 2900°K in a hydrogen-oxygen atmosphere, almost 100% of Be particles ignite.
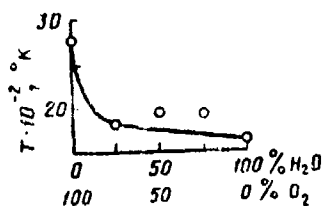
Fig. 51. Ignition temperature of thin beryllium wires in an H_2O-O_2 medium; P = 7 atm.

These data are very limited. However, they confirm [129] (also very limited) the results of the ignition of finely dispersed particles of beryllium (d = 35-45 μm) in a complex flame of combustion products from a system of ammonium perchlorate-trihydroxymethylene, whose characteristics are presented in Fig. 22. Full pressure in the installation varied from 2.4 to 50 atm.

Particles began to ignite at a temperature around 2380°K if partial oxygen pressure exceeded 4-6 atm. As the oxygen concentration in the flame decreased the ignition of beryllium became more difficult and at $P_{O_2} < 0.1$ atm failures were observed even at temperatures near 2650°K. Thus, in enriched fuel mixtures the critical temperature of the flame, necessary for the ignition of individual particles, approaches the boiling point of beryllium (Fig. 52). Let us emphasize that, in this case, we are speaking of the temperature of medium and not the temperature of the particles at the moment of ignition, as was the case during the ignition or breaking of thin wires heated electrically. For the latter the heating mode and heat losses can differ sharply from those of particles. Undoubtedly, for beryllium the self-heating of particles due to heat release during the chemical reaction of high-temperature oxidation plays a more noticeable role than for aluminum.

Fig. 52. Ignition temperature of beryllium particles as a function of P_{O_2}. Solid line corresponds to ignition limit. □ - no ignition; ○ - ignition.

3. Induction Period

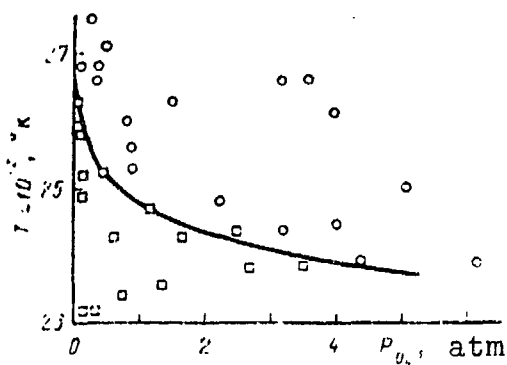Quantitative parameters for the ignition of Be particles are determined under the specific conditions of the flame from a gas burner (P = 1 atm, partial pressure of oxygen 0.16-0.43 atm, of carbon dioxide 0.42-0.56 atm, T = 2400-2920°K) [254].

144

The dependence of the experimental $\tau'_{вп}$ on diameter is not subject to square law: $\tau'_{вп} \sim d^{2.5}$.

Table 16 presents the values of the directly measured, i.e., "conventional," induction period $\tau'_{вп}$ and the induction period $\tau_{вп}$ with allowance for a correction (according to (III.1)) for the velocity lag from the gas flow.

Table 16. Values of $\tau'_{вп}$ and $\tau_{вп}$ for beryllium particles with an average diameter of d = 32 μm [254].

Partial oxygen pressure p, atm	$\tau'_{вп}$	$\tau_{вп}$	$T_{ип}$, °K
0.16	11,2	13,2	2590
0.23	12,4	14,4	2690
0,36	11,4	13,4	2510
0,43	10,4	12,4	2400

For particles 32 μm in diameter this correction is small, 10-20%. The possible error connected with the inaccuracy of parameters η and V_θ is much less substantial for beryllium than for aluminum.

If, in the preflame period, the particle is heated from ambient gas exclusively by thermal conductivity and subsequently burns in a diffusion mode in vapor phase, then $\tau_г$ and $\tau_{вп}$ must be proportional to d^2. When these assumptions are valid with respect to beryllium, the graph (Fig. 53) must be a straight line passing strictly through the origin of coordinates. In reality this is not accomplished: the extrapolation of straight lines in coordinates $\tau_{вп} - \tau_г$ to the origin of coordinates intercepts the positive segments on the axis of ordinates. The reason for this lies in the more complex mechanism of preflame particle heating, which combines the heat transfer due to thermal conductivity with the supplementary chemical heating on the surface of the particle.

The use of expression (III.2) to solve the reverse problem -
finding the ignition temperature of a particle at the moment of
ignition, according to the experimentally determined value of
the induction period - qualitatively confirmed this assumption
(see Table 16).
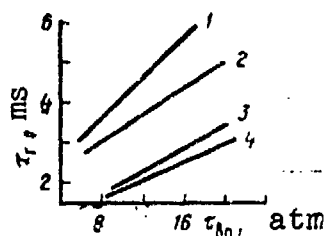
Fig. 53. Burning time τ_Γ versus $\tau_{вп}$
for beryllium particles (d = 32 ± 6 μm)
at different P and T: $1 - P_{O_2} = 0.16$ atm,
T = 2970°K; $2 - P_{O_2} = 0.23$, T = 2950;
$3 - P_{O_2} = 0.36$, T = 2880; $4 - P_{O_2}$ =
= 0.43 atm, T = 2830°K.

From Table 16 it follows that the degree of self-heating
increases as the partial oxygen pressure in the medium increases:
$T_{вп}$ drops with an increase in P_{O_2}.

4. Characteristics of the Ignition
Process of Beryllium Particles

The ignition process of Be is heterogeneous in nature and
similar to the ignition of aluminum. However, at the same time,
it has several specific differences. First, for beryllium the
transition to the stage of stationary self-sustained burning is
less clearly expressed: the particle begins to glow distinctly
even before the onset of vapor-phase burning. Second, the
ignition of beryllium occurs at a higher temperature of the medium:
$T_{cp} \geq 2000°K$. Third, the induction period of beryllium is very
sensitive not only to temperature but also to the composition of
the ambient medium (in the first place, to the O_2 and H_2O concen-
tration). In addition, $\tau_{вп}$ is not strictly subject to a square-
law dependence on diameter and is proportional to $\sim d^{2.5}$.

The explanation of these features should first of all be considered from the point of view of the structure and physical properties of the film coating the particle in its natural state. For beryllium the Pilling-Bedworth criterion is $\beta = 1.68$. This means that the oxide film has no less protective properties than that of aluminum. In a high-temperature oxidizing atmosphere (O_2, H_2O, CO_2) in the 1500-1800°K region (i.e., in the region of beryllium's melting point) the oxidation of beryllium increases sharply and is proportional to the pressure of the oxidizing reagent to the degree 0.5 (O_2 or H_2O medium) - 0.8 (NO_2 medium). In the same temperature range the oxidation process in time occurs according to linear law.

Hence it follows that the oxide layer which forms during heating in an active medium does not limit the subsequent oxidation of the metal and is not such an active diffusion barrier as it is with aluminum.

A possible reason also is the impairment of the structure (cracking) of the BeO film because of the differences in the coefficients of thermal expansion for the molten metal and the solid oxide and the presence of low-temperature impurities, additions, and coatings (natural or special).

Since the reaction rate and, consequently, the heat release, other conditions being equal, depends on the oxidizer concentration and the temperature, the strong dependence of $\tau_{\text{вп}}$ on medium activity and temperature, as well as the glow of the particles in the induction period, have a reasonable explanation.

The second factor, which should also be taken into consideration when studying the ignition process, is the thermophysical properties of the medium (heat capacity, heat conductivity). In the temperature range where intensive self-heating of particles begins as a result of chemical reaction and the temperature of the

147

particle becomes greater than the temperature of the medium, the latter plays the role of heat drain with respect to the particle. It is natural that the intensity of heat loss to the outside will be determined by the coefficient of heat transfer and the radiating capacity of the particles of beryllium oxide, which is greater than the radiating capacity of Al_2O_3. For example, in an argon medium the process of cooling a beryllium particle occurs approximately 3 times as fast as in air (Fig. 54).

Fig. 54. Temperature variation of a beryllium specimen over a period of time in different media. 1 - Air; 2 - argon.

Thus, the minimum temperature of the medium which ensures the ignition of beryllium particles in it will be determined by the chemical activity (Fig. 55) and the properties of the medium [282]. They, in conjunction with the physical properties of the BeO oxide film, are the main reasons for the stronger (than square-law) dependence of $\tau_{вп}$ on particle diameter. At the same time, the temperature of particles at the moment of ignition and burning, just as in the case of Al, is apparently equal to the boiling point of the pure metal. However, it is not possible to obtain vapor-phase burning of beryllium samples or, in the extreme case, to increase their temperature to $T \geq 2200°K$ in an H_2O (vapor) atmosphere. At the same time, the oxidation of the metal, in this medium, occurs quite actively and is accompanied by the formation of an oxide which has a complex double structure: an upper thick porous layer and a lower thin dense layer which protects the particle from oxidation.

148
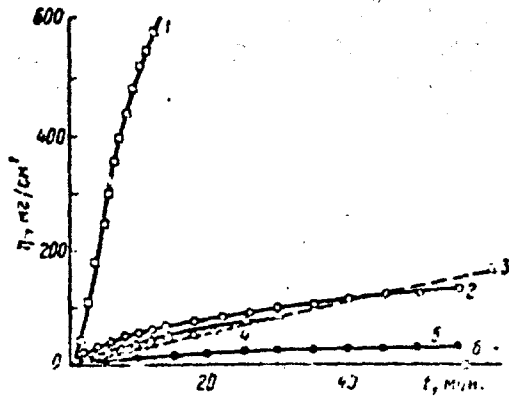
Fig. 55. Quantity of gas which has reacted during the oxidation of a beryllium specimen (l = 12 mm, d = 4 mm) at 1870°K in the following media: 1 - (O_2 (p = = 228-480 mm Hg); 2 - N_2 (p = = 306-387); 3 - CO_2 (p = 632-660); 4 - CO (p = 403-454); 5 - NO (p = = 330-358); 6 - H_2 (p = 500 mm Hg). Designations: мг/см^2 = mg/cm^2; мин = min.

The exclamation lies in the fact that during the reaction of beryllium with water free hydrogen is formed. Its liberation loosens the upper oxide layer and suppresses (because of the reduction in the rate of heat release and the diffusion of the oxidizer, as well as the increase in heat transfer) the reaction of vapor-phase burning.

Of the theoretical analyses on the ignition of Be particles, reference [253] should be noted. For each specific particle three heating stages are examined: the first stage consists of the heating of the particle to melting point; the second stage consists of the isothermal transformation; the third stage consists of the heating of the liquid drop to ignition temperature. The heating of particles occurs because of the heat exchange with the ambient medium without taking the chemical reaction into account.

The following assumptions are also made: a) the velocity of motion differs from the velocity of the gas by constant quantities; b) the effect of this difference in velocities on heat exchange is not negligible; c) the change in particle density and diameter during melting is not small.

149

The results of calculating the temperature of a particle over a period of time and the value of the induction period during heating to a given temperature are presented in Fig. 56. However, these data are rather illustrative in nature.
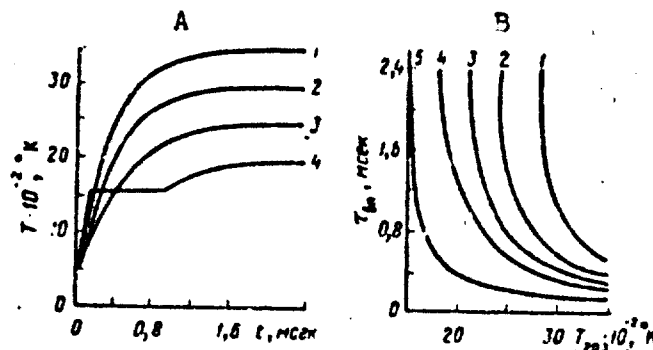
Fig. 56. Variation in temperature (A) and $\tau_{\text{вп}}$ (B) of a beryllium particle, d = 20 μm (T_0 = 500°K). The difference in the velocity of particle motion and the flow rate ΔV = = 5791-6096 cm/s. A: 1 - 3500; 2 - 3006; 3 - 2500; 4 - 2000°K; B: 1 - 2820; 2 - 2400; 3 - 2100; 4 - 1800; 5 - 1500°K.

Designation: мсек = ms.

[газ = gas]

§ 3. Ignition of Boron

Boron can be conditionally placed in the category of metals having a volatile oxide.

The Pilling-Bedworth criterion for boron is β = 2.46. This means that the surface of the particles during oxidation must be coated with a protective layer creating an effective barrier to the flow of the gaseous oxidizer.

The ignition of boron occurs only in a high-temperature oxidizing medium. All attempts to ignite a particle of ultrafine powder (d = 0.02-0.06 μm) of boron in a nitrogen atmosphere below T ≤ 1170°K have been unsuccessful. It has been established by

150

chemical analysis that after calcination, less than 1% N_2 was contained in the products. A similar result was obtained during the heating of boron powder in a CO_2 atmosphere (T $\leq$ 1200°K) [249].

Later studies have shown that the ignition temperature of crystal boron at atmospheric pressure is a function of the activity of the medium and depends on the initial particle size of boron.

In the work of Gurevich and colleagues [255] the critical temperature of the medium, necessary for the ignition of crystal boron (particle shape near parallelepiped), was evaluated according to the cessation (beginning) of particle burning in a flow having a velocity of 10-20 m/s.

Figure 57 presents the results of an experimental change in critical temperature as a function of particle size with various contents (per volume) of oxygen or water vapor (diluent - argon or nitrogen). Regardless of the composition of the medium, critical ignition temperature was lower for a large particle. In the size range 50-250 μm the difference in critical temperature was $\sim$500°C.
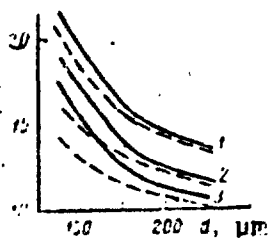
Fig. 57. Ignition temperature of boron particles as a function of their size with different contents of H_2O (solid lines) and O_2 (dashes) in a mixture with Ar and N_2. 1 - 15%; 2 - 30%; 3 - 45% H_2O (or O_2).
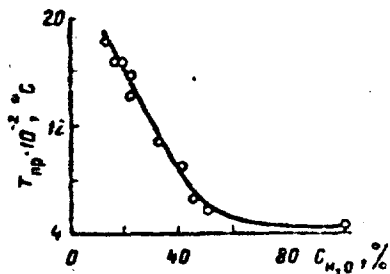
Fig. 58. Ignition limit of clusters of boron 150 μm in size as a function of the percent of H_2O in a mixture with N_2(T = 900°C) and N_2 + Ar (T > 900°C).

For large particles (d = 200-250 µm) with low concentrations of the oxidizing reagent, the replacement of H_2O by O_2 has less effect on critical temperature than in the case of fine particles (d ∿ 50 µm). The critical ignition temperature of particles with a diameter of less than 50 µm in an oxidizer concentration not exceeding 50% is above 1700-1800°K.

Clusters of fine particles (hundreds of Å) of amorphous boron are ignited rather easily at even lower temperatures (Fig. 58) than particles of crystal boron of equivalent size. In a water vapor medium, clusters with a diameter of 25 µm begin to ignite even at 1070°K, and with a diameter of 150 µm at 600°K. This result could be expected. This case is virtually equivalent, in its nature, to a reduction in the ignition limits of powdered metals during the heating of the latter on a base or in a flow of gas (increased concentration of particles) and has the same explanation: a decrease in heat losses to the outside, an increase in heat supply (thermal conductivity and radiation) from neighboring particles, a division of surface, and an increase in the role of self-heating due to chemical reaction.

However, the temperature of the particle itself ($T_{вп}$) at the moment of ignition, as a rule, does not coincide with critical temperature.

The temperature of boron particles at the moment of ignition was evaluated in reference [256]. A study was made, using a gas burner, in combustion products of CO or propane in oxygen (p = 1 atm) (Table 17).

The distance $x_{вп}$ from the point of particle injection into the flow to the point of the appearance of a visible particle glow is an experimentally determined quantity. The particle ignition temperature is given by the solution to the following system of equations:

152

$$\frac{dT}{dt} = \frac{6!}{\mu d}\left[\frac{k\,\mathrm{Nu}}{d}(T_1 - T_\cdot) - \varepsilon \sigma T^4\right], \qquad (\text{III.4})$$

$$\frac{dV}{dt} = \frac{3}{4}\frac{\alpha}{d}\frac{\rho_r}{\rho}(V_r - V)^2, \qquad (\text{III.5})$$

$$\frac{dz}{dt} = V \qquad (\text{III.6})$$

on the assumption that the particle is spherical with an average diameter d and there is no self-heating of the particle due to chemical reaction.[1]

Table 17. Temperature, velocity and composition of flame (in mole fractions) [256].

Compo-sition No.	$T, \,^\circ K$	$V_r,$ cm/s	Composition of flame						
			H_2O	CO_2	CO	N_2	O	OH	O_2
1	2280	265	0	0,30	0	0,45	0,01	0	0,23
2	2430	340	0	0,33	0,01	0,43	0,01	0	0,20
3	2870	600	0	0,11	0,29	0,09	0,03	0	0,23
4	2230	420	0,16	0,11	0,01	0,50	0	0,01	0,19
5	2330	1180	0,16	0,12	0,01	0,47	0	0,01	0,21
6	2430	1380	0,19	0,13	0,02	0,45	0	0,02	0,19
7	2650	2280	0,21	0,15	0,03	0,35	0,01	0,04	0,20
8	2040	365	0	0,35	0,03	0,32	0,01	0	0,28
9	2150	360	0	0,34	0,02	0,25	0,01	0	0,37

The results of corresponding measurements $(x_{вп})$ and $(T_{вп})$ are presented in Table 18.

From an analysis of the tabular data, it follows that the temperature of the particle at the moment of ignition does not depend on d or the temperature of the ambient medium. However, in a humid medium, containing 16-21% H_2O (compositions 5-8), it is approximately 130° lower than in a dry (compositions 1-3) medium, i.e., 1992 ± 16°K and 1860 ± 24°K. This difference can

---

[1]The radiative capacity of a B particle coated with a film of liquid B_2O_3 is taken as $\varepsilon \approx 0.5$.

be connected with the chemical nature of the reaction of high-temperature oxidation. We know [87] that in the reaction of boron with water it is possible to form metaborcn acid HBO_2 which has very noticeable volatility. However, we cannot exclude inaccuracy in the method of evaluating T_{en}.[1]

Table 18. Average distance x_{en} and T_{en} of boron particles [256].

Composition No.	$d = 30.5$ μm		$d = 45.2$ μm	
	x_{en}, cm	T_{en}, °K	x_{en}, cm	T_{en}, °K
1	2,37±0,18	1980	3,97±0,83	1970
2	2,50±0,31	2000	3,31±0,20	1970
3	1,88±0,28	1999	3,14±0,41	1990
4	5,83±0,65	1840	10,75±1,13	1930
5	4,97±0,56	1850	9,60±0,72	1880
6	5,68±0,40	1810	7,45±1,12	1800
7	7,40±1,42	1960	8,11±0,98	1810
8	2,50±0,37	2030	3,42±0,17	2010
9	2,26±0,25	1990		

The ignition temperature of boron particles 30-50 μm in diameter, determined by the shock tube method in an air medium (p = 1 atm), is ~1900°K. The fact that the temperature of the particle at the moment of ignition is below the melting point of boron and the boiling point of B_2O_3 is noteworthy. This means that on the solid surface of the particle there is a film of liquid oxide which creates additional resistance to the diffusion of the oxidizer toward the particle.

An approximate evaluation of the ignition temperature of large boron particles in oxygen at a pressure of 1 atm was made by Tally [144]. The evaluation was made under the condition

---

[1]The average velocity V_r of gas in the second group cf compositions is greater by a factor of 5 than in the first (see Table 17). Since the calculation assumes that $V_0 = u$ it is possible to have an error connected with the inaccuracy of the determination of particle velocity at the moment of entrance into the flame front.

that at the moment of ignition the heat release due to chemical reaction Φ_1 was equal to the heat losses from radiation Φ_2 in accordance with Stefan-Boltzmann law (the radiating capacity of boron particles was taken as 0.8).

Under these assumptions, $\Phi_2 = 0.65 \cdot 10^{-10} \, T^4$ cal/cm^2 $\cdots$. The expression for the rate of heat release was obtained on the basis of kinetic data of boron oxidation at $T \leq 1500°K$.

$$\Phi_1 = 6.0 \cdot 10^{10} \cdot \exp(-38\,000/RT), \quad \text{cal/cm}^2 \cdot \text{min}.$$

The condition $\Phi_1 = \Phi_2$ is satisfied by the value $T_{\text{вп}} = 2200°K$. This temperature is taken as the ignition temperature of boron particles. This evaluation is naturally only approximate because of the approximate character of the assumptions and the kinetic parameters. However, in spite of this, the obtained value for ignition temperature is near the earlier introduced experimental data.

The induction period of individual boron particles in a medium of 36% H_2O + 64% Ar was determined according to the distance between injection points and the origin of the visible glow and the velocity of particle motion. The values for ignition delay are presented below.[255]:

d, μm	T, °K	$\tau_{\text{ви}}$, ms
73	2370	14
115	2070	19
115	2370	17
115	2770	11
200	2370	28

The above examined qualitative and quantitative experimental factors dealing with the ignition of individual particles of crystal boron make the following conclusions possible. The process of boron particle ignition in a high-temperature oxidizing medium has a heterogeneous nature. Below 1500-1900°K the particle burns

almost entirely due to heat conductivity from the surrounding
gas without a noticeable effect from the chemical reaction of
oxidation. At these temperatures the particle has a yellow glow.

Beginning at 1900°K and above a substantial heat release
sets in because of the chemical reaction of oxidation on the
surface of the particle. This additional source of heat either
competes with the heat release to the outside if the particles
are heated to temperatures exceeding the temperature of the ambient
medium or accelerates the heating of particles if the temperature
of the medium is greater than the temperature of the particle.
Ultimately the temperature of the particle increases and the
ignition stage changes into the burning stage.

The temperature of the particle at this moment lies between
the melting point (according to data from [255], the particles
are in liquid state during burning) and the boiling point of
boron (at p = 1 atm, $T_{\text{кип}}$ = 2850°K).

The differential equation describing the average temperature
of the particle in the ignition stage can be written in the form
[256]

$$\frac{dT}{dt} = \frac{6z}{d\rho c} \exp\left(-E/RT\right) c_{0_2} \Delta H + \frac{6k\,Nu}{d^2\rho c}(T_r - T_0),$$ (III.7)

where z, E, ΔH are the preexponents, activation energy, and heat
of chemical reaction on the surface of the particle; c_{0_2} is the
concentration of oxygen in the medium.

The first term on the right side of the equation describes
the change in particle temperature due to the chemical reaction
of oxidation; the second takes into account the heat exchange
with the ambient medium.

With a decrease in particle diameter the coefficient of gas-particle heat transfer (Nu = const) increases. Hence it follows from the equation that although the rate of temperature increase due to the reaction on the surface grows in inverse proportion to the diameter, the increase in the rate of heat exchange due to convection plays a more substantial role.

Small particles in a medium with comparatively low temperature reach an equilibrium temperature significantly higher than the temperature of the gas. If equilibrium between heat transfer to the outside and heat supply due to the chemical reaction of the particle is achieved at temperatures below the boiling point of boron, the reaction occurs on the surface of the particle.

With small particle diameter the surface reactions are the determining mechanism in the burning of boron.

§ 4. Physical Model of Metal
Particle Ignition

Most metals have on their surface an oxide film whose properties can be very different in various media and temperature ranges (see Chapter I). As we have seen, this leads to the fact that for given metals the rate of the oxidation reaction depends not only on temperature and concentration of the oxidizing reagent in the ambient medium, but also on the protective properties of the oxide film.

An analysis of the characteristics of the particle ignition process which occur because of the peculiarities of the kinetic laws of metal oxidation is presented in reference [355] by Khaykin, Bloshenko, and Merzhanov.

Conditions for the ignition of spherical metal particles are found from the joint solution of the equations of heat balance (III.8) and the kinetic law of oxidation (III.9):

$$\frac{1}{3} c \rho r_0 \frac{dT}{dt} \approx Q \rho \frac{d\delta}{dt} - \frac{\lambda}{2r_0} Nu\,(T - T_t),$$ (III.8)

$$\frac{d\delta}{dt} = \frac{k_n c_{OH}^m}{\delta^n} \exp\,(-E/RT),$$ (III.9)

where r_0, δ are the radius of the particle and the thickness of the oxide film; k_n, E, m are the preexponent, activation energy, and the order of reaction with respect to the oxidizer in the appropriate law of metal oxidation; c_{OH} is the concentration of the oxidizer on the surface of the particle; T_0, T are the temperatures of the ambient medium and the particle; c, ρ is the specific heat capacity and density of the metal; λ is the coefficient of thermal conductivity for the gas; Q is the thermal effect of the reaction for 1 g of oxide multiplied by the density ratio of the oxide and metal.

The index n represents the dependence of the oxidation rate on the thickness of the oxide film, i.e., oxidation law (n = 0 - linear law, n = 1 - parabolic, n = 2 - cubic, etc). The authors have limited themselves to an examination of only the power laws of oxidation, assuming that the characteristics of the logarithmic (i.e., stronger) laws of oxidation will be manifested in a stronger dependence of oxidation rate on δ, while the laws governing oxidation will be similar to the case with a large value for index n.

The conditions for metal particle ignition are determined by the rate of heat release due to the oxidation reaction and the rate of heat drain from a particle to the ambient gas und r the following initial conditions:

$$t = 0 \rightarrow T = T_H,\quad \delta = \delta_H,$$

where δ_H, T_H are the initial thickness of the oxidizing film and the temperature of the particle.

158

By ignition, as usual, we mean the interruption of thermal equilibrium leading to a self-accelerating increase in the temperature of the particle. For small particles, i.e., for small Re numbers, the Nusselt number is near 2 (Nu $\approx$ 2).

By a replacement of variables, the system of equations is brought to dimensionless form, which is similar, in form, to the system of equations describing a thermal explosion [274]:

$$\frac{d\theta}{d\tau} = \varphi(\eta) \exp\left(\frac{\theta}{1-\beta\theta}\right) - \frac{\theta}{\varkappa};$$

$$\frac{d\eta}{d\tau} = \gamma\varphi(\eta)\exp\left(\frac{\theta}{1+\beta\theta}\right);$$

$$\varphi(\eta) = (1+\eta)^{-n},$$

$$\tau = 0; \quad \eta = 0; \quad \theta = -\theta_{\text{H}},$$

where

$$\eta = \frac{\delta - \delta_{\text{H}}}{\delta_{\text{H}}}, \qquad \theta = \frac{E}{RT_0^2}(T - T_{\text{H}});$$

$$\tau = t\,\frac{3Q}{c}\,\frac{E}{RT_0^2}\,\frac{k_{\text{n}}c_{\text{OK}}^{m}}{r_0\delta_{\text{H}}^{n}}\exp(-E/RT_0),$$

$$\varkappa = \frac{Q\rho}{\delta_{\text{H}}^{n}}\,\frac{E}{RT_0^2}\,\frac{r_0}{\lambda}\,k_{\text{n}}c_{\text{OK}}^{m}\exp(-E/RT_0),$$

$$\beta = \frac{RT_0}{E}, \qquad \theta_{\text{H}} = \frac{E}{RT_0^2}(T_0 - T_{\text{H}}), \qquad \gamma = \frac{r_0}{3\delta_{\text{H}}}\,\frac{cRT_0^2}{EQ}.$$

The basic difference lies in the form of function $\phi(\eta)$.

In the theory of thermal explosion, function $\phi(\eta)$ is taken in the form $\phi(\eta) = (1 - \eta)^{n}$ where η is the burn-up of the substance. Solution of the system is possible only for case $\gamma < 1$.

In the examined problem, parameter η characterizes the relative increase in the thickness of the oxide film, and the character of the solution to the system of equations, to a significant extent, is determined by the value of parameter γ. For small values of $\gamma(\gamma \ll 1)$ the form of the function slightly affects the critical conditions for particle ignition and they are determined by the critical value of parameter

$$x_{\text{кр}} = \frac{1}{c}.$$

The critical ignition temperature of metal particles drops with an increase in their diameter. The condition $\gamma \ll 1$ in the examined problem, is fulfilled for rather fine particles coated with a very thick oxide film.

The case $\gamma \gg 1$ is more realistic for metals.

To study the critical conditions of particle ignition when $\gamma \gg 1$, a change in variables is made $\eta = \gamma z - 1$ and the equations are changed to the form:

$$\frac{d\theta}{d\tau} = \frac{1}{z^n} \exp\left(\frac{\theta}{1+\beta\theta}\right) - \frac{\theta}{\Omega};$$

$$\frac{dz}{d\tau'} = \frac{1}{z^n} \exp\left(\frac{\theta}{1+\beta\theta}\right);$$

$$\tau' = 0; \quad z = 1/\gamma; \quad \theta = -\theta_{\text{н}},$$

where

$$z = \frac{\delta \cdot 3QE}{r_0 c R T_0^2}, \quad \tau' = \frac{\tau}{\gamma^n} = \left(\frac{3QE}{cRT_0^2}\right)^{n+1} t \frac{k_n c_{\text{ок}}^m}{r_0^{n-1}} \exp\left(-\frac{E}{RT_0}\right),$$

$$\Omega = \frac{\varkappa}{\gamma_n} = \left(\frac{3QE}{cRT_0^2}\right)^{n+1} \frac{c\rho}{3\lambda} \frac{k_n c_{\text{ок}}^m}{r_0^{n-1}} \exp\left(-\frac{E}{RT_0}\right).$$

If we assume $z = 1/\gamma = 0$ as an initial condition, we finally obtain solution in the form

$$\left(\frac{3QE}{cRT_{0\,\text{кр}}^2}\right)^{n+1} \frac{c\rho}{3\lambda} \frac{k_n c_{\text{ок}}^m}{r_0^{n-1}} \exp\left(-\frac{E}{RT_{0\,\text{кр}}}\right) = \Omega_{\text{кр}} = \text{const.} \tag{III.10}$$

The value of the constant $\Omega_{\text{кр}}$ is obtained by a numerical solution to the problem and is

$$\Omega_{\text{кр}} = \begin{cases} 1,57 & (\theta_{\text{н}} = 0) \\ 2,33 & (\theta_{\text{н}} \gg 1) \end{cases} (n=1); \quad \Omega_{\text{кр}} = \begin{cases} 7,45 & (\theta_{\text{н}} = 0) \\ 13 & (\theta_{\text{н}} \gg 1) \end{cases} (n=2).$$

160

According to the solution obtained, for a linear law of oxidation
(n = 0) equation (III.10) reduces to the ordinary law of hetero-
geneous ignition and $T_{кр}$ drops with an increase in particle size.
For n = 1, ignition temperature does not depend on particle size.
If, however, the rate of oxidation depends on δ more strongly
than during parabolic law (n > 1), then $T_{кр}$ increases with particle
growth (Fig. 59).
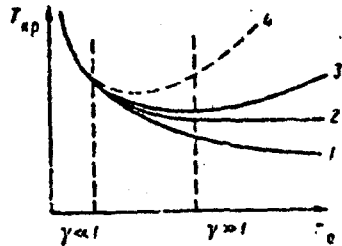
Fig. 59. Ignition temperature versus
particle radius for various oxidation
laws. 1 - n = 0; 2 - n = 1; 3 - n =
= ¹; 4 - n >> 1.

If the critical ignition conditions are not fulfilled, then
the temperature of the particle passes through maximum and
approaches the temperature of the ambient gas. However, if during
heating, the temperature of the particle exceeds the temperature
at which the film loses its protective properties (for example,
melting point of aluminum oxide), this leads to a change in the
kinetic law of oxidation and, in this case, particle ignition
can occur.

The solutions obtained, from the physical point of view,
can be interpreted as follows. As we know, the rate of heat
drain in large particles is less than in small. However, for
the heating of a particle there is required a large amount of
time and heat, whose release is connected with an increase in
the oxide film. With the weak dependence of oxidation rate
on oxide film thickness (n < 1) the first factor predominates
and the ignition temperature decreases with an increase in
diameter.

_____

¹Omission in original Russian document.

With a strong dependence of oxidation rate on $\delta(n > 1)$ the second factor predominates and the ignition temperature increases with diameter size.

Allowing for heat loss on radiation in the equation of thermal balance leads to a criterion of the following form:

$$k_R = \frac{2\varepsilon s E T_0^2}{R\lambda \, \mathrm{Nu}} r_c.$$

When $k_R \ll 1$ heat transfer by radiation can be disregarded as compared with heat transfer by thermal conductivity.

For small particles $(d < 30 \ \mu m, \ \lambda = 2.4 \cdot 10^{-4}$ cal/cm·s·deg, $T_0 = 2300°K, \ E = 50$ cal/mole, $\varepsilon = 0.4, \ \mathrm{Nu} = 2)$ the parameter $k_R \approx 0.45$, i.e., heat transfer by radiation has a correction nature even at high values for the temperature of the ambient medium.

For large particles the ignition temperature, with allowance for radiation, is an increasing function of particle size even with a parabolic law of oxidation.

An examination of the partial evaporation of metal (for example, Mg) in the proposed model $(n = 0)$ shows that at the moment the thermal equilibrium is disturbed, the temperature of the particle can be less than the temperature of the ambient medium. The conductive heat drain for evaporation, under these conditions, plays the role of conductive heat supply, which disturbs the balance between the rate of heat release from the chemical reaction and the rate of heat absorption for evaporation.

The results presented above on the ignition of individual particles of Al, Be, and B can agree qualitatively with the conclusions of the proposed model.

The independence of critical temperature from particle diameter in the experiment of Friedman and Macek [256] gives a basis for assuming that, in this case, aluminum was used, which oxidizes according to parabolic law (n = 1), characteristic for metals whose oxidation is limited by diffusion through the oxide film.

At the same time, in order to explain the increase in $T_{кр}$ with particle size, demonstrated in references [355], it is necessary to assume that the studied aluminum had a stronger dependence of oxidation rate on δ than parabolic.

The results of determining critical ignition temperature for boron particles whose oxide film melts at the low melting point of B_2O_3 (420°C) can be included in the examined model with the value n = 0 (linear law of oxidation).

The case of metal particle ignition in high-temperature combustion products of mixed fuel-oxidizer systems does not contradict the arguments given. Under these conditions, ignition, as already indicated, is connected with the impairment of the integrity of the oxide film and the increase in the rate of heat release due to the reaction of active metal oxidation. This corresponds to a change in the general law of metal oxidation and a transition of the particle to a subcritical ignition mode.

CHAPTER IV

COMBUSTION OF METAL

§ 1. Combustion of Aluminum

The basic methods of studying processes of ignition and burning of metals were outlined in Chapter II. These include, in some sequence or in totality, the following stages of observation:

1. Study of the picture of combustion of particles from results of microcinematography and photography; study of trails - the tracks obtained during motion of hot particles relative to the recording material (photographic film, photoplate, etc.).

2. Visual micro- and macrostudies of the products of combustion of metals and their compounds.

3. Thermometric and spectroscopic analysis of metal flames.

4. X-ray diffraction, chemical, and mass spectrometry analysis of combustion products drawn off from the burning zone by sampling instruments of various original designs.

Only detailed analysis and comparison of results from investigations on all the enumerated stages make it possible to approach closely to an exploration of the mechanism by which particles of metal burn. However, in this case two other factors must be borne in mind.

164

Since combustion of metals occurs in a certain medium (in our case gaseous), the parameters of this medium should render a definite influence on the nature of the development and steady-state condition of combustion. First of all these parameters include composition, temperature, and pressure. Finally, of course, there are the properties of the metal particles themselves: degree of purity, activity, shape, degree of dispersion, concentration, etc.

Naturally, the totality of these factors sharply complicates any understanding of the general picture of combustion of the particles. Nonetheless, a comprehensive and systematic study of their role is an inseparable link in the pattern of study of all heterogeneous processes, a necessary and mandatory condition without which it would be impossible to construct the overall picture of combustion of metals.

1. General Picture of the
Combustion of Aluminum Particles

One of the most effective methods of studying the mechanism of combustion of metals is, as in the case of any other complex process, the visualization of all available phenomena by applying methods of high-speed micro- and macrocinematography and still photography [129, 138, 155, 257].

As has already been pointed out, for aluminum particles the transition to self-sustaining steady-state combustion is accompanied by a sudden appearance of intense light (Fig. 60). During photography at a speed of 5000-10,000 frames/s this transition is accomplished for particles 100-200 μm in diameter during exposure of one or, at the most two frames - i.e., in a period of time less than 0.2-0.3 ms.

The zone of brightness which appears around the particle is so brilliant that it frequently screens the surface of the particle

from the observer. The diameter of the brightness zone at the
moment of ignition is only slightly larger than the diameter of the
initial particle. However, subsequently the width of this zone is
rapidly increased (Fig. 61) and during steady-state combustion it
can exceed the diameter of the initial particle by 1.5-3.5 times.
The value of the latter figure depends on the composition of the
ambient medium. In a "dry medium" enriched by oxygen and contain-
ing no water vapor or hydrogen, the width of the brightness zone
is 2.5-3.5 times greater than the diameter of the particle at the
moment of its ignition. In a "wet" atmosphere the brightness zone
approaches the surface of the particle and may equal as little as
1.5 times the diameter of the latter [258]. If combustion occurs
in a moving medium the region of brightness around the particle
is gradually drawn off along the flow. A so-called "tail" will
appear (Fig. 62). The "tail" grows rapidly and in the end exceeds
the initial size of the burning particle by several times. The
intensity of the "tail's" brightness indicates the possibility
that exothermic reactions may occur in it.

Fig. 60. Cineframes from high-speed
photography of burning particles of
aluminum.

166
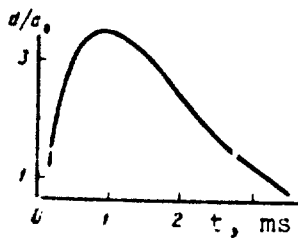
Fig. 61. Ratio of the diameter of the brightness zone, d, to the initial diameter of the particle, d_0.

Fig. 62. Burning of Al particles in a high-temperature gas flow.

Individual, extremely small, and brightly glowing points - particles - appear along the periphery of the symmetrical zone of brightness or "tail" on the boundary with the medium (Fig. 63). These points are particles in continuous motion. Their size is gradually reduced with time. During collision individual particles merge together or capture smaller particles.

Upon achievement of a certain critical size, sometimes close to the diameter of the initial d op (50-100 μm), individual particles are ejected from the brightness zone or the "tail" into the surrounding atmosphere, owing to the action of gravitational and convective forces. There they gradually harden in the form of extremely small spheres, white in color.

167

Fig. 63.   Combustion of Al particles during
a reduction in pressure.

After the lapse of a certain amount of time the burning particles
of aluminum frequently begin to acquire rotation.   The beginning
of rotation is preceded by a sudden asymmetrical inflation - expan-
sion of the flames surrounding the particle.   The speed of rotation
grows quite rapidly and reaches up to 10^4 Hz in order of magnitude
(Fig. 64).

Fig. 64.   Rotation and fragmentation of
hot Al particles.

The concluding stage of combustion of Al particles can proceed
in two directions.   The first is the simplest and most typical
variant.   The width of the combustion zone is gradually reduced
in diameter, the intensity of its brightness weakens, and the
particle ceases to burn.   In the second case there is a sudden
expansion and flash of intensity of the combustion zone brightness,
after which the particle flys apart into a number of much smaller
burning pieces.   The scattering pattern is fan-shaped.   The

scattering angle can vary from 0 to 180° with respect to the direction of the initial particle motion.

Combustion of aluminum in an active medium at subatmospheric pressure permits qualitative examination of the surface of the particle, since the burning zone is not so dense and lies at a substantial distance from the surface of the drop (see Fig. 63). The particles are in the molten state. The combustion products, made up of aluminum oxide Al_2O_3, diffuse from the flame zone primarily in the form of extremely fine smoke of submicron size.

Useful additional information is obtained from observation of combustion of thin metallic wires, 0.5-1.0 mm in diameter, in an oxidizing medium [236, 237]. After ignition the wire is broken. Its er drop downward almost to the vertical and begin to burn with a brightly glowing flame. Under the action of gravity the metal flows out of the oxide shell covering the wire as though out of a trough, forming spherical drops on the ends of the shell. If the pressure of the medium is low the oxidation reaction proceeds in the gaseous phase. The combustion products which are formed diffuse from the reaction zone into the medium in the form of thick white smoke.

Combustion in this case is analogous in nature to burning of drops of hydrocarbon fuels [259, 260].

At high pressures and high oxygen concentrations ignition of the wire proceeds, as in the case above, in one place. However, the flame propagates rapidly and in the end covers the entire wire. As it is heated the wire melts and is transformed under the effect of surface tension forces into a group of drops. The size of the latter can amount to several millimeters. Each drop burns independently. The surfaces of the drops differ in brightness. On certain segments the liberation of gas can be observed; from the sections bright trails are drawn off, caused by condensation of the oxide in the surrounding cold medium. It is

probable that the surfaces are partially covered with a layer of oxide and that this is the reason for the effects which are observed. The burning process is frequently terminated by crushing of the drops. As a rule the drops are rotating during combustion.

Another method of optical investigation of the burning of metal particles - the most widely applied method - is by photographing them on fixed photographic film or on a photoplate (Fig. 65). The moment of sudden appearance of light on these photographs corresponds to the beginning of aluminum combustion. Immediately after ignition the width of the track exceeds the initial size of the particle only slightly (by approximately 1.2-1.5 times). Subsequently it is increased and on the segment of steady-state combustion it can exceed the size of the burning particle by 3-4 times. The latter situation depends on the composition of the ambient medium. In a medium with a high moisture or hydrogen content the tracks are much narrower and sharper than in a "dry" medium.
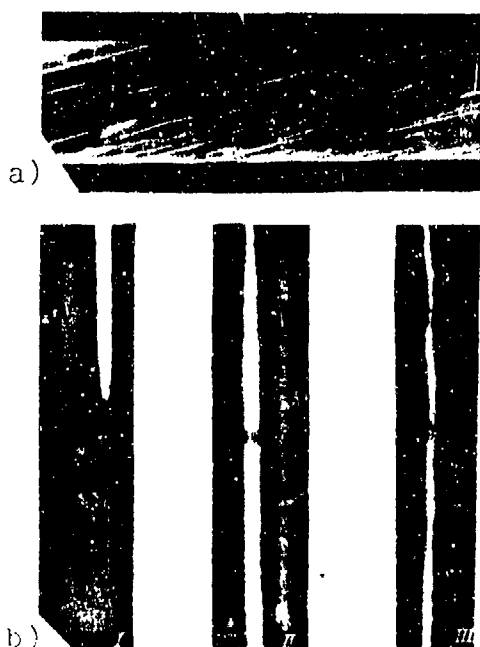

Fig. 65. Tracks of hot aluminum particles, obtained on moving (a) and fixed (b) film.

The time of track development - i.e., the time from the moment of ignition to the moment when the track reaches maximum width - increases with a growth in particle diameter. For a particle

50 µm in diameter the duration in time of the conical part of the
track amounts to about 0.1 ms. An intensively glowing core is
seen in the middle portion of the track. Its size corresponds
approximately to the diameter of the particle. In the initial
stage of combustion the track is a straight and even line which
glows symmetrically and is uniformly bright. Then, following the
period of steady burning of the particle, attenuation and discon-
tinuities in the glow appear on the track; the track is transformed
into a broken line.

As the process develops the frequency of brightness pulsations
increases up to 10^4-10^5 Hz. Here distortions of the rectilinearity
of particle motion are frequently observed - the track becomes
wavy.

Simultaneous cinematography and photography on stationary film
of a burning particle of aluminum makes it possible to conclude
that pulsations in brightness on the track are the result of rota-
tion of the particle. The track terminates either in gradual
attenuation of the glow or in a star-shaped peak from which some-
what finer rays - tracks - travel out at various angles. At this
moment an intensification of the glow is observed on the track.
Such a picture is characteristic for fragmentation of the particles.

Thus, both methods of optical recording give matching results
and thus emphasize the reliability of the general ideas obtained
on combustion of particles of aluminum in an active gaseous medium.

2. Products of Aluminum Combustion

As is indicated by statistics, the overwhelming fraction of
solid final products of the combustion of aluminum particles
represent fine spherical particles with a dimension on the order
of 1 µm and less (Fig. 66). The particles are solid, white in
color, and consist of aluminum oxide. Along with them there will
be a certain quantity of larger solid spheres, 10 µm in diameter,

171

and also a certain quantity of spheres which equal the initial
particle in size or even exceed it by 2-3 times. These spheres
are hollow, semitransparent, matte spheres (see Fig. 66). Their
wall thickness is constant and equals 1-3 μm. These spheres are
ground up and crushed by even comparatively small forces, not
infrequently by the mere impact against a plate at the moment of
sampling. The amount of aluminum involved in the formation of
such hollow spheres is estimated to be ∿30-40% of the weight of
the initial particle.
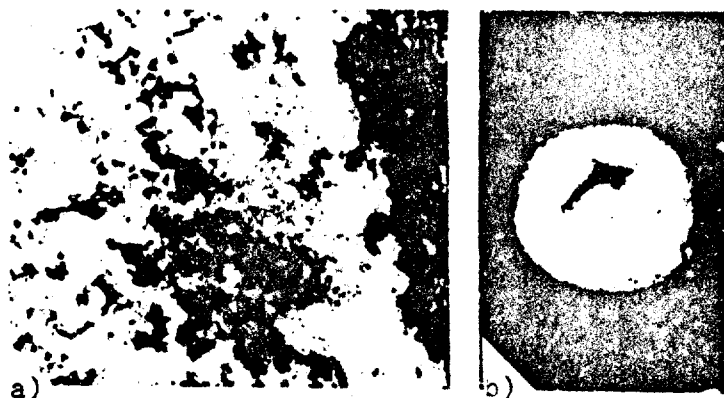
Fig. 66. Subdispersed products (a) and
hollow spheres (b) form during combustion
of aluminum.

If the aluminum is burned on a support (graphite rod or tungsten
plate) the final product is a "shell" and in the general case is
commensurate in magnitude with the initial particle (Fig. 67).
A dense ring of subdispersed particles of oxide is formed around
it. In a medium of carbon dioxide the ratio of the radius of the
ring to that of the shell equals 3-4, while in water vapor it is
1.5-2.

When aluminum particles are burned in the suspended state in
a flow of gas, at the moment when they approach heat-conducting
elements of the installation or plates which are especially
located in the flow, clear tracks appear on the latter due to the
continuously forming combustion products. The indicated traces

172
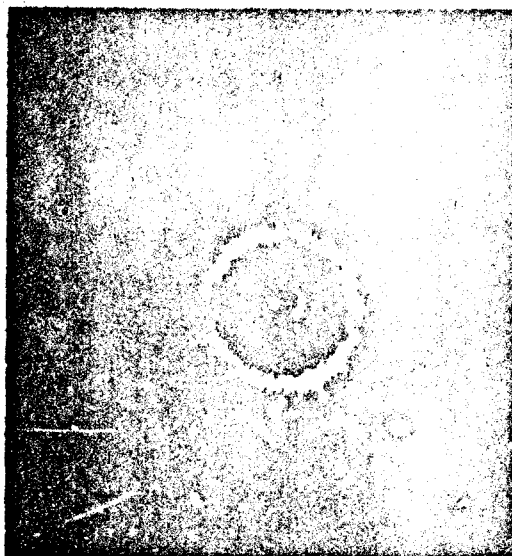
Fig. 67. Products of combustion
of Al particles on a substrate.

have extremely varied and eccentric shapes: rectilinear and twisted,
wavy and helical, narrow and wide, ending in a point or resembling
the picture of motion of a comet, etc. The base of the track, as
before, is made-up of subdispersed particles of aluminum oxide.
Along the periphery of the track and in its tail segment the size
of the condensate is, as a rule, somewhat greater than that in the
center and in immediate proximity to the extinguished particle.
Growth of the oxide occurs mainly in the gaseous phase and is
apparently caused by such a phenomenon as condensation and
agglomeration of finer particles due to the presence of convective
flows in the combustion zone or close to it.

A comparatively small quantity of larger particles. 5-10 μm in
diameter, exist against the general background of subdispersed
particles (Fig. 69, see page 175). The shape of the particles is
not necessarily strictly spherical; some may be teardrop-shaped.
They are found over the entire length of the track, but it is
difficult to identify any sort of law governing their appearance.

The peak of the track frequently ends in a spherical particle. Its size depends on the previous history of combustion. It may be both smaller or equivalent in size to the initial particle. An annular halo of subdispersed oxide is formed around it on the substrate. In the general case the picture is similar to that obtained during combustion of aluminum particles on a substrate. From this it is possible to draw the particular conclusion that after deposition on the plate the particles continue to react actively with the ambient medium for a certain period of time.

Another type of track peak is gradual narrowing and thinning. The width and shape of the track left by a burning particle of aluminum depends, just as the width of the track on the photoplate, on the composition of the medium. With a substantial content of oxygen and in the absence of water vapor or hydrogen the tracks are wide and slightly blurred. The presence of water vapor or hydrogen results in narrowing them by half; they are much clearer and are much more clearly outlined. In this case hollow thin-wall spheres of Al oxide always exist in the combustion products.

Figure 68 shows a double helical track left by a hot particle during its travel along the sampling instrument immediately before deposition on its surface. The extinguished particle is visible at the head of the track. Usually such tracks are left by particles during combustion in a highly active medium. With an oxygen concentration greater than 15% (atmospheric pressure) trajectories of particles can be distorted. However, the changes will have a more or less smooth nature. If the partial pressure of oxygen becomes equal to 0.35 atm and more and if the temperature of the medium equals ~3000°K [135], the track is progressively more uneven, with sudden and sharp changes in direction. Frequent ejections of oxide toward the side are observed. Like the main track, the radial rays are short and blurred in a "dry" medium and long and sharply defined in the presence of hydrogen or its compounds.

174

Fig. 68. Double track-trail of
a hot rotating aluminum particle.

Fig. 69. Peak of a track on a plate
in the sampling device.

Immediately after ignition spherical particles 150 μm and more
in diameter are broken up at the moment of collision with the plate
in the flame zone, leaving behind fan-shaped radial tracks (see
Fig. 36). The picture is typical for head-on collision of a liquid

175

drop against a solid barrier. If the indicated particle flys beyond
the flame zone into the atmosphere prior to ignition no crushing of
the particle occurs. With a reduction in particle size deformation
during collision with the surface of the plate becomes ever less
sharply expressed and for particles less than 50 μm in diameter
it virtually ceases to be noticeable. The oxide film covering the
particle of molten metal apparently congeals so rapidly that at
the moment of collision with a cold plate there is no noticeable
motion of the material of the particle. In this respect the
collected particles are extremely representative from the point of
view of shape and size in the period of combustion before quenching.
The majority of particles which are extinguished immediately after
ignition contain a metallic core.

Figure 70 shows photographs of particles (a and b) collected
from the flame of an oxygen-hydrogen burner on a later stage, at
the moment of steady-state combustion. On the extinguished
particles hollow bubbles of oxide are located in random fashion.
This gives a basis to assume that the formation of hollow spheres
is not directly connected with the mechanism of aluminum quenching,
but is one of the particular features of the mechanism of its
combustion.

Thus, as the result of study of trails and tracks and of analysis
of the products from combustion of aluminum three characteristic
features of the considered process are revealed: a) rotation of
particles in the period of steady-state combustion; b) breakup of
particles on the concluding stage of combustion; c) the formation
of hollow transparent spheres of aluminum oxide in the combustion
products.

Since these phenomena are directly connected with the process
of particle combustion, we will pause to consider in more detail
the conditions their formation.

a. Formation of hollow spheres. The formation of such spheres
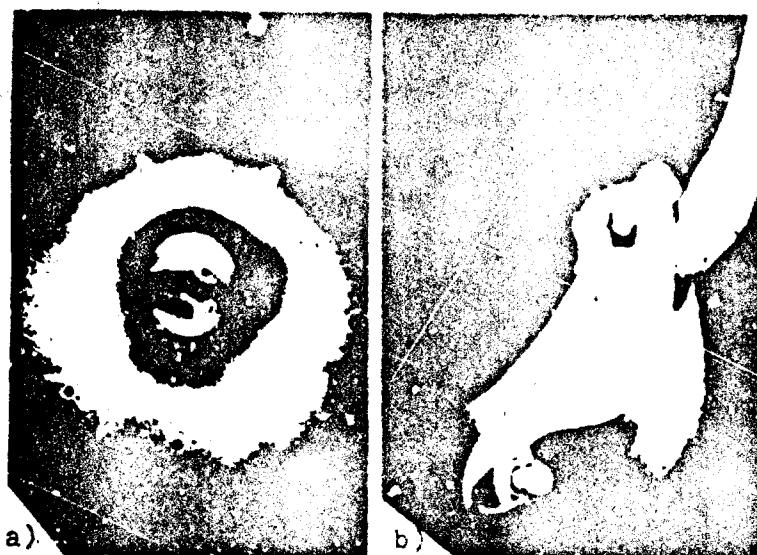
Fig. 70. Motion of burning particles of
aluminum along a plate of the sampling device.

during combustion of aluminum was apparently first noted in the
literature by Fassel, Papp, et al. [137]. Their observations
related to experiments with a gas burner, in which ordinary
natural gas was used as the fuel. The possibility that drops of
active metal or alloy might be contained within such a sphere was
pointed out. However, this was observed, as a rule, during
combustion of large particles under the condition that sampling
was carried out on an early stage of combustion.

Friedman and Machek [133] detected similar hollow spheres during
combustion of Al in the flame of a gas burner using a propane-
oxygen-nitrogen mixture. In this medium (the flame) the quantity
of moisture amounted to approximately $14-18\%$, while the content of
pure oxygen ran up to $25-48\%$ (depending on the flame temperature).
With respect to degree of dispersion the hollow shells frequently
turned out to be equivalent to the initial aluminum.

According to assertions by these same authors, when burning alumi-
num in a "dry" carbon monoxide-oxygen flame containing less than
0.5% H_2 (introduced to stabilize the flame), there was no forma-
tion of hollow spheres. But if an additional $5-10\%$ of hydrogen

177

was introduced into such a flame large oxide spheres appeared once
again. Residues of metallic aluminum were frequently detected on
the outer side of the walls of the spheres in the form of extremely
fine tiny balls.

A similar picture was observed during combustion of aluminum
in a methane-oxygen-nitrogen flame [267] and in an oxygen-hydrogen
flame from a gas burner [139]. In the latter case even larger
spheres were observed: with an initial aluminum particle
diameter of 70 μm the size of the hollow transparent spheres of
oxide reached a magnitude of 150-200 μm. Tiny drops of pure
aluminum were found on the inner and outer walls of the spheres.

At the same time, products of combustion of aluminum in a pure
cyanogen-oxygen flame (p = 1 atm) [203] consist of white oxide in
the form of smoke; there are no large particles or spheres. With
forced quenching the aluminum particle is wholly or partially
covered with a film of oxide. If hydrogen is gradually introduced
into the flame, hollow spheres begin to predominate in the products.

At first glance the data presented above confirm a direct
connection between conditions for formation of hollow shells and
the presence of hydrogen or its compounds in the medium in which
the aluminum is burned. However, later studies cast doubt upon
this position: large hollow spheres of aluminum oxide were detected
with burning of aluminum in a medium free from hydrogen.

Davis [246] observed their formation in a carbon monoxide-oxygen-
nitrogen flame (0.5% H_2), along with finely dispersed aluminum oxide
(<1 μm). Gordon et al. [262] established their presence during
burning of spherical aluminum particles at normal atmospheric
pressure in a CO + O_2 flame. It is noteworthy that with a ratio of
fuel and oxidizer corresponding to a high-temperature flame the
hollow shells appeared in large quantities. But as the temperature
of the flame was reduced by changing the flow rates of the carbon
monoxide and oxygen the number of spheres dropped sharply. The

results of this work lead to the extremely interesting conclusion that the temperature of the medium has a strong role in the question of the formation of hollow shells during combustion of metals.

The question arises of whether hollow spheres are formed during burning of metallized powders or of heterogeneous condensed systems containing additions of Al. The composition of the gaseous products (H_2O, CO_2, CO, HCl) and the temperature of the flame jet (2500-3300°C) of the powders are favorable from the point of view of conditions for appearance of spheres. Actually, after burning of metallized solid rocket propellants a large quantity of condensate remains. A certain part of the latter is made up of hollow spheres. However, it should be emphasized that in some they comprise a comparatively small percentage of the total quantity of aluminum oxides. These spheres are virtually no different from those obtained during burning of aluminum particles in gas burners. During burning of propellants rich in carbon a deposit of soot particles is observed on the surface of the hollow spheres, giving them a grayish cast. As pressure is increased a tendency is noted toward a reduction in the quantity and size of the spheres. Their distribution over the cross section of the jet is not distinguished by uniformity.

Summarizing the material outlined above, we arrive at the conclusion that the formation of hollow transparent spheres of oxide can occur during combustion of aluminum in any chemically active oxidizing gaseous medium. A basic condition in this case is high temperature of the medium or of the flame.

Spheres appear directly on the surface of the burning particles. In the case of forced extinguishing they remain bound to the particles (see Fig. 70).

The presence in the flame of hydrogen or compounds of it of the water type (vapor) serves to activate the process of growth of the hollow spheres, both qualitatively and quantitatively.

Certain differences of opinion which arose concerning the determining role of hydrogen might proceed from the fact that a change in the concentration of hydrogen in the flame was apparently inextricably bound with a change in the flame temperature.

b. **Crushing.** This interesting phenomenon occurs, as a rule, on the concluding stage of combustion, when the process has already been completely formulated (see Fig. 64).

In a propane-oxygen-hydrogen flame crushing (fragmentation) proceeds actively in the case when the concentration of free oxygen in the medium reaches 28-38% [133]. Here no small role is played by the temperature of the flame. As the concentration of oxygen in the flame is reduced the limit of crushing of particles is increased with respect to temperature. If the flame temperature comprises 2250-2400°K - i.e., close to the boiling point of aluminum - the concentration of oxygen required for the appearance of the phenomenon of fragmentation exceeds 38%.

In a carbon monoxide-oxygen-nitrogen flame [246] crushing of particles is observed at approximately this same concentration of free oxygen. The lower concentration limit in terms of oxygen equals 32% in this case.

Drew et al. [139] indicate that in a steady oxygen-hydrogen flame from the "Corning Universal" forced burner combustion of aluminum particles terminates with crumbling if the particles leave the flame and reach a zone of contact with the ambient atmosphere.

The phenomenon of crushing of burning particles of aluminum is clearly manifested during combustion of condensed compositions based on ammonium perchlorate (in air or in constant-pressure installations with a medium of inert gas) [173]. In this case free oxygen may either be absent from the flame or may be present in a concentration substantially lower than the limits which are

180

characteristic for gas burners. Thus in an ammonium perchlorate-trioxymethylene flame [246] the quantity of oxygen did not exceed 9%, while products from combustion of a propellant made up of ammonium perchlorate and polyurethane fuel contain virtually no oxygen in the free state, but nonetheless fragmentation of aluminum took place in these cases. However, this occurred only when the particles escaped from the high-temperature zone of the flame and entered the cold atmosphere or a region of lower temperature.

During burning of metallized compositions under conditions of insulation from the external medium - for example, in a typical rocket engine or in a semiclosed volume installation (under conditions when motion and combustion of the particles occurs in a flow of virtually constant temperature) - crushing of aluminum particles is very rarely observed. As pressure increases the probability of appearance of crushing is reduced even further, with fragmentation virtually ceasing to occur at pressures of 20-50 atm (according to observations). At the same time it should be emphasized that an increase in the pressure in constant-pressure instruments does not completely eliminate the crushing effect, although it does lead to a certain degree of quantitative reduction in it [173].

It follows from the given examples that one of the basic factors facilitating crushing of particles on the stage of steady-state self-sustaining combustion is a sharp drop in temperature of the ambient medium along the trajectory of particle motion.

c. **Rotation of hot aluminum particles.** Rotation arises after self-sustaining combustion of the particle has already been established. For particles 100-150 µm in diameter in a carbon monoxide-oxygen flame this process begins to develop approximately 0.1 ms after ignition. Usually it is preceded by a sudden expansion of the diffusion zone of brightness around the particle. Subsequently the speed of rotation is gradually increased and at the limit amounts to 10^4-10^5 pulsations per second.

The trajectory of motion of a rotating particle frequently takes on a wavy nature and terminates with sharp ejection of aluminum in vapor form (crushing) or with a sudden sharp change in the direction of travel (see Fig. 64). The pulsating nature of combustion of individual particles is noted during combustion of aluminum both in gas burners with "dry" and "moist" flames, and in the products of combustion of metallized solid fuels - i.e., in a gas-phase flow which is complex in composition and at a high temperature. However, the total number of particles subjected to rotation during combustion is not great. The latter fact is particularly noticeable during combustion of aluminum in a composition of powders.

3. Temperature of the Zone of
Combustion of Aluminum Particles

The process of combustion of aluminum falls in the class of highly exothermic processes.

In any thermal theory of combustion the temperature fields and gradients are the basic initial characteristics. Since measurement of temperatures and their gradients is extremely complex and difficult to realize in practice for individual particles moving in a gas flow, in this case (as in similar ones) larger-scale bodies are selected as the object of study - thin wires, strips, and drops of aluminum.

During the study of peculiarities of combustion and of the so-called "aluminum sun" (burning of a drop of aluminum in oxygen), Gross and Conway [145] carried out measurements of temperature of the reaction zone by means of an optical pyrometer (Fig. 71). According to their measurements the temperature of the flame lies within the limits 3300-3800°K. Since the drop of aluminum is in the molten state and its surface is free of aluminum oxide, the authors proposed that the temperature of the metal surface is no higher than the boiling of aluminum and is approximately equal to it.

182
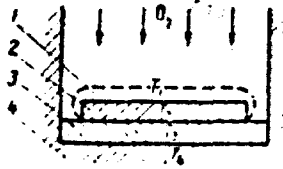
Fig. 71. Distribution of temperatures during combustion of a drop of aluminum. 1 – combustion zone where $3000 < T_1 < 3800°K$; 2 – molten metal, $T_3 < T_2 < 2740°K$; 3 – Al_2O_3, $T_3 < 2318°K$; 4 – substrate, $T_4 < 2318°K$.

A second source of information on the maximum temperature of the zone of combustion of aluminum is study of brightness and light temperatures of oxygen-aluminum flashbulbs [263]. The maximum temperature (from pyrometric measurements) equals 3800°K for all types of bulbs. Their brightness temperature, with consideration of thermal losses, is somewhat lower and falls in the limits 3200-3450°K.

In works [173, 174, 206, 237] the temperature of combustion of aluminum particles in a jet of flame from mixed compositions was evaluated by the spectral-optical method (see Fig. 73). Measurement of the distribution of energy in the visible region of the continuous spectrum from the investigated flames showed that it maybe described by the Wien formula with a single color temperature. Results from evaluations of the temperature of aluminum combustion in the products from combustion of ballistite and mixed compositions by spectral-optical methods are given in Table 18a.

By comparing the measurement results we arrive at the conclusion that the temperature of the zone of combustion of aluminum particles at normal atmospheric pressure equals 3600-3850°K - i.e., it approximately corresponds to the boiling temperature of aluminum oxide Al_2O_3, 3800°K. No specific experimental data are available with respect to measurements of the temperature of the surface of an individual drop or particle. However, the experimental data examined above on combustion of aluminum particles indicate that during combustion aluminum is in the liquid state and therefore the temperature of the particle surface should be limited by the boiling temperature of aluminum.

183

Table 18a. Temperature (in °K) of aluminum in the flame of metal-lized compositions [173, 174].

Composition	Continuous spectrum method	Resonance line method	Photometric method
Ballistite composition (d = 40-70 μm)	3100 ± 150	3400 ± 150	3200 ± 150
High temperature ballistite composition (d = 40-70 μm)	3400 ± 150	3700 ± 150	3600 ± 150
Polyformaldehyde, ammonium perchlorate, and aluminum (d < 50 μm)	3500 ± 150	3750 ± 150	3700 ± 150

4. Spectroscopic Studies

The application of spectroscopic methods to the study of processes of metal combustion is extremely promising, since it provides information which is virtually impossible to obtain by other methods. However, in view of the specific peculiarities of this method its successful application in questions of studying the mechanism of the combustion of individual finely dispersed particles of metal at a given stage is connected with great difficulties.

In their work, Brzustowski and Glassman [143] used strips of aluminum and magnesium 9 cm in length and with an average cross section of 0.3×0.013 cm^2. The spectra were photographed on "Kodak-III" spectroscopic plates by means of a quartz prismatic spectrograph produced by the firm "Hilgar." The photomaterial emulsion was sensitive in the wavelength region 0.24-0.68 Å. Spectral lines were identified from a handbook [264]; the molecular bands of the spectrum were identified from the tables [265].

Spectra which are developed in time (resolution in time 2.1 ms/mm of the image slot) for aluminum foil during its combustion and for flashbulb are continuous. At the maximum of the flash it begins approximately in the region of 3300 Å wavelengths and extends right

up to the red limit of spectral sensitivity of the photographic material. At the very moment of the flash the aluminum lines 3944 and 3961 Å appear in the spectrum. At approximately 5-16 ms they are turned and exist in absorption, after which they are turned once again. Over the entire period of the flash of a foil AlO bands with the most noticeable edges 4648, 4852 and 5079 Å exist in the emission spectrum. The AlO bands never appear in absorption. A few milliseconds after the flash bands in emission on a background of a continuous spectrum exist only in the form of weak "ripples" and become virtually indistinguishable at the maximum of flash intensity. However, at the end of the flash, when the brightness temperature of the continuous spectrum is reduced, they reappear. Figure 72 shows the results of measurements of optical density of the spectrum of aluminum combustion as developed in time. Since the AlO bands exist only at the very high temperature in emissions and do not exist in absorption, in the opinion of the authors this indicates that AlO is formed in the flame as a result of dissociation of Al_2O_3. The subsequent repeated appearance of Al lines on the background of a continuous spectrum first in absorption and then in emission should be considered from the point of view of the nonisothermicity of the process in the flashbulb. At the moment when the flash appears the average temperature of the sources of the continuous spectrum is low. Aluminum lines are manifested in emission. With development of the process of aluminum oxidation particles of aluminum oxide appear - the source of a continuous spectrum with a temperature higher than the boiling temperature of the pure metal. Aluminum lines are now present in the absorption spectrum. On the last stages of the flare the average temperature of condensing Al_2O_3 particles can become lower than the temperature of aluminum vapors, owing to the sharper and more rapid cooling of the particles. Aluminum lines are turned and once again appear in emission. Spectra of the combustion of aluminum wire 0.89 mm in diameter in an oxygen-argon atmosphere are given in work [237]. The experiments were carried out at pressures up to 31.6 atm; the quantity of oxygen was varied in the range 0-100%. The spectra were taken on "Kodak" type I spectroscopic film by means of a 1.5 m grating spectrograph. The first

185

order dispersion region was varied from 3700 to 7400 Å with a linear dispersion of approximately 1.5 Å per 1 mm. Slot width was 60 µm and exposure duration was 1-5 seconds.
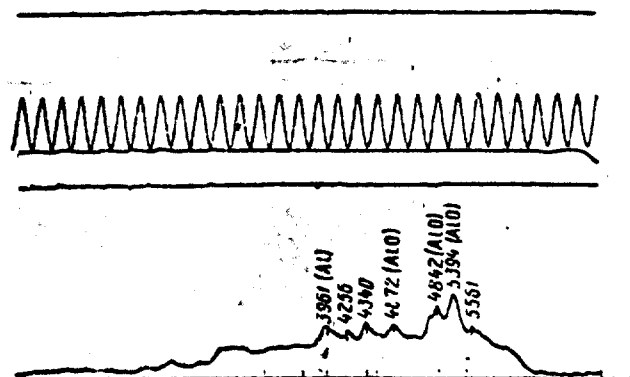
Fig. 72. Optical density of the spectrum of aluminum combustion [173].

Against a background of the continuous spectrum the following bands and doublet lines of Al were singled out: 3082.15, 3092.71, 3944.03, and 3961.53 Å, as well as nine systems of AlO bands with strong band edges at 2942.5, 3022.2, 3114.3, 4352.6, 4470.5, 4648.2, 4842.3, 5079.3, and 5336.9 Å. Systems in the ultraviolet spectral region were determined from wavelengths [266]. Aluminum lines were observed in emission only to a pressure of 7 atm. At a higher pressure they become indistinguishable against a background of a continuous spectrum. Aluminum lines were absent from the absorption spectrum.

In the region of subatmospheric pressures and high oxygen concentrations the flame spectra during combustion of aluminum in an oxygen-water vapor mixture coincided with spectra of flames in an oxygen-argon atmosphere. No differences were detected between combustion spectra for pure and anodized aluminum.

In carbon dioxide and oxygen and carbon dioxide and argon in the pressure interval 1-2.5 atm and with a change in the oxygen concentration from 0 to 100% or 0 to 40% for argon, and also in

the region of reduced pressures in carbon dioxide and oxygen (O_2 concentration 40-100%), the spectra were analogous to spectra of aluminum combustion in oxygen and argon. Two doublets of aluminum and nine AlO bands were clearly distinguished. Despite the fact that they fall in the working range of the spectrograph, it was impossible to detect the presence of CO_2, CO, and C_2 bands.

Study of the spectrum of emission from the flame of metallized powders and solid rocket propellants in the 1-30 atm range was carried out successfully by the authors of works [173, 206, 247]. A diagram of an installation especially developed for this purpose and a description of it are given in Section II (page 95). The spectrum has much in common with those examined above.

The radiation of the flame jet has a continuous spectrum. Its intensity drops gradually in the direction of a reduction in wavelength. Vibration bands caused by molecules of AlO and AlH are manifested against the background of the continuous spectrum in the pressure interval 5-10 atm. In the visible and near ultraviolet regions resonance lines of atomic aluminum are singled out: 3961, 3944, and 3082 Å. They are manifested at a distance of 1 mm and achieve an intensity maximum at a distance of 2 mm from the combustion surface of the specimen. Anomalies sometimes occur in the continuous spectra; without exception, these can be connected not only with candoluminescence and chemoluminescence, but also with scattering of light by extremely fine particles of Al_2O_3 which are formed in the jet during combustion.

It should be noted that the transparency of such a flame is less than 10^{-2} - i.e., the flame jet (specimen diameter 5 mm) with additions of aluminum and magnesium is not transparent. The distribution of energies in the spectrum was constructed in order to study the nature of the continuous spectrum of the investigated flames (Fig. 73). As distance from the combustion surface of the charge is increased, the quantity of energy emitted by the flame

in the wavelength interval 0.3-0.6 μm grows and reaches a maximum at a distance of 1.5 mm from the burning surface. It remains virtually constant up to a height of 3.5 mm and then begins to drop as the combustion products begin to cool. The obtained intensity distribution is adequately described by the Wien formula

$$E_\lambda = u_{\lambda,\,T} c_1 \lambda^{-5} \exp(-c_2/\lambda T),$$

from which it is possible to conclude that the obtained spectra are identical in nature to spectra of thermal radiation of a gray body. From this it follows that the continuous spectrum of the flame jet for compositions with aluminum is due to thermal emission of Al_2O_3 particles. The glow is additionally intensified by the thermal radiation of AlO (or MgO) molecules.
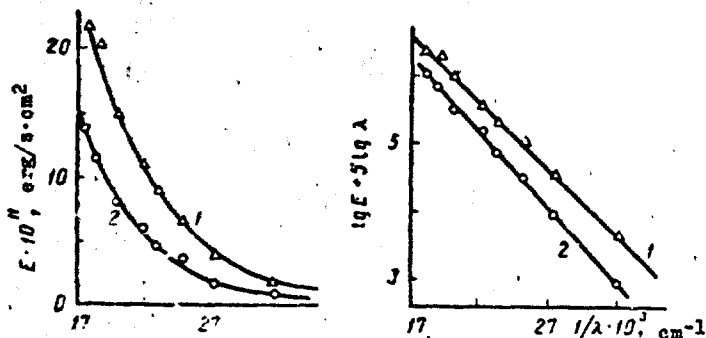
Fig. 73. Distribution of energy over the height of a flame jet for the composition PF + ammonium perchlorate + 20% aluminum at 25 atm. a - in the coordinates E, 1/λ; b - in the coordinates lg E + 5 lg λ, 1 λ. 1 - h = 3 mm; 2 - h = 9 mm.

Figure 74 shows the relative intensity of Al and AlO resonance lines over the height of a flame jet for a composition with 10% Al. The presence of AlO bands in the radiation spectrum is interpreted as proof of the fact that the process of aluminum combustion in the flame jet for premixed condensed systems occurs partially through the intermediate products, with the formation
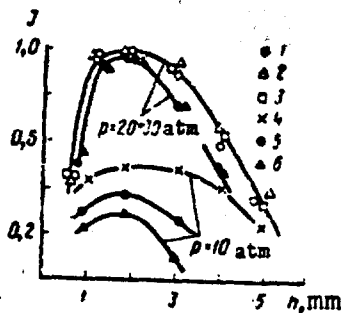
Fig. 74. Relative intensity of Al and AlO resonance lines over the height of the flame jet. For AlO: 1 - 4866(42) Å; 2 - 4672(48) Å; 3 - 5399(54) Å; 4 - 4842 Å; Al: 5 - 3961(44) Å; 6 - 3082(92) Å.

of lower oxides. It is noted that although the spectrum of the flame remains continuous with an increase in pressure (up to 5 atm), it contains no Al and AlO bands.

From the above it follows that the spectrum of a flame of burning aluminum in active gaseous medium is continuous, independent of the medium composition. The continuity of the spectrum is the result of thermal emission of condensed oxide. A number of lines and bands can be singled out against the general background of the spectrum: two doublets of aluminum and nine AlO bands.

During steady-state combustion the lines of aluminum and its alloys are present only in the absorption region. The presence of aluminum lines in emission can be observed in the spectrum only in the period of development or the very concluding stage of combustion of the metal - at the moment of quenching (for example, in flashbulbs). With an increase in pressure there is a drop in the intensity of the individual lines with respect to the general background of the continuous spectrum, and at a pressure greater than 7-10 atm some of them become, in general, quite difficult to distinguish. Since strong doublets of aluminum and AlO bands are manifested in the flame spectrum only during emission, this serves as evidence of the existence in the flame around the particle of either a field of high temperatures or an active chemical reaction, during which these elements are formed in the excited state.

In the region of moderate oxygen concentrations (30-55%) and a pressure $p \geq 1$ atm, strong aluminum oxide bands can be distinguished against the background of the continuous spectrum [237]. Their appearance maybe the result of thermal excitation. One of the probable mechanisms of aluminum oxide formation is the surface reaction between particles of liquid Al_2O_3 and Al, in the course of which Al_2O and Al are formed [287]. The presence of all of the bands of aluminum oxide in the region of low pressures against the background of a continuous spectrum in emission indicates the probability that aluminum oxide is formed as the result of a vapor-phase reaction directly within the flame.

5. Chemical Composition of the
Combustion Products

Study of condensates collected successively during the combustion of aluminum in various oxidizing media provides a basis for the conclusion that the phase state of the final products of combustion depends on the condition of their formation.

According to the results of X-ray diffraction analysis the major fraction of condensed products from aluminum combustion usually comprises the α-modification Al_2O_3 - i.e., corundum. This modification is the most common and most stable. It predominates during combustion of aluminum in the range of atmospheric and higher pressures and at moderate values of oxygen concentration in the medium [237]. As the oxygen concentration is increased and, especially, with conversion of the combustion process into the subatmospheric region, the high-temperature γ-modification appears. Usually the $γ-Al_2O_3$ is a mixture of three modifications, κ-, γ- and $θ-Al_2O_3$. At temperatures above 700°C this modification undergoes an irreversible transformation into $α-Al_2O_3$ [267]. Sharp cooling of the combustion products - for example, during their deposition on heat-conducting elements of the installation - prev nts the indicated transformation and thus, under certain conditions, will facilitate the forced appearance of $γ-Al_2O_2$ in the final products.

During combustion of aluminum in a CO_2-O_2 medium with an increased content of carbon dioxide a yellow crystalline deposit is detected in the condensate; at lower temperatures this reacts with water vapor with the liberation of a hydrocarbon gas.

In terms of chemical composition and properties this product is Al_4C_3. In a medium with a high content of halogens or of their derivatives - for example, Cl or HCl - the formation of aluminum halides of the $AlCl_3$ type is observed along with that of corundum. Compunds of aluminum with carbon and chlorine can be present in a substantial quantity (>1%) among the products of combustion of metallized solid fuels based on ammonium perchlorate. The probability of their appearance grows as the initial composition of the propellant is enriched with fuel and with aluminum.

At the same time suboxides of aluminum AlO and Al_2O, whose presence or possible existence in the flame is confirmed by spectrograms or by thermodynamic calculations [137], are not found in the final products of aluminum combustion.

6. Time of Particle Combustion

The time of combustion of particles of aluminum and its dependence upon various factors are extremely important parameters from a practical and theoretical point of view. In the end it is precisely this parameter which determins the effectiveness with which the metallic additives are utilized in combustion chambers of various power plants, including solid-propellant rockets.

Since the majority of studies have been carried out in tracking installations and burners, the quantitative experimental data on the time of particle combustion relate mainly to atmospheric conditions. However, comparison of results will not infrequently run into major difficulties, since the authors often do not give the detailed characteristics of the conditions under which the data were obtained.

In the flame of a flat propane-oxygen-nitrogen burner the combustion time of aluminum particles 23 and 50 μm in diameter comprises 4 and 13 ms, respectively. Combustion time τ_r is roughly proportional to the diameter of the particles, d, in a power of 1.5 [133].

In a $CO-O_2$ flame [134] combustion time for spherical aluminum particles 35 and 49 μm in diameter varies as a fun tion of the content of free oxygen and water vapor in the flame.

In a "dry" atmosphere (7.9% free oxygen and 0.5% H_2O) it equals 6.6 ± 0.7 and 12 ms. With the addition of hydrogen to the flame (18.1% H_2O + 5 8% O_2) the time grew to 10.5 ± 0.5 ms for particles with d = 35 μm and to 19 ms for particles with an average diameter of 49 μm (the quantitative composition of the remaining reagents was not indicated, but it is not impossible that the concentration of CO_2 varied with a change in the H_2O concentration; T = 2510°K).

Work [261] gives averaged value of τ_r for aluminum particles 15-50 μm in diameter in a methane-oxygen flame (Fig. 75). These results have a more illustrative significance, since neither temperature nor flame composition are reported. However, the fact that the combustion time for 50-um particles exceeds that of similar particles as given in work [134] by 3-4 times allows us to assume low activity of the flame.

Approximate evaluation of the connection of τ_r with particle dimension d shows that τ_r is proportional to diameter to a degree of 1.7-2.0.

More detailed information on the effect of reactivity of a gas-burner flame on combustion time for aluminum can be drawn from work [246] (particles with d = 53-66 μm, medium CO + O_2, p = 1 atm).

The results of the measurements are shown on Fig. 76. In the upper portion of the figure the concentration of the basic reagents

192

and the flame temperature are given. From the curve it follows that
with a constant flame temperature (2500°K) and at atmospheric pressure
the combustion time for aluminum is approximately inversely pro-
portional to the partial pressure of oxygen. Since we noted earlier
that the nature of the combustion process for aluminum and the com-
positions of its product are significantly influenced by the presence
of hydrogen or water in the oxidizing medium, the question arises
of the effect of "humidity" of the medium on the time of particle
combustion.
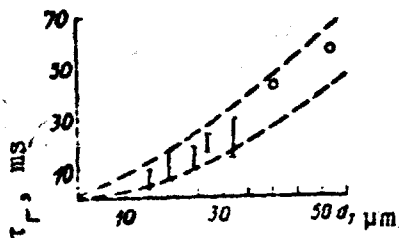
Fig. 75.
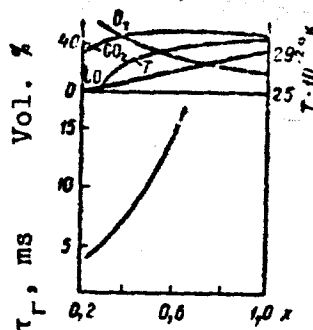
Fig. 76.

Fig. 75. Combustion time for Al particles in a
methane-oxygen flame.

Fig. 76. Concentration of main reagents and com-
bustion time for spherical Al particles in a flame
with $xCO + 0.5\ O_2$.

At first view the experimental data outlined above confirmed
the hypothesis of a sharp intensification of aluminum combustion
in the presence of moisture. However, from this point of view
these results cannot be considered correct, since no data are given
on the remaining reagents besides the concentrations of H_2O and
O_2. This concerns first of all CO_2, which can participate actively
in reactions with aluminum. But comparison of experimental data on
combustion rate indicates that it occurs too rapidly (especially in
a "moist" medium) to be caused only by diffusion of oxygen.

193

Actually, more recent investigations [135] of conditions of aluminum combustion in a gas burner have shown that combustion time for aluminum in "moist" and "dry" atmospheres differs very little; τ_r for particles 32 μm in diameter comprises 2.8 ms for a "dry" flame and 3.2 ms in the case of a "moist" flame. These values were determined with great accuracy and have high reproducibility. The differences are extremely small and can be ascribed to the action of carbon dioxide, whose content in the "dry" medium is higher than the total quantity of CO_2 and H_2O in the "moist" atmosphere. In both cases τ_r is proportional to the square of the diameter.

In considering the time parameters of combustion of finely dispersed aluminum in a high-temperature gas flow, it is necessary to single out the case of combustion in products of the gasification of solid fuel or heterogeneous condensed systems in constant-pressure instruments or in installations with a semiclosed volume like a model end-burning microthruster. An outstanding feature of the latter is the fact that the required level of pressure and high-temperature flow are created in them as a direct result of burning of the powder or of fuel-oxidizer compositions which simulate powders. The basic method of introducing aluminum particles into a flow which is thus created is preliminary pressing of them into specimens of the propellant.

As the specimen is burned up the metallic particles are continuously injected into the flow of gaseous decomposition products escaping from the surface of fuel and oxidizer combustion. The concentration of particles per unit volume of the flow is determined by their quantity in the specimen. If the main problem is to determine the induction period or combustion time of individual particles of one metal or another, the quantity of it in the composition of the specimen usually does not exceed 0.01%. At this concentration there is adequate basis to consider that the interaction of the burning particles in the gas flow is negligibly small.

Work [154] presents a broad study of combustion time for individual aluminum particles as a function of the basic parameters of the flow: pressure, temperature, and composition. Preliminary thermodynamic calculation of a number of compositions on an electronic computer made it possible to vary the composition and temperature of the medium in wide limits, independently of one another. The temperature measurement interval comprised 1600-3000°K (Fig. 77).

As has already been emphasized, the composition of a flow created by the indicated method is extremely complex and can include up to 50-80 different compounds, radicals, and elements. At the same time the basic reagents containing oxygen and therefore capable of taking an active part in the reaction of aluminum oxidation are H_2O, CO_2, CO, OH, O_2, O, etc. With the exception of the first three, the remainder are, as a rule, present in extremely limited quantities (fractions of a percent) and do not have any essential influence during the combustion of aluminum. But the first three are not of equal significance. The energy of molecule dissociation is given below for the compounds which are most characteristic from the point of view of the considered medium [268]:

Bond	E, kcal/mole
H_2-O	119.2
CO-O	127.2
C-O	256.9

Dissociation energy with respect to oxygen for the molecules CO_2 (CO - O) and H_2O(H - O_2) is about half that of CO(C - O). From this it follows that with concentrations of the indicated reagents in the flow which are identical in order of magnitude the process of oxidation of aluminum should proceed primarily due to its interaction with carbon dioxide and water - which are equivalent to each other with respect to reactivity with aluminum.

Thus the rate of combustion of aluminum in a flow which is created by the products of combustion of a condensed system is
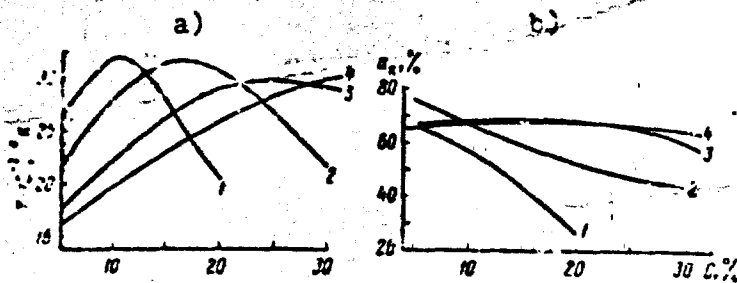
Fig. 77. Adiabatic temperature of the flame (a) and relative concentration $a_{\text{и}}$ of active oxygen-containing reagents (b) in the flame for ammonium perchlorate compositions with different fuels. 1 - polyethylene; 2 - polymethyl methacrylate; 3 - polyformaldehyde; 4 - ballistin N.

determined by the total concentration of active oxygen carriers - H_2O and CO_2. In this case carbon dioxide in reaction with aluminum is reduced predominantly to CO rather than to pure carbon, although with respect to energy the latter would be preferable:

$$2Al + 3CO_2 \rightarrow Al_2O_3 + 3CO + 195.2 \text{ kcal/mole.}$$
$$2Al + 3/2CO_2 \rightarrow Al_2O_3 + 3/2C + 257.2 \text{ kcal/mole.}$$
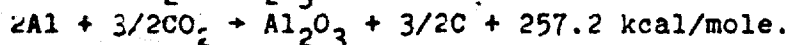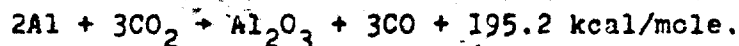
Figure 77b shows graphic curves of the change in relative concentration of $H_2O + CO_2 + O_2$ (parameter $a_{\text{и}}$) in flames of a number of compositions of polymer fuel and oxidizer (APC) as a function of the percentage ratios of the component.

The parameter $a_{\text{и}}$ was calculated by the expression

$$a_{\text{и}} = \frac{n_{H_2O} + n_{CO_2} + n_{O_2} + \cdots}{\Sigma n_i} \cdot 100 \text{ %,} \qquad (IV.1)$$

where n_1 is the molar or volume concentration of individual reagents. Naturally, if the concentration of H_2O and CO_2 in the products of specimen combustion is small, aluminum can and will enter into reaction with other compounds.

196

These assumptions find confirmation in a series of thermo-
dynamic calculations of the process of combustion of metallized
compositions with an increased aluminum concentration.

Since the curves of the change in composition and temperature
of the medium (see Fig. 77) were compiled for the same systems,
there is broad possibility for an independent change of each of
the parameters named above.

On the basis of a large series of experiments it was established
[154] that the time of combustion for particles of finely dispersed
aluminum is virtually unchanged with constant pressure and with
a change in medium composition in the temperature interval 2000-
3300°K (Fig. 78). In the region of lower temperatures τ_Γ grows
somewhat. However, this growth is not great. For particles 70 μm
in size at T ≈ 1600°K it comprises approximately 10% of the τ_Γ for
the same particles at 2400°K. In the general case the time of
burning of particles of a given size is approximately inversely
proportional to the relative concentration of H_2O and CO_2 in the
flame jet: $\tau_\Gamma \sim 1/a_{\text{H}}^{0.9}$ or, for practical purposes, $\tau_\Gamma \sim a_{\text{H}}^{-1}$
(Fig. 79).

Davis [246] obtained a similar result for conditions of a gas
burner: τ_Γ is inversely proportional to the partial pressure of
oxygen.

Results on the dependence of burning time of aluminum on pressure
are no less interesting (Fig. 80). At pressures about 25 atm it
virtually ceases to depend on pressure (composition and temperature
being constant). Beginning at 20 atm and below the rate of high-
temperature oxidation of aluminum is reduced and τ_Γ grows. A more
sharply expressed growth in τ_Γ with a reduction in pressure was
obtained in a series of experiments carried out in a constant-
pressure instrument on the system APC - polyformaldehyde - aluminum
[246] (Fig. 81). The limiting pressure which marks the beginning
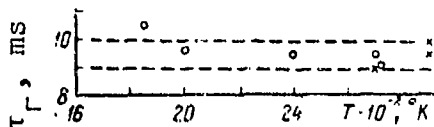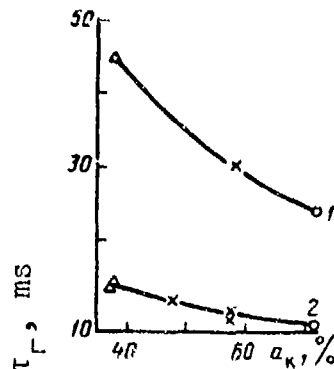
Fig. 78.   Fig. 79.

Fig. 78. Time of combustion of Al particles (d =
= 70 μm) as a function of temperature.

Fig. 79. Effect of the parameter a_H on τ_Γ of
aluminum. 1 – d = 140 μm; 2 – d = 70 μm.

of $\tau_\Gamma \approx$ const is shifted into a region of higher values of p
(70÷100 atm). This pressure is the higher, the greater the size
of the particles. The reasons for the divergence in magnitude
of maximum pressures are not clear. However, the quantitative
values of equal-size particles in the $\tau_\Gamma \neq f(p)$ region (with
consideration of the parameter a_H) as given in works [154, 246]
differ very little.

One of the central questions is that of the burning time for
particles as a function of their size. For spherical aluminum
the diameter of the particle is the dimension concerned here.
Under the conditions in a gas burner at atmospheric pressure the
majority of investigations for aluminum indicate a law which is
quadratic or close to it, $\tau_\Gamma \sim d^2$. This is emphasized by the
sharp growth in burning time of particles with [an increase in]
diameter and the similarity of processes of metal combustion to
diffusion burning of hydrocarbon fuel [259].

During burning in a composition of condensed systems with
p ≈ 1 atm burning time for spherical aluminum particles is also
proportional to d^2. However, as pressure increases the square law

198
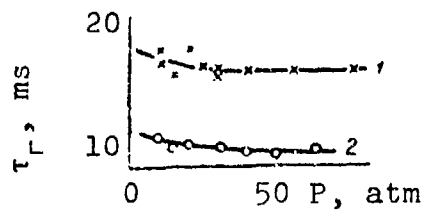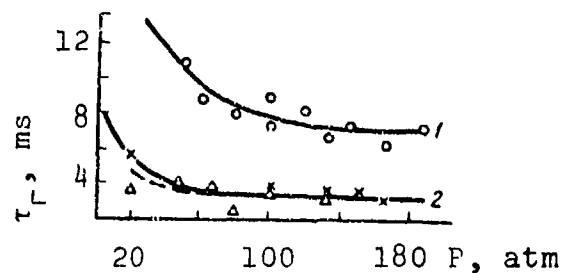
Fig. 80.

Fig. 81.

Fig. 80. τ_Γ as a function of P. $1 - a_{\text{H}} = 37.5\%$; $2 - a_{\text{H}} = 71.5\%$.

Fig. 81. τ_Γ as a function of P. $1 - d_{A1} = 80{-}103$; $2 - d_{A1} = 53{-}66$ μm.

is constantly replaced by weaker relationships. In the pressure region above the maximum τ_Γ is proportional to the diameter to a power of 1.5 (Fig. 82) and is independent of the speed of the high-temperature oxidizing flow, W (Fig. 83). The transition from a quadratic law to a power of 1.5 occurs without sharp changes. The nature of the change in τ_Γ with particle diameter is virtually independent of the activity of the medium - i.e., of the magnitude of the parameter a_{H} ($30\% \le a_{\text{H}} \le 60\%$). However, it should nonetheless be noted that with a sharp drop in the concentration of H_2O and CO_2 in the flame ($a_{\text{H}} < 25\%$) the exponent drops even lower (to 1.4 or less).

Thus during combustion of aluminum in the combustion products from condensed systems, where the basic oxygen-containing oxidizing reagents are H_2O and CO_2, burning time τ_Γ is virtually independent of the medium temperature ($T \ge 2000°C$) and of pressure ($p \ge 25$ atm), but at the same time it varies strongly with a change in particle diameter and in the activity of the medium, a_{H}.

In the general case for the indicated conditions

$$\tau_r = k \frac{d^{1.5}}{a_{\text{H}}^{0.5}}, \quad \text{ms}.$$
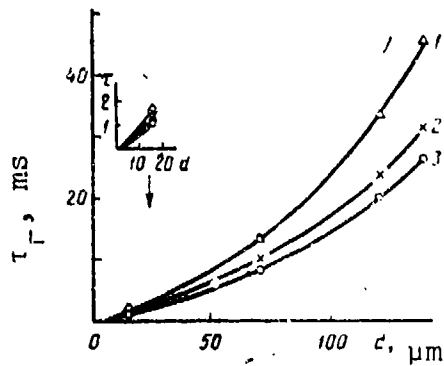
Fig. 82.   Fig. 83.

Fig. 82. τ_Γ as a function of particle diameter. 1 - a_H = 37.5%; 2 - a_H = 57.3%; 3 - a_H = 71.5%.
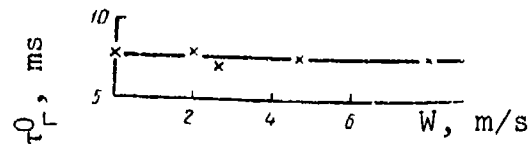
Fig. 83. τ_Γ as a function of the speed W of the high-temperature flow for d = 70 μm.

If the time is measured in milliseconds and the diameter in microns the proportionality factor k will equal 0.67. Calculation by the proposed formula

$$\tau_\Gamma = 0.67 \cdot \frac{d^{1.5}}{a_K^{0.9}} \cdot \text{ ms} \qquad (IV.2)$$

will give satisfactory agreement with experiments. For example, for particles 50 μm in diameter we find from the calculation in a flame with a_H = 57.5% values of τ_Γ = 6.4 ms. The experimental value of burning time for the same conditions is 6.5 ms.

In order of magnitude the average rate of burnout over the radius comprises 5-10 mm/s for spherical aluminum 15-20 μm in diameter. This is comparable with burning of ordinary two-component fuel mixtures based on APC [156].

No systematic data are available on the combustion of aluminum as one of the components of heterogeneous systems in a constant-pressure instrument.

Nonetheless the available data make it possible to state that the conclusion concerning equality of average burning rate for fine particles of aluminum and the normal rate of combustion of solid rocket propellants remains valid.

7. Effect of Medium Composition and Pressure on the Combustion of Aluminum

Medium and pressure have a direct influence on the process of burning of metal. Their role in the combustion of finely dispersed aluminum has been touched upon in virtually every section of this chapter. We will pause once again to consider their basic features.

1. The process of burning of aluminum, as a diffusion process, is activated as the activity of the medium is increased and with an increase in oxygen concentration or the concentration of oxygen-containing reagents of the H_2O and CO_2 type. Carbon dioxide and water vapor are equivalent from the point of view of activity: combustion time for aluminum in a "dry" and "wet" medium virtually coincide with identical concentrations of the oxidizer.

2. A high content of oxygen, the most highly active oxidizer during combustion, contributes to crushing (fragmentation) of the particles. When a substantial quantity (30%) of water vapor is present in the medium favorable conditions are created for the formation of hollow translucent spheres of oxide in the products from combustion of aluminum. With an increase in oxidizer concentration the brightness and density of the glowing reaction zone around the particle will increase.

3. The glowing zone of combustion of a particle in a "moist" atmosphere is 1.5-2 times wider than in the absence of H_2O or compounds of hydrogen.

4. An increase in pressure p leads to an increase in the rate and to weakening of the dependence of combustion time of aluminum

on particle size. The exponent of d drops from 2 to 1.5 with a growth in p from atmospheric level to 30-80 atm.

5. The width of the reaction zone grows with a reduction in pressure, while the density of the glow around it is reduced.

6. In the region of elevated pressures the phenomenon of fragmentation of particles occurs more rarely than when $p \leq 1$ atm.

We should pause for separate consideration of studies on the influence of pressure and chemical activity of the medium on burning of aluminum wires [236-239, 269].

Drawing of heat to the electrodes, intensive thermal radiation incident on parts of the installation, ignition from an internal heat source (electrical discharge) rather than from an external source, the need to maintain mechanical integrity in the period of ignition - all of these are specific features of the combustion of wires and tapes and are not encountered in carrying out experiments with spherical particles in a gas flow, to say nothing of solid propellants. Therefore certain special features and conditions of combustion which are observed during burning of wires cannot be transferred to the case of particles. However, there is unquestionably utility in research of this type and consideration of the procedures and results.

Diagrams taken from works of Brzhustovski, Glassman, and Mellor show the basic regions which are specific for burning of aluminum wires (anodized and unanodized) which are ignited in mixtures of oxygen and argon [237] or oxygen and carbon dioxide or carbon dioxide and argon [236].

With ignition in the region of low pressures and high oxygen concentrations (Fig. 84, region 1) a bright blue flame appears on the tips of the wires, progressing rapidly toward the electrodes.
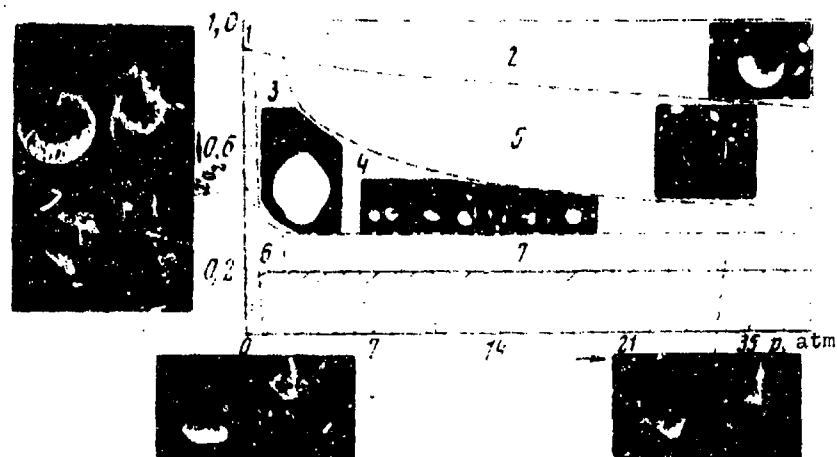
Fig. 84   Combustion of aluminum wires in an
O_2-Ar medium.

With an increase in pressure (region 2) the density of the
flame grows; its color becomes an intense white. The combustion
products are made up of a fine white smoke with bits of ceramic
on the electrodes.

Region 3 is an area of low pressures and moderate concentrations
of oxygen. In external appearance the flame on the tips of the
wires is similar to hydrocarbon flames. In the upper left corner
of the figure we see (clockwise) flame of a   wire 0.9 mm in di-
ameter at p = 100 mm Hg and oxygen concentration n_{O_2} = 70%, and
then p = 50 mm Hg and n_{O_2} = 60%. The figure also shows combustion
products on the electrodes and the flame at p = 50 mm Hg with
n_{O_2} = 80%.

Bright spots are visible on the surface of the wire - tiny
spheres of liquid aluminum oxide. Tracks caused by condensation
of Al_2O_3 in the surrounding atmosphere travel out from the drop
surrounded by the flame. The appearance of bright tracks is the
result of turbulence in the velocity field around the drop. The
surface of the latter is not uniform in brightness: deposits of
oxide cover part of the surface, causing asymmetrical evaporation
of the Al.

With an increase in pressure (region 4) the flame becomes less transparent and draws closer to the drop or metal. Bright particles are seen in the zone of the flame, gradually moving out of it.

The unburned wire is covered with gray vitreous drops. The combustion products on the floor of the chamber consist of translucence spherical particles 50-100 μm in diameter. Certain of them reach a maximum diameter of 100-1000 μm. Only the very largest particles are hollow. The deposit on the electrodes is made up of glassy spherical particles less than 10 μm in diameter. A protective layer of aluminum oxide is formed comparatively slowly on the surface of the liquid metal and thus cannot serve to inhibit the reaction.

In region 4 (see Fig. 84) we see a flame at a pressure of 2 atm with an oxygen content ≈60%. After initially covering the entire drop, the flame moves upward along the surface. The shape of the flame indicates that the flame does not sit directly on the surface of the drop.

In region 5, at low pressures, the flame is analogous to that in region 4, but less bright; it goes out quickly. Metallic drops 3-4 mm in size with a dull surface are collected on the bottom of the installation; there is no vitreous material. At higher pressures a flash occurs at the moment when the protective layer is melted. Brightly glowing particles drop from the point of fracture; the remainder of the wire is not ignited.

The rate of the aluminum oxidation reaction on the pure surface of the metal is so great that the metal is rapidly covered with a layer of oxide which prevents further development of the reaction. The existence of this region is connected with destruction of the integrity of the specimen and, consequently, with termination of heat supply (Joule heat) in the wire. The vapor-phase combustion mechanism is not applicable to this region and its existence for spherical particles burning in a high-temperature flow is doubtful.

When the concentration of oxygen in the medium drops to 20-30% (regions 6 and 7) the burning of the aluminum wire is characterized by a rise in the solid deposit in the diffusion flame. The flame is supplied with metal draining through the solid oxide shell covering the wire. The flame front is virtually invisible. On the tip of the hollow [oxide] shell a solid white deposit is detected. The figure shows the flame and the products from combustion at pressures of 300 mm Hg and 2.1 atm and an oxygen concentration of 30%. With an increase in pressure (region 7) a dense greyish mass is formed, which was not observed at low pressure (region 6).

With a concentration of free oxygen in the medium of less than 20% it was not possible to ignite aluminum wires in the investigated interval of pressures. The observed picture of combustion of wires is unchanged if anodized aluminum is used instead of the pure form.

Figure 85, whose boundaries are also tentative, shows the picture of combustion of aluminum in a medium of carbon dioxide with oxygen and argon.
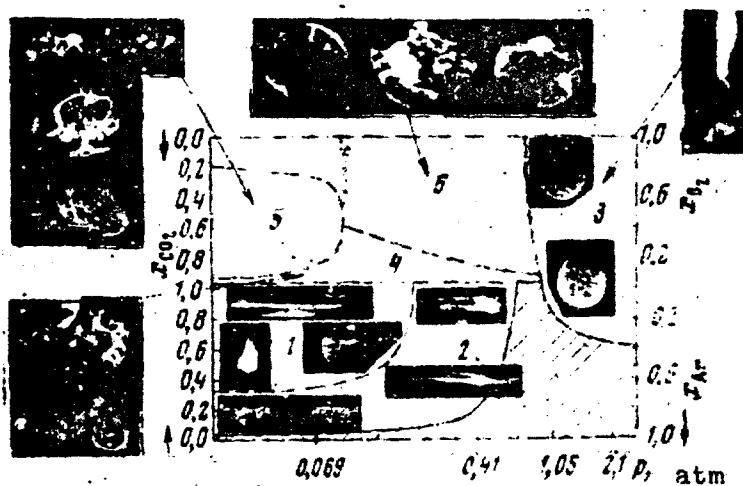
Fig. 85. Burning of anodized aluminum wires in a CO_2-O_2-Ar medium.

Thin anodized aluminum wires burn in a mixture of carbon dioxide and oxygen (region 3) with any ratio of O_2 and CO_2. In a carbon dioxide and argon medium the region of ignition is sharply narrowed, especially at pressures above 0.5 atm. Burning occurs only with an oxygen concentration higher than 70-90%. Ignition is connected with destruction of the wire. However, if ignition has occurred the process is analogous to burning of aluminum in an oxygen and carbon dioxide medium at the same pressures (p > 1 atm).

The observed flames correspond to flames in regions 3 and 4 (low pressure) on Fig. 84. The flame travels rapidly along the wire and at the tip takes on a spherical shape. With an increase in pressure the flame front draws closer to the surface. At high oxygen concentrations the color of the flame is bright blue. At the top of the photo related to region 3 we see a flame in pure carbon dioxide at a pressure of 2 atm; the bottom photo shows the flame during burning of aluminum in a carbon dioxide and oxygen medium (50/50) at a pressure of 1 atm. The condensate is equivalent to the condensate in regions 3 and 4 of the preceding setup (see Fig. 84), with the exception of the fact that in this case a larger quantity of gray and black flakes and spheres is present. The dark color increases with a growth in carbon dioxide concentration. This indicates the formation of pure carbon in this region during the reaction $Al + CO_2$.

In a carbon dioxide and argon medium ignition is facilitated with a decrease in pressure: at pressures below 0.3 atm wires are oxidized even at an argon concentration of more than 90% (10% CO_2). Two regions of combustion are distinguished here: region 1 at high CO_2 concentrations and pressure below 0.2 atm, and region 2 with pressure up to 0.5 atm and an oxygen concentration from the determining limit of the ignition region up to values which relate to region 1 (see Fig. 85).

In region 1 a cylindrical flame is formed around the wire immediately after ignition (at p = 50 mm Hg, 50% CO_2). At the

206

moment when the wire breaks we see on its tips balls of aluminum, leaking downward, surrounded by a diffusion flame. The total time of the process, including ignition and burning, comprises 1-7 seconds. The deposit is of a grayish color and is predominantly a mixture of Al_2O_3 and carbon.

In general features region 2 is similar to region 1, which again serves to emphasize the tentative nature of the division of aluminum combustion into regions.

A cylindrical flame is also formed after ignition; however, it is located somewhat closer to the wire than in region 1. This flame does not disappear even after the wire breaks. Owing to the extremely small burning time (0.4-2.4 s) the molten aluminum is unable to run down to the end of the wire. Figure 85 shows a specimen of cylindrical flame at a pressure of 300 mm Hg and a molar fraction of carbon dioxide equal to 0.9, and also the hollow shell which remains after its quenching.

A translucent deposit is formed on the electrode at high CO_2 concentrations in regions 1 and 2. The diameter of the smallest particles equalled 5-10 μm. A few darker particles are present − the result of the presence of carbon.

Region 4 falls in the class of low pressures (less than atmospheric), high CO_2 concentrations, and low O_2 concentrations. The mechanism and products of combustion are analogous to those in region 6 or Figure 84. The photograph gives a picture of combustion at a pressure of 300 mm Hg and an oxygen content of 10%. The duration of the process is up to 12 seconds. In the period of existence of a diffusion flame a solid deposit builds up on the wire. The reaction occurs at the expense of molten aluminum covered with an oxide film. A white deposit with a small quantity of black carbon plates or flakes is noted on the electrodes.

Region 5 is characterized by large sky-blue flames. It is similar to region 3 in terms of the diagram of combustion in a mixture of oxygen and of argon. There is a small quantity of a yellow deposit which is absent in oxygen and argon mixtures; this can be identified as Al_4C_3. The total burning time is 10-20 seconds. These photographs were obtained at a pressure of 50 mm Hg: for the upper photo the O_2 content was 50%, and in the lower photograph it was 40%.

In region 6 we observe a combination of the mechanisms of combustion in regions 3 and 4. The two types of flames are present simultaneously or separately. If they exist simultaneously the appearance of the flame characteristic for region 4 precedes that of the flame characteristic for region 3. This region can also be included in region 3 of Fig. 84. The time of the total burning process equals 1-28 seconds. Region 6 is a buffer between regions 3 and 4. The photographs were obtained at 100 mm Hg, with the one on the left being taken with a 60% O_2 concentration and the one on the right in 100% O_2.

Thus the pressure and composition of the medium are unquestionably important during burning of metal. But it must be emphasized once again that certain of the examined specific regions for burning of wires may not necessarily apply to the combustion of aluminum particles.

8. Effect of Additives on Aluminum
Combustion

Metals of high purity were used to obtain the optimum characteristics of combustion. There is no question of the need and substantiation for this requirement. However, during solution of practical problems certain additives are deliberately used.

One of the additives most frequently applied is magnesium. Magnesium forms a strong alloy in any ratio with aluminum. The

eutectic alloy contains 11% magnesium and 89% aluminum. This is one of the metals which activates the burning of aluminum and at the same time introduces a comparatively small reduction in the power capacities of the metal as a component of rocket propellant. In terms of activity of metals magnesium is in second place behind aluminum.

Of the various alloys the one which burns most quickly is an alloy consisting of 65% Al and 35% Mg [137]. Cinephotographs of the burning of aluminum-magnesium alloy particles indicate that a two-stage process occurs in this case.

On the first stage, immediately after ignition, there is predominant burning out of the magnesium. Then the aluminum ignites and is burned. On the first stage the track is similar to the track for combustion of magnesium: its width substantially exceeds the width of the track of an aluminum particle of similar size. At the same time the possibility of partial evaporation and combustion of aluminum is not completely excluded. Spectroscopic measurements show that AlO lines exist in the flame in this stage.

On the second stage virtually pure aluminum burns with traces which are characteristic for its features and properties. In certain cases the transition of combustion from the first to the second stage is accompanied by a drop in the intensity of the glow. This is favored by a low temperature of the medium.

The phenomenon of fragmentation is expressed more sharply during burning of the magnesium-aluminum alloy than during combustion of aluminum.

The products from combustion of the alloy are extremely similar to products from aluminum combustion. Along with a subdispersed condensate, hollow spherical shells are formed. The X-ray composition of the products from burning of aluminum-magnesium alloys is shown in Table 19.

Table 19. Radiography of products from the combustion of Al-Mg alloy [137].

Combustion	Basic oxides	Second-stage oxides
Al	α-Al$_2$O$_3$	γ-Al$_2$O$_3$
Al — 5% Mg	γ-Al$_2$O$_3$	MgAl$_2$O$_4$
Al — 12% Mg	MgAl$_2$O$_4$	γ-Al$_2$O$_3$ (нет α-Al$_2$O$_3$ и MgO)
Al — 36% Mg	MgAl$_2$O$_4$	α-Al$_2$O$_3$, γ-Al$_2$O$_3$
Al — 43% Mg	MgAl$_2$O$_4$	γ-Al$_2$O$_3$ MgO
Al — 50% Mg	MgAl$_2$O$_4$, MgO	γ-Al$_2$O$_3$
Al — 55% Mg	MgAl$_2$O$_4$, MgO	α-Al$_2$O$_3$, γ-Al$_2$O$_3$
Al — 65% Mg	MgAl$_2$O$_4$, MgO	Нет Al$_2$O$_3$
Al — 80% Mg	MgO	MgAl$_2$O$_4$
Al — 90% Mg	MgO	MgAl$_2$O$_4$
Mg	MgO	—

[нет = "no"; и = "and"]

The predominance of MgAl$_2$O$_4$ in the combustion products attests to the formation of this compound directly in the process of the reaction. The time of steady-state combustion of the alloy particles, without fragmentation, depends on the ratio of Al to Mg. As the magnesium fraction in the alloy is increased this time is reduced, gradually approaching the combustion time for a particle of pure magnesium. Under identical conditions and with equal spherical dimensions of the particles the combustion time of aluminum is approximately 3 times as great as that for magnesium (Fig. 86).
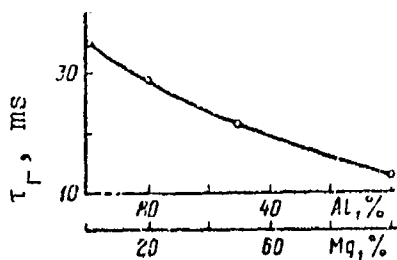
Fig. 86. Burning time τ_Γ for particles of Al-Mg alloy.

It is noted [137] that the addition of a small quantity (2%) of Li, B. Ti, Zr, V, Mo, Cr, Mn additives to an aluminum-magnesium alloy containing 65% aluminum sharply reduces the burning rate (by 5-6 times).

Combustion of the lithium aluminum hydride LiAlH$_4$ occurs in three stages. First the gaseous hydrogen which is formed during decomposition is burned off. Then the lithium evaporates and burns. Finally on the concluding stage there is the remaining aluminum, which burns in the fashion characteristic for it. The multistage nature of combustion is inherent to many other compounds and hydrides of aluminum.

9. Models of Combustion of
Aluminum Particles

As a result of experimental study of the process of self-sustaining combustion, analysis of combustion products, spectroscopic and fluoroscopic investigations, and generalization of the obtained quantitative and qualitative data, two model mechanisms of the combustion of aluminum particles have been advanced.

One of these is the "bubble" model of Bartlette, Fassel, et al. [261]. According to this model a molten spherical drop of aluminum is encased in a solid shell of aluminum oxide which in turn is at a temperature close to the boiling temperature. The rate of combustion is limited by the diffusion of gaseous reagents through the oxide film.

The second model is that of vapor-phase combustion. The rate of the process is determined by mutual diffusion transfer of aluminum and oxidizer vapors into the high-temperature zone of the reaction. In its general features this model is analogous to the diffusion model of combustion of drops of hydrocarbons developed by G. A. Varshavskiy, D. A. Frank-Kamenetskiy, et al.

The bubble model is depicted schematically on Figure 87. The authors have tentatively broken it down into three time periods.

The first period is that of surface oxidation of the aluminum. The reaction rate is determined by the slow diffusion of reagents

through the solid film of oxides which covers the particle of
metal. This is the so-called preignition period. Its extent in
time determines the delay in ignition of the particle, τ_{an}. In
this period there is a gradual heating of the metal up to the melt-
ing point and further heating of the melted particle to a tempera-
ture equal to the melting temperature of the oxide shell (~2300°K).
The melting point of Al_2O_3 is the temperature limit of the first
region. Heat transfer to the particle is accomplished mainly by
thermoconductivity from the surrounding medium and partially through
the reaction of slow surface oxidation of the metal through the
oxide film and by radiation. In the course of the reaction the
thickness of the oxide film is gradually increased.

Transition of the process to the second period is connected
with melting of the oxide film covering the molten particle of
metal. This demarcation is indicated by a sharp increase (t
several orders of magnitude) in the rate of diffusion of reagents
within liquid substances as compared with that in solids [132, 270].
The temperature interval of the region ranges from the melting
point of Al_2O_3 up to the boiling temperature of pure aluminum.
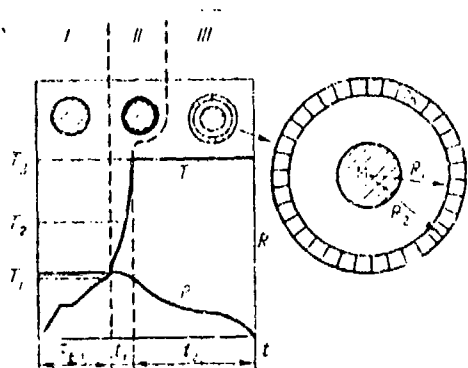
Fig. 87. Diagram of the "bub-
ble" model of particle combus-
tion. T_1 - ignition tempera-
ture; T_2 - boiling temperature
of the metal; T_3 - boiling
temperature of the oxide.
I - ignition delay; II, III -
evaporation and burning of the
metals; M - metal particle;
OK - oxide.

The main source of heat is the chemical reaction of aluminum
oxidation. The supply of heat from the gas by conduction is
insignificant.

Since the pressure of aluminum vapors is lower than the pressure of the surrounding medium the molten oxide film is located directly on the liquid drop of metal. This coating prevents evaporation of the aluminum. The radius of the particle changes insignificantly and only as a result of partial oxidation of the metal. The duration of the second period, t_1, is determined by the time required to raise the temperature of the particle to the boiling temperature of aluminum.

The quantity t_1 is found from equality of the heat which is liberated as a result of the chemical reaction of aluminum oxidation, Q_1, and the heat Q_2 which is required to heat the metal from the ignition temperature $T_{вп}$ up to the boiling temperature $T_{кип}$. The supply of heat from the medium can be ignored. For particles with initial radius R_0 and oxide film thickness $R_0 - R_M << R_0$ the weight rate of oxidation of the metal is approximated by the diffusion law for a flat surface:

$$\frac{dm/A}{dt} = \frac{D_{1,2}\Delta C}{(R_0 - R_M)\rho_M \rho_i}, \tag{IV.3}$$

where $D_{1,2}$ is the coefficient of diffusion of reagents in the liquid aluminum oxide; ΔC is the gradient of reagent concentrations; ρM – is the density of the metal; ρ_i is the density of metal ions in the aluminum oxide.

On the other hand, the rate of oxidation of a spherical particle is connected with a change in its radius by the relationship

$$\frac{dm/A}{dt} = -\frac{dR}{dt}. \tag{IV.4}$$

By equating expressions (IV.3) and (IV.4) and integrating the obtained expression (after substitution of boundary conditions: with $t = 0$ $R_M = R_0$), we find that the thickness of the oxide layer will equal

$$(R_0 - R_M) = \left[\frac{2\rho_i D_{1,2}\Delta C t}{\rho_m^2}\right]^{1/2}. \tag{IV.5}$$

From this the quantity of heat liberated in the course of the chemical reaction will be

$$Q_1 = 4\pi R_0^2 \, [2\rho_t D_{1,2} \Delta C t]^{1/2} \, \Delta \overline{H} \qquad (IV.6)$$

($\Delta \overline{H}$ is the heat of formation of aluminum oxide in the temperature interval $\Delta t = 2300\text{-}2740°K$).

Considering the fact that $R_0 - R_M \ll R_0$, the quantity of heat necessary to heat the particle from ignition temperature to the boiling temperature of aluminum will equal

$$Q_2 = \tfrac{4}{3}\pi\rho_M R_0^3 \, (\Delta H_{T_{КИП}} - \Delta H_{T_{ВП}}) \qquad (IV.7)$$

($\Delta H_{T_{КИП}}$, $\Delta H_{T_{ВП}}$ are the enthalpies of the molten metal at the boiling temperature and the ignition temperature in cal/g^3).

Time t_1 is found from the equality $Q_1 = Q_2$. Specific calculations were carried out for particles with $R_0 = 50$ µm for three values of $D_{1,2}\Delta C$ equal respectively to 10^{-4}, 10^{-5} or 10^{-6} g/cm·s. The selection was based on the fact that for liquids (except for polymer liquids) diffusion coefficients depend weakly on temperature and chemical composition and are very close to one another – usually $10^{-4}\text{-}10^{-5}$ cm^2/s.

In the calculation it was assumed that $\Delta H = 6400$ cal/g, $\Delta H_{T_{КИП}}$ – $\Delta H_{T_{ВП}} = 115$ cal/g, $R_0 - R_M = 0.3$ µm.

According to the calculations the duration of the second period – i.e., the time t_1 – equals $1.56\cdot10^{-2}$, $1.56\cdot10^{-1}$, and 1.56 ms respectively.

In comparison with the total combustion time the time t_1 is extremely small and therefore the assumptions which were made in order to simplify the calculation (ignoring heat exchange from the

ambient medium, introduction of average value of ΔH, etc.) are
fully justifiable. For the indicated reason the role of pressure
is also not great.

In the third period with achievement of the boiling point of
the metal evaporation of Al occurs into the space between the
surface of the drop and the inner surface of the oxide shell
(see Fig. 87).

The radius of the oxide shell is determined by the equality of
the mass rates of evaporation and oxidation of the metal. Since
diffusion of reagents through the oxide shell is the limiting stage,
the reaction should occur on one of the shell surfaces. The latter
situation depends on the ratio of the diffusion coefficients of the
metal and the oxidizer in molten Al_2O_3. The temperature of the
particle equals the boiling temperature of Al; the shell has a
higher temperature, determined by conditions of the thermal balance.

The rate of mass transfer of metal in the radial direction is
expressed through the rate V_r of diffusion of metal in vapor form
in the same direction:

$$W_r = \frac{dm}{dt} = 4\pi r^2 \rho_v V_r.$$

(IV.8)

where ρ_V is the density of the metal in the vapor state.

It is assumed that the latter quantity is sufficiently small
and the oxide film is adequately mobile for pressure gradients to
be absent between its inner and outer surfaces.

The distribution of temperatures between the surface of the
metal and the shell is given by the equation

$$\rho_v c_p V_r \frac{dT}{dr} = \frac{\lambda}{r^2} \frac{d}{dr}\left(\frac{r^2 dT}{dr}\right).$$

(IV.9)

The coefficient of heat conductivity of the vaporized metal,
λ, is taken as equal to the average value at a temperature

$1/2(T_{кип} + T_{cp})$, according to the theory of monoatomic dilute gases.

The equation of the heat balance on the drop,

$$W_{\nu}\Delta H_{исп} = (-4\pi R_1^2 k^2 q)|_{r=kR_1} \qquad (IV.10)$$

is found from conditions of equality of heat expenditures on evaporation of the metal and heat input to the drop by the flow of heat $q = -\lambda\frac{dT}{dr}$ from the region filled with vaporized metal.

The solution is found in the form

$$\frac{4 \pi D_{1,2}\Delta C\,(1-k)}{k} \div \left\{ \frac{R_M}{k} \left[(R_0^3 - R_M^3)\frac{\rho_M}{\rho_i} + \left(\frac{R_M}{k}\right)^3 \right]^{-1/3} - 1 \right\} \times$$

$$\times \left\{ \left(\frac{4\pi k_V}{\bar{c}_{\rho V}}\right) \ln \left[\frac{\bar{c}_{\rho V}\,(T_{cp} - T_{кип})}{\Delta H_{исп}} + 1 \right] \right\} = 0. \qquad (IV.11)$$

In this equation all of the constants except T_{cp} are known or can be calculated. In the absence of heat losses to the outside, T_{cp} is assumed to be equal to the adiabatic temperature of the flame of high-temperature oxidation of aluminum.

In the opinion of the authors, at atmospheric pressure the error in determining T_{cp} will play an insignificant role, since the quantity enters into the expression in the form $(T_{cp} - T_{кип})$. However, with an increase in pressure the role of accuracy in determining T_{cp} grows (in view of the increase in the boiling temperature). Solution of equation (IV.11) for $R_0 = 50$ µm was used to calculate the change in the radius of the aluminum drop in time, according to

$$\frac{dR_M}{dt} = -\frac{W_r}{4\pi R_M^3 \rho_M} \qquad (IV.12)$$

It was assumed that $T_{cp} = 3700°C$ and the value of the product $D_{1,2}\Delta C = 10^{-4}, 10^{-5},$ and 10^{-6} g/s·cm.

Comparison of the calculations with an experiment on the burning of spherical particles of aluminum carried out in a carbon dioxide-oxygen flame (Fig. 88) shows that for correlation of the indicated data the required value of $D_{1,2}\Delta C$ should lie in the interval between 10^{-4} and 10^{-5} g/s·cm.
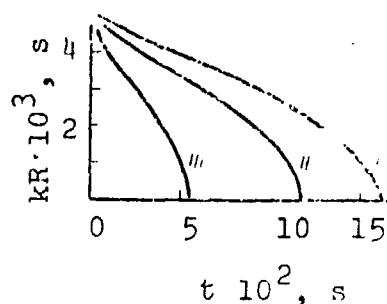
Fig. 88. Change in particle radius in time (calculated) (p = 1 atm; T = 3700°K. I – DΔC = 10^{-6} g·cm·s^{-1}; II – DΔC = 10^{-5}; III – DΔC = 10^{-4}.

If the burning time of 50-μm aluminum particles determined from experiment falls in the limits 40-65 ms, according to the calculations τ_2 will equal, respectively, 56 ms ($D_{1,2}\Delta C = 10^{-4}$), 117 ms ($D_{1,2}\Delta C = 10^{-5}$) and 160 ms ($D_{1,2}\Delta C = 10^{-6}$). We will emphasize that the uncertainty of the product $D_{1,2}\Delta C$ remains a weak point in the question of quantitative checking of the proposed model.

The considered model gives a natural and simple explanation for certain specific features of the combustion of aluminum. This includes first of all such phenomena as fragmentation, rotation, and distortion of the particle motion trajectory in the process of combustion in a gas flow. As has already been stated, the shell of molten aluminum oxide located around the evaporating drop of aluminum in the proposed model is a unique regulator of the rates of evaporation and oxidation of the metal. If because of certain conditions the shell loses its elasticity or if its role as a diffusion barrier is increased, the pressure of the vaporized metal may exceed the pressure of the ambient medium plus the mechanical strength of the shell. In this case the shell is torn or fragmented.

In the first case vapors of metal which escape from the fracture lead to the appearance of an asymmetrical reaction force and as a

a result to rotation and distortion of the particle motion trajectory. In the case when the sphere is broken up the liquid drop of metal is shattered into a number of fragments which fly off in a radial direction and burn up as a totality of individual fine particles.

The "bubble" model is supported by the sharp definition of the combustion zone and by the presence of clear sharp tracks during visual investigation of the burning of aluminum in a "moist" medium.

But for the most part this model is either difficult to explain or is contradicted by the majority of experimental results on combustion of aluminum. Investigations of the process of aluminum particle combustion by methods of forced quenching and high-frequency cinematography indicate, as we saw earlier, a connection of the flame with segments of the surface of the particle which are more likely free of oxide than covered with it. A diffusion cloud of subdispersed Al_2O_3 exists around the burning particle; it is extremely difficult to explain the formation of this cloud in the presence of a solid oxide film. This is true to an equal degree with regards to the blurred form of the track during combustion of Al in a "dry" medium.

At the same time τ_r of aluminum particles of equal dimension in mixtures of H_2O and CO_2 in equal proportions or in an atmosphere with oxygen, are correspondingly equal.

If we work on the basis of the "bubble" model positions, this equality should not exist. Judging from the differences in the external picture, the liquid Al_2O_3 should create a barrier of variable density on the path of the H_2O and CO_2. From this point of view burning of aluminum in a medium enriched with oxygen should not demonstrate any essential qualitative differences in the presence or absence of water vapor.

Furthermore, the calculated values of combustion time τ_r obtained by Bartlett et al. [261] by a calculation scheme which

218

they developed appear, despite agreement with (their own) experiment, to be extremely overstated. To correlate the calculation with experimental values in this case it was necessary to take a value of $D_{1,2}\Delta C$ an order of magnitude higher ($D_{1,2}\Delta C \approx 10^{-3}$) than those selected as characteristic for diffusion processes in liquids [270]. According to maximum evaluations the rates of aluminum burning under these conditions correspond to the rates of diffusion of oxidizer in a gaseous medium without any additional resistance, such as that offered by a film of liquid oxide.

Finally, in the considered model the question of removal of aluminum oxidation products from the reaction zone is no simple matter. Since the reaction rate is determined by diffusion through the oxide shell, the combustion front should be connected with one of its surfaces (inner or outer). The temperature of the shell and, consequently, the zone of combustion are limited by the boiling temperature of aluminum. From this situation two possible variants arise. The first is a gradual accumulation of oxide on the surface of the shell, increasing its thickness and conseqeuntly leading to a gradual reduction in reaction rate - i.e., and the rate of aluminum burning. The second path is the existence of a mechanism for removing reaction products beyond the limits of the shell - for example, by evaporation of Al_2O_3 (of low probability) or as the result of the formation of suboxides of aluminum during burning (AlO, Al_2O), existing in the gaseous state at the reaction temperature and diffusing into the surrounding atmosphere. In the latter case additional complexities arise, connected with the presence of a zone of completed reaction and condensation.

Thus, the sum total of the pros and cons regarding the "bubble" model of combustion of particles of metal of the aluminum type indicates that the greater portion of the experimental results are difficult to explain from the positions of this model. These results find a more reasonable explanation if we take the diffusion model of combustion as the basis.

We will pause to consider the diffusion model of vapor-pause combustion.

Vapor-phase combustion is one of the most possible and probable forms of steady-state combustion of aluminum in a high-temperature gas flow. The burning of such metals has many features in common with the process of combustion of drops of hydrocarbon fuel, the theory of which was formulated by Varshavskiy [259]. Therefore it is quite natural that the first descriptions of the process of burning such metals were based on analytical methods similar to those developed previously for hydrocarbons. At the same time it was clear that quantitative and even, to a certain degree, qualitative differences exist between these processes. This is first of all concerned with the level of temperatures, gradients, and thermal fluxes, conditions of equilibrium and phase states of the final combustion products, etc.

According to the initial hypothesis of Glassman [271], if the boiling temperature of the oxide of the metal is higher than the boiling temperature of the metal itself, steady-state combustion of the metal occurs in the vapor phase. The boiling point of the oxide limits the temperature of the combustion zone. If, on the other hand, the boiling temperature of the metal is higher than that of the oxide the process of combustion is localized on the surface of the particle.

Limitation of the temperature of the combustion zone from the top for a number of metals, including aluminum, is postulated by the fact that for them the heat $\Delta H_{\text{кип}}$ of evaporation and dissociation of the oxide at $T_{\text{кип}}$ is greater than the heat of the oxidation reaction, Q:

$$\Delta H_{\text{исп}} > Q - (H^{\circ}_{\text{кип}} - H^{\circ}_{298}).$$

Simple calculation shows that the expenditure of heat for evaporation of a single mole of the oxide Al_2O_3 at the boiling

220

temperature is equivalent to the quantity of heat liberated during burning of 1.2 moles of the metal in oxygen under adiabatic conditions. Heat transfer into the surrounding space by conductivity and radiation facilitates an intensification of the inequality given above.

Glassman includes Al, Be, Zr, Mg, Li, Si in the class of metals which burn in the vapor phase.

Subsequently Glassman and Brzustowski updated the basic postulate concerning the burning of metals in the vapor phase [143]. In the first variant it is necessary that the boiling temperature of the oxide of the metal exceed that of the metal itself, but this is not a sufficient condition for vapor-phase combustion. And, on the other hand, if the boiling temperature of the metal is higher than that of its oxide, this is considered a sufficient but not necessary condition for the surface reaction. Whether or not combustion occurs in reality in the vapor phase is a question which depends on the intensity of heat losses from the flame zone.

Gordon [138] proposed that metals and their compounds which he had studied be broken down into five groups or classes in accordance with the boiling points of the metals and their oxides.

Brzustowski and Glassman, accepting the Gordon classification in principle, subjected it to detailed analysis with consideration of the modified criterial thermodynamic position concerning vapor-phase combustion which they advanced. The following chemical elements are examined: Li, K, Na, Be, Mg, Ca, Al, Zr, Si, Ti, B. They were divided into volatile and nonvolatile. The nonvolatile types were divided into classes according to the solubility of the oxide. In contrast to the first classification, within the limits of each class a distinction is drawn individually for fine and large particles and account is taken of the conditions of their heat exchange with the ambient high-temperature oxidizing medium.

High heat transfer intensity;
low accumulation of oxide on
the surface

Small   Droplet   Diffusion
particle   flame

Low heat-exchange intensity;
significant formation of oxide on surface

Large   Drop with   Diffusion flame   The metal boils, the
particle   some oxide   over a porous   layer of oxide is
             on surface   layer of oxide,   shattered. Hot drops
                           reverse heat   of metal burn in a
                           transfer from   diffusion flame
                           the gas to the
                           liquid

Fig. 89.   Diagram of the combustion of particles of volatile metals.

a.   **Volatile metals, Mg (Fig. 89).**   The boiling temperature of
metal in this group is lower than the boiling temperature of their
oxides.   The ratio of the volume of the oxide to the volume of
consumed metal – the Pilling-Bedvors criterion – is smaller than
unity and therefore during combustion the surface of the metal
particle is not covered with a solid oxide film.   With considera-
tion of the criterion of vapor-phase combustion it is assumed that
the indicated metals burn in the diffusion regime:

Small particles.   The size of particles which are considered
to be small is determined by the temperature and composition of
the surrounding atmosphere, the rate of surface oxidation, and
the vapor pressure of the metal at a given temperature.   For small
particles the ratio of surface area to volume is high (inversely
proportional to their diameter).   They are heated up to the melting
point quite rapidly.   During the heating period a small quantity
of oxide is formed on the surface, but does not prevent evaporation

and diffusion of metal vapors into the reaction zone. Since the vapor pressure of the metal depends strongly on temperature and is very great in absolute magnitude at the high temperatures which are characteristic for burning of solid rocket propellants, vapor-phase oxidation of the metal occurs at a small rate. A glowing zone of diffusion flame exists around the burning particle.

Large particles. The rate of growth in temperature is small. Oxide accumulates on the surface of the particle. Since the oxide has a porous structure and does not form a solid protective film, evaporating metal diffuses into the reaction zone and burns in a slow diffusion flame. The liberated heat warms the drop of metal located beyond the gradually thickening layer of oxide. Its temperature can reach the boiling point of the metal. As a result of overheating the drop breaks up the oxide shell and flies apart into a number of very small particles. Each of these burns according to the mechanism of combustion of small drops.

Any gas which is previously dissolved in the metal can strongly lower its boiling temperature (the partial pressure of the gas is added to the vapor pressure of the metal) and therefore fragmentation can occur at an even lower temperature.

b. **Nonvolatile metals.** This class includes aluminum, beryllium, silicon, titanium, zirconium, and boron. For these metals β is greater than unity (1.3-2.7). The oxides of aluminum, beryllium, and silicon cover the surface of the particle solidly with a protective layer. This layer inhibits oxidation of the metal. Aluminum, beryllium, and silicon form a group of nonvolatile metals with insoluble oxides. Titanium and zirconium can form a solid solution of the oxide in the metal. There is no clearcut interface between the metal and the oxide. Combustion is not terminated even if the particle is covered with a thick layer of oxide. These belong to the group of nonvolatile metals with soluble oxides. The boiling temperature of the oxides of all these metals (except silicon) is higher than the boiling temperature of the metal.

Therefore the criterion (necessary condition) of vapor-phase combustion is fulfilled for them. However, the actual realization of combustion in the vapor phase is questionable in the case of titanium and zirconium. Despite the fact that the boiling temperature of the oxide is higher than that of the metal, the difference between them is no greater than 500°. Losses of heat from the burning particle by heat conductivity and by radiation convert the process to conditions of slow surface combustion.

Boron is a member of the group of nonvolatile metals with a soluble oxide. The oxide of boron has low melting and boiling temperatures (lower than for the metal). The form of combustion depends on heat exchange with the ambient medium.

c. **Nonvolatile metal, insoluble oxide (Fig. 90).** *Large particles.* During heating and before melting a protective layer of oxide is formed on the surface of the particle. Surface oxidation occurs. There is no combustion as such.

Small particles. The rate of temperature rise up to the melting point is high. Surface oxidation is unable to form a large larger of oxide. Heat exchange with the medium determines the form of steady-state combustion:

1. The temperature of the surface does not exceed the melting temperature of the oxide. The mechanism of combustion is analogous to burning of large particles.

2. The temperature of the particle exceeds the melting temperature of the oxide. A shell of liquid oxide limits the rate of oxidation of the metal. Since the rate of diffusion through the liquid oxide is higher than diffusion through the solid form, the time required for the particle to burn up is less than that in case 1.
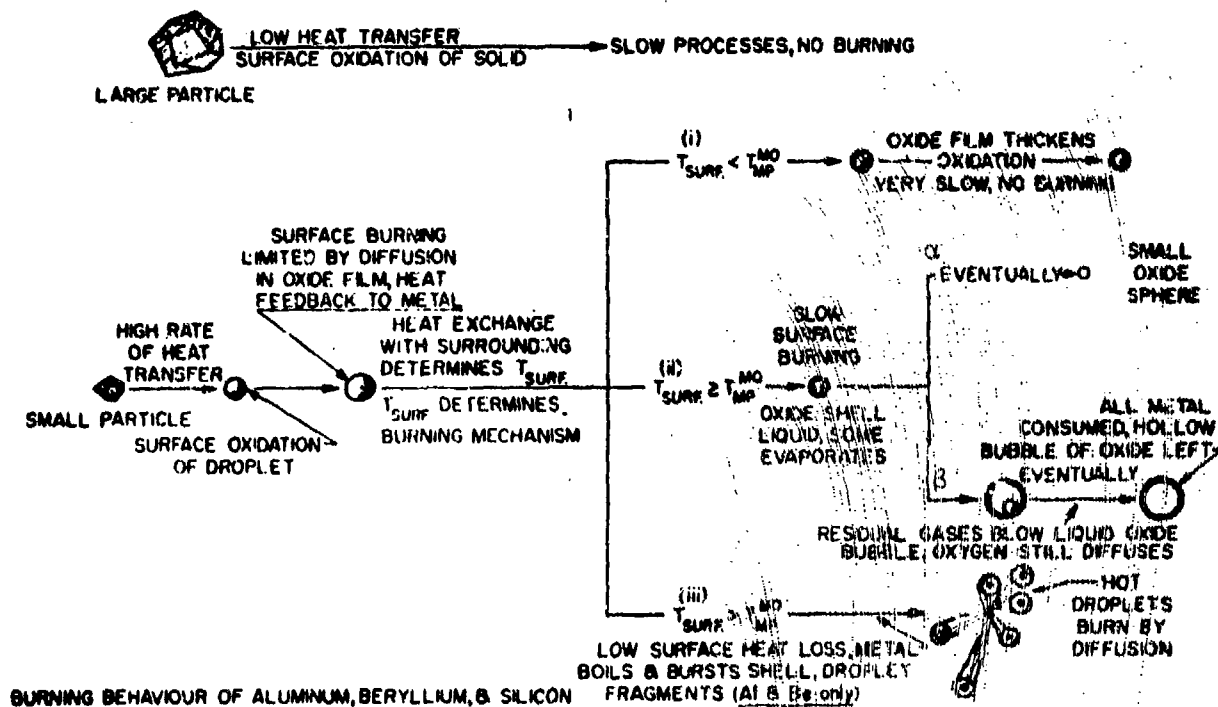
Fig. 90. Diagram of the combustion of particles in the "non-volatile metal, insoluble oxide" system.

Surface burning may be accompanied by partial evaporation of the oxide (variant α, see Fig. 90). The layer of oxide retains its thickness. If burning goes to the end the final product is a drop of oxide. If combustion is terminated before complete combustion of the metal, the residue is a drop of metal surrounded by a thick-walled shell of oxide. When a certain amount of soluble gas is present in the metal the liberation of the gas may result in inflation of a shell of liquid oxide (variant β, see Fig. 90). The metal is burned out on the surface of the particle due to diffusion of oxygen through the shell. The type of residue is a hollow thick-walled spherical shell.

3. High temperature of the ambient medium. Low heat losses. Overheating of the metal and destruction of the shell surrounding it are possible. This variant is impossible for silicon: the temperature of the flame is limited by the boiling temperature of the oxide, which is lower than the boiling temperature of silicon.

225

d. **Nonvolatile metal; soluble oxide (Fig. 91).** *Small particles.*
A thick layer of oxide cannot be formed on the surface of the
particle before it melts. The combustion reaction is limited by
diffusion through the oxide. Temperature and heat exchange with
the surface of the particle play an important role:

1. Heat losses from the surface are great, and the oxide
temperature does not reach the melting point. The rate of combus-
tion is determined by diffusion of metal and oxygen through the
solid oxide. A gradual reduction in the drop of metal is accompa-
nied by a growth of the oxide. The final product is a particle
of oxide which is approximately equal to the initial particle of
metal.
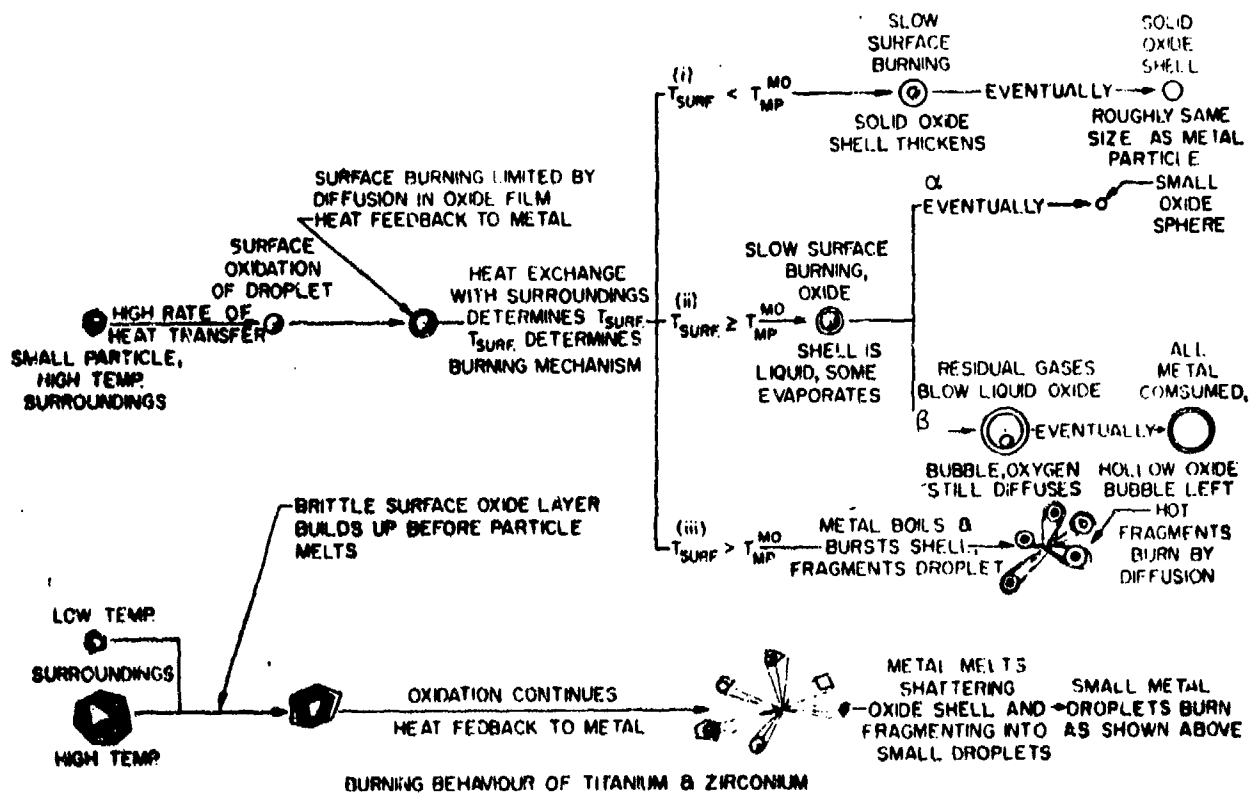
Fig. 91. Diagram of combustion of particles in the "nonvolatile
metal, soluble oxide" system.

2. The temperature of the particle surface reaches the melting point of the oxide. In this variant the picture of combustion is analogous to that which is characteristic for burning of metals from the "nonvolatile metal, insoluble oxide" group.

3. The boiling temperature of the particle inside the oxide shell reaches the boiling temperature of the metal. Explosion of the shell is accompanied by escape of drops in the form of a number of small particles which burn under diffusion vapor-phase conditions. It is considered that there is little probability of realization of the variant for particles of titanium and zirconium in products from combustion of solid propellants, owing to the strong thermal losses by radiation.

Large particles. Before the particle melts its surface is covered with a layer of oxide which forms a solid solution with the metal. Surface burning occurs as the result of mutual diffusion of vapors of the metal and oxidizer through the solid layer. Reverse flow of heat to the solid particle may cause it to melt.

Since there is no boundary between the metal and oxide the brittle film of oxide is destroyed in the process of melting and the particle breaks down into individual droplets. These drops maybe joined to part of the oxide. Further combustion occurs by the mechanism of burning of small particles.

e. **Nonvolatile metal, volatile oxide** (Fig. 9?). The metal (especially boron) remains in the solid state. An exception to this is the case of very high temperatures of the ambient medium, when some of the metal is melted. Particle dimensions have no effect. The state of the oxide depends on heat exchange with the medium and on radiant heat losses from the surface of the particle. Three variants are possible:

1. If, because of intensive heat losses, the temperature of the oxide does not reach the melting temperature slow surface

227

VERY SLOW
BURNING RATE
LIMITED BY
OXYGEN DIFFUSION
THROUGH SOLID
OXIDE

SURFACE TEMP 720°K

SLOW
BURNING RATE
LIMITED BY
OXYGEN
DIFFUSION
THROUGH
LIQUID OXIDE

SURFACE TEMP 720→2520°K

STEADY COMBUSTION

H/T AND SURFACE OXIDATION

METAL ALWAYS
SOLID, OXIDE
STATE DEPENDS
ON HEAT LOSSES

NO SHATTERING
OF OXIDE LAYER

SURFACE TEMP 2520°K

BURNING RATE
LIMITED BY
DIFFUSION OF OXIDE
VAPOUR AWAY FROM
PARTICLE
METAL MAY MELT

BURNING BEHAVIOUR OF BORON

Fig. 92.   Diagram of combustion of particles in the "non-volatile metal, volatile oxide" system.

oxidation of the metal takes place. The rate of oxide buildup is limited by diffusion through the solid oxide shell. With a growth in the layer of oxide the oxidation process is inhibited.

2. The intensity of thermal losses is lower and the oxide reaches the melting point and melts. The reaction rate is considerably higher and is determined by diffusion through the liquid layer of oxide. If the temperature is sufficiently high evaporation of the oxide reduces the size of the particle.

3. The temperature of the liquid oxide reaches boiling temperature. The rate of combustion can be limited both by the rate of diffusion of oxide in the vapor form and products of dissociation from the particle surface and also by an increase in the thickness of the layer in the liquid oxide. Each of these processes will be limiting and depends on the expenditure of heat in evaporation of the oxide and on heat exchange with the ambient medium.

For boron water vapor accelerates evaporation of the oxide due to the formation of the highly volatile metaboric acid HBO_2.

228

In accordance with the above classification, Brzustowski and Glassman developed an analytical model of vapor phase combustion of metal particles. The group of metals for which this model may be applicable includes aluminum, magnesium, beryllium, etc. They based their consideration on the theory of diffusion vapor-phase combustion of drops of hydrocarbon.

The spherical particle of molten metal A (Fig. 93) is surrounded by an infinitely thin reaction zone B, located at a certain distance from it. The reaction zone is bounded on both sides with a region of immobile gas: on the particle side by spherical region AB and on the side of the ambient atmosphere by region BC. The outer boundary of BC is assumed to be located at infinity. It is considered that the fuel and oxidizer diffuse into the reaction zone in a stoichiometric ratio.
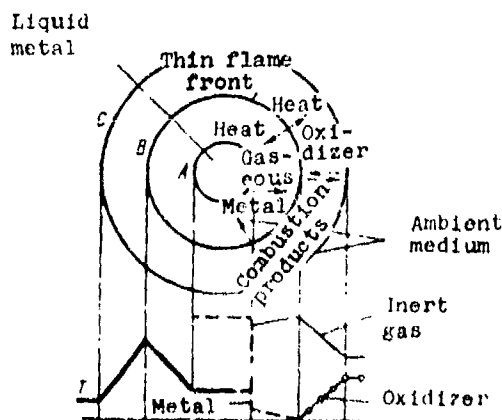
Fig. 93. Diagram of the vapor-phase model of combustion of particles.

The transfer of reaction products outside creates additional diffusion resistance for the oxidizer. The model is assumed to be isobaric and quasi-stationary.

Five basic physical processes are taken into account in the theoretical analysis: 1) evaporation of particles at temperature

T_A; 2) diffusion of oxidizer into the flame zone through region BC; 3) diffusion of metal in the vapor phase from the surface of the particle to the flame zone B through region AC; 4) transfer of heat from the flame zone B to the particle surface (conductivity and radiation); and 5) heat transfer from the flame zone (conductivity and radiation) into the ambient medium.

The initial parameters which determine the physical and chemical properties of the system during the solution are the radius of the metal particle R_A, total pressure P and temperature T_{cp} of the medium, partial pressure P_{ok} of the oxidizer in the ambient medium, the oxidizer, and the metal. The unknown parameters are the radius of the reaction zone R_B, temperature of the metal T_A, the molar flow rate of condensed metal, and the partial pressure of vapors of the metal at the particle surface, p_r.

In region AB the concentration of reaction products and of oxidizer is considered equal to zero: the flow rate of fuel is determined by the rate of evaporation of the particles. In region BC there are three gaseous substances: oxidizer (ok), inert gas (i), and combustion products in the vapor phase (p).

The following relationship is valid for an ideal gas:

$$p_i + p_0 + p_p = P. \qquad (IV.13)$$

Flow rates of oxidizer (ω_0) and gaseous combustion products (ω_p) are mutually connected by the equation of conservation of matter:

$$\omega_p = - m_{cr} \alpha \omega_0 .$$

where α is the fraction of evaporating condensed combustion products; m_{cr} is the stoichiometric coefficient.

From this the condition for existence of a flow from reaction zone B into the ambient medium is written as

$$\alpha m_{cr} > 1. \qquad \qquad \text{(IV.14)}$$

In the physical sense this means that for each mole of oxidizer which is consumed in the flame more than 1 mole of gaseous reaction product should be formed. Simultaneously, fulfillment of this condition can be called the criterion of the possibility of transfer of condensed combustion products from the flame zone. The indicated inequality is normally fulfilled for burning of hydrocarbon drops.

In general form the conclusions of Brzustowski and Glassman reflect the experimentally observed features of combustion of particles of aluminum and magnesium - the dependence of process rate on the concentration of oxidizer, the ratio between the combustion zone and the radius of the particle, and the degree of influence of the temperature of the medium. But even for a medium in which the basic oxidizer is oxygen the rates of combustion (evaporation) of particles of finely dispersed aluminum as calculated by this theory differ substantially (are understated) from experiment. The latter is also true of the quantity R_{p}/R_{A} and the temperature of the surface of the burning aluminum (Fig. 94). One reason for this lies in the fact that, as has already been stated, a number of parameters used for the solution are not entirely accurate.

According to the valid conclusion of the authors themselves, the significance of the proposed theory consists in the fact that it shows the probability and certain special features of vapor-phase combustion of drops of aluminum and magnesium with favorable ambient conditions.

The work by Kuehl [253] represents a certain refinement of the quasi-stationary theory of combustion of metals in the vapor phase put forward by Brzustowski and Glassman. The basic assumptions remain as before, but the determining equations are converted

for oxidizers which, in contrast to oxygen, form noncondensed
inert products of the hydrogen or nitrogen type in the reaction.
For example, such oxidizers include water vapor, carbon dioxide,
etc. Although the inert products which are formed do not partici-
pate in the reaction they must be taken into account in the general
equation of the heat balance. To ignore these facts is to distort
the real physical model of combustion of particles of metals of
the aluminum type and leads to understating the calculated rate
of the process being analyzed.
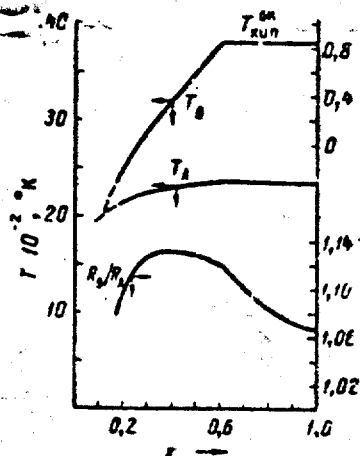
Fig. 94. Particle temperature
T_A, combustion zone temperature
T_B, and R_B/R_A as a function of
O_2 concentration.

A further improved model was proposed by Klyachko [272]. In
the theoretical analysis of combustion of metal particles which
he developed the process is assumed to be quasi-stationary. Within
the framework of the quasi-stationary theory of combustion diffusion
of oxide in the vapor form into the particle is, strictly speaking,
possible only in the presence of a parallel process of its condensa-
tion. Therefore in the general case the problem reduces to solu-
tion of second-order nonlinear differential equations. However,
by introducing effective parameters (effective temperature of com-
bustion and effective concentration of oxide in the vapor phase)
as well as a number of simplifications, the solution is carried out
within the framework of linear theory.

As in the preceding considerations, the effect of radiation from the flame zone and partial evaporation or dissociation of the reaction products (oxides) on the process of combustion of metal is taken into account. The diagram of the physical model of combustion, with the exception of the presence of two-way flow of reaction products (oxides) in the vapor form out of zone B, is analogous to that given on Fig. 93.

The following assumptions were made:

1) the particle is at the equilibrium temperature of evaporation of the metal;

2) the combustion zone is infinitely thin and the concentration of reagents in it equals zero;

3) the rate of diffusion of condensed combustion products in the reaction zone equals zero;

4) the transfer coefficient in the corresponding zones is averaged in terms of temperature and composition;

5) the effective degree of evaporation of reaction products equals the arithmetic mean value between the degree of their evaporation in zone B at infinity and on the drop surface - i.e., $\alpha_{\text{э}\phi\phi} = \alpha/2$;

6) the fraction of oxide in the vapor form, k, which diffuses to the surface of the particle is equal to one-half of the total vapor oxide formed in the reaction zone.

The temperature T_R of the radiating layer of the combustion zone is taken as equal to $T_{\text{пл}}^{\text{пр}}$ of the oxide Al_2O_3 if $T_{\text{г}} \geq T_{\text{пл}}^{\text{пр}}$ ανφ; equal to $T_{\text{г}}$ if $T_{\text{г}} < T_{\text{пл}}^{\text{пр}}$.

233

The reduced degree of blackness, ε_π, of the particle surface is assigned by the Christiansen formula [273], which is valid for the case of heat exchange between a convex body and a shell surrounding it:

$$\epsilon_{n} = \frac{1}{\frac{1}{\epsilon_{\kappa}} + \frac{r_{\kappa}^{2}}{r_{r}^{2}}\left(\frac{1}{\epsilon_{r}} - 1\right)}. \qquad (IV.15)$$

The system of basic equations which describe the combustion process includes the following:

Equation of heat balance in the zone AB:

$$\mathcal{J}_{M} H_{M}(T) - \mathcal{J}_{M}^{\text{кон}} H_{\kappa}(T_{M}) = 4\pi r^{2}\lambda\frac{dT}{dr} + Q_{R}^{\kappa}. \qquad (IV.16)$$

The effect of diffusion and condensation of oxide in the vapor phase into this region is taken into account during the solution by introducing the effective temperature of combustion.

Equation of heat balance for the combustion zone B:

$$\mathcal{J}_{M} H_{M}^{\text{кон}}(T_{M}) - \mathcal{J}_{\text{ок}} H_{\text{ок}}(T) - \mathcal{J}_{\text{пр}} z H_{\text{пр}}(T) - \mathcal{J}_{\text{пр}}(1-z) H_{\text{иг}}^{\text{кон}}(T_{r}) =$$
$$= -4\pi r^{2}\lambda\frac{dT}{dr} + Q_{R}^{r}. \qquad (IV.17)$$

Since the process is quasi-stationary the connection between the flows of metal vapors $\mathcal{J}_M$, oxidizer $\mathcal{J}_{\text{ок}}$, and products $\mathcal{J}_{\text{пр}}$ is assigned by the equation of the reaction and by stoichiometric coefficients of this equation:

$$\frac{\mathcal{J}_{M}}{v_{M}} = \frac{\mathcal{J}_{\text{ок}}}{v_{\text{ок}}} = \frac{\mathcal{J}_{\text{пр}}}{v_{\text{пр}}}. \qquad (IV.18)$$

In the designations used the quantity $Q_{R}^{\kappa} = 4\pi r_{\kappa}^{2}\,\varepsilon_{n}\sigma(T_{R}^{4} - T_{M}^{4})$ is the radiation flux from the reaction zone to the surface of the particle; $Q_{R}^{r} = 4\pi r_{r}^{2}\,\varepsilon_{r}\sigma(T_{R}^{4} - T_{\infty}^{4})$ is the radiation flux from the reaction zone into the external zone. The subscripts к, г, M, ок, пр., and кон designate, respectively, a drop, the combustion zone, metal, oxidizer, products and the condensed state.

According to Frank-Kamenetskiy [274] the expression for flows of metal and oxidizer vapors, under the condition of equality of diffusion coefficients of all components in each region, will be written in the form

$$\mathcal{I}_{OH} = 4\pi r^2 \frac{D_2 P}{RT} \cdot \frac{1}{1-\left(1-\frac{a(1-A)v_{np}}{v_{OH}}\right)m_{OH}} \cdot \frac{dw_{OH}}{dr} \qquad (IV.19)$$

$$\mathcal{I}_{M} = -4\pi r^2 \frac{D_2 P}{RT} \cdot \frac{1}{1-\left(1-\frac{zAv_{np}}{v_M}\right)m_M} \cdot \frac{dw_M}{dr} \qquad (IV.20)$$

Heat content of the oxidizer H_{OH}, the metal vapors H_M, and of the gaseous reaction products H_{np} is written as

$$H_{OH}(T) = H_{OH}(T_\infty) + c_{p_{OH}}(T-T_0),$$

$$H_{np}(T) = H_{np}(T_\infty) + c_{p_{np}}(T-T_\infty), \qquad (IV.21)$$

$$H_M(T) = H_M(T_0) + c_{p_M}(T-T_0).$$

Equations (IV.15)-(IV.20) are integrated under the following boundary conditions:

1. On the boundary of the particle $(r = r_H)$ $T = T_M$, the partial pressure of the metal vapors is equal to the pressure of saturated vapors and is a known function of T_M, the partial pressure on the products equals zero, $P_{np} = 0$.

2. In the zone of combustion when $r = r_\Gamma$ $T = T_\Gamma$, $P_M = P_{OH} = 0$.

3. In the ambient medium when $r = \infty$ $T = T_\infty$, $P_M = P_{np} = 0$, $P_{OH} = P_{OH} = \infty$.

After integration with consideration of simplifying assumptions for the flow of oxidizer and metal we will have

235

$$\mathcal{J}_{\text{ок}} = -4\pi r_{\text{г}} \frac{\bar{D}_1 P}{RT} \frac{1}{1 - \frac{\alpha v_{\text{пр}}}{4 v_{\text{ок}}}} \ln \frac{1}{1 - \left(1 - \frac{\alpha v_{\text{пр}}}{4 v_{\text{ок}}}\right) m_{\text{ок}\,\infty}}, \qquad (IV.22)$$

$$\mathcal{J}_{\text{м}} = -\frac{4\pi r_{\text{к}}}{1 - \frac{r_{\text{к}}}{r_{\text{г}}}} \frac{\bar{D}_1 P}{RT} \frac{t}{1 - \frac{\alpha v_{\text{пр}}}{4 v_{\text{м}}}} \ln \frac{1}{1 - \left(1 - \frac{\alpha v_{\text{пр}}}{4 v_{\text{ок}}}\right) m_{\text{ок}\,\infty}}. \qquad (IV.23)$$

Subsequently, from equations (IV.16) and (IV.17) the author obtains an expression for determining the degree of evaporation of reaction products, α, or the temperature $T_{\text{г}}$ in the zone of combustion:

$$\frac{1}{1 - \frac{v_{\text{пр}}}{v_{\text{ок}}} \alpha \frac{r_{\text{пр}}}{r_{\text{ок}}}} \times$$

$$\times \ln \left\{ 1 + \frac{\bar{c}_{p_2}(T_{\text{г}} - T_{\infty})}{H_{\text{ок}}(T_{\infty}) + \frac{v_{\text{м}}}{v_{\text{ок}}} H_{\text{м}}^{\text{исп}}(T_{\text{м}}) - } \right.$$

$$\left. - \frac{v_{\text{пр}}}{v_{\text{ок}}} \left[\alpha H_{\text{пр}}(T_{\infty}) - (1 - \alpha) H_{\text{пр}}^{\text{исп}}(T_{\text{г}}) \right] - \frac{Q_R^{\text{г}}}{\mathcal{J}_{\text{ок}}} \right\} =$$

$$= \frac{\bar{D}_2}{\bar{c}_2} \frac{1}{1 - \alpha \frac{v_{\text{пр}}}{v_{\text{ок}}}} \ln \frac{1}{1 - \left(1 - \frac{\alpha v_{\text{пр}}}{4 v_{\text{ок}}}\right) m_{\text{ок}\,\infty}}, \qquad (IV.24)$$

where

$$\bar{c}_{p_2} = \bar{c}_{p_{\text{ок}}} - \frac{v_{\text{пр}}}{v_{\text{ок}}} \alpha \bar{c}_{p_{\text{пр}}}; \qquad \bar{a}_2 = \frac{\bar{\lambda}_2 RT}{\bar{c}_{p_{\text{ок}}} P},$$

and from (IV.20) and the expression for $Q_R^{\text{г}}$ we obtain

$$\frac{Q_R^{\text{г}}}{\mathcal{J}_{\text{ок}}} = \frac{\varepsilon_{\text{г}} r_{\text{г}}^2 \sigma (T_R^4 - T_{\infty}^4)}{\frac{\bar{D}_2 P}{RT} \frac{1}{1 - \frac{\alpha v_{\text{пр}}}{4 v_{\text{ок}}}} \ln \frac{1}{1 - \left(1 - \frac{\alpha}{4} \frac{v_{\text{пр}}}{v_{\text{ок}}}\right) m_{\text{ок}\,\infty}}}. \qquad (IV.25)$$

The equation is solved in the following sequence. It is assumed that $\alpha = 0$. If the found $T_{\text{г}}$ does not exceed the boiling temperature of the oxide, $T_{\text{пр}}^{\text{кип}}$, the calculation is terminated.

236

If $T_\Gamma > T_{np}^{\text{кип}}$, the temperature in the combustion zone is considered to equal the boiling temperature of the oxide and the fraction of evaporating oxide, α, is found.

The product $\varepsilon_\Gamma r_\Gamma$ is regarded as a parameter.

From equations (IV.24) and (IV.25) it follows that for fine particles α differs from zero; with a growth in particle diameter the magnitude of α is reduced.

Consideration of the thermal flux imparted to a particle by vapor-phase oxide of the metal diffusing to its surface is accomplished, as was noted, by introduction of the effective combustion temperature $T_\Gamma^{\text{эфф}}$ into the consideration — the temperature taken on by the combustion products if they remain in the condensed phase ($T_\Gamma^{\text{эфф}} > T_{np}^{\text{кип}}$). The effective combustion temperature is found from equation (IV.24), by artificially substituting the fraction of vapor phase oxide $\alpha = 0$ into the left side of the equation. This approach was carried over to the problem of combustion of metals from methods of calculating thermal flux from a dissociated gas to a cold wall [275].

As a result the equation for calculating $T_\Gamma^{\text{эфф}}$ is brought to the form

$$\ln\left\{1 + \frac{\bar{c}_{p_{\text{ок}}}(T_\Gamma^{\text{эфф}} - T_\infty)}{H_{\text{ок}}(T_\infty) + \frac{\nu_{\text{M}}}{\nu_{\text{ок}}} H_{\text{M}}^{\text{кон}}(T_{\text{M}}) - \frac{\nu_{np}}{\nu_{\text{ок}}} H_{np}^{\text{кон}}(T_{np}^{\text{кон}}) - \frac{Q_R^\Gamma}{\mathcal{J}_{\text{ок}}}}\right\} =$$
$$= \frac{\overline{D_2}}{a_2} \frac{1}{1 - \frac{x\nu_{np}}{\mathcal{J}\nu_{\text{ок}}}} \ln \frac{1}{1 - \left(1 - \frac{x\nu_{np}}{\mathcal{J}\nu_{\text{ок}}}\right)m_{\text{ок}\infty}}. \quad \text{(IV.26)}$$

After T_Γ is found by integration of equation (IV.16) for the thermal balance in zone AB, an expression is found for determining the flow $\mathcal{J}_{\text{M}}$ of vapors of the metal:

$$\mathcal{J}_{\text{M}} = \frac{4\pi r_{\text{к}}}{1 - \frac{r_\text{к}}{r_\Gamma}} \frac{\lambda_1}{c_{p_{\text{M}}}} \ln\left[1 + \frac{c_{p_{\text{M}}}(T_\Gamma^{\text{эфф}} - T_{\text{M}})}{T_{\text{M}} - \frac{Q_R^\text{к}}{\mathcal{J}_{\text{M}}}}\right]. \quad \text{(IV.27)}$$

237

where $L_M = H_M(T_M) - H_M^{KOH}$ is the latent heat of evaporation of the metal at its boiling temperature.

Then from this equation and equation (IV.19), applying the condition of stoichiometric flows (IV.18), the calculation of the ratio of the radius of the combustion zone r_Γ to the radius of the particle r_H is carried out with a combustion zone temperature equal to $T_\Gamma^{\mathfrak{Z}\Phi\Phi}$:

$$\frac{r_\Gamma}{r_H} = 1 + \frac{v_{OK}}{v_M}\frac{d_1}{D_1}\left(1 - \frac{\varkappa v_{\text{пр}}}{4v_{OK}}\right)\frac{\ln\left[1 + \frac{\bar{c}_{P_M}(T_\Gamma^{\mathfrak{Z}\Phi\Phi} - T_M)}{L_M - Q_R^K/\mathcal{I}_M}\right]}{\ln\left[1 - \left(1 - \frac{\alpha v_{\text{пр}}}{4v_{OK}}\right)m_{OK\,\infty}\right]^{-1}}. \qquad (IV.28)$$

By substitution of r_Γ/r_H into (IV.20) the final equation for the flow of metal is obtained in the form

$$\mathcal{I}_M = 4\pi r_H \omega, \qquad (IV.29)$$

where

$$\omega = \frac{v_M}{v_{OK}}\frac{\bar{D}_1 p}{RT}\frac{1}{1 - \frac{\varkappa v_{\text{пр}}}{4v_{OK}}}\ln\frac{1}{1 - \left(1 - \frac{\varkappa v_{\text{пр}}}{4v_{OK}}\right)m_{OK\,\infty}} + $$
$$+ \frac{\lambda_1}{c_{P_M}}\ln\left[1 + \frac{c_{P_M}(T_\Gamma^{\mathfrak{Z}\Phi\Phi} - T_M)}{L_M - Q_R^K/\mathcal{I}_M}\right]. \qquad (IV.30)$$

The time τ of combustion of the particle is found from the condition of equality of the flow of metal in vapor form by the change in the weight of the particle:

$$\mathcal{I}_M = 4\pi r_H^2 \frac{\rho}{\mathfrak{N}_M}\frac{dr_H}{d\tau}$$

or, with consideration of (IV.30), after integration,

$$\tau_\Gamma = \frac{\rho_H}{\mathfrak{N}_M}\int_0^{r_H}\frac{r_H\,dr_H}{\omega}. \qquad (IV.31)$$

And, finally, simultaneous solution of equations (IV.23)-(IV.27) gives the expression for calculating the temperature of a drop of metal, T_M:

$$\frac{1}{1-\frac{x}{4}\frac{v_{\text{пр}}}{v_{\text{ок}}}}\ln\frac{1}{1-\left(1-\frac{x}{4}\frac{v_{\text{пр}}}{v_{\text{ок}}}\right)m_{\text{ок}}}=\frac{a_1}{D_1}\ln\left[1+\frac{\bar{c}_{p_M}(T_i^{\text{эф}}-T_M)}{L_M-Q_R^{\text{к}}/\mathcal{F}_M}\right].\ (IV.32)$$

The system of equations was solved by the method of successive approximations. Owing to the absence of precise data on transfer coefficients for vaporized metals and oxides at high temperatures the diffusion coefficients and the thermal conductivity were calculated according to data from work [277]. Reaction constants for molecules of metals and their oxides were determined from boiling temperature and the parameters of the crystal lattice. The reaction potential for the molecules is determined by the Lennard-Jones potential.

The values accepted for the coefficients in a medium of air and in an oxygen-nitrogen mixture at P = 1 atm and 1200°K are given below:

	Magnesium	Aluminum
λ_1, kcal/m·s·deg	$27.7 \cdot 10^{-6}$	$26.7 \cdot 10^{-6}$
λ_2, kcal/m·s·deg	$32.4 \cdot 10^{-6}$	$29.2 \cdot 10^{-6}$
$\bar{D}_2$, m^2/s	$7.35 \cdot 10^{-4}$	$6.2 \cdot 10^{-4}$

The degree of blackness was taken as equal to $\varepsilon_{\text{к}} \approx 0.2$; $\varepsilon_{\text{г}} \approx 0.5$.

The calculation proposed by Klyachko for parameters of combustion of particles of metals with consideration of partial diffusion of vaporized combustion products to the surface of the metal with respect to the nature of the basic relationships corresponds more exactly to the experimental results (Figs. 95 and 96).

An essential distinction of the theory which takes into account the process of evaporation of the metal oxide in the reaction zone
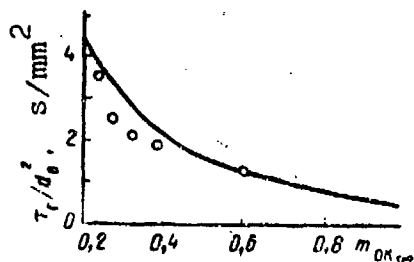
239
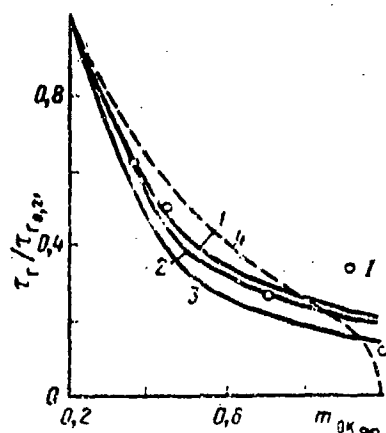
Fig. 95.　　　　　　　　　　　　　Fig. 96.

Fig. 95. Relative time of combustion for an aluminum
particle, τ_r/d_0^2 as a function of m_{0H}. Solid line –
calculation (T = 2500°K); points – experiment.

Fig. 96. Ratio of the combustion time for magnesium
particles in an O_2-N_2 medium to time $\tau_{r\cdot 0.21}$ in air
as a function of O_2 content. O – experiment; 1, 2, 3 –
calculated relationships with consideration of evapora-
tion of the oxide for d = 50, 100 and 500 μm; 4 – cal-
culated relationship without consideration of oxide
evaporation.

and of its diffusion is the possibility of calculating the time
parameters of combustion of finely dispersed metallic particles
in pure oxygen. In the opposite case the calculation leads to a
clear contradiction with experiment: the calculated time of
combustion turns out to be equal to zero.

However, the analysis proposed by Klyachko contains absolutely
no discussion of the question on the nature and future fate of
the vaporized oxide condensing on the surface of the particle.
If we assume that condensation occurs uniformly over the entire
surface, in the course of time the aluminum particle turns out to
be enclosed in a shell of molten oxide. The rate of particle
evaporation will gradually be slowed and the model of vapor-phase
combustion is actually converted into a model of "bubble" combus-
tion [261].

240

The question of the real fraction of metal oxide and of the possibility of its condensation directly in the zone AB also remains open.

In an analogous statement [272], i.e., with consideration of evaporation of the metal oxide in the flame front and its partial diffusion in the direction of the particle surface, Kuehl and Zwillenberg examined the problem of combustion of particles of metal in the vapor phase. It is postulated despite its two-way diffusion from the reaction zone B the total quantity α of evaporating or dissociating oxide remains the same as during the soltuion which takes into account directivity of the flow of reaction products into the ambient medium, BC.

It is further considered that vaporized oxide which reaches the surface of the particle is completely condensed. Its quantity αk stands dependent on the total evaporation of oxide in the flame front, α (quite naturally), and on the ratio between the dimensions of the combustion zone and particle radius, R_B/R_A. No condensation of the oxide occurs in region AB - i.e., between the flame front and the particle.

The relationship between the flow of evaporated metal, $\mathscr{I}_M$, in the presence of reverse diffusion of the oxide to the particle and the flow $\mathscr{I}_{1M}$ without reverse diffusion is given by the expression

$$(\mathscr{I}_{2M} - \mathscr{I}_{1M})\, H_M^{\text{кип}} = \mathscr{I}_{2M}\, \frac{v_{\text{пр}}}{v_M}\, \alpha k \psi,$$

where ψ is the heat of condensation of the oxide and $H_M^{\text{к ип}}$ is the heat of evaporation of the metal. After conversion it is found that

$$\frac{\mathscr{I}_{2M}}{\mathscr{I}_{1M}} = \frac{1}{1 - \dfrac{\psi}{L_M^{\text{кип}}}\, \dfrac{\alpha k v_{\text{пр}}}{v_M}}. \qquad (\text{IV.33})$$

The condition for existence of a solution follows from this expression:

$$\frac{\psi}{H}\frac{\alpha k v_{np}}{v_M} < 1. \qquad (IV.34)$$

With the numerical values of parameters entering into inequality (IV.34) the maximum quantity of oxide which reaches the surface of the particle will not exceed $\alpha k = 0.125$ ($v_{np} = 2.67$, $v_M = 1.33$; $\psi = 2.8 \cdot 10^5$ cal/mole, $H_M^{\text{ккп}} = 7.0 \cdot 10^4$ cal/mole).

In final form the problem is reduced to solution of the following equation by the method of successive approximations:

$$f(\alpha, k, R_B/R_A) = 0. \qquad (IV.35)$$

Calculation of particle combustion time is carried out by the formula

$$\tau_r = \int\limits_M^0 \frac{d_M}{[(1-B\alpha k)M + B\alpha kM]^{1/3}\left(\frac{\mathcal{Y}_M}{r}\right)} \qquad (IV.36)$$

under the assumption that αk and $\mathcal{Y}_M/r$ are constants (here $A = 3/4 \pi\rho_M$, $B = \frac{3}{4}\pi\rho_M$, $B = \frac{3}{4\pi H}\frac{\mathcal{Y}_{ok}}{\mathcal{Y}_M}\frac{v_{np}}{v_M\rho_{ok}}$).

Quantitative calculation was carried out for two metals which show promise and interest in a practical respect: aluminum and beryllium. The authors considered the problem of the influence of reverse oxide diffusion on flame temperature, particle temperature, the ratio R_B/R_A, and the rate and time of combustion of particles 1-1000 µm in diameter in the pressure interval 0.01-100 atm. Oxygen was selected as the major oxidizer; the inert diluent was argon.

The following points can be noted from the results of this work: the minimum concentration of oxidizer $X_{\text{мин}}$ at which self-sustaining combustion of aluminum and beryllium is still possible

242

does not depend in practice on the dimension of the particles (with the exception of the very largest - larger than 300-500 μm) or on pressure. On the other hand, the critical oxygen concentration X'_{O_2} at which the temperature in the reaction zone still equals the boiling point of the metal oxide is a strong function of pressure and particle size (Fig. 97). From Fig. 97 it clearly follows that according to the proposed theory the process of vapor-phase combustion is most probable for fine particles of metal at low pressures. With an increase in pressure and in particle size the quantity X'_{O_2} grows sharply. With $X_{мин} < X < X'_{O_2}$ a process of accumulation of condensed oxide occurs in the flame zone. The particle is covered with an oxide film. The rate of diffusion and, after it, the rate of combustion are reduced and in the end the particle is quenched.
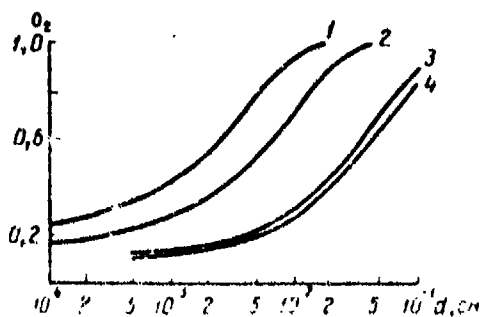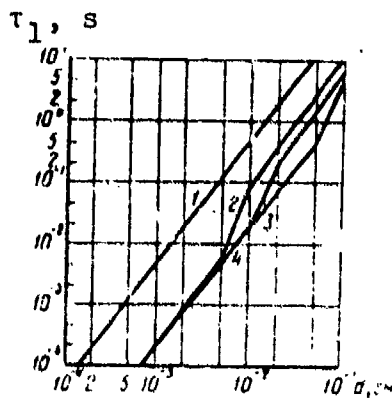
Fig. 97.   Fig. 98.

Fig. 97. Minimum concentration of oxygen at which the flame temperature T^B equals the boiling temperature of aluminum oxide (2, 4) and of beryllium oxide (1, 3) ($T_0 = 300°K$). 1, 2 - p = 100; 3, 4 - p = 10^{-2} atm.

Fig. 98. Combustion time for Be particles in a medium of xO_2-Ar with consideration of reverse diffusion of the oxide to the surface of the particle (p = 10 atm, $T_0 = 300°K$). 1 - x = 10%; 2 - x = 40; 3 - x = 70; 4 - x = 100%.

It also follows from the calculation results that, other conditions being equal, combustion in the vapor phase is of higher preference for aluminum than for beryllium. As we will see below, in reality this corresponds to experimental results.

We will note that the concentration limit of vapor-phase combustion falls below that given by the theory, which does not take into account the presence of a flow of oxide to the particle.

For a broad range of particle sizes (1-100 µm) in an oxygen-argon mixture the combustion of aluminum and beryllium obeys a quadratic law: $\tau_r \approx d^2$. The size of the particles for which this law is fulfilled is reduced with an increase in pressure and a reduction in oxygen concentration in the medium (Fig. 98). In terms of absolute value the combustion rate for beryllium and aluminum will grow if reverse diffusion of the oxide to the particle is considered in the calculation. There is a simultaneous growth in the ratio of the radii of the flame, R_B and of the particle, R_A - i.e., R_B/R_A (Fig. 99).
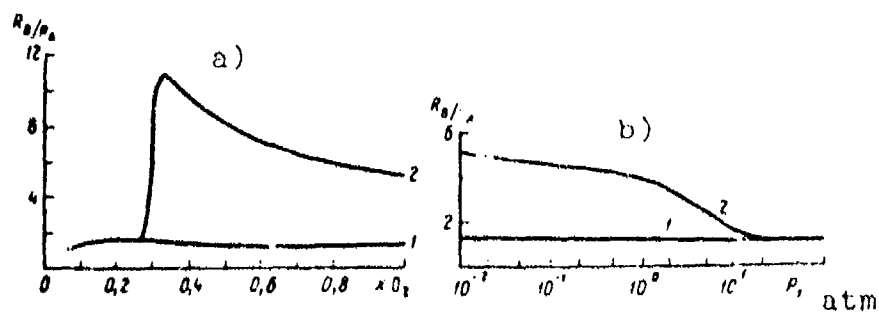
Fig. 99. The quantity R_B/R_A as a function of oxygen concentration xO_2 (a) (d = 50 µm, p_0 = = 0.1 atm) and as a function of pressure (b) (d = 260 µm, O_2-Ar medium, 80/20) during combustion of aluminum: 1 - without reverse diffusion of the oxide; 2 - with reverse oxide diffusion.

For aluminum (d ≤ 200 µm) in an 80/20 oxygen-argon medium at a pressure less than atmospheric the ratio R_B/R_A equals 4-5

(according to theory without consideration of diffusion and condensation of the oxide on the particle it equals 1.5-1.7, independently of pressure). With an increase in pressure the indicated quantity drops and at P = 10 atm it is almost equal to ∿1.75. It should be noted that at such a pressure (and particle size) the concentration of oxygen in the medium approaches the limiting value $x_{O_2}^{мин}$ (Fig. 97), corresponding to the case $\alpha = 0$. Without question the course of the change in R_B/R_A with pressure which is considered here corresponds more exactly to experimental observations.

According to calculation the temperature of the surface of the aluminum particle at $P \geq 1$ atm lies substantially above the melting temperature of Al_2O_3. Therefore the oxide which condenses on the particle surface will be in the molten state. This does not lead to any sharp change in the rate of combustion up to the finishing stage.

At a pressure $P \geq 10$ atm the temperature of the surface of a Be particle also exceeds the melting temperature of BeO, and therefore the process of beryllium combustion will be similar to that for aluminum.

Thus, of the two analytical models considered the model of vapor-phase combustion more completely reflects the quantitative peculiarities and the basic laws governing combustion of particles of metals of the aluminum, beryllium, etc. type. This relates first of all to theories which take into account the partial dissociation of the oxide which forms during the reaction and its diffusion from the flame zone, not only into the ambient medium but also in the direction of the particle surface. These theories make it possible, within reasonable limits, to evaluate the relationships between radii of the flame zone and the particle, the temperature of the flame and that of the particle surface, the overall dependence of time or rate of combustion on particle diameter, and the temperature and activity of the medium (when oxygen is the major oxidizer).

However, a number of the questions and physical phenomena which are observed during the combustion of aluminum in experiments are not explained within the framework of these theories.

Theories of vapor phase combustion in the form in which they have been developed at present do not reflect essential differences between the combustion of particles of aluminum in "dry" and "moist" atmospheres (even if oxygen is the major oxidizer); they do not reveal the causes of the formation of hollow spheres and the phenomenon of particle rotation, nor do they explain the reduction in τ_r with an increase in pressure.

The effect of natural and forced convection is not taken into account. The basic reason for the incomplete state of existing theories of the combustion of metal particles unquestionable lies in the absence at present of exhaustive and fully substantiated presentations on the mechanism of combustion in various media and in the virtually complete absence of quantitative data on the parameters of the transfer of vaporized metals and products of their reactions under the conditions and at the temperature characteristic for the flame.

In this section the sum total of experimental factors obtained by various methods and characteristic for combustion of particles and thin wires of aluminum in chemically active gaseous media are considered.

On the basis of the above it is possible to present, in general outlines, a picture of the basic processes of steady-state self-sustaining combustion of particles of aluminum in a high-temperature gaseous medium.

10. The Physical Picture of
Combustion of Aluminum Particles

At atmospheric pressure (p ≈ 1 atm) in a medium of air or one with a substantial (∼50% and greater) concentration of

oxidizing reagents (oxygen, water vapor, carbon dioxide), the combustion of aluminum particles occurs mainly in the gaseous phase and as the result of reaction between vapors of the metal and of the oxidizer. The process is bound to the free surface of the metal: evaporation and diffusion of vapors into the reaction zone are unlimited by their passage through a liquid layer of aluminum oxide. During combustion the particle is in the molten state.

Melting and evaporation of aluminum occur as the result of heat transfer (heat conductivity, radiation, etc.) from the reaction zone. At atmospheric pressure the zone of the vapor-phase reaction is separated from the particle surface by a distance of 1-3 radii: $R_B/R_A = 2-4$. The latter quantity is determined by the state and temperature of the ambient medium. The temperature of the reaction zone is limited by the boiling temperature of the oxide, since even in pure oxygen the heat of the oxidation reaction is less than the heat required for total dissociation or evaporation of the condensed products (Al_2O_3) which form at $T_{кип}$. Since their concentration here is maximum, the products diffuse from the reaction zone both in the direction of the particle surface and outward from it. Thus the possibility of diffusion to the particle surface of condensed products is not excluded. As was pointed out earlier, in order of magnitude the size of particles of subdispersed Al_2O_3 is comparable with the average size of the molecules of ordinary gases ($\sim 10^{-8}$ cm). A constant flow of vaporized oxidation products in the direction of the particle is possible in the case when a certain and also constant mechanism of absorption or removal is present. Condensation in the space between the burning zone and the particle and on the surface of the particle can be such a mechanism. In the region of the particle surface there is a gradual drop in temperature down to the boiling temperature of aluminum.

Condensation and cooling of Al_2O_3 to the temperature of the metal surface is a third additional method of heat transfer to

the particle, leading to a growth in the temperature of the drop and to an increase in the rate of aluminum evaporation.

Expansion of the combustion zone, predicted qualitatively by the theories, is the result of the existence of a reverse flow of reaction products and of their condensation.

Since it is poorly soluble in the metal, the condensed aluminum oxide can either coagulate into larger particles or enter into reaction with the aluminum. In the first case we obtain a picture which is essentially similar to that observed during combustion of a large drop of aluminum ("aluminum sun") [145]: formation of fine spheres of oxide on the metal surface, which skate about on the surface and unite with spheres which developed earlier.

If combustion occurs on a substrate, used to stabilize the particles in the field of view, we find that because of the comparatively low temperature as compared with that of the flame zone condensed Al_2O_3 gradually accumulates on the particles. As a result a particle is formed which is comparable in size with the initial particle (see Fig. 67). The same thing apparently takes place during sampling of particles onto object glasses.

During combustion of aluminum in the suspended state the gradual accumulation and coagulation of the oxide on the particle surface leads to a situation in which at some critical dimension the force of gravity and of the outflow of vaporized aluminum causes separation of a drop of oxide from the surface of the particle. This phenomenon can be partially explained by the presence of solid white spheres 10-15 µm in diameter among the products of aluminum combustion (see Fig. 66). But we cannot completely exclude the possibility of direct interaction of the oxide with the metal.

In work [277] it was established that at 1900°C a mixture of $Al + Al_2O_3$ (15-µm sample) can evaporate completely from the

surface of the heated element. It is shown that the volatility of Al_2O_3 is increased by approximately 2 orders of magnitude in the presence of aluminum. Since the temperature of the particle surface is about 2000°C, it is reasonable to designate the actual reaction by the equation

$$4Al(\text{ж}) + Al_2O_3(\text{ж}) \to 3Al_2O(\text{г}),$$
$$Al(\text{ж}) + Al_2O_3(\text{ж}) \to 3AlO(\text{г}),$$
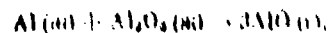
ж = liquid;
г = gas.

The reaction products – gaseous lower oxides of aluminum – can subsequently diffuse back into the reaction zone and there once again undergo oxidation up to the final product Al_2O_3. It is appropriate to note here that the presence of lower oxides of aluminum in the reaction zone was detected by spectral analysis.[1] In such a variant the combustion of aluminum particles resembles the combustion of particles of carbon [278].

Both versions of the removal of oxide from the particle surface are acceptable. Their simultaneous existence is not contradictory, but they rather supplement one another.

The process of diffusion of the oxides back to the particle and their condensation on it is also a reasonable explanation of such phenomena, specific to the combustion of metal particles, as rotation and fragmentation of the particles.

Asymmetry in the accumulation of oxide causes the appearance of force components connected with the outflow of evaporating aluminum – forces which do not pass through the center of mass of the particle. The eccentricity of the force causes the particle

---

[1]This does not exclude the possibility of the formation of lower oxides of aluminum directly within the reaction zone.

to rotate. Localization of molten oxide on the surface of the particles requires a certain amount of time. Therefore rotation does not set in at the moment of particle ignition, but rather within the period of steady-state combustion, after the appearance of a fully developed glowing track.

Condensation and cooling of the products down to the surface temperature are extremely effective additional sources of heat transfer to the particle. If the heat liberation and the temperature of combustion in the reaction zone are great and if losses of heat are small (for example, characteristic for metal-containing rocket propellants and high-temperature gas burners ($2500-300°K$)), dissociation and evaporation of the reaction products and a flow of them in the direction of the particle and condensation on its surface can reach significant magnitudes, sufficient to cause heating of the particle above the boiling point. The results of such heating will be fragmentation of the particle.

The presence of impurities of more volatile metals (e.g., magnesium) in the aluminum will increase the vapor tension and the probability of explosions of particles during combustion. In this case there is a direct analogy with fragmentation of drops of emulsion of the reverse type. During rapid heating of a drop of oil, containing admixtures of water, the latter explode with characteristic spattering of fine drops in radial directions. The combustion and destruction of emulsions of the reverse type was studied in detail by N. F. Pokahil.

It is also of some interest to note that during burning of finely dispersed carbon containing volatile substances it is possible to observe fragmentation of the carbon particles and the formation of hollow spheres, the so-called "senospheres"[1] [279, 280].

---

[1]Term not found; transliteration of Russian prefix "сено" — Translator.

The fact that the fragmentation phenomenon occurs in a high-temperature flame independently of the presence or absence of hydrogen in it emphasizes the determining role of temperature in this process. However, there is also an influence of medium composition: in a "wet" atmosphere fragmentation of particles is observed much more frequently than in a medium containing no water vapor or hydrogen.

Finally, the latter fact can be interpreted from a purely thermal point of view. According to experiments, with equality of the rates of combustion the reaction zone has more sharply defined boundaries in a moist atmosphere and is located about half as far from the particle surface as in the case in a carbon monoxide and oxygen flame. This proximity of the high-temperature zone intensifies heat transfer (primarily by radiation) to the particle and thus increases the probability that it will be over-heated and fragmented. It is also possible that the addition to a burner flame of 18-20% hydrogen will simply raise the flame temperature to the necessary critical level. But the above must be classed as an assumption.

At the same time the presence of nitrogen ($\sim$5%) in the ambient medium causes destruction of hot drops of zirconium, while carbon dioxide favors fragmentation of drops of iron during combustion [148, 281]. These facts indicate that completely defined gases exist for hot particles of certain metals, gases which in small concentrations will lead to breakdown of the steady-state process of particle combustion. Their existence close to the particle is connected either with the initial presence in the medium (for example, nitrogen) or with their formation in the reaction zone during oxidation of the metal (e.g., water vapor or carbon dioxide).

Diffusing to the surface of the particle, the gases may be partially dissolved in the metal or in its oxide. If the solubility of the gases changes significantly with temperature or with conversion of the metal and oxide from one phase state into another,

a small change in particle temperature (e.g., possible if the particles suddenly leave the flame jet) will be accompanied by intensified gas liberation. As a result we can expect fragmentation of the particle or expansion of hollow spheres ("bubbles"), as occurs during combustion of particles of carbon [279, 280].

When aluminum is burned under standard conditions only a small part of the oxide can dissociate in the reaction zone. According to calculations within the framework of the theory of vapor-phase combustion (with consideration of two-way diffusion) the total quantity of them will not exceed 30%. A large part of the products exist in the reaction zone in the condensed form. Their diffusion into the surrounding space creates a glowing zone around the particle and creates a characteristic track on the substrate, consisting of fine subdispersed particles. A part of these will be accumulated into larger drops close to the zone of combustion. Agglomeration is favored by existence of flows of natural and forced convection around the particle of metal. The latter is especially manifested in relief during combustion in a moving medium. High-speed cinematography makes it possible to fix their intensive displacement, growth, and ejection from the zone of combustion. Together with drops which leave the surface of the metal, they are comprised of a group of condensate particles of medium diameter (up to 10-15 μm).

The agglomeration and coagulation of oxide close to the combustion zone are expressed more sharply in a moist medium than in a dry one. This leads to sharpness in the outlines of the tracks. It is possible to assume that the great width of the glow zone in a dry atmosphere is not a consequence of separation of the reaction zone from the particles surface, but is rather explained by the great extent of the zone of condensation and afterglow of finely dispersed condensed products in the direction away from the particle. In reality the difference between the radii of the reaction zone in the indicated media is substantially less than that determined from the glow or from the width of the tracks.

One of the basic laws governing vapor-phase combustion is
fulfilled with satisfactory accuracy for aluminum at a pressure
of ~1 atm: the time of combustion of the particles is proportional
to the square of their diameter.

However, with an increase in pressure an essential change is
observed in the overall picture of combustion. The rate of burning
of the particles is gradually increased; at a pressure of 10-30 atm
combustion time is proportional not to the square of the diameter,
but to a power of 1.5 and less of the diameter. The
reaction zone draws closer to the surface of the particles; the
ratio of the radius of the flame to the particle radius at 40
atm comprises 1.5-1.7.

Such a change in the laws governing combustion of individual
aluminum particles can be the result of a gradual transfer of the
reaction from the gas phase to the particle surface with a growth
in pressure and also of an increase in the role of convection as
pressure increases.

§ 2. Combustion of Beryllium

Works dealing with a systematic study of processes of beryllium
combustion have only begun to appear. As has already been repeatedly
emphasized, the reason for this position is connected with the
toxicity of finely dispersed beryllium and of the products of its
oxidation.

The reaction of beryllium with oxygen or oxygen-containing
compounds of the H_2O and CO_2 type has a clearly expressed exo-
thermic character.

In contrast to aluminum, the process of steady-state self-
sustaining combustion of beryllium is preceded by self-heating of
the particles with a weak but clearly distinguishable glow (Fig.
100). Combustion of the particles in the normal conditions

obtaining in the flame of a flat gas burner [254] is accompanied by a bright, intense glow, which grows with an increase in the oxygen concentration.
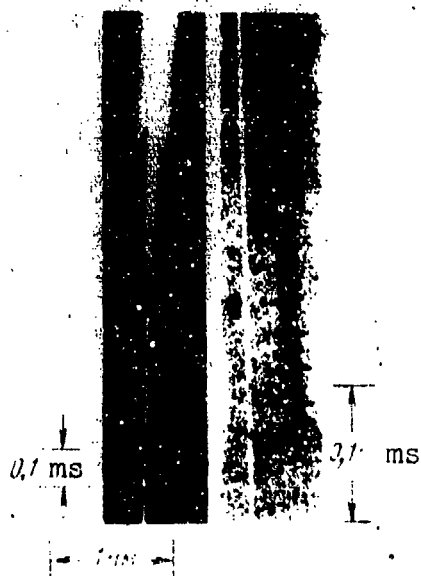
Fig. 100. Track of a burning particle of beryllium [254].

For the most part the trajectories of the particles are rectilinear and they rarely terminate in the star-shaped burst characteristic of the phenomenon of fragmentation.

At low pressures, a low level of medium activity, and high temperatures the burning particles form straight lines and sharply outlined tracks on photographs. A high oxygen content, high pressure, and low temperatures will, on the other hand, favor the appearance of blurred wide tracks - one of the characteristic features of vapor-phase combustion.

In a dry atmosphere the ratio of the flame zone diameter to the diameter of the particle comprises 1.3-1.4. In a moist atmosphere it is less, approximately equal to 1.1. In this medium the vapor-phase flame itself is less sharply expressed. If the partial pressure of oxygen is less than 0.1-0.2 atm the flame around the particle loses its brightness and draws closer to the surface of the particle.

A brighter core is seen in the center of the track. Its size is 10-20% greater than the diameter of the initial particle of beryllium.

Just as in the case of aluminum a periodic change in the intensity of the glow is, as a rule, observed on the track. This actually indicates asymmetry of the combustion process and rotation of the particle during its movement in the flow. The frequency of rotation comprises 10,000 Hz. The pulsations of illumination arise immediately after ignition of the particle; their termination can serve as a criterion for completion of the combustion process.

The size and shape of products of beryllium combustion depend on the temperature of the ambient medium. If the temperature of the medium exceeds the melting point of beryllium oxide (2820°K) the condensed products will have the form of spheres and their size will not exceed 1 μm in diameter. If the medium temperature is lower than the melting point the combustion products are formed as rod-shape crystals up to 10 μm long.

Among the combustion products the particles of oxide can be distinguished by their dimensions, equivalent to the initial particles of the metal. This occurs most frequently at the moment of forced sampling and of quenching of the particles on a heat-removing plate (Fig. 101). Such particles (a and b) can contain (by evaluation) up to 60% of the total oxide formed during combustion of a beryllium particle.

There are no specific data on the temperature of the flame of the Be particle. As in the case of aluminum, the boiling temperature of the oxide is the upper limit; this equals 4100°K.

In works [143, 276, and 279] it is postulated that beryllium oxide is formed in both the liquid and the gaseous phase in the reaction zone.

Fig. 101.   Products from the combustion of
beryllium particles.

Table 20 gives the average di meter $\bar{d}$ of beryllium particles,
the temperature of the medium, partial pressure of oxygen P_{O_2} and
of water vapor P_{H_2O} in the flame, and the average burning time τ_Γ
of the particle.

Table 20.   Burning time of beryllium
particles [254].

$\bar{d}$, μm	T, °K	P_{O_2}, atm	P_{H_2O}, atm	τ_Γ, ms
32	2830	0,43	0,005	1,8
32	2880	0,36	0,005	2,2
32	2950	0,23	0,005	3,5
32	2970	0,16	0,005	4,5
25	2880	0,36	0,005	1,4
25	2880	0,36	0,015	1,8
32	2730	0,31	0,22	(2,3)
25	2790	0,31	0,22	1,4
25	2690	0,31	0,19	1,3

From the table it follows that the burning time for beryllium
particles at atmospheric pressure will, in the general case, obey
a quadratic law: $\tau_\Gamma \sim d^2$, characteristic for a spherically
symmetrical model of vapor-phase combustion.

The presence or absence of water vapor in the flame has an essential influence on the rate of burning of the particle. For example, an increase of water vapor in the flame from 0.5 to 1.5% will cause a 30% growth in the time required for combustion of partic' s 25 μm in diameter (Table 20, lines 5 and 6). Since the addition of such small quantities of water cannot change the thermodynamic properties and mass-transfer properties of the medium, the indicated change can be ascribed only to the chemism of the reaction.

Kuehl [253], during experimental examination of the combustion of fine beryllium wires in a gaseous medium, notes that in the presence of water the process is slower than in pure oxygen. Study of unreacted or partially burned wires shows that in the presence of water vapor a coating of greater volume is formed, consisting of the lower or higher hydroxide of Be. Combustion in oxygen is accompanied by the formation of a large number of extremely fine spherical particles of the oxide.

For purposes of comparison combustion times are given below for beryllium and aluminum particles of equal size under conditions as similar as possible (with respect to oxygen concentration in the flame) [135, 246]. The diameter of the beryllium particles equaled 32 μm; by means of the d^2 law the data on aluminum were brought to the same diameter. The medium was CO_2, CO, with a small quantity (0.5%) of H_2:

P_{O_2}, atm	$(\tau_r)_{Be}$	$(\tau_r)_{Al}$
0,43	1,8	2,1
0,36	2,3	3,1
0,23	3,5	—
0,18	4,5	2,8

In view of the paucity of information on combustion of beryllium, there is unquestionable interest in data on such combustion for specimens other than particles. Work [143] contains, along with a study of high-temperature oxidation of beryllium,

a series of experiments on the qualitative consideration of the picture of combustion of cylindrical specimens (d = 3 mm, h = 12 mm) of beryllium in an oxygen-hydrogen medium. Ignition was accomplished by a heat flux from the flame of a burner.

In a flame rich in fuel (O_2/H_2 = 0.33) no vapor-phase combustion as such occurred with heating of the specimen up to the melting point of beryllium. It appeared that the reaction in individual burning points proceeds inside a thick porous oxide layer growing up on the surface of the specimen. Such a thick porous layer of beryllium oxide cannot serve as a reliable protection from subsequent oxidation. However, a second thinner, dark layer in direct contact with the metal was detected under the first layer on quenched specimens; this second layer will, apparently, fulfill a basic protective function under ordinary conditions In a flame enriched with oxygen (O_2/H_2 = 0.99) specimens were ignited (if the initial flux of heat was not too low) and burned with the formation of a hot diffusion flame.

The transition from the fast reactions occurring on the surface of the specimen (or close to it) to a vapor-phase diffusion flame located at a certain distance from the specimen was accomplished at a surface temperature above 2200°K in less than 10^{-2} seconds. During vapor-phase combustion a significant portion of the specimen was transformed into a finely dispersed condensate, while the remaining portion lost the initial cylindrical shape.

It was noted that in a flame in which water vapor was the single active reagent the beryllium specimen was sometimes not heated to the temperature above 2000°C which is necessary for the development of vapor-phase combustion. However, the reaction of beryllium oxidation occurred very actively. The process of beryllium oxidation by water vapor is accompanied by the liberation of hydrogen:

$$Be + H_2O \rightarrow BeO + H_2$$

Experiments in burning cylindrical specimens of Be confirm the special and unique role of water vapor as a reagent in the oxidation and combustion of beryllium.

The sum total of available data on combustion of beryllium in an active medium indicates that this process can occur at different levels. One mode of combustion can be vapor-phase combustion, analogous to the burning of aluminum particles. Its appearance is favored by high-temperature of the medium, a high concentration of oxygen in the medium, and a low content of moisture. A determining factor is diffusion of the oxidizer into the reaction zone, which is located some 0.1-0.3 radii from the surface of the particle. The combustion products can diffuse from the reaction zone both inward, in the direction to the particle surface, and also outward. Since the temperature of the particle surface is, although close, less than the melting temperature of the oxide, condensation of the oxide on the surface is possible. This possibility is confirmed by the observed periodicity of the change in the light radiation from the burning particle, occurring as a result of disturbance of the symmetrical combustion front and the appearance of large spherical condensed drops of oxide in the combustion products after extinguishing of the particles; this is the same as in the case of aluminum.

In this version the theory of vapor-phase combustion with reverse condensation of the reaction products [272, 276] is applicable to the combustion of beryllium. Calculated values of flame temperature T_B, particle temperature T_A, the fraction of oxide diffusing to the particle surface, the ratio of radii of the flame zone and the particle R_B/R_A, and of τ_r for a drop of beryllium 50 μm in diameter burning in an argon-oxygen mixture at $T_0 = 300°K$ and atmospheric pressure are presented on Figs. 97, 98. The quantitative divergence between the time of combustion obtained in work [276] and those given in Table 20 is significant and cannot be explained by a difference in initial conditions.

A second possible version of beryllium combustion is "burning" the metal in a medium with low (0.1-0.2 atm) oxygen content. In essence this is the reaction of surface oxidation of the metal, occurring on individual local burning segments of the surface at a very high rate.

According to results from experiments with cylindrical specimens [283], one condition for transition from surface oxidation to vapor-phase combustion is achievement of a temperature higher than 2200°K on the surface of combustion. It is postulated that at this temperature the rate of heat liberation resulting from the reaction of surface oxidation of Be becomes adequate to ensure conditions for evaporation of the metal and transition to vaporphase combustion. The melting point of beryllium oxide is the temperature at which the second, dense subsurface layer of oxide loses its protective properties.

The combustion of beryllium in a high-temperature flame containing water vapor is a unique phenomenon.

It was indicated above that the presence of even small quantities of H_2O in the flame sharply reduces the rate of beryllium combustion or even terminates it altogether. The explanation should be sought, apparently, in the fact that in the preflame period a thick layer of oxide or hydroxide is formed on the particle as the result of the oxidation reaction, and this layer reduces the rate of oxidation and increases outward heat losses.

In addition, in this case hydrogen is liberated during the reaction; at a high temperature hydrogen will for practical purposes not react with beryllium and creates an additional diffusion barrier in the path of the oxidizer.

If the concentration of water vapor in the medium is great vapor-phase combustion will not develop at all. In an oxygen-containing medium hydrogen has the possibility of secondary

oxidation to H_2O. It should be noted that the role of hydrogen and of water vapor has not been reflected in theoretical works.

§ 3. Combustion of Boron

The first information on combustion of elemental boron in oxygen was apparently obtained by Talley [144] in his experiments with rods (d = 1 mm). The linear velocity of flame propagation was measured during combustion of a rod from the face in a flow of oxygen at 2500°K. In these experiments it was established that boron remains solid during combustion, except for the case of extremely high temperatures. A thick viscous oxide is formed on the surface of the rod and is retained in a broad range of temperatures.

In the flame of natural gas enriched with oxygen and having a temperature of 1800°K boron burns "relatively slowly." With an increase in temperature to 1800-2100°K the rate grows smoothly to a value of 1 cm/min. This is the normal steady-state rate of self-sustaining combustion of elemental boron under the given conditions. In this case the reaction rate is virtually independent of pressure. A further rise in temperature to 2480°K leads to melting of the end of the boron rod.

It should be noted that such phenomena as fragmentation or crushing, characteristic for combustion of metal particles, are absent in the case of combustion of metallic rods.

A study of the combustion of particles of crystal boron on a jet of hot gas was undertaken by Gurevich et al. [255]. A mixture of water vapor or oxygen with nitrogen and argon was used as the oxidizing medium. The flow rate equaled 10-20 m/s and the pressure was 1 atm. An arc plasma burner was used to obtain the jet of hot gas. The experiments were carried out with powdered particles obtained by grinding large crystals of 99.99% boron.

Results of cinephotography established the fact that the shape of the track will, as a rule, be curved (Fig. 102a). The initial width of the track is close to the diameter of the initial boron particle and is a clearly defined thin line. As combustion develops the track is gradually thickened, with simultaneous blurring of the boundaries. A brighter central portion is seen in the middle part of the track. During combustio. in water vapor the thickening track sometimes terminates in a star-shaped peak, characteristic of fragmentation of particles (Fig. 102b). Tracks with virtually unchanging width were observed along with tracks of the first type.

Fig. 102. Tracks of burning particles of boron (p = 1 atm) [255].

a) b)

Selection of samples of burning particles and their combustion products on glass plates showed that incompletely burned particles are spherical drops of metalic boron with diameters 2-20 times smaller than those of the initial particles. No traces of oxide were found on the drops of boron.

262

If combustion occurred in an atmosphere of water vapor no condensed combustion products were detected in the section corresponding to termination of combustion of the boron particles. In an oxygen-containing medium the combustion products consisted of melted transparent particles of oxide whose size is both comparable in order of magnitude to the original and "very much smaller." Agglomerates 10-20 µm in size are noted.

According to the observations, the boron particle remains in the liquid state for a substantial portion of the combustion time. A particle of crystalline boron 1-3 µm in size placed in a flow of gas (20% H_2O + 80% Ar) at 1700°C was heated up to a bright glow, melted, and took on a form close to spherical within 3-4 seconds. The time required for combustion of individual particles of boron, determined during combustion in a mixture of water vapor and argon, is given below [255]:

d, µm	H_2O, %	τ_r, ms
75	36	40
105	47	34
105	36	62
105	25	82
145	36	97

In the course of the combustion process the temperature of the medium was varied from 2100°C to 800-1000°C. It was assumed that combustion time is essentially independent of medium temperature.

According to the measurement results, the dependence of combustion time on particle diameter is weakly quadratic: $\tau_r \sim d^{1.3}$. At the same time τ_r is a very strong function of the concentration of the oxidizer - water vapor.

Since the shape of particles used for quantitative evaluation of combustion time differed essentially from spherical, the given

results can be considered more or less as preliminary.

Maček et al. [256] studied the combustion of single particles of pure crystalline boron in a high-temperature gas-burner flame of known composition (p = 1 atm; see page 58). It is noted that the trajectory of burning particles of boron consists of a central, brightly glowing core surrounded by a wide and ill-defined region with a greenish color. The size of this region is increased with an increase in temperature of the medium. A two-stage nature of the process is a characteristic feature of combustion of boron particles under the considered conditions. Immediately after ignition the particle burns very brightly for comparatively short period of time. Then a tendency toward attenuation is noted, but the particle does not go out. After a short time the brightness of the particle grows once again and remains virtually unchanged up to termination of combustion. The second stage is of longer duration than the first.

The two-stage process of combustion of boron particles is reflected especially sharply in a medium with an increased concentration of oxygen; a region with an absence of glow exists on the track between stages. If the concentration of oxygen is reduced the transition from the first stage to the second is gradually smoothed; the beginning of the second stage of combustion is determined by a sudden increase in the glow. It was established by a special check that the observed effect cannot be the result of the presence of impurities in the boron.

Spectroscopic studies in the wavelength range 3500-6500 $\overset{c}{A}$ and on the first and second stages of combustion reveal systems of B_2O_3 bands which are absolutely identical both in structure and in brightness. The authors determined the combustion time of boron particles in the media whose composition and temperature are given in Table 17.

Measurements were made of time τ_1 counted off from the moment of ignition of the particle up to the beginning of the second

264

stage of combustion and also of time τ_2 of the second and concluding stage of combustion for particles 34.5 and 44.2 μm in diameter. Table 21 presents values of τ_1, τ_2, and $\tau_r = \tau_1 + \tau_2$ obtained by averaging a series of measurements of combustion time for individual boron particles.

The data in Table 21 indicate that the rate of combustion of boron particles is increased somewhat with a growth in the temperature of the medium.

Table 21. Combustion time for boron particles [256].

Composition No.	$\bar{d} = 34.5$ μm			$\bar{d} = 44.2$ μm		
	τ_1	τ_2	τ_r	τ_1	τ_2	τ_r
1	4,4	16,6	21,0	5,5	20,1	25,6
2	4,8	15,7	20,5	5,7	18,9	24,6
3	3,4	7,8	11,2	5,0	13,8	18,8
4	5,0	17,3	22,3	—	—	—
5	4,0	11,2	15,2	7,2	—	—
6	3,5	10,5	14,0	5,8	—	—
7	3,8	10,8	14,6	6,1	—	—
8	2,8	7,0	9,6	5,6	—	—
9	—	—	38,7	—	—	—
10	3,6	10,3	13,9	(7,4)	16,2	(23.6)
11	2,1	7,7	9,8	—	—	—

From comparison of compositions 2, 9, 10, 11, which have virtually identical temperature but which differ in oxygen concentration, it is evident that the rate of combustion is, with adequate accuracy, directly proportional to the molar fraction of free oxygen in the medium (Fig. 103).

The presence of water increases the rate of burning of the particles. This effect maybe connected with participation of H_2O in the reaction of boron oxidation. If we consider that a mole of H_2O is equivalent to 0.5 mole O_2 in reaction with boron, then with particles of the same size compositions 6 and 7 will give one and the same combustion time as compositions containing no water vapor.

265

The following formula is proposed for calculation of combustion time under the assumption that the process is determined by diffusion of the oxidizer to the particle:

$$\tau = \frac{(\rho/M)\gamma_i}{8\delta\beta p_i} d^2,$$
(IV.37)

where γ_i is the stoichiometric reaction coefficient (for the reaction of B (Al) with oxygen it equals 3/4); $\delta = R_B/R_A$ is the ratio of the radius of the reaction zone to the radius of the particle ($\delta = 1$); ρ/M is the ratio of density to the molecular weight of the metal; $\beta = D/RT$, where D is the diffusion coefficient; $\beta = 4 \cdot 10^{-5}$ mole/cm·s·deg·atm; $p_i = p\ln(p/p_i - x_i p)$; x is the molar fraction of the i-th component.
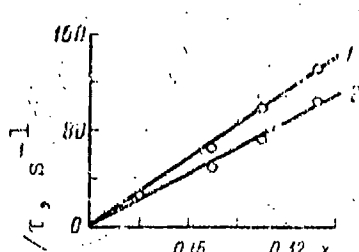

Fig. 103. Value of $1/\tau_1$ and $1/\tau_2$ as a function of xO_2 concentration in the medium. 1 – $1/\tau_2$; 2 – $1/\tau_1$; d = 34.5 μm; T_1 = 2400-2500°K.

Calculation of combustion time for boron particles in a dry atmosphere by the indicated formula with consideration of the fact that oxygen and CO_2 operate simultaneously as oxidizers will give satisfactory agreement with experiment (on the average the divergence does not exceed 10-20%).

One of the possible causes of quantitative differences between calculation and experiment is considered to be the possibility that the reaction of surface oxidation of boron may occur, with the formation of the gaseous lower oxide BO, which in the gas phase is subsequently oxidized to the final oxide B_2O_3. Formally, in the equation this leads to an increase in the parameter $\delta = R_B/R_A$.

At the same time it should be noted that results from work [256], just as those from [255], indicate that the quadratic law $\tau_r \sim d^2$ which is characteristic for the diffusion conditions of combustion is not fulfilled for boron.

In his interpretation of the obtained experimental results on the combustion of boron rods, Talley [144] singles out five characteristic regions in temperature/pressure coordinates (Fig. 104).
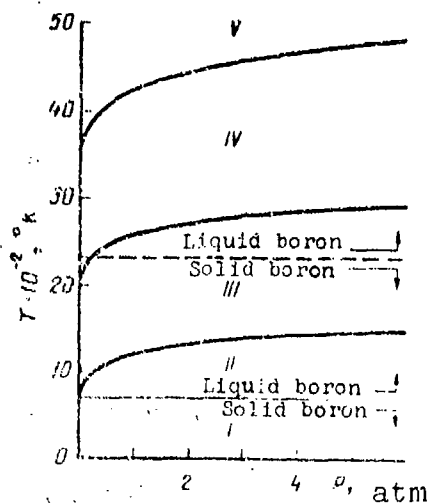
Fig. 104. Diagram of combustion of boron in oxygen as a function of temperature and pressure.

Region I. The intensity of heat losses during combustion is such that the temperature of the oxide which forms on the surface of the particle is lower than its melting temperature, that is, $723°K$. This is a region of slow oxidation, limited by diffusion of oxygen through the solid oxide. The layer of oxide is gradually thickened. The law governing the change in the oxidation rate is parabolic.

Region II. This region is bounded below by the melting temperature of the oxide, $723°K$. In this region, after a certain period of time, dynamic equilibrium sets in between the rate of formation of the oxide and the rate at which it flows off under the action of gravity. In this region the law governing the change in time of the rate of burning or oxidation of boron becomes linear.

The process is limited by the diffusion of oxygen through the layer of liquid oxide.

Region III. The temperature of the surface exceeds 1100°K. Removal of oxide from the surface of the particle occurs as the result of evaporation. The thickness of the oxide film and the process rate are limited by the diffusion of oxide vapors into the ambient medium. The rate of combustion is inversely proportional to the pressure and depends on temperature according to Arrhenius' law with an activation energy value equal to 77 kcal/mole. A strong influence of water vapor is observed in this region. In the presence of H_2O the rate of combustion grows and the value of E is reduced to 56 kcal/mole. The determining factor in the process is the evaporation of the metaboric acid forming on the surface of the particle as the result of the reaction of boron with H_2O.

Region IV. The temperature of the film of liquid oxide reaches the boiling temperature of B_2O_3 (with $p \geq 1$ atm, $T > 2520°K$). The surface of the particle is freed from the oxide film. The surface of the liquid metal is bounded by the gas phase. The rate of combustion is limited by diffusion of oxygen through the B_2O_3 vapor to the surface of the particle.

Region 5. The boundary of the region is determined by the boiling temperature of boron. The vapor pressure of boron exceeds the pressure of the ambient medium. The determining process is evaporation of boron. Vapor-phase combustion takes place (in work [144] this mode was not realized experimentally).

In a plasma burner [255] in a medium of oxygen or water vapor with an inert gas as the diluent the combustion of boron particles occurs in conditions when the temperature of the particle exceeds the boiling point of the oxide (the particle is in the liquid state). This means that there is no oxide film on the particle and the oxidation reaction proceeds on the surface of the metal. The

268

limiting stage is diffusion of the oxidizer through the vaporized B_2O_3 oxide. The absence of condensed oxide during combustion in water vapors is testimony to the fact that the reaction occurs through the formation of volatile boron-hydrogen compounds of the metaboric acid type. The presence of transparent particles with a broad spectrum of sizes among the products of combustion in oxygen should apparently ascribed to the process of their condensation and coagulation in the ambient atmosphere. In this respect the conglomerates noted in work [255], consisting of a large number of fine particles, are characteristic. Growth of B_2O_3 particles may also occur due to condensation on them of the vaporized oxide formed in the subsequent (in time) stages of combustion.

At the same time, the sharp expansion of tracks and fragmentation of particles in a medium of water vapor, noted by the authros of [255], indicate the possibility of overheating of the boron particles and partial conversion of the burning condition into the vapor phase. In order for the vapor tension at atmospheric pressure to equal the external pressure, the temperature of the boron particle must be close to 2800-3000°K. Achievement of such temperatures by the particles in a high-temperature medium is possible in principle, but requires additional experimental confirmation.

The considered modes of combustion of particles correspond to burning of rods in the fourth and fifth regions (Fig. 104).

Since the ignition temperature for boron lies below the boiling point of B_2O_3, combustion of a particle begins under conditions when a solid oxide film is present on its surface. This makes it possible to explain the two-stage nature of combustion observed in experiments [256] in a medium with a high concentration of oxygen.

With ignition the temperature of the particle begins to grow because of the oxidation reaction and at some certain moment

reaches the evaporation temperature of B_2O_3. The flow of vaporized oxide, directed away from the particle surface, creates a strong diffusion barrier for the oxidizer and slows the rate of the oxidation reaction.

After complete evaporation of the initial oxide film and condensation of B_2O_3 in the outer zone new and favorable conditions are created for diffusion of the oxidizer to the surface of the particle. A new dynamic equilibrium of diffusion flows of oxidizer and reaction products sets in, more favorable to the reaction of boron oxidation. In this case the reaction rate is increased and the brightness of the glow around the particle once again begins to grow, indicating that the second stage of combustion has begun.

The rate of the reaction in the first stage of combustion is lower than that in the second. The two-stage mechanism of combustion of particles is, according to the Talley scheme [144], the transition of boron combustion from region III into region IV.

CHAPTER V

AGGLOMERATION OF METAL POWDERS DURING COMBUSTION OF CONDENSED SYSTEMS

One of the particular features of the combustion of condensed systems containing additions of metal powder is the enlargement of particles due to accumulation and fusion on the burning surface of the specimen - i.e., the phenomenon of agglomeration.

This phenomenon was first discovered and investigated during a study of the combustion of ballistite compositions and mixtures of typical compositions by Nokhio, Logachev, and Mal'tsev [172-174, 247]. Sampling condensed combustion products in direct proximity to the burning surface of the specimen, they established that the particles escaping into the gas phase differed essentially from the initial aluminum in degree of dispersion. Their size was significantly greater.

Today the basic laws governing agglomeration have been clarified and qualitative and semiquantitative connections have been established between this phenomenon and the structure and physical chemical parameters of the initial composition, the conditions of combustion, and the degree of dispersion and concentration of the particles.

The methods and the basic setups for sampling and hardening the condensate escaping from the surface of the charge are outlined in Chapter I.

As a rule the results are developed in the form of integral curves of the distribution of particles with respect to volume [G(d)] or directly, in terms of visible size, F(d).

The arithmetic mean diameter or the mean volumetric diameter are frequently used as brief characteristics of the distributions. The volumetric mean size can be calculated by the formula

$$G(d) = \left[\int_0^\infty d^3 f(d)\, dd \right]^{1/3} = \left[\Sigma d_i^3 \frac{N_i}{N} \right]^{1/3},$$

where N_i is the number of particles in the i-interval; N is the total number of particles; d_i is the average size of the particles in the i-interval.

During combustion of metallized condensed systems the agglomeration of the metal particles is influenced by many factors: the nature of the binder and the oxidizer, the concentration and dispersion of the introduced metal, the size of the oxidizer crystals, etc. However, other conditions being equal, the combustion rate of the propellant is the determining factor. Any factor which leads to an increase in the rate of combustion will lead to a reduction in agglomeration of metal particles during burning of the propellant.

The role of individual factors in enlargement of particles of the metallic ingredient on the combustion surface is examined below.

§ 1. Concentration and Dispersion
of Metal Particles

The threshold concentration at which agglomeration effect
begins to be significant is directly dependent on the size of
the particles: the smaller the particles, the earlier agglomer-
ation sets in.

For aluminum powder with an average size d $\leq$ 1 μm agglomera-
tion begins to appear at concentrations of aluminum as low as
<1%; with a volumetric mean size d $\approx$ 10 μm the threshold concentra
tion equals 2-3%. For the 50-70 μm fraction it is increased to
5-7%, while particles with d $\approx$ 160 μm are not accumulated up to
a concentration of 10%.

From Tables 22 and 23 and Fig. 105 it follows, quite definitely,
that the transition from finely dispersed aluminum to large aluminum
is accompanied by an increase in the degree of agglomeration of
the particles. For example, in an ammonium perchlorate and
polyformaldehyde composition with 7% aluminum the formation of
agglomerates equal to the volumetric mean size requires uniting
of approximately 5000 aluminum particles (d $\leq$ 1 μm) - i.e., 2 orders
of magnitude greater than for aluminum for the fraction 5-10 μm
($\sim$70 particles). In compositions with concentrations of Al or Mg
no greater than 20-25% the maximum of agglomeration coincides
with the maximum of concentration of the initial metal. At the
same time, the greater the dispersion of aluminum or magnesium,
the lower will be the volumetric mean size of the agglomerates
which are formed. With increasing distance from the surface of
the charge the size of the fusing particles of metal drops in
the course of combustion, with the effect being the more sharply
evidenced, the higher the initial pressure $\bar{p}$.

Table 23. Dependence of the characteristic size of agglomerates on the dispersion of aluminum in a composition of 85% APC + 15% PMMA + 7% Al[1].

Fractional composition of aluminum, %		Size of aluminum particles, µm		Size of agglomerates, µm		D_{50}/D_{50}^0	D_{90}/D_{90}^0
50→70 µm	fine	D_{50}^0	D_{90}^0	D_{50}	D_{90}		
100	0	62	70	60	92	1.0	1.2
50	50	38	60	50	82	1.3	1.4
1C	90	19	42	41	72	2.1	1.7
0	100	17	28	42	70	2.5	2.5

[1]Sample taken by the setup with a "rotating" drum [248].

§ 2. Effect of Pressure and Combustion Catalysts

With an increase in pressure (Table 24) the volumetric mean size of aluminum particles forming as a result of accumulation on the surface of the charge is reduced. This is not a random effect. Virtually all investigators [172, 173, 203] using various methods to study the behavior of aluminum during combustion of metallized condensed systems note that the size of particles escaping from the condensed phase into the gaseous phase drops with a growth in pressure.

Table 24. Effect of pressure on agglomeration of aluminum in an APC + polyester + 7% Al mixture (D_{50}^0 = 16 µm, D_{90}^0 = 28 µm).

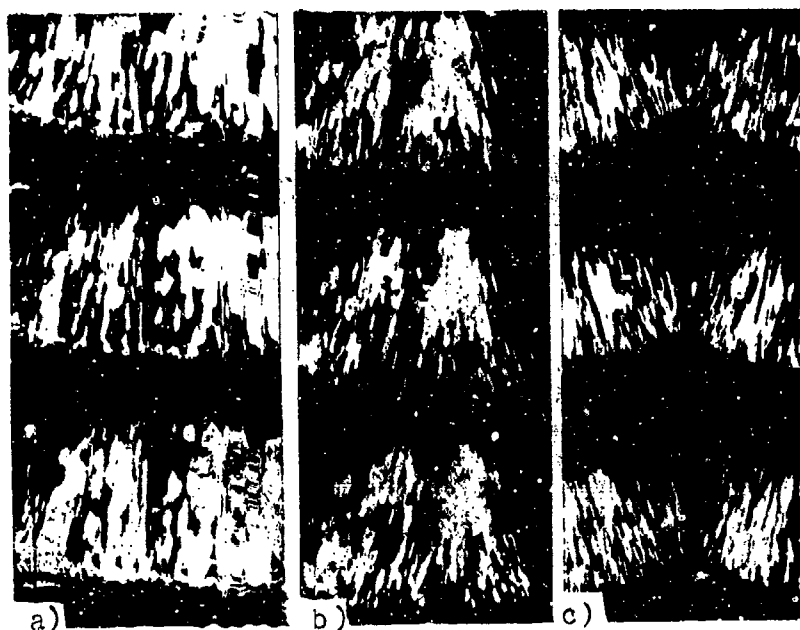| Pressure, atm	Agglomerate size, µm		D_{50}, D_{50}^0	D_{90}, D_{90}^0
	D_{50}	D_{90}		
1	40	60	2,35	2,15
20	30	40	1,75	1,43
40	19	32	1,2	1,4

PRECEDING PAGE BLANK

Fig. 106.   Surface of a metalized powder
(20% aluminum).   a) 1 atm; b) 15 atm;
c) 30 atm.

From Fig. 106 it is clear that enlargement of particles occurs directly on the surface of the burning composition. The quantity and size of glow sites increases with an increase in pressure p. At high concentrations of Al or Mg and high p the impression is created that the surface consists solidly of brightly glowing points. The appearance of the condensate itself is extremely interesting. At pressures of 2-20 atm this is made up of large agglomerates of particles which are joining together with each other and with heat-resistant products of the decomposition of nitrocellulose. They have an irregular shape (Fig. 107, a-g). At p = 60 atm their shape becomes almost spherical. Besides the relatively large particles there is a large quantity of smaller particles, 2-3 μm in size. Individual cracks and even extremely fine defects are visible on the surface of the large particles (200-400 μm) [173].
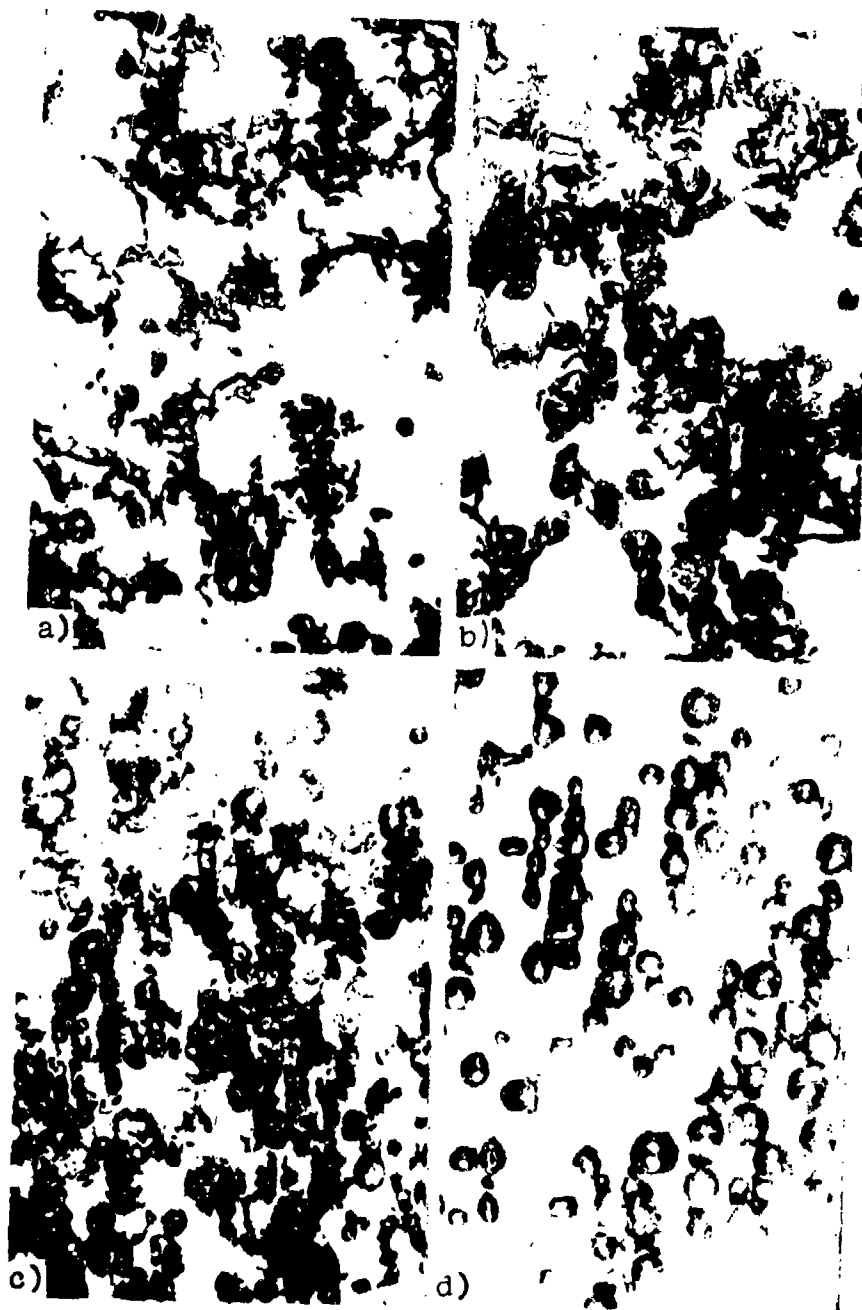
Fig. 107. Condensed products from the combustion of metallized powder $H(d_{Al} = 1{-}40 \ \mu m)$

10% Al: a) 2; b) 10; c) 25; d) 60 atm.
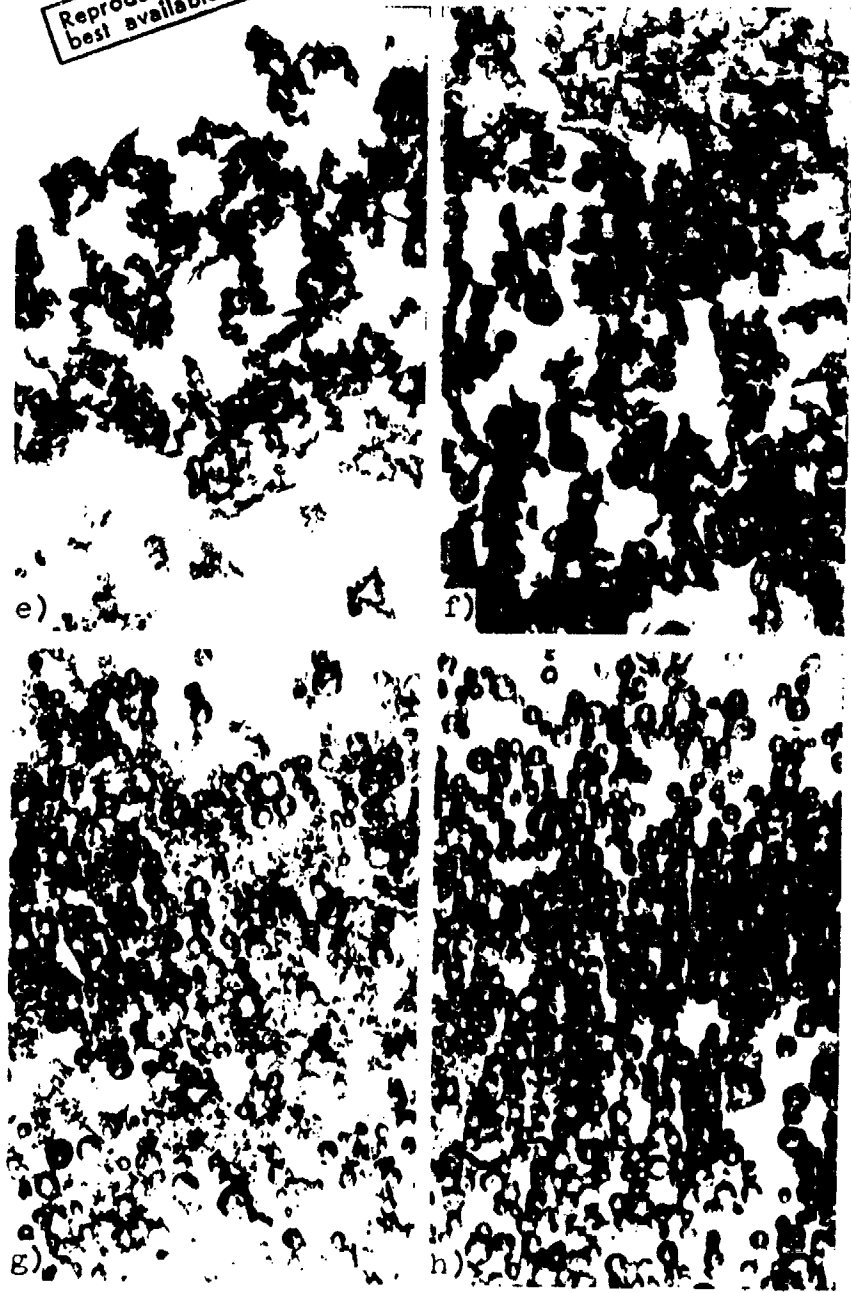20% Al: e) 2; f) 10; g) 25; h) 60 atm.

Fig. 107 Cont'd.

These same photographs emphasize once again the quantitative differences examined above, arising during a change in the degree of dispersion [248] (see Table 23).

With an increase in pressure from atmospheric up to 40 atm the volumetric mean diameter of the agglomerates for a composition with 7% Al (Table 24) is reduced by more than half [172, 174, 204].

Povinelly and Rosenstein [203] note that for polybutadiene-acrylonitrile propellants studied by them the degree of agglomeration of aluminum on the combustion surface was reduced in proportion to $p^{-0.3}$ (Fig. 108). The authors characterize the effectiveness of the agglomeration process by the percentage of particles which exceed the initial aluminum in size. For convenience they introduce coordinates in which the function of distribution of aluminum particles by diameter is linear (Fig. 109).
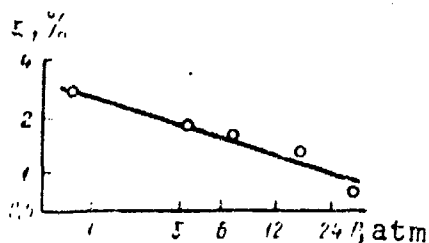
Fig. 103. Degree of agglomeration ξ as a function of p.
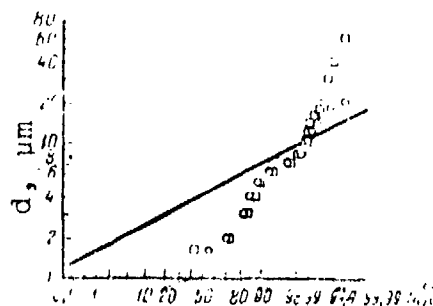
Fig. 109. Degree of agglomeration at 15 atm (d – particle diameter; N – number of particles).

For the overwhelming majority of powder mixtures a growth in pressure (especially in the low-p interval) is inextricably connected with an increase in the linear rate of combustion V. However, combustion rate is a factor which in itself is capable of rendering a definite influence on the nature of the behavior of a metallic additive and the length of time it is located on the burning surface. This change in the burning rate is primarily a change in the mass flow rate of removal of gaseous products of

decomposition from the burning surface; these products arc the basic cause of removal of particles from the surface of the condensed phase [173, 174].

According to the continuity equation

$$U_{\kappa}\rho_{\kappa}S_{\kappa} = U_{r}\rho_{r}S_{r}$$

(the subscripts r and κ designate the gaseous and condensed phases, respectively). Since $V_{\kappa} \sim P^{\nu}$ for the surface of combustion, with an increase in $P(S_{\kappa} \cong S_{r})$ there is a proportional growth in the flow rate $U_{r}\rho_{r}$; consequently the force acting to remove a particle is increased. Examination of a model of the escape of an aluminum or magnesium particle to the surface during combustion of a model composition with consideration of the forces acting on the particle indicated that a "leg" 10^{-6} cm in radius between the surface of the charge and the particle of the metal, consisting of the liquid phase of the reaction layer, is sufficient for the particle to remain on the surface of charge combustion at the existing velocities of outflow of the products from combustion of the powder. Tracing the mechanism by which the size of agglomerates depends on the combustion rate without changing other parameters of the propellant is extremely difficult. As a rule this is inevitably connected with a change in pressure, composition, or degree of dispersion of the components of the propellant. Therefore a method was selected which satisfies the condition of a constant level of the majority of the propellant parameters. It consists in a change in the gravitational density of the specimen. It is known from numerous works [283, 284] on combustion of heterogeneous condensed systems and powders that the rate of combustion of pressed compositions grows with a reduction in charge density. Under certain conditions (high pressures and low densities) combustion can develop right up to detonation modes. In the pressure range 1-50 atm and the range of relative densities

Δ = 0.7-1.0 combustion occurs at a rate which is virtually constant, but elevated. For a PF + APC + 7% Al (d = 5-10 μm) system a change in density from ρ = 1.69 to a value of ρ = 1.37 g/cm^3 at a pressure of 30 atm will lead to growth in the normal rate of combustion from 5.8 to 7.6 mm/s. This is equivalent to a change in the mass flow rate of the gas outflow from 0.98 to 1.04 $g \cdot cm^2/s$. Actually, with an increase in a burning rate the volumetric mean size D_{50} of the aluminum particles (h $\approx$ 0.5 mm) is reduced from 32 to 21 μm - i.e., by one third.

It is clear that any factor which leads to an increase in the rate of burning of a solid propellant (catalytic additives, pressure, type of oxidizer) should reduce the degree of enlargement of the particles. Thus, during experiments with a binary mixture of APC + 10% aluminum (D_{50}^0 = 60 μm) at 60 atm the size of the agglomerates forming on the burning surface of the perchlorate as a result of accumulation of fine particles reached 1-2 mm. With addition of 2% of the catalyst Cu_2O into this binary composition the size of the particles was reduced to 0.1-0.5 mm. The effect of cuprous oxide on the thermal decomposition and burning rate for compositions based on APC has been more or less definitely established [156].

Thus, the reduction in the degree of agglomeration in the given example is also confirmation of a positive role of burning rate (rate of decomposition) of the composition in the formation of agglomerates.

§ 3. The Role of the Fuel
and the Oxidizer

Figure 110 and Table 25 show integral curves of the distribution and characteristic dimensions of aluminum particles and particles of condensed combustion products from a number of investigated compositions based on ammonium perchlorate. The initial aluminum had D_{50}^0 = 16 μm and D_{90}^0 = 28 μm.
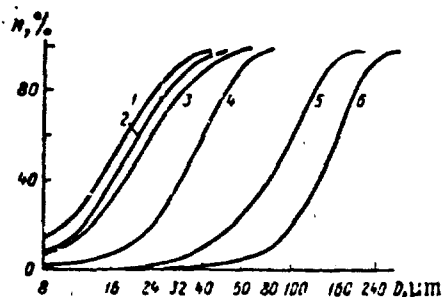
Fig. 110. Integral curves of the volume distribution of particle agglomerates of Al in compositions: 1 - Initial Al; 2 - 7% Al + 15% polyester; 3 - 8% Al + 10% PMMA; 4 - 10% Al + + 40% H; 5 - 10% Al + 20% PF; 6 - 20% Al + 20% PF.

These data once again clearly emphasize the influence of aluminum concentration in the composition on the degree of agglomeration. But at the same time they indicate that the fuel-binder is by no means the last thing to be considered in this question. It is difficult to explain the almost twofold difference in distributions between the first and second or the third and fourth compositions - for example, differences in burning rates. Thus, as we saw earlier, this is also important.

Table 25. Characteristic sizes of agglomerates on compositions with different fuels (P = 40 atm, D_{50}^0 = 16 μm, D_{90}^0 = 28 μm).

No.	Fuel	Aluminum concentration, %	Size of agglomerates, μm	
			D_{50}	D_{90}
1	Polyester, 19%	7	18	35
2	Polymethyl methacrylate (PMMA), 15%	7	33	56
3	Ballistite (chip), 20%	10	54	80
4	Polyformaldehyde (PF), 24%	10	120	185
5	Polyformaldehyde, 24%	20	240	350
6	Powder II, 90%	1°	-	300

282

The role of the binder and the oxidizer was studied in more detail in works [173, 174]. Typical pressed compositions based on $KClO_4$ and NH_4ClO_4 as oxidizers and polymethyl methacrylate, polyformaldehyde, carbon (carbon black), and naphthalene were studied (Table 26).

Table 26. Volumetric mean size D_{50} of agglomerates forming during combustion of mixed and ballistite compositions.

Composition	Percentage of additive	Size, μm		
		5 atm	20 atm	40 atm
NH_4ClO_4 + polymethyl methacrylate	10	48	41	32
	20	67	58	46
NH_4ClO_4 + polyformaldehyde	10	46	41	35
	20	51	47	42
NH_4ClO_4 + naphthalene	10	190	150	100
	20	300	240	180
NH_4ClO_4 + carbon + 0.5% paraffin	10	210	180	110
	20	320	270	200
$KClO_4$ + polymethyl methacrylate	10	–	34	21
	20	–	48	37
$KClO_4$ + polyformaldehyde	10	–	30	27
	20	–	36	31
$KClO_4$ + naphthalene	10	–	90	60
	20	–	150	105
$KClO_4$ + carbon + 0.5% paraffin	10	–	120	80
	20	–	170	130
Nitroglycerin composition	10	Aggregates	120	90
	20	–	200	140
Pyroxylin composition	10	Aggregates	165	110
	20	–	250	180

Potassium perchlorate falls in the class of oxidizers which melt during combustion; APC is, for the most part, decomposed during burning (sublimates), with a very thin molten layer (2-3 μm) [201]; carbon is a nonvolatile, nondecomposing, nonmelting fuel; naphthalene is a fuel which melts but is highly volatile (easily sublimated); polymethyl methacrylate and polyformaldehyde melt with the composition during burning. In order to retain a constant level of the ratio between fuel and oxidizer aluminum was introduced in a quantity above 100%. Sampling of the condensed products was carried out 0.5 mm from the surface of charge combustion by the electromagnetic method [172-174].

First of all in mixed compositions with identical fuels the dimensions of agglomerates are in all cases greater on ammonium perchlorate than on potassium perchlorate. This is true independently of the aluminum concentration. Secondly, such polymer fuel-binders as polymethyl methacrylate and polyformaldehyde differ sharply (3-4 times) from the fuels naphthalene and carbon in terms of the degree of effect on enlargement of aluminum on the surface of combustion. Thirdly, there is a definite difference between mixed and ballistite compositions. With identical concentrations and degrees of dispersion of the metallic powder, ballistites form larger particles during combustion than the mixed propellants. In individual cases agglomerates reach 1.0-1.5 mm in diameter, despite elevated pressure (Fig. 111). One reason for the increased potential for agglomeration is the formation of filament-shaped carbon black aggregates on the surface of the molten layer of the charge. This, in particular, explains the high agglomeration on ballistite and pyroxylin powders.

During combustion of pyroxylin compositions a significant quantity of carbon "threads" (more than during combustion of nitroglycerin compositions) will be formed on the surface. Representing unique centers for grouping of metal particles, which are comparatively mobile on the molten surface, they are

dispersed together with the latter into the high-temperature
zone of the flame. In this zone the particles of aluminum are
fused together, forming large agglomerates of the type which
are demonstrated on Fig. 111.[1] Extremely large particles are
also formed when ballistite powder is used in combination with
APC (see Table 25).
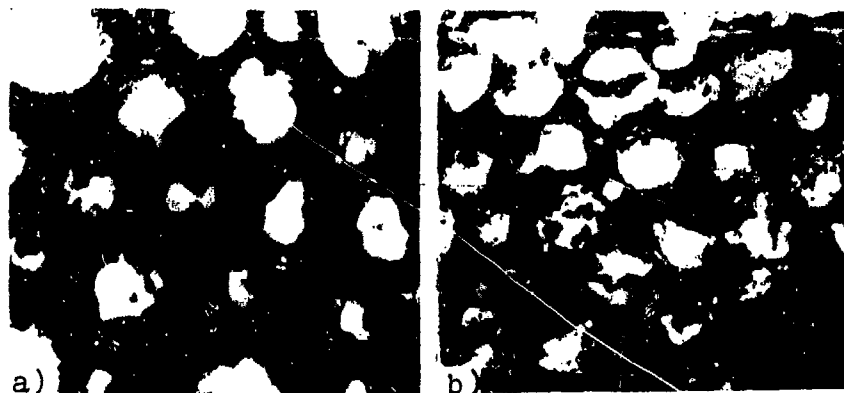
Fig. 111. Agglomerates of aluminum particles
of ballistite (a) and mixed (b) compositions.

But the property of formation by the components of a liquid
phase during combustion is not a determining factor in all cases.
Potassium perchlorate melts, but the degree of enlargement of
aluminum particles during combustion of mixtures based on it is
lower than that for equivalent compositions based on APC.
Apparently a decisive role is played here by differences in the
combustion rate. Other conditions being equal, mixed compositions
based on PPC usually burn at a higher rate than those based on
APC.

_____

[1]It must be noted that the rate of combustion of pyroxylin
powders is lower than that of nitroglycerin compositions.

The experimental material available at present does not allow us to draw final conclusions concerning the role of the physicochemical properties of the fuel and oxidizer in the process of enlargement of metal particles on the surface of the burning powder. However, there is no question that they influence the process of enlargement of metal particles. This influence is manifested through the rate of normal combustion, the phase state of the surface of combustion, volume concentration, ability to decompose with the formation of gaseous products, etc. For example, a composition of $NH_4ClO_4 + C + 20\%$ Al at a pressure of 40 atm burns at a rate of 0.8 cm/s, while the composition NH_4ClO_4 + polyformaldehyde + 20% Al at 20 atm burns at a rate of 0.75 cm/s - i.e., they are very similar with respect to rate of combustion. However, the degree to which particles of aluminum are joined together in the first composition is approximately 60 times higher than that in the second. The fact is that, apparently, in contrast to carbon the polyformaldehyde, despite melting, is almost completely gasified during combustion. The active liberation of gas during decomposition favors dispersion of condensed substance from the liquid-phase reaction layer. Control experiments in heating binary mixtures of polyformaldehyde and aluminum and polystyrene and aluminum on molten aluminum plates confirm the fact that melting, vigorous decomposition, and foaming of these compounds occurs in the temperature interval 200-350°C, with a clearly expressed process of dispersion of the material. The deposits remaining after the experiment comprised 40-60% by weight of the aluminum imbedded in the specimen.

With heating of a mixture of carbon + 0.5% paraffin + + aluminum no changes of any kind were observed up to 1000°C. In all probability in combination with an oxidizer carbon plays the same role as formations of carbon black on the surface of ballistite powders.

It must be emphasized that compositions with a gasifying fuel possess a higher degree of gas formation (per unit volume of substance) than compositions with fuels which are not gasified or gasify only poorly (carbon type); this unquestionably favors more active removal of condensed particles into the gas phase before they can join together.

Comparison of Tables 25 and 26 reveals at first glance certain contradictions: the mean volumetric size of agglomerates with one and the same concentration of aluminum in a PF-APC composition is significantly higher in the first case than in the second. In actual fact the contradiction is only apparent. These compositions differ with respect to degree of dispersion of the oxidizer (it is larger in the first case) and in the type of polyformaldehyde (the polymer has different molecular weight). Besides this, the indicated data were obtained by different sampling methods and at inadequate distances from the surface of combustion.

§ 4.   Dispersion of Components

The degree of dispersion of components of polymerized compositions is determined mainly by the dimensions of the oxidizer particles. The same thing can be said of pressed compositions, since in these the particles of the fuel are, as a rule, substantially smaller than those of the oxidizer.

As the oxidizer is enlarged the degree of agglomeration grows sharply. With an increase in APC particle diameter from 5-10 to 100-200 μm the size of agglomerates is practically doubled. The effect of enlargement of aluminum with a growth in oxidizer particle size was also noted in work [203] (degree of agglomeration was increased by 2%). An increase in pressure smooths the difference slightly. The final size of agglomerates depends not only on the degree of dispersion and the fractional composition of the system, but also is influenced by the method used to prepare the mixture.

One and the same mixture (10% PMMA) was prepared by two different methods: by the usual mechanical mixing of the components in a rotating drum or by the "gelling" method, which consists in introducing the aluminum and the oxidizer into a previously prepared solution of fuel in dichloroethane. After evaporation (with careful agitation) of the solvent an extremely uniform mass is formed. The fuel surrounds particles of aluminum and of APC in a very thin layer.

During combustion of specimens of the "gelled" composition (7% Al) the characteristic size D_{50} and D_{90} of the agglomerates was a third less than specimens of a mixture prepared by the usual method:

	D_{50}, μm	D_{90}, μm
"Gelled"	34	58
Mechanical mixing	58	81

§ 5. "Blasting" of the Surface
of Combustion

Structures of combustion chambers for rocket engines are designed in many versions for channel burning of solid-fuel charges. In such engine structures a high-temperature gas flow of variable velocity exists along the burning surface. The magnitude of velocity can, under certain conditions, reach a value such that the flow begins to act directly on the surface of the condensed phase. The mode of "erosion" combustion appears [4]. The rate of charge combustion becomes different from the rate of normal combustion and is a function of the velocity of the flow.

Since the effect of enlargement of metal particles occurs on the surface of the charge, the presence of a transverse flow is one of the factors which influences agglomeration.

288

Povinelly and Rosenstein [203] indicate that at a velocity of approximately 60 m/s on compositions with a coarse oxidizer the transverse flow increases the number of particles which surpass the initial particles in size by about 2 times. Applying the method of sampling condensed combustion products by the "slit charge" setup [283], we obtained a blowing velocity 10-15 times higher.

The velocity of the transverse flow of high-temperature products from combustion of the investigated composition, averaged along the length of the charge and in time, exceeded 100 m/s in the general case. An important point is the fact that in this case the flow is two-phase, since a high percentage of heterogeneous particles is present in it.
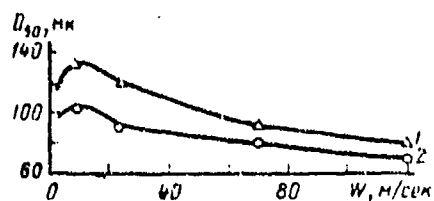

Fig. 112. The quantity D_{50} as a function of the velocity of a gas flow.

Designations: мк $= \mu m$, м/сек $= m/s$.

The point on the ordinate (Fig. 112) corresponding to a zero blowing velocity $W = 0$ (time for sampling and hardening of particles 70-100 μm and less in diameter is 1 ms) was obtained during end-burning of a flat specimen. Curve 1 corresponds to experiments in which the distance from the cut of the "slotted" specimen to the surface of the quenching liquid in the sampling instrument equals 3 mm; curve 2 – h = 30 mm. In terms of time this is equivalent to ∿1 and ∿4 ms, respectively. The time difference between curves 1 and 2 comprises 0.5-3 ms, depending on the interval of velocity W.

With an average velocity W on the order of 15 m/s the volumetric mean size D_{50} passes through a maximum; a further increase in velocity leads to a reduction in the size of agglomerates. In the

289

considered example the integral curves of distribution of particles obtained during end burning (W = 0) and during blasting of the surface of a burning specimen by a flow at ~100 m/s virtually coincide.

This result is of interest from another point of view. It means that at the initial moment, when the agglomerate escapes from the surface of combustion and enters the gaseous phase, it is burned out at a rate which exceeds the rate of combustion of aluminum.

§ 6.   The Effect of the Properties
of the Metal

The phenomenon of agglomeration is characteristic for combustion of virtually all metallized compositions with an increased concentration of metallic particles. It is also noted on magnesium compositions and on powders containing particles of boron, beryllium, etc. Table 27 gives the results of studies of the degree of agglomeration of particles during burning of a APC-polyformaldehyde-magnesium composition.

Under completely identical conditions of burning, sampling, and hardening of the condensate the size of agglomerates in compositions with Mg is noticeably smaller than for aluminum. With increasing distance from the surface of the specimen the degree of dispersion of agglomerates is rapidly reduced and at a distance of 5 mm the volumetric mean diameter falls in the limits 1-2 μm.

As in the case of compositions with addition of aluminum, for compositions with magnesium we observe a dependence of the volumetric mean size of particles formed as a result of accumulation of powder on the surface on pressure (rate of combustion of the charge) and on the percentage addition of the metal.

290

Table 27. Volumetric mean size of magnesium particles formed during combustion of the composition APC-PF-Mg ($d_0 \leq 1.5$ µm).

Pressure, atm	Distance from surface of charge, mm	Addition of Mg, %	Size of particles, µm
1	0.5	7	18
	0.5	20	23
30	0.5	7	11
	0.5	20	16
1	5	7	3
	5	20	6
30	5	7	1.0
	5	20	2.0

However, the degree of fusion of particles is less for magnesium than for aluminum. Thus, for example, for the composition APC + polyformaldehyde + 20% Mg ($a \leq 1.5$ µm) with $p = 30$ atm the volumetric mean size of particles $D_{50} = 16$ µm (see Table 27), while with an analogous composition with 20% Al ($d \leq 1$ µm) under the same experimental conditions $D_{50} = 22$ µm. The interaction of the particles and all of the processes which influence agglomeration in one way or another occur on the surface of the specimen and mainly prior to particle ignition.

Magnesium has a melting temperature which is virtually identical with that of aluminum, but the ignition temperature is lower and it also has a small period of preignition heatup. Besides this, compositions with additions of magnesium have a higher burning rate than those with aluminum (at identical percentage contents and identical particle size). Therefore in this respect the fact that agglomeration is less expressed as compared with particles of aluminum is a fully understandable factor.

§ 7. Structure of Agglomerates

The process of agglomeration frequently leads to the formation of large particles on the surface of charge combustion; the size of the particles exceeds the largest particles of initial metal powder by an order of magnitude. This problem is quite important, since it can determine the effectiveness with which metallized compositions are utilized in combustion chambers. The time of combustion of metal particles, as is known, is a function of their diameter.

Whereas large agglomerates are uniform in terms of structure and have exclusively metallic base, their incomplete combustion in installations or rocket engines can bring to naught the entire positive energy effect achieved by the application of a metallic powder in the fuel. However, as was first established on ballistite powders [172, 173] and later studied in more detail on mixed compositions [248], agglomerates are not uniform. Individual large particles collected from the surface of combustion of an aluminized charge were sintered for several hours at 350-500°C. This temperature interval was deliberately selected below the melting point of pure aluminum and its oxide, but higher than the decomposition temperature of the remaining components of the mixture. In the case when the latter are present in agglomerates they should be decomposed during sintering and thus should reduce the strength of the investigated particles. The experiments showed that agglomerates held at a high temperature are very easily crushed and broken down into much smaller particles.

The second method used for qualitative analysis of the structure of agglomerates was to evaluate their average density. For this purpose agglomerates ($d > 100$ µm) preliminarily separated into individual fractions were selected and packed into cylindrical specimen holders under a pressure $p \sim 4000$ atm. At such a pressure

ammonium perchlorate and the polymer fuel are packed to a relative density virtually equal to 1.0, while aluminum powder is packed to an absolute density of 2.62 g/cm^3. It was found that the average density of specimens pressed in this way does not exceed 2.1 g/cm^3.

Both of these facts indicate that the composition of large agglomerates contains, besides aluminum and its oxides, a significant quantity of substances with lower density. Such substances can only be incompletely decomposed fuel ($\rho \sim 1.0$ g/cm^3) and APC ($\rho = 1.96$ g/cm^3) or nitrocellulose.
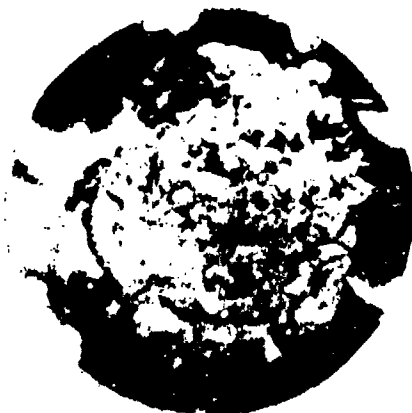
Fig. 113. Internal structure of a large agglomerate.

Cutting sections of the largest individual agglomerates (Fig. 113) clearly confirms the nonuniformity of the structure. In fact some of them have an internal cavity. In view of this measurement of the density of individual particles by the methods used in the case of dispersed media is always connected with a probability of error. By using the developed procedures we are able to evaluate the fraction of aluminum in the agglomerates.

The procedure developed to investigate the combustion of single particles of metal [154] was used to measure the combustion time of individual agglomerates in a flow of products from the combustion of a known composition. Subsequently the laws

combustion of individual particles (IV.2) and the measured
combustion time were used to calculate the "effective" diameter
of the agglomerate, D_{eff}. Thus the diameter of an aluminum
particle for which burning time under the given conditions is
identical to that of the agglomerate is taken as the "effective"
diameter of the latter. The ratio of the "effective" diameter
D_{eff} to the initial diameter of the particle D_0 characterizes the
fraction of aluminum in the agglomerate, in the first approx-
imation. Results of individual measurements are presented in
Table 28.

Table 28. Combustion time τ_r and "effective" diameter of agglom-
erates.

Size of ag-glomerates, D, µm	Burning time of agglomer-ates, ms	Burning time of aluminum particles, ms	"Effective" diameter of agglomerates, µm	Fraction of aluminum in the agglom-erates $(D_{eff}/D)^3$
50	4.8	6.0	43	0.63
80	7.8	12.0	57	0.36
120	12.6	22.0	83	0.33
160	19.0	34.0	108	0.30
200	25.0	45.0	130	0.27

The first column of the table gives the initial dimensions
of the agglomerates, while the second contains the experimentally
measured combustion times. For comparison the third column gives
the time required for complete combustion of aluminum particles
equal in size to the agglomerates. The combustion time for the
agglomerates is noticeably less than that for analogous aluminum
particles, with the difference being the greater the larger the
size of the agglomerates. The fourth column gives the "effective"
diameters of agglomerates as calculated from their combustion
time. It is clear that in large agglomerates (diameter greater
than 80 µm) the fraction of aluminum does not exceed 40% and is
reduced with an increase in agglomerate diameter. Combustion
time of the agglomerates depends on the quantity of aluminum

294

contained in them. Such an evaluation is, of course, approximate, since it is impossible to identify combustion time of solid aluminum particles completely with the time required for complete burning of the aluminum out of agglomerates which possess a complex structure.

Thus, although agglomeration leads to a noticeable increase in combustion time, direct utilization of the dimensions of formed agglomerates for evaluation of τ_r can lead to very substantial errors.

§ 8.   The Physical Nature of
of Agglomeration

Analysis of photographs of propellant combustion surface shows that agglomeration of aluminum is realized in both ballistite and mixed propellants basically by accumulation, although the presence of growth of agglomerates of aluminum by means of collision is also noted (but in a substantially lower degree).

From works [195, 196] we know that in the initial stage of burning of powders decomposition of a small portion of the composition into gaseous combustion products occurs in the reaction layer of the condensed phase. A large part of the condensed material of the reaction layer is dispersed with the formation of a smoke and gas mixture. During combustion of ballistite compositions a "grid" of threadlike aggregates is formed on the surface; these consist predominately of carbon. These heat-resistant products are, as it were, centers for grouping and cementation of particles, leading to their accumulation.

On Fig. 107 we can see aggregates of aluminum particles adhering to one another and to carbon-rich heat-resistant products of the decomposition of nitrocellulose. The adhesion of a substantial quantity of aluminum particles to particles of carbon

black occurs on the surface of the composition with the formation of a grid, after the destruction of which its individual bits (aggregates) are carried off by the gaseous combustion products. In the low-pressure region p < 20 atm (Fig. 107, a, b, c, e, f, g) and, consequently, at low combustion temperatures at which complete combustion of the ballistite composition is not achieved the aggregates have an irregular shape and arbitrary dimensions.

At $p \geq 60$ atm, when complete combustion is achieved (Fig. 107), particles of spherical shape are formed. Cracks and other defects are visible on large round particles (whose dimensions reach 250-300 μm). The particles are dark in color due to the presence of carbon black.

Since the temperature on the surface of ballistite compositions is less than half the melting point of aluminum and magnesium, particles of these metals are found on the surface in the solid state.

Gaseous products of decomposition of the powder flowing away from the specimen surface carry off agglomerates into the high-temperature gas phase. Here the agglomerates are melted and become spherical, while the individual particles of metal in them are blended together into larger sizes.

Thus, the process of enlargement of metallic particles in compositions similar to ballistite powders occurs in two stages. The first stage is adhesion of the particles with products of decomposition of the condensed phase, while the second stage is their fusion close to the surface of the charge in the gaseous phase. During burning of mixed compositions, if the temperature of the burning surface is lower than the melting temperature of aluminum and if the components form a solid molten layer in the course of decomposition, we can regard such a mechanism of agglomerate formation as one of the most probable.

High-speed cinephotography of the burning surface gives a clear idea of the processes occurring on it. With a proper magnification factor it is possible to note that particles are rotating and move, coalescing with neighboring particles and being carried into the gas phase. On these same frames individual particles remain in place for several milliseconds after emergence on the surface, virtually unchanged in diameter, and then are immediately thrown out into the flow (Table 29).

Table 29. Average size and duration of stay of agglomerates on the surface of the charge.

Composition	Particle size, μm	Pressure, atm	Average agglomerate size, μm	Average stay time of agglomerate, ms
Powder H + 2% Al	1	10	400	-
Powder H + 10% Al	1	10	1000	23
The same	1	40	250	10
The same	40-70	40	400	-
Mixed composition	-	80 mm Hg	230	5-7
The same	-	5	80	1-2

If the temperature of the composition surface exceeds the melting temperature of the metal the process of adhesion of particles can begin directly on the surface of the charge [172].

The possibility of fusion and adhesion of individual drops of aluminum with a temperature of the surface which equals or exceeds the melting point of aluminum and despite the presence on them of a refractory oxide film was demonstrated in work [241]. Figure 38 clearly demonstrates that growth of particles occurs on points where the oxide shell is fractured and the surface of the pure aluminum is exposed. Cracking of the shell during heating of particles occurs because of differences of thermal coefficients of volume expansion for aluminum and its oxide.

297

An analogous idea of the enlargement of aluminum particles
on the surface of the grain by their motion and mutual collision
was developed in work [203]. According to results in this work
the average speed of travel of particles and the degree of their
agglomeration are reduced with a growth in pressure in proportion
to $p^{-0.3}$. It is postulated that the appearance of the phenomenon
of partical agglomeration requires fulfillment of two conditions;
first of all the time during which the particle remains on the
surface of combustion must be greater than the time required for
the particles to adhere and, secondly, agglomeration time must be
less than the combustion time of the particles.

Using several assumptions concerning the nature of combustion
of aluminum particles, their distribution in the powder composition,
and a number of assumptions (surface temperature independent of
pressure, proportionality of the speed of motion of particles
to the burning rate of the fuel, etc.), the authors obtained an
expression which permits calculation of the critical aluminum-
particle diameter necessary for the appearance of agglomeration.

Thus, according to the calculations in the case of the
fuel RVAA + NH_4ClO_4 + 9% Al the aluminum particle diameter required
for agglomeration is 3.5 µm at atmospheric pressure and 6.5 µm
at a pressure of 30 atm. However, despite the apparently good
coincidence of experimental and theoretical data the proposed
criterion does not explain the laws governing the phenomenon
of agglomeration given above.

During combustion of heterogeneous metallized compositions
with binders which are poorly gasified, a somewhat different
method of formation of agglomerates is possible; this was proposed
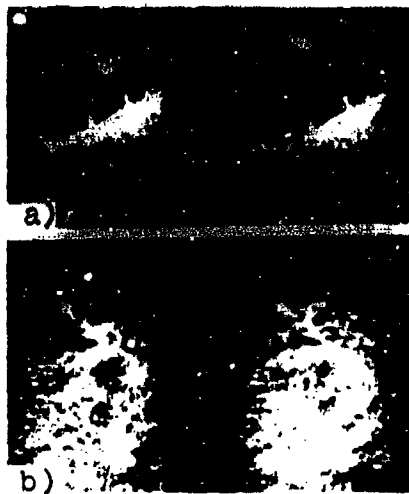by Belyayev, Frolov, and Korotkov [248].

Fig. 114. Cineframes of the surface
of a burning specimen with 15%
aluminum, taken with triple (a) and
sevenfold (b) magnification.

Figure 114 shows frames from motion pictures of the surface
of a burning specimen containing 15% finely dispersed aluminum.
Large agglomerates in the form of "flakes" with a flat irregular
shape are visible on them, flying away from the surface of the
specimen. Against the general background of "flakes" individual
bright spots of aluminum particles can be singled out. These
particles are separated from one another by the basic substance
of the agglomerates. The large "flakes" or agglomerates can
remain close to the surface of burning for a comparatively long
time, still connected to it by thin connectors - "legs."
During this period finer particles, which escaped previously from
the surface of combustion, can adhere to them.

Only small transverse displacements of the flakes are
recorded at the moment of separation from the surface. Upon
entering the high-temperature zone of the jet the agglomerates
melt rapidly and take on a spherical shape. At this moment cavities
can be formed inside the agglomerates. Other conditions being
equal, the size of the agglomerates depends on the ability of the
fuel to decompose and melt during pyrolysis. If the "flake"
agglomerates are sufficiently large and if the sampling and
hardening time is small, their surface will have noticeable
roughness and irregularities (see Fig. 111).

299

As was noted earlier, condensed systems have an unordered nonuniform structure and consist of crystals of oxidizer separated by gaps which are filled with the polymer fuel containing particles of metal (aluminum, magnesium). The greater the fraction of APC the thicker will be the interlayer of fuel and the greater the amount of aluminum in it. The latter fact also depends on the degree of dispersion and concentration of the powder metal, on the uniformity of component mixing, and on the density and concentration of the fuel.

In the general case the rate of decomposition of the fuel and the APC will be different. The decomposition process occurs most rapidly along the boundary of contact between the components. Under certain conditions the rate of propagation of the combustion front is wholly determined by the average rate of propagation of the "tips" between the fuel and oxidizer [156]. In view of this individual segments of fuel containing aluminum burn gradually on all sides at points of contact with crystals of APC, break away, and are carried off by the flow of gaseous products leaving the surface. In a high-temperature oxidizing medium the fuel is subjected to rapid pyrolysis, opening the way for direct interaction and ignition of the particles of metal included in the agglomerate. With an increase in pressure the thickness of the heated layer of propellant is reduced and the rate of decomposition of the components is increased. This results in a reduction in the size of agglomerates. Naturally, the two considered versions are not only not mutually exclusive but, just the opposite, they supplement one another.

Thus the mechanism for enlargement of metal particles during combustion of metallized solid fuels and explosive proposed by the authors of [172-174, 248] and involving their accumulation on the burning surface of the propellant grain and subsequent accumulation and adhesion to heat-resistant products from decomposition of the binder makes it possible to explain all of the basic laws governing the phenomenon of agglomeration.

300

CHAPTER VI

COMBUSTION OF POWDERS WITH POWDER-LIKE METAL ADDITIVES

§ 1. Combustion of Metal
Particles in Powder Compositions
[285]

Flameless combustion represents the initial combustion stage for powders and occurs in a virtually isolated form under vacuum conditions. Stability in flameless combustion results from the thermal effect of reactions which occur in the reaction layer of the condensed phase [195, 196]. It is evident that if the metal particles react during flameless combustion of metallized compositions, then this will be reflected in the heat effect of the reactions which occur in the reaction layer of the condensed phase (k-phase).

From results obtained in igniting solid fuels it was found that in order to achieve combustion of compositions in a vacuum ($p = 10^{-2}$ mm Hg) the specimen must first be heated to a certain temperature T_U. If we know the preheating T_0 and the temperature on the surface of the specimen $T_{пов}$ in flameless combustion, then we can estimate the thermal effect Q of the total exothermal process in the reaction of the k-phase:

$$Q = \bar{c}_p (T_{пов} - T_0).$$

where $\bar{c}_p = 0.4$ cal/g·deg is the average heat capacity of the substance.

It was established that ballistite powder burns steadily and flamelessly when preheated to $T_0 = 110°C$, a pure mixture of polyformaldehyde and ammonium perchlorate [APC] (ПХА) - to $T_0 = 200°C$. Quantity $T_{пов}$ of these compositions is equal, respectively, to 300 and 480°C.

In the case of flameless combustion of ballistite powders with aluminum added the surface temperature remains practically the same (T = 280-290°C) as for the ballistite powders without the metal additive. The aluminum particles ignite and burn not on the surface of the powder, but in the smoke-gas zone of the flame near the surface of the charge.

Flameless combustion of mixed powder with aluminum, magnesium, and their alloys added (50/50) is accompanied by a steady increase in $T_{пов}$ in proportion to the increase in the concentration of the metal up to 20% (115). At the same time $T_{пов}$ is increases in proportion to the decrease in the particle size of the metal which is added to the solid rocket propellant [SRP] (TP]). The AFC/PF composition with 5% Al and above and a diameter of $d \leq 1$ μm, when heated to 200°C, burns at a very rapid rate (with an explosion), which does not enable correct measuring of the $T_{пов}$ value. The growth of $T_{пов}$ is accompanied by an increase in the amount of heat (Fig. 116) which is released as a result of the oxidation reactions of Al, Mg, and the aluminum-magnesium alloy, and this oxidation also increases with an increase in the percent of the additive, reaching 40% for Mg (d = 1-10 μm), 35% for Al/Mg (50/50) (d = 10-100 μm), and 25% for Al (d = 20-60 μm) in relation to the total amount of heat release in the k-phase. The great reaction capacity of magnesium in the k-phase as compared to the aluminum is caused by differences in the oxide film properties of Al and Mg (see Chapter 1).
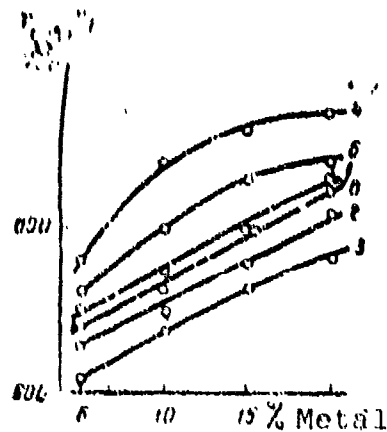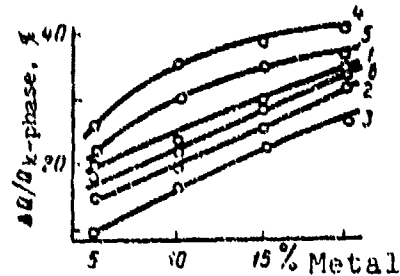
Fig. 115.   Fig. 116.

Fig. 115. Surface temperature ($T_{пов}$) as a function of concentration of metal in powder: Particle size (in μm): For Al: 1 - 5-10; 2 - 12-15; 3 - 20-60; Mg: 4 - 1-10; 5 - 80-90; Al-Mg (50/50); 6 - 10-100.

Fig. 116. Ratio of heat release during oxidation of metal to total amount of heat released in k-phase: Particle dimension (in μm): For Al: 1 - 5-10; 2 - 12-15; 3 - 20-60; Mg: 4 - 10;] 5 - 80-90; Al-Mg (50/50); 6 - 10-100.

Figure 117 shows the ratio of heat released through the oxidation of the metal in the k-phase to the total heat which is realized in complete combustion of the metal in the powder. There is a maximum for all studied compositions in the additive range of 10-13%, where in the k-phase 3-4% Al and 10% Mg of the original quantity of the metal react. The decrease in this ratio as the concentration of metal in the powder is increased up to 20% is caused by the growth of a negative oxygen balance in the SRP and the agglomeration of metal particles on the surface of the burning charge (see page 281). As pressure increases up to 20-25 atm (at which complete combustion of the mixed compositions is achieved [219-222])the amount of metal which reacts on the charge surface increases.
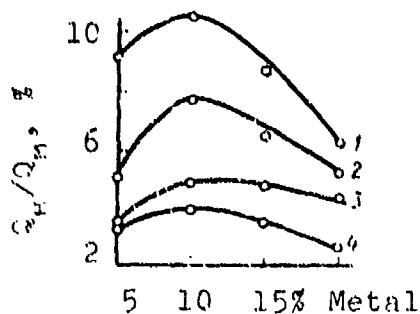
303

Fig. 117. Ratio of heat released during oxidation of metal in k-phase to heat realized in complete burn-up of metal: Particle size (in μm): For Mg: 1 - 1-10; 2 - 80-90; Al: 3 - 20-60; Al-Mg (50/50); 4 - 10-100.

How is it possible that aluminum particles covered with a solid oxide film of Al_2O_3 can be oxidized at the relatively low temperatures of 500-600°C? Since the vapor pressures of aluminum and magnesium at this temperature are extremely low (vapor pressure of aluminum at 660°C is $5.25 \cdot 10^{-7}$ mm Hg, magnesium at 751°C - 10 mm Hg), then their reaction with the oxidizer can occur only on the charge surface of the metal. The diffusion coefficient of the gases (O_2, CO_2, N_2 etc) through the solid shell is too low to cause the rate of heat release, equal to 0.3-0.6 cal/cm^2s, which was observed in the experiment. Apparently there are two ways that this might happen. The first and most probable is that because of the different linear expansion co-efficients β, during heating the particle shell cracks and the aluminum is stripped. The second is that the carbon which is formed in the decomposition of the fuel bond may restore the Al_2O_3 oxide film and form the carbide AlC_3 (see Chapter I).

Near the charge surface in the region of relatively low temperatures metal oxidation reactions occur as a rule on the surface of the particles. With an increase in pressure and, consequently, temperature the role of reactions in the vapor phase also increases. Here, the higher the combustion temperature of the SRP and the lower the boiling temperature of the metal, the greater the heat which is released from reactions occurring in the vapor phase. For example, magnesium, whose boiling temperature at atmospheric pressure is equal to 1107°C and 1850°C at 50 atm (below the com-bustion temperature of the SRP flame), combusts in the vapor phase.

Metal such as tungsten, which has a boiling point of 5000°C under atmospheric pressure, should burn in the condensed phase. Aluminum, however, whose boiling point at atmospheric pressure is equal to 2050°C and 3600°C at p = 50 atm occupies an intermediate position.

During combustion there is an accumulation of metal particles on the charge surface. In the case of ballistite powders there is first a fusing of aluminum and magnesium particles with the thermoresistant decay products of the nitrocellulose, which subsequently fuse near the charge surface. When model mixture systems are burned fusion of the aluminum particles can occur on the surface of the powders, since its temperature is sufficient to melt the aluminum and magnesium. Ignition of the aluminum particles with respect to flame height depends on particle size. Evidently, the greater the particle size, the greater the time required to heat it up to the ignition point ($\tau_{вп} \approx d^2$) and the higher (up the flow) will be their ignition. A spectral study on the height of the flame in metallized powders indicated that radiation in a wave length interval of 0.3-0.6 μm has a spectrum whose intensity gradually declines toward short wavelengths. Against the background of a continuous spectrum in a pressure interval of 5-10 atm for a fuel with an aluminum additive and 2-5 atm for SRP with a magnesium additive oscillating bands appear, which are caused by the molecules of AlO, AlH and MgO. Moreover, in the visible and near ultraviolet region atomic lines of aluminum and magnesium are observed.

The presence of an intensive continuous spectrum in the near ultraviolet and visible regions during combustion of metallized SRP is explained by the radiation of condensed metal combustion products (Al_2O_3, MgO) (see page 184). The characteristic form of energy distribution in the spectrum as a function of wavelength λ along the flame during the combustion process of the APC-PF charge with 10% Al at 20 atm is shown in Fig. 73. The experimental points were taken only from the places on the spectrum free of oscillating bands of AlO (λ = 4866, 4842, 4672, 4648 Å), AlH (λ = 4259, 4241 Å).

The amount of energy released by the flame in the studied wavelength range of 0.3–0.6 μm increases with an increase in distance from the charge surface and reaches a maximal value at a distance of 0.8–1 mm. Further, at a distance of up to 3 mm it becomes steady, then falls as the combustion products of the SRP cool.

The distribution of intensities is well described by the Wien formula [217, 218], i.e., the obtained spectra are identical in nature to that of heat radiation from a gray body. The intense visible emission of the SRP flame with aluminum and magnesium added is related primarily to the selective emission of condensed particles of aluminum and magnesium oxide [180]. Moreover, this emission is intensified by thermoradiation of AlO molecules which are formed in the flame (when aluminum is added in the case of SRP combustion) and the MgO molecules which are formed in the gas phase (when magnesium is added in SRP combustion). The combustion temperature of the aluminum and magnesium particles in the flame jet of the SRP grows with pressure and reaches a maximal value in the range of 18–20 atm for aluminum at $3500° \pm 150°K$ and the range of 7–10 atm for magnesium at $3400 \pm 150°K$. The combustion temperature of the aluminum particles is $400-500°C$ higher than that of the fuel flame jet [206].

The transparency of the SRP flame jet with 5 and 10% aluminum and magnesium added was, according to [173, 206], less than $\gamma \leq 10^{-2}$, i.e., the flame jet of the metallized powders was not transparent. On the basis of studies of flames close to the indicated [224, 229] it maybe concluded that their reflectivity changes with temperature in the relatively narrow range of $\beta = 0.15-0.2$. Since transparency γ, absorptivity α, and reflectivity ρ are linked by the relationship $\alpha = 1 - \gamma - \rho$, then the absorptivity of the SRP flame jet with aluminum and magnesium added should be equal on the average to $\alpha = 0.80-0.85$.

The obtained emissivity of the zone around the particles proved to be considerably greater than the absorptivity of the

gaseous combustion products. This is explained by the formation in the zone surrounding the particle of extremely fine, condensed oxides Al_2O_3 and MgO, which are also the main source of heat emission in the burning particle.

In summing up what has been said, the following brief notes should be made.

1. When ballistite powders are burned with aluminum and magnesium additives, as a result of the accumulation on the charge surface there is a fusing of the metal particles with the thermostable decomposition products of the nitrocellulose, which subsequently fuse near the charge surface. In a case where model mixture systems are burned the fusion of the aluminum particles has already begun on the charge surface.

2. In the initial combustion stage of model mixed fuels with aluminum and magnesium added, i.e., in the reaction layer, oxidation reactions with a positive thermal effect begin on the surface of the metal particles. Here 3-4% (in the case of the aluminum additives) and 5-10% (in the case of the magnesium additive) of the total heat achieved in complete combustion of the metal in a SRP flame is released in the reaction layer.

3. The temperature of the combustion zone of the aluminum particle exceeds the flame jet temperature by 400-600°C.

§ 2. Combustion Time of Aluminum

Of the great diversity of problems which arise when metals are introduced into fuel compositions, one of the most important is that of the completeness of the chemical reaction of the original components.

Since combustion completeness of non-metal fuel-oxidizer systems with finely ground components at pressures of 10-25 atm is

reached very near the combustion surface in an extremely short
time, then combustion completeness in mixtures containing aluminum
or magnesium particles will be determined entirely by the chemical
reaction time of the latter.

It was shown earlier that the oxidation process of aluminum
or magnesium begins directly in the heated layer of the condensed
phase. Nevertheless, the fraction of reacted metal is extremely
small, not exceeding 5% on the average. The main metal oxidation
process - the combustion process - occurs in a high-temperature
flame. The flame jet in condensed systems consist essentially of
the gaseous combustion products of the decomposing fuel and oxi-
dizer as well as the burning metal particles in this medium.

The macrokinetics of the combustion process of such a jet
flame should be based on the laws govering the combustion of the
individual particles taking into account size distribution. It
is also important to consider that in the case of heterogenous
fuel compositions particles burn in concentrations of active
reagents in the medium which are complex in composition and variable
(in time).

The combustion of condensed systems with a high concentration
of powder-like metals is distinguished by the fact that the process
of active particle agglomeration is observed on the burning surface
[172]. For this reason particles which differ (sometimes dras-
tically) from the original in their dispersion and composition
enter the flame jet. The combustion time of large agglomerates
is not determined by visible size, rather it depends on the amount
of aluminum contained in them, i.e., on the "effective"
diameter (see Table 28).

At the present time there is no qualitative theory of metal
particle agglomeration for the combustion of metallized systems
which would consider all of the structural features and properties
of the fuel compositions and the physicochemical parameters of the
original metal powders. Thus, the problem of combustion completeness

308

of the metal in the combustion of metallized compositions and powders begins in each specific case with an investigation of the degree of particle agglomeration.

With all of this considered, a rough estimate has been made below[1] of the combustion of 10 and 20% aluminum contained in condensed mixtures based on APC. The average mass diameter of the particles in the original aluminum powder is 16 µm, and the size distribution of the particles·(agglomerates) corresponds to that shown in Fig. 110.

In the calculation the following was assumed: a) the flame jet was semi-infinite; b) there was no heat exchange between the carrier gas phase and the particles suspended in it; c) transverse molecular and turbulent transfer of components in the flame was negligible; d) the composition of the medium along the flame jets as the result of the oxidation of the metal changed constantly, forming quasi-stationary fields of concentration of the main oxidizing reagents; e) combustion of the particles in the flow occurred because of the H_2O and CO_2, which are equivalent in the metal oxidation reaction; f) the rate of movement of the particles was equal to the velocity of the flow, i.e., there was no velocity lag in the particles; g) the combustion time of the agglomerates was determined by their "effective" diameter.

Let us designate the density of the fuel as ρ, the concentration of aluminum in the fuel as c_0. Thus the total mass of aluminum entering the flow from one unit volume of fuel is $m_0 = \rho c_0$. If the density function of the distribution with respect to the dimensions of the particles which enter the gas phase is $f(D_0)$, and the law of mass loss of particles in time $Z(D_0) = (D) D_0$,

[1]Yu. V. Frolov, A. I. Koromkov. Report at seminar of the division of the Institute of Chemical Physics of the AS USSR, 1968; FGV, 1972 (in press).

then the mass of unreacted aluminum for time dt in a particle interval of $(D_0 - (D_0 + dD_0)$ will equal

$$dm = 2\pi\rho f (D_0) Z (D_0 t) dt\, dD_0.$$ (VI.1)

Hence, the total expression for determining the amount of active aluminum in the flow during time t will equal

$$m = 2\rho_0 \int_0^t \int_0^\infty Z(D_0 t) f (D_0) dt\, dD_0.$$ (VI.2)

Function $f(D_0)$ of the distribution density of the particles with respect to size is plotted on the basis of the experimental data with consideration of the structure of the agglomerates, i.e., according to $D_{\text{эфф}}$. Figure 118 shows a specific example of functions $f(D_{0\text{эфф}})$ for fuels containing 7, 10, and 20% aluminum (corresponding to the integral distribution of particles in the volume shown in Fig. 110).

Expression (IV.2) is used in deriving the law $Z(D_0 t)$ of mass change in the aluminum particles in time.

If τ_0 is the time of complete combustion of particles with diameter D_0 and D and t are the current diameter and combustion time, respectively, of particles in the medium of the gas phase, then

$$Z = \left(\frac{D}{D_0}\right)^3 = \left(1 - \frac{t}{\tau_0}\right)^3 = \left[1 - k\frac{t}{D_0^2}\right]^3,$$ (VI.3)

where

$$k = \frac{a_{\text{K}}^{0.9}}{0.67}.$$

In the solution one must remember that parameter a_{K} — the relative concentration of oxidizing reagents in the flame — changes gradually as the aluminum is burned up, i.e., it in turn represents the burn-up function of the metal $(1 - m/m_0)$ or the

310

current concentration of aluminum c:

$$a_{\text{к}} = a_{\text{к}}^0 - \alpha (c_0 - c).$$

(VI.4)

where $a_{\text{к}}^0$ and $a_{\text{к}}$ and c_0 and c represent the initial and current concentrations of active reagents and aluminum in the flow, respectively.

For compositions based on·APC which were selected as examples. coefficient $\alpha \approx 1.9$. In the general case

$$\alpha = \frac{a_{\text{ок}} - a_{\text{к кон}}}{c_0}.$$

(VI.5)

where $a_{\text{к кон}}$ is the final value of the parameter. which corresponds to total burn-up of the metal; coefficient α can also be expressed somewhat differently.

According to the oxidation reaction equation of aluminum in H_2O or CO_2 each mole of aluminum reacts with 1.5 moles of H_2O or CO_2:

$$Al + 1,5H_2O \rightarrow 0,5Al_2O_3 + 1,5H_2$$

or

$$Al + 1,5CO_2 \rightarrow 0,5Al_2O_3 + 1,5CO.$$
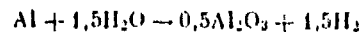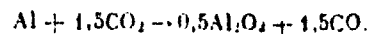
Here the total number of moles n (per unit weight of the fuel) of the gas-phase compounds in the medium does not change. Thus, in the symbols selected earlier,

$$a_{\text{к}} = a_{\text{к}}^0 - \frac{1.5}{n} \frac{100}{\mu} c_0$$

(VI.6)

or

$$\alpha = \frac{150}{2n} = \frac{5,55}{n}.$$

311

Fig. 118. Function $f(D_{0 \, \text{эфф}})$ for compositions containing Al (in %) 1 - 7; 2 - 10; 3 - 20%.
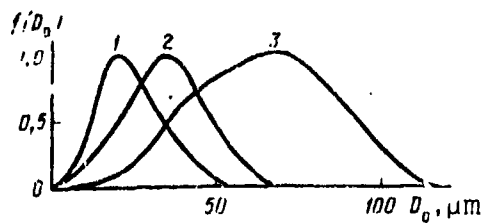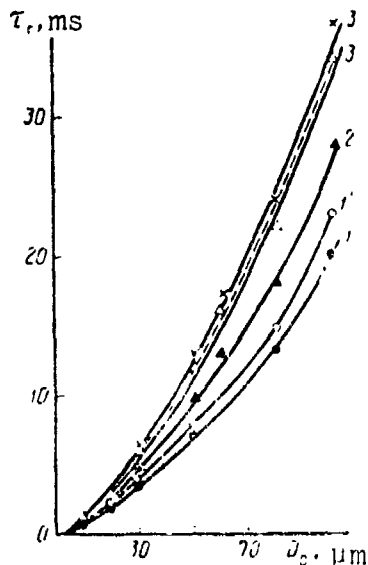

Fig. 119. Combustion time of aluminum particles as a function of particle diameter; Al concentration: 1 - 7; 2 - 10; 3 - 20%.

The combustion [burn-up] time of the aluminum in the flame is calculated together with the solution to equations (VI.2) and (VI.4).

Figure 119 shows how the combustion time of the individual particles changes depending on their diameter and on the initial concentration of aluminum in the fuel. The graphics give an idea of the time required to complete an aluminum oxidation reaction in a flame of a metallized composition based on APC, assuming that the agglomerates which leave the surface of the specimen form a fraction with an effective diameter $D_{\text{эфф}}$ equal to D_0. The completeness of combustion $(1 - m/m_0)$ = N, % of time for three monofractions with a particle dimension of D_0 = 50, 70, and 100 µm can be followed on Fig. 120. The time process is uneven; in the first third of the total time more than one half of the original mass of particles has a chance to react, or more than one half of the active aluminum which enters the flame from the k-phase.

Burn-up (by mass) of the aluminum in the flame for the case
with the corresponding integral D distribution shown in Fig. 110 and
corresponding distribution density shown in Fig. 118 was calculated
for a composition with a parameter value of $a_H \approx 50\%$ in $c_0 = 20\%$
(Fig. 121). The maximal time required to complete the aluminum
combustion reaction was 45-50 μs. This is the total combustion
time of the largest particle. However, the bulk of the aluminum
mass (about 90%) was able to react within approximately the first
20-25 μs. If we consider that average mass diameter D_{50} for the
studied example is equal to 70 μm, then replacement in the calcu-
lation of the polydispersed distribution by a monodispersed dis-
tribution with a particle size of $D_0 = 70$ μm reduces the combus-
tion period by approximately 2 times (Fig. 120). This emphasizes
the inadmissibility of replacing the actual distribution of
agglomerates with respect to $D_{эфф}$ even in rough estimates by a
monofraction with a particle size which is equal to the mean
average size in the corresponding distribution. Such calculations
for compositions with a 10% concentration of aluminum indicate
that the complete burn-up period of aluminum is in this case equal
to 20-25 μs.

Simplifying the calculation system by averaging parameter a_H,
i.e., by replacing the quasi-stationary concentration distribution
of active reagents with respect to the length of the flame jet by
a constant value $a_H = a_H^0 - \alpha/2\, c_0$ corresponding to the oxidation
condition of half of the original aluminum mass, reduces the degree
of burn-up $(1 - m/m_0)$ at the initial moment and increases it in
the final stage by an average of 5-10%.

The results of the rough estimates determining the burn-up time
of aluminum in a flame for heterogenous compositions of fuel
and oxidizer were verified experimentally on a semi-closed unit -
the end-burning micromotor (page 75). Optimal combustion condi-
tions for aluminum are found by successively increasing the free
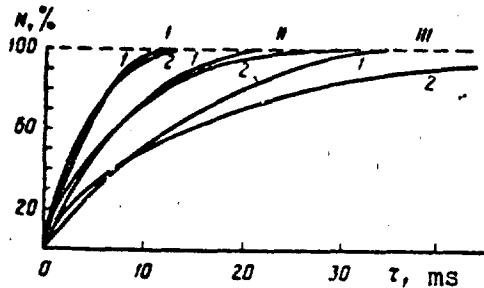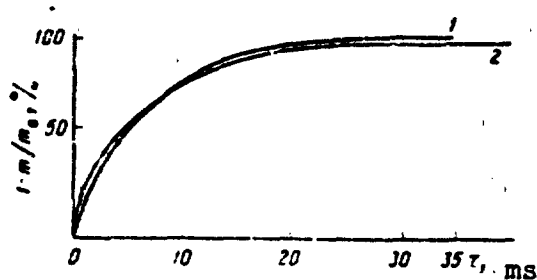volume in the combustion chamber above the surface of the burning

Fig. 120.   Fig. 121.

Fig. 120. Calculating completeness of aluminum burn-up (mono-fraction) in high-temperature (T = 3000°K) active medium. I - D_0 = 50; II - D_0 = 70; III - D_0 = 100 μm. 1 - $a_к$ = $\bar{a}_к$ = const; 2 - $a_к$ = $a_к(c)$.

Fig. 121. Burn-up of polydisperse aluminum in flame jet in time. 1 - $\bar{a}_к$ = const; 2 - $a_к$ = $a_к(c)$.

specimen by increasing chamber length H (see Fig. 25). The fixed variable in the experiments was specific impulse $\mathcal{J}$. The inde-pendence of $\mathcal{J}$ (considering correction for thermal losses in the unit) from H was considered by means of the condition of total completion of chemical reactions in the flame jet. The hold-up time of the combustion products in the engine was determined by corresponding recalculation of height H.

Results of such experiments show that the average time re-quired to obtain the optimal specific impulse value is equal to 12 and 27 μs for compositions with 10 and 18% aluminum, respec-tively. According to the calculation (see Fig. 121), during this time more than 96-98% of the aluminum should react. Here we must add that after-burning of the large particles, constituting 10-15% of the mass, occurs in an atmosphere which is rather poor in active reagents and is a very drawn out process. If we were to follow this process from the increase in the specific impulse, it would be necessary to considerably increase the height of the chamber H, which involves an increase in thermal losses and

involves additional difficultes, which is the reason for the limited sensitivity threshold of this method.

In order to eliminate chemical losses in such units, the time in which the combustion products of the metallized solid fuels remain in them should be comparable to the combustion time of the largest particles (agglomerates).

There are two ways to actively affect the combustion process: a) decrease the degree of agglomeration of the particles and b) enrich the gas phase of the fuel by active reagents of the H_2O and CO_2 type or, for example, by flourine compounds (F_3Cl) [287].

There are different ways to decrease the agglomerates. Among them, for example, are attempts at chemical inclusion of the aluminum or boron into the molecule of the binding agent instead of individual carbon atom [288], reducing the dispersion of the original components [172, 251], increasing the combustion rate of the composition, etc [173, 174, 206].

One promising method of reducing agglomerates might be that of first covering the aluminum particles with a material which has a high melting point. Here a certain improvement in the ignition characteristics of anodized or chromated aluminum is indicated [240, 253]. True, it should be mentioned that a deterioration in the energy parameters of the fuel could result from this cladding.

§ 3. Effect of Metal Additive
on Specific Impulse of Jet Fuel

The specific impulse of a reactive force is an important energy characteristic in the rocket charge [289]. To a great extent it determines the velocity, flight range, and carrying capacity of the rocket. For example, for an intercontinental ballistic rocket with a flight range of 11,000 km and a specific vacuum impulse of

$\mathcal{J}$ = 310 kg·s/kg the increase in $\mathcal{J}$ by 1% is equivalent to a 500 km increase in range [290].

One method of creating high-thrust solid rocket fuels and powders is to use powder metals with a high heat producing value as additives to modern fuel compositions.

As we know, the energy possibilities of fuels can be estimated from specific impulse formulas:

$$\mathcal{J} = 9.33 \sqrt{\eta_t \Delta H}, \quad \text{kg·s/kg}, \qquad (VI.7)$$

or

$$\mathcal{J} = \frac{V}{g} = \sqrt{\frac{2k}{k-1} \frac{R_0}{\mu g} T_\kappa \eta_t} \quad \text{kg·s/kg}, \qquad (IV.8)$$

where ΔH is the difference in formation heats of the reaction products in the chamber; k - adiabatic exponents; g - free-fall acceleration; R_0 - gas constant; T_κ - temperature in combustion chamber; V - exhaust velocity of combustion products from nozzle; $p_0 p_\kappa$ - ratio of pressures at outlet and in combustion chambers; μ - molecular weight of combustion products, $\eta_t = [1 - (p_\kappa/p_0)^{\kappa-1\kappa}]$ - thermal efficiency of engine.

Thermal efficiency (in addition to ratio p_κ/p_0) describes that part of the thermal energy which is released during combustion of the fuel and is converted directly into work.

Let us briefly examine the effect of the main parameters on quantity $\mathcal{J}$ in order to determine the way in which the metal additives affect the power of the fuel.

1. As it increases ratio p_κ/p_0 has a favorable effect on the specific impulse value (Fig. 122) in the range of low values of $p_\kappa \leq 20$ atm. A pressure increase causes complete burn-up of the

316

fuel and suppresses dissociation of the combustion products at high temperatures. Yet along with this there are certain limita-tions which are imposed, first, by the design features of the engine and, second, by the fact that increasing pressure places an undesirable burden on the system. Thus, the optimal working pressure range is not high and generally lies in a range of 30-100 atm.

2. Temperature T_{κ} is determined by the energy characteristics of the fuel. The specific impulse and the exhaust velocity of the gas from the nozzle of the engine are directly proportional to the square root of T_{κ}. Thus, it is desirable to use a fuel with a high flame jet temperature. Yet even here there are limitations. The first is related to heat insulation of the engine. The high temperature increases demands on the materials of the chamber and the nozzle. The second limitation is due to the fact that at high temperatures there is an increase in dissociation of gaseous combustion products. Since dissociation is an endothermic process, then in practice this limits T_{κ} to a temperature of $\sim 3500°K$.

3. The effect of indicator $k = c_p/c_V$ on is more complex, since it exist simultaneously in η_t and in ΔH. Thermal efficiency η_t increases with an increase in k, thus causing an increase in the specific impulse (Fig. 123). The second term $k/(k-1)$, which actually determines the enthalpy of the products in the chamber ($H = c_p T_{\kappa}$), conversely decreases as k increases. As a result the specific impulse of the fuel declines slightly with an increase in k.

4. As for molecular weight μ, the question is solved unam-biguously. In order to provide high values of $\mathcal{J}$ most desirable are products with a low molecular weight, for example, hydrogen. To this we might add that as the combustion products become more complex, the thermal efficiency of the engine declines. When $p_{\kappa}/p_0 = 50$ for diatomic gases (H_2, N_2, CO, Cl) $\eta_t = 0.582$, for

317

triatomic (CO_2, H_2O) - 0.446, and for pentatomic gases - n_t = = 0.248.

Figure 124 shows how the specific impulse magnitude changes for a simultaneous change in temperature and molecular weight.

Thus, in order to increase the specific impulse of the fuel we must find a composition whose combustion products would have increased enthalpy and a high combustion temperature.

Table 30 of Fig. 125 in [4] shows the heating capacity and thermal effect of the combustion reaction of several fuels with ammonium perchlorate.

From this table it is evident that the power characteristics of beryllium, aluminum, boron, and magnesium are significantly greater than those of hydrocarbons (mixed with APC). The most advantageous of the these is undoubtedly beryllium. Thus, despite the fact that beryllium is difficult to use because of the toxicity of its combustion products, a number of foreign firms are conducting an intense study on beryllium solid rocket fuels.

Figure 126 shows how the specific impulse of a fuel consisting of ammonium perchlorate and polyester $C_{23}H_{28}O_4$ changes as aluminum, boron, and magnesium are introduced. Although the boron has greater energy per unit weight, the most effective is the aluminum. Even if a correction is made for two-phase losses, aluminum still provides a thrust increase of up to 10 units.

The energy parameters of binary mixtures of a metal and an oxidizer can be correctly evaluated from the data presented in Table 31.

Based on their specific impulse with ammonium perchlorate the metals are arranged in the following order: Al, B, Mg. This

318
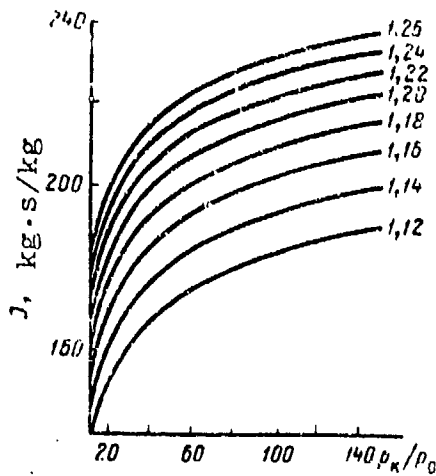
Fig. 122.

Fig. 123

Fig. 122. Specific impulse $\mathcal{J}$ as a function of ratio $p_{\text{к}}/p_0$ for different value os $k (p_0 = 1$ atm; $Q = 1000$ Cal/kg).
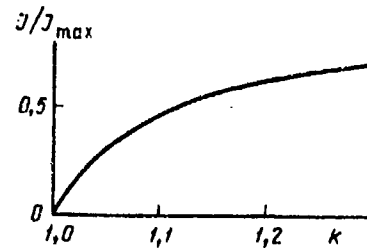
Fig. 123. Effect of magnitude of k on $\mathcal{J}/\mathcal{J}_{\max}$ ($p_{\text{к}}/p_0 = 20$; $T = 3000°K$).
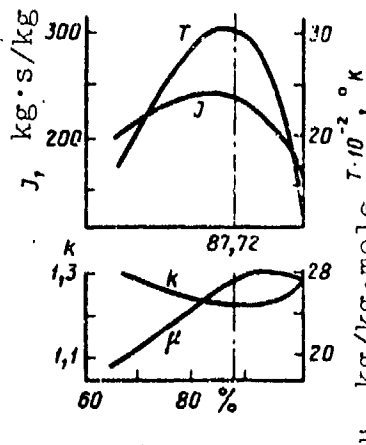
Fig. 124.

Fig. 125.

Fig. 124. Specific impulse as function of temperature of combustion products $T_{\text{к}}$, their molecular weight μ, and specific heat ratio k for a mixed APC - polyether fuel ($p_{\text{к}} = 70$ atm).
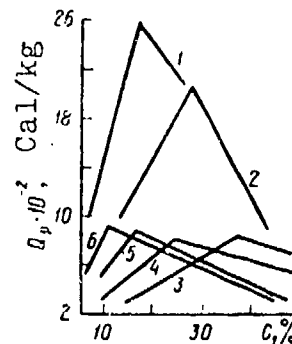
Fig. 125. Rate of values of thermal effect in combustion reaction of solid rocket fuel consisting of APC and various combustibles as a function of the concentration of combustibles: 1 - Al; 2 - Be; 3 - polyurethane rubber; 4 - polysulfide rubber; 5 - carbamide resin; 6 - butadiene-styrene rubber.

319

Table 30. Energy properties of fuels for mixed solid rocket propellants [287].

Fuel	Enthalpy Q, Cal/kg	Thermal effect of reaction with APC (α = 1), Cal/kg
Rubber		
natural	10,270	960
butadiene-styrene	9,530	930
polysulfide	5,600	880
polyurethane	5,115	810
Resin		
phenol-formaldehyde	7,540	950
carbamide	3,495	935
polyester	5,070	885
epoxy	7,317	920
Plastics		
polyisobutylene	10,475	950
polymethyl methacrylate	6,138	930
polyvinyl chloride	5,380	872
polyamide	7,168	913
nitrocellulose	2,250	837
Metals		
aluminum	7,450	2060
beryllium	16,210	2600
lithium	13,950	2360
magnesium	6,000	2040
boron	13,950	1860

320
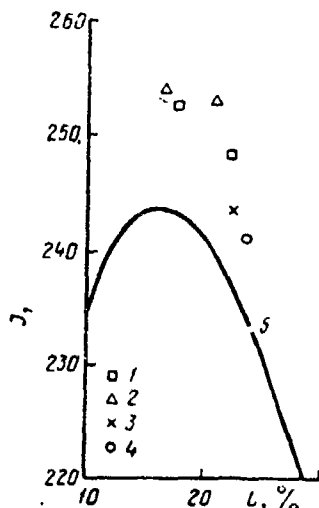
Fig. 126. Change in specific impulse of mixed composition when Al, Mg, and B are introduced [288]. 1 = 10%; Al; 2 - 15% Al; 3 - 10% Mg; 4 - 5% B; 5 - original composition.

sequence changes if in place of NH_4ClO_4 we use NH_4NO_3. The optimal concentration of aluminum in the ammounium perchlorate composition is approximately 30%. In its energy characteristics this composition is 10 units higher than the binary stoichiometric mixture of rubber $+NH_4ClO_4$. Yet in practical application of these metals we must remember another important fact.

Since oxides Al_2O_3, BeO and B_2O_3 have high boiling and melting temperatures, then at the temperatures which exist in the combustion of fuels with metal additives, these oxides will be found in the condensed phase. If the part by weight of the condensed oxides is designated as z, then the apparent molecular weight of the two-phase flow of combustion products will be equal to

$$\mu = \frac{\mu_0}{1 - z},$$

where μ_0 is the average molecular weight of the gaseous combustion products. In other words, as the concentration of the metal and, consequently, of the condensate increases, then the specific impulse of the fuel decreases in proportion to $\sqrt{1 - z}$.

The second parameter which is influenced by the presence of condensed combustion products in the gas flow is adiabatic exponent k.

321

If we assume that the temperature and velocity of the particles and the gas are equal, and if we ignore the specific volume of solid particles in relation to the specific volume of the gases, then we can write

$$\bar{c}_p = (1-z)c_p + zc,$$
$$\bar{c}_v = (1-z)c_v + zc. \qquad (VI.9)$$

Since heat capacity c of oxides Al_2O_3 and MgO is less than that of the gases c_p, then as the part by weight z of the oxide increases, quantity k of the two-phase flow decreases. In its final form the expression for calculating the specific impulse of fuels containing condensed particles will be

$$\mathcal{J} = \sqrt{\frac{2\bar{k}(1-z)}{2(\bar{k}-1)}\frac{R_0}{\mu}T_{\kappa}\left[1-\left(\frac{P_0}{P_{\kappa}}\right)^{(\bar{k}-1)\bar{k}}\right]}. \qquad (VI.10)$$

Thus, the introduction into fuels with high-enthalpy metals increases, on the one hand, the efficiency of the fuels by increasing combustion temperature T_{κ} and ΔH and, on the other, decreases efficiency due to the formation of condensed combustion products. The final result is determined by the ratio of these two factors.

Let us examine a particular example. The adiabatic exponent of the gas phase $k = 1.25$; $c_p = 0.421$ Cal/kg·deg. The specific impulse is $\mathcal{J} = 227$ kg·s/kg. Let there be 10% condensed particles ($z = 0.1$) with a specific heat capacity of $c_p = 0.35$ Cal/kg·deg for the same composition and temperature of the gases. According to (VI.9) we get $\bar{k} = 1.225$, while according to the formula of (VI.10) we find that $\mathcal{J} = 218$ kg·s/kg, i.e., introducing the combustion products of 10% of the condensed phase into the composition without considering the additional heat release and increase decreases the specific impulse by 4% [291].

The ratio between z and T_{κ}, which enter into the specific impulse expression, explains why the optimal concentration of metal additive in the actual fuel does not coincide with its quantity in the composition of maximal power.

Composition of fuel mixture		Density, g/cm³	H, Cal/kg	n_t	$\mathcal{I}$ kg·s/kg	Specific gas formation, l/kg
NH_4NO_3	(94,5)	—	955	0,472	198	970
C_nH_{2n}	(5,5)					
NH_4ClO_4	(90,9)	1.77	1260	0,486	232	840
$C.H.$	(9,1)					
NH_4ClO_4	(68,5)	—	1260	0,49	232	—
$C_6H_2(NO_2)_3CH_3$	(31,5)					
trinitrotoluene)						
$KClO_4$	(88)	—	805	0,48	180	530
C_nH	(12)					
$KClO_4$	(85)	1,92	1300	0,48	234	650
C_nH_{2n}	(15)					
NH_4NO_3	(60)	2,02	1070	0,52	203	—
Al	(40)					
NH_4ClO_4	(61,8)	2,19	1250	0,534	242	514
Al	(38,2)					
NH_4ClO_4	(80)	2,06	1560	0,48	254	660
B	(20)					
$LiClO_4$	(55,6)	2,54	1560	0,40	232	—
Al	(44,4)					
NH_4ClO_4	(78)	1,70	1530	0,51	260	—
B_5H_{11}	(22)					
NH_4NO_3	(52)	—	2300	0,582	218	440
Mg	(48)					
NH_4ClO_4	(71)	—	2440	—	200	314
Mg	(29)					
KNO_3	(89,2)	—	450*	0,428	120	530
C_nH_{2n}	(10,8)					
$C(NO_2)_4$	(82,3)	—	2190	0,42	283	—
B	(17,7)					
$C(NO_2)_4$	(64,5)	1,91	1800	0,42	253	—
Al	(35,5)					
$C(NO_2)_4$	(80,5)	1,44	2150	0,48	300	—
$B_{10}H_{14}$	(19,5)					
B	(31,5)	—	3180	0,248	264	320
O_2	(68,5)					
Al	(54,3)	—	2200	0,248	220	220
O_2	(45,7)					

*770 Cal/kg when K_2O is in solid state.

323

The optimal concentration of aluminum in compositions where rubber or polyurethane resins are used as fuels is 18-20% on the average. The increase in specific impulse achieved by introducing Al reaches 6-8%. In absolute magnitude the specific impulse of the poly-urethane-APC composition increases to 240-250 kg·s/kg, and up to 250 kg·s/kg when nitrided binding agents are used.

Figure 127 shows, using a stoichiometric composition of poly-propylene and APC as an example, how the specific impulse magnitude changes when the oxidizer is replaced by finely dispersed powder aluminum.

It is characteristic that despite substantial differences in absolute values, the experiment rather fully reflects the course of the calculated curve right up to 18-20% aluminum. Yet past this point the experimental magnitude of specific impulse falls much more drastically than one might expect from the thermodynamics data. The explanation for this is that beginning at a certain limit in the given micromotor (page 75) chemical losses resulting from incomplete combustion of the aluminum rise sharply.

Using a fuel composition of a nitrided combustible and TNT one can easily study the limits within which the energy characteristic of the systems change under a discrete substitution of aluminum for each of the components. Since the stoichiometric composition in the given APC-TNT mixture is 68.5/31.5, and 72/28 for the ammonium perchlorate-aluminum mixture, then the range in which aluminum replaces TNT and APC is very wide with respect to weight (Fig 128).

The effectiveness of using aluminum in place of the oxidizer is 7-8 units higher with respect to the specific impulse than using it in place of the nitrided combustibles. A qualitatively similar pattern is observed when magnesium and boron additives with a high heating value are added (Fig. 129).
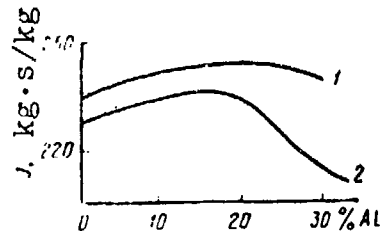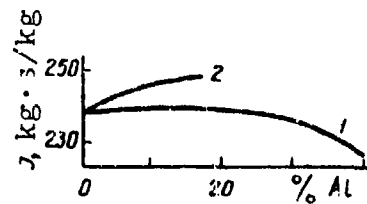
Fig. 127.   Fig. 128.

Fig. 127. Change in specific impulse of PP-
APC system when finely dispersed aluminum
(p_H = 40 atm) is introduced. 1 - calculation;
2 - experiment.

Fig. 128. Change in specific impulse of TNT-APC
system when finely dispersed aluminum is added
(p = 40 atm). 1 - in place of oxidizer; 2 - in
place of TNT.
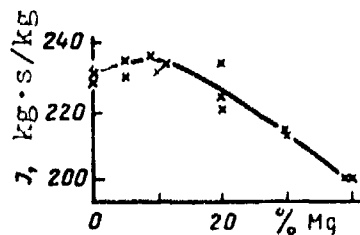
Fig. 129. Effect of Mg (in place
of APC) additive on J (p = 40 atm).
Experimental data.

Thus, metal additives can be introduced into mixed solid rocket
propellants in the place of the polymer combustible or the oxidizer.
Yet the ultimate increase in specific impulse gained by reducing
the combustible is lower and is achieved at a lower concentration
of the metal combustible in the fuel than that obtained by decreas-
ing the oxidizer. A combined substitution is possible.

CHAPTER VII

EFFECT OF METAL ADDITIVES ON COMBUSTION RATE OF CONDENSED SYSTEMS

§ 1. Combustion Rate of Condensed Systems with Metal Additive

The rate of combustion of a fuel, as well as the nature of the dependence of the combustion rate on the properties of the fuel and on the conditions under which it burns are some of the most important factors used to determine the applicability of a fuel for one or another purpose.

Condensed systems are distinguished by an exceptionally great diversity in purpose, the properties of their components, the ratio between the components and the nature of the fuel and the oxidizer. Thus, condensed systems can be broken down into mixed solid fuels for rocket, jet, and hydraulic jet engines [4, 8, 156, 292-296], and pyrotechnic mixtures (incendiary, illumination, ignition, and other compositions) [2].

There are two ways to express the combustion rate quantitatively: the linear combustion rate v can be determined (this rate is determined directly in the experiment), and then from the known value of the linear rate the mass combustion rate u = ρv can be determined, where ρ is the density of the composition.

For condensed systems, as well as gas mixtures, the combustion rate changes significantly with a change in the pressure at which the fuel burns, and this dependence v(p) is often approximated at a constant temperature by the exponential function:

$$v = bp^{\nu}.$$
(VII.1)

However, in literature the combustion rate has often been represented as a binomial formula in the form of

$$v = a + bp^{\nu},$$
(VII.2)

which describes the experimental values with sufficient accuracy and over a broad pressure range. Evidently formula (VII.1) is a particular case of formula (VII.2) (a = 0), yet it is better to use the monomial formula (VII.1) (breaking down the entire range into the necessary number of segments), since this form of dependence v(p) is convenient for comparison to the theory [289, 297] and in calculating pressure in the combustion chamber of an engine operating on solid fuel [156, 287, 296].

An investigation in which the combustion rate of nitroglycerin powders N and NB with aluminum added [173] was studied as a function of pressure showed (Fig. 130) that the combustion rate of such compositions can be described by equations characteristic of pure N and NB fuels. From the results of the experiment the exponent $\nu = 0.82-0.86$ for a composition of N + Al, i.e., the same as for pure N powder ($\nu = 0.8-0.9$); for the composition consisting of NB + Al $\nu = 0.6-0.64$, while without the additive $\nu = 0.6-0.7$ (in a pressure range of 20-80 atm).

One is struck by the fact that the combustion rate of N and NB powders containing aluminum with a particle size of 350-450 μm increases by a greater value with the increased percentage of aluminum than in the case of a smaller particle size at the same

pressure. Since the combustion rate $u \sim \lambda^{0.5}$, where λ represents the heat conductivity of the powder, then it is natural to assume that the increase in the rate of combustion is caused by an increase in the heat conductivity of the powder with aluminum added. For this purpose experiments were conducted to determine heat conductivity using the nonstationary heat flux method [298].

In the experiments a differential copper-constantan thermocouple with a wire diameter of 0.1 mm was used. One junction of the thermocouple was introduced into the specimen, the other was placed in a thermostat with water, whose temperature was held constant during the experiment (60°C). The specimen was immersed in the thermostat at 20°C. Thus, all quantities by which heat conductivity was determined referred to an average temperature of 40°C.
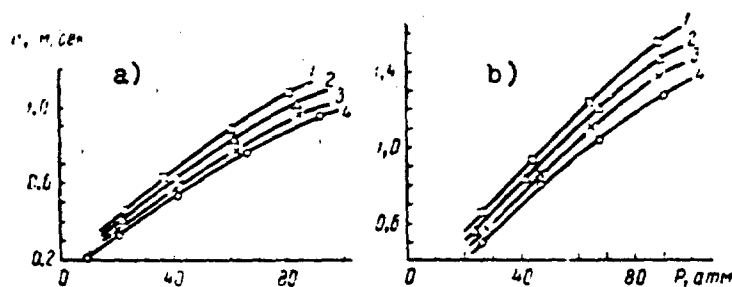

Fig. 130. Combustion rate of metallized ballistic powders as a function of pressure.

a) Powder N + 9% Al. Particle size of Al (in μm): 1 - 350-450; 2 - 40-70; 3 - ≤1 μm; 4 - powder N.

b) Powder NB + 13% Al. Particle dimension of Al (in μm): 1 - 350-450; 2 - 160-280; 3 - 40-70 μm; 4 - NB.

Designations: cm/сек = cm/s; атм = atm.
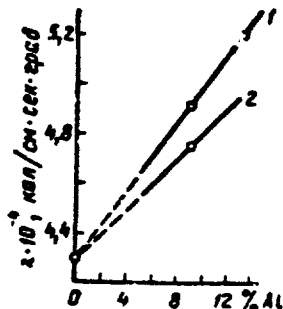
Fig. 131. Change in heat conductivity of N powder as a function of percent of additive and particle diameter of Al (in µm): 1 - 350-450; 2 - ≤1.

Designation: кал/см·сек.град = cal/cm·s·deg.

As we see in Fig. 131, the heat conductivity of N powder with aluminum added increases with the percent concentration of aluminum and the increase in particle size.

Interesting from the standpoint of studying the combustion mechanism of solid fuels with metal additives are studies by Pokhil and Romodanova [299, 300] on the combustion rates of model compositions based on oxidizers $KClO_4$ and NH_4ClO_4 with metals under vacuum conditions (p $\approx$ 10^{-2} mm Hg). Steady-state, flameless combustion of these compositions is determined by the reactions occurring in the reaction layer of the condensed phase with a total exothermic heat effect on the combustion surface of the metal. Here the initial combustion stage (flameless combustion) is achieved by the formation of a smoke-gas combustible mixture, which later burns down under certain conditions in the zone above the charge surface to final combustion products.

The subjects of the study were stoichiometric compositions based on the oxidizer $KClO_4$ and fuels W, Zr, Mo, and Ti and the oxidizer NH_4ClO with Al and Mg. The charges, 5 mm in diameter, were compressed to maximal density.

It was learned that compositions based on potassium perchlorate can burn steadily and flamelessly in a vacuum (p $\approx$ 10^{-2} mm Hg) not only at room temperature, but also at a negative temperature. Thus, compositions of $KClO_4$ + Mo (25-60 µm) and $KClO_4$ + Zr (20-60 µm) burn at an initial temperature of -30°C; the composition

329

$KClO_4$ + W (d ≤ 60 µm) begins to burn at a specimen temperature of -5°C, while $KClO_4$ + Ti (20-40 µm) can burn steadily in a vacuum only when preheated to 200°C. Charges based on NH_4ClO_4 with aluminum (d ≤ 1 µm) and magnesium (d ≤ 10 µm and 80-90 µm) burned in a vacuum only when preheated to a temperature exceeding 200°C (Table 32). Here, compositions containing aluminum particles measuring 20 µm in diameter generally cannot ignite at pressures of 10^{-2} mm Hg, although mixtures based on $KClO_4$ and NH_4ClO_4 with aluminum particles of less than 1 µm burn quite intensely with an explosion.

Table 32. Combustion characteristics under vacuum conditions (p = 10^{-2} mm Hg) of compositions based on oxidizers $KClO_4$ and NH_4ClO_4.

Composition	Particle size of metal, µm	Initial temperature of specimen, °C	Surface temperature, °C	Combustion rate mm/s	Percent of metal reacting with oxidizer
$KClO_4$ + Al	1	260		Note[1]	7.0
Al	20—60	Does not ignite	—	—	--
Al	70—100		—	—	—
Mg	10	290	790	0.19	4.0
Mg	80—90	290	700	0.10	—
Al/Mg	10—100	280	820	0.15	Al ~ 6.0 Mg ~ 6.0
W	60	20	850	0.22	12
W	100	20	—	0.12	—
Mo	60	20	610	—	—
Zn	20—40	20	860	0.15	7.0
Ti	20—40	200	640	—	—
NH_4ClO_4 + Al	1	450—500		Note[1]	—
Al	20—60	Does not ignite	—	—	—
Al	70—100	The same	—	—	—
Mg	10	200	510	0.086	—
Mg	80—90	200	420	0.044	—
Mo	25—60	200	530	—	—
Al/Mg	10—100	20	560	0.073	—
W	60	20	560	—	—
Zn	20—40	230	540	—	—
Zn	20—40	20	470	0.061	—
Ti	20—40	—	515	—	—

[1]Combustion is intense with explosion. Thermocouple torn off.

In view of the fact that the aluminum is covered with a solid, durable oxide film, for compositions based on potassium and ammonium perchlorates and aluminum spontaneous ignition is more difficult than for compositions based on the same oxidizers and magnesium.

The increased temperature of the surface of compositions based on potassium perchlorate and metal combustibles in the case of flameless burning in a vacuum up to 700-800°C and for compositions based on ammonium perchlorate and metal combustibles up to 500°C is caused by the total exothermic process of deep composition in the reaction layer of the condensed phase of the mixtures. As we see in Table 32, the flameless combustion rate of the composition depends on the particle size of the fuel. The smaller the size of the metal particles, the greater will be the rate of flameless combustion. A similar relationship between the combustion rate of model composition consisting of ammonium perchlorate, polyformaldehyde, and metal under vacuum conditions $(p \sim 1^{-2}$ mm Hg) and the particle size of the aluminum and magnesium was obtained in [173].

The effect of the metal particle diameter on combustion rate under increased pressures has been specially studied in [301]. Experimental data [156] show that for the gasified components dependents $U(d)$ is relatively weak, and the integral of change due to the change in d, which is described by the quantity $\theta = U_0 U_\infty$ (ratio of combustion rate of limiting finely dispersed mixture $U_0 = U_{|d=0}$ to the combustion rate of the limiting coarsely dispersed mixture $U_\infty = U_{|d \to \infty}$) is not great. Conversely, for nonvolatile components the dependence $U(d)$ is considerably stronger, while quantity θ is considerably greater. Otherwise the combustion rate might change much more intensely as a result of the change in the particle size of the nonvolatile component than as a result of the change in the particle size of the easily gasified component. N. N. Bakhman attributes this phenomenon

to the mass-exchange coefficient, which for systems consisting of gasified components (for example, an organic fuel with NH_4ClO_4 or $KClO_4$), depending on temperature and pressure, has an order of $A = 10^{-2}-10^{-4}$ g/cm·s, and for mixtures with a nonvolatile component (for example, a fuel consisting of tungsten, carbon, and aluminum with NH_4ClO_4 or $KClO_4$) $A = 10^{-8}-10^{-26}$ g/cm·s. Thus it follows that for systems with gasified components the mixing of components can occur rather rapidly even in the warming zone. Accordingly, the combustion rate is to a great extent determined by kinetic factors, and dependence U(d) is weak (nonexistent at rather low d values, since mixing is achieved completely within the limit of the warming zone). On the contrary, for systems where one component (usually the oxidizer) is gasified and the other is nonvolatile, mixing can only occur simultaneously with the reaction. In this case combustion occurs in a regime which is close to diffusion, and dependence U(d) (where d is the particle size of the nonvolatile component) is strong. From the dependence of the combustion rate of composition $W + KClO_4$ on the particle diameter of tungsten (Fig. 132), which was plotted in a logarithm scale, we see that there is a plateau at middle values of d = 19-160 μm. In other words, at low values of d = 3-19 μm the dependence U(d) appears strong (U ~ 1/d); at middle values of d = 19-160 μm it weakens, thereafter at high values of d = 160-550 μm it again approaches U ~ 1/d. If dependence U(p) is written in the form of exponential function $U = bp^{\nu}$, then exponent ν will depend on the size of the metal particles (Table 33). From the table it follows that the value of ν is in general noticeably higher at greater d values.

The theoretical study of the combustion of model mixed powders, representing a mechanical mixture of two substances of different properties, one of which was not easily gasified, the other easily gasified (oxidizer), conducted in [2, 303], showed that the combustion rate of the fuel U should (in a diffusion combustion regime) depend on pressure and particle size as follows:

332

$$U \sim \frac{p^{n.5}}{d}.$$ (VII.3)

If, however, we assume that the particles begin to react (burn) in the diffusion regime immediately after they leave the surface of the condensed phase (taking into account the actual movement of the particles), then the combustion rate dependence can be represented in the form of

$$U \sim \frac{p^{1.5}}{d}.$$ (VII.4)
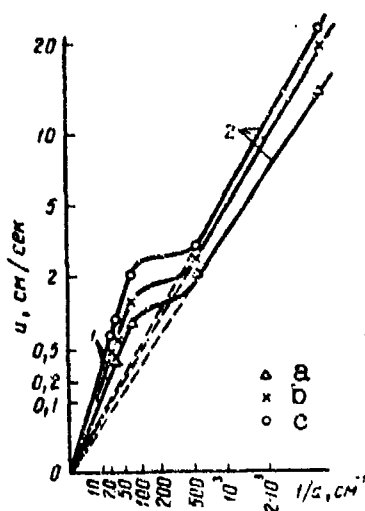
Fig. 132. Combustion rate of composition with 90% W + 10% $KClO_4$ as a function of particle diameter. a - 10, b - 50; c - 100 atm.

Table 33. Exponent v as a function of particle size of the metal.

Mixture composition	$\varkappa$	v				
		2,7 μm	10 μm	100 μm	300 μm	550 μm
80% W - 20% $KClO_4$	0,15	0,21	—	—	0,53	—
90% W - 10% $KClO_4$	0,2	0,23	0,20	0,42	0,30	0,37
95% W - 5% $KClO_4$	0,1	0,20	—	—	0,33	—

333

As we see, there is qualitative agreement between the theory and the experiment for fine particle fractions of 2.7 and 19 μm. The experimental dependence for a mixture consisting of 90% W + + 10% $KClO_4$ was obtained in the form of $U \sim p^{0.23}$ at d $\sim$ 2.7 μm and $U \sim p^{0.2}$ with d $\sim$ 19 μm, the theoretical - from expression (VII.4) in the form of $U \sim p^{0.33}$. Yet it is too early to speak of quantitative agreement. First, in the theoretical studies it was assumed that the particles begin to react from the moment that their velocity coincides with that of the gas stream flowing off of the surface of the fuel, i.e., that there is no velocity lag (this condition requires d < 0.1 μm); second, a stoichiometric mixture was studied, not a super-rich mixture (the part by weight of the tungsten was very high - 0.9). This is even truer of mixtures with large tungsten particles.

Romodanova [300] studied the dependence of the combustion rate of the stoichiometric mixture of NH_4ClO_4 on the activity of aluminum powder (d $\leq$ 1 μm) in a pressure range of 1-120 atm. Aluminum with activities of 75, 83, and 99% were taken. From the results shown in Fig. 133 we see that the activity of the aluminum has no effect on the nature of the combustion rate/pressure dependence. In the low-pressure range an increase in the combustion rate is observed, and this reaches a maximal value for a composition of NH_4ClO_4 + Al with an aluminum activity of 75% in the pressure range 65-70 atm, for a composition with an aluminum activity of 83% - in a pressure range of 65-75 atm, and for a composition with aluminum activity of 99% - the pressure range of 80-90 atm. As pressure continues to increase up to the maximal value the combustion rate of the mixtures indicated above decreases.
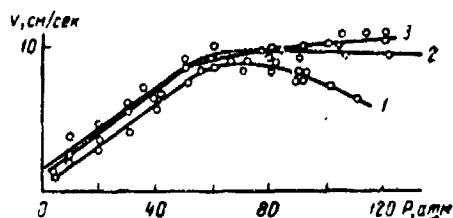

Fig. 133. Combustion rate as a function of pressure.
Mixtures: 1 - NH_4ClO_4 + Al; 2 - NH_4ClO_4 + Al + 0.5% V_2O_5; 3 - NH_4ClO_4 + + Al + 0.5 Fe_2O_3.

When 0.5% Fe_2O_3 or V_2O_5 are added to NH_4ClO_4 + Al no maximum is observed for the curves representing the combustion rate as a function of pressure. Hence it is apparent that additions of Fe_2O_3 and V_2O_5 may not only increase the combustion rate of NH_4ClO_4 + Al, but also change the nature of the combustion rate dependence.

Vanadium pentoxide may, when it reacts with metal oxides, form vanadates. The corresponding change in volume which occurs here is accompanied by the formation of a porous film, which has a poor bond with the metal. Here, very small quantities of V_2O_5 [304] are required to cause prolonged acceleration of the oxidation process.

Brasunas [305] and Monkman [306] performed a chemical analysis of the oxide film and found that on the interface between the metal and the oxide the concentration of vanadium is greater than its average concentration in the film (less than 5%). Studies on the effect that the nature, dispersion, and percent of metal additives in a wide pressure range with different types of oxidizers have on solid rocket propellants were performed in [156, 283]. Bitumen was used primarily as the binding agent.

As we see from Tables 34-36, the combustion rate has a rather strong dependence on the dispersion of the metal and a somewhat lesser dependence on the percent of the additives, the ratio between the fuel and the oxidizer depending on the dispersion of the oxidizer, and on the pressure. Thus, the combustion rate, even in an overwhelming majority of cases, decreases (Z < 1) when large particles of aluminum (d $\geq$ 190 μm) are introduced into the model mixture, whereas sub-dispersion particles (d $\bullet$ 0.09 μm) increase the combustion rate by Z = 2.0-2.5 times (it should be mentioned that a composition of polyformaldehyde, APC, and Al (d $\leq$ 1) burns in a vacuum with an explosion [173]).

335

Table 34. Effect of large metal particles on combustion rate [283].

Oxidizer	d_{ox}, µm	a	Metal	d_M, µm	Percent of metal	$Z = U/U_0$ 0 atm (gage)	5 atm (gage)	10 atm (gage)	50 atm (gage)	100 atm (gage)
NH₄ClO₄	10	1,5	Al	190	13,1		0,92	1,0	1,1	1,04
	10	1,0	Al	190	13,1		0,86	0,84	0,88	0,92
	10	0,75	Al	190	13,1	0,90	0,90	0,94	0,98	1,0
	180	1,5	Al	190	13,1	—	0,93	0,97	0,97	1,1
	180	1,0	Al	190	13,1	2	1,1	1,04	1,02	0,85
	180	0,75	Al	190	13,1	0,95	0,97	0,93	0,92	0,95
	10	1,0	Al	190	31,1	—	0,81	0,81	0,82	0,90
	180	1,0	Al	190	31,1	—	0,88	0,92	0,96	0,88
	10	1,0	Al	560	13,1	0,93	0,93	0,92	0,96	0,94
	10	1,0	Mg	190	13,1	1,1	—	1,02	1,07	1,01
	10	1,0	W	320	13,1	0,73	0,90	0,87	0,96	1,0
KClO₄	10	1,0	Al	170	13,1	1,08	0,98	0,95	1,03	1,02
	10	1,0	Al	560	13,1	—	—	0,94	1,04	0,99
	200	1,0	Al	170	13,1	0,92	1,06	1,1	0,86	0,71
	10	0,75	Al	190	13,1	0,99	0,95	0,94	0,92	0,65
	200	0,75	Al	190	13,1	—	0,79	0,90	0,80	0,81

Table 35. Z is a function of d_M with addition of 13.1% finely dispersed aluminum.

Oxidizer	d_{ox}, µm	a	d_c, µm	Z 1 atm (gage)	5 atm (gage)	10 atm (gage)	50 atm (gage)	100 atm (gage)
NH₄ClO₄	10	0,75	0,09	1,94	1,38	1,55	1,69	1,63
			3	1,23	1,26	1,33	1,21	1,38
			12	1,08	1,11	1,03	1,10	1,11
	180	0,75	0,09	2,0	1,61	1,73	1,37	1,22
			12	1,38	1,15	1,12	0,99	0,91
KClO₄	10	1,0	0,2	6,45	2,72	2,31	1,65	1,69
			12	1,44	1,30	1,20	1,06	1,01
	200	1,0	0,2	4,1	2,74	2,62	2,23	1,98
			12	1,21	1,26	1,20	0,92	0,84

336

Table 36. Effect of percent added of finely dispersed aluminum on combustion rate of stoichiometric mixtures of an oxidizer and bitumen.

Oxidizer	d_{ox}, μm	d_{al}, μm	Metal, percent	z				
				1 atm (gage)	5 atm (gage)	10 atm (gage)	50 atm (gage)	100 atm (gage)
NH₄ClO₄			6,5	1,15	1,07	1,07	1,04	—
	10	0,09	13,1	1,72	1,63	1,55	1,65	—
			31,1	3,46	3,46	3,8	--	2,87
	180	0,09	13,1	1,85	1,73	1,76	1,62	1,51
			31,1	3,41	3,02	2,78	2,70	2,37
KClO₄			6,5	2,8	—	2,02	1,58	1,34
	10	0,2	13,1	6,45	2,72	2,31	1,65	1,69
		0,09	31,1	—	--	2,74	2,23	2,4

Table 37. Combustion rate of some compositions consisting of an oxidizer ($\sim$10 μm) + + bitumen + 31.1% Al (0.09 μm).

Oxidizer	x_0	U, mm/s				
		0 atm (gage)	5 atm (gage)	10 atm (gage)	50 atm (gage)	100 atm (gage)
NH₄ClO₄	1	5,4	19,5	32,3	56	86,1
	0,75	5,75	15,5	25,8	60,8	—
KClO₄	1	—	—	18,4	43,4	79

However, the increase in the combustion rate (Table 37) is far from proportional to the decrease in the aluminum particle size. This is due to the fact that on the surface of a burning charge the metal particles fuse and form relatively large drops. The greater the percent of additive and the smaller the particle size, the greater will be the extent of the fusion [173-251] (the initial particles fused into a single particle). Thus, the particles which burn on the charge surface and in the flame jet greatly exceed the original particles in size. However, the large particles (d ≥ 160 μm), although not subject to fusion, have no substantial reaction on the surface or near the surface of the charge, but only take up heat for their heating and melting.

Indicator ν in the formula $u = bp^\nu$ undergoes a rather unusual change when finally dispersed aluminum is added (Table 38).

Table 38. Effect of adding finely dispersed aluminum on indicator ν in formula $U = bp^\nu$ (indicator ν_0 refers to original system without aluminum added).

Fuel	Oxidizer	d_f μm	x_f	d_{Al} μm	Al, %	ν_0	ν	Pressure, atm
Plexiglas	NH_4ClO_4	6	0,66	2,7	10	0	0,49	40—6?
			0,83	2,7	10	0.37	0,5?	40—6?
Bitumen	NH_4ClO_4	180	0,75	0,09	13,1	0,54	0,43	10—100
				3	13,1	0,54	0,42	10—100
♦				12	13,1	0,54	0,48	10—100
				0,09	13,1	0,54	0,495	10—100
			1,6	0,09	31,1	0,54	0,49	10—100
		10	1,0	0,09	13,1	0,57	0,60	10—100
Bitumen	$KClO_4$	10	2,0	0,2	13,1	0,62	0,56	5—100
				12	13,1	0,62	0,60	5—100
		200	1,0	0,2	13,1	0,65	0.55	5—100
				12	13,1	0,65	0,53	5—100
		10	1,0	0,2	6,5	0,75	0.61	10—100
				12	13,1	0,75	0,69	5—100

As we see in Table 38, if the combustion rate of the model mixture without the metal additive can be described by an exponent of $\nu_0 < 0.5$, then the metal increases the combustion rate less intensely at low p values and more intensely at high values. If, however, $\nu_0 \geq 0.5\text{-}0.6$, then, conversely, the metal weakens the rate/pressure dependence.

The effect of the additive on the combustion rate of SRP can be explained based on the thermal conbustion theory of [297]. As Logachev and Pokhil were the first to prove in [172], the metal begins to react in the reaction layer of the condensed

338

phase of the charge with a positive thermal effect. Here, due to heterogeneous reactions in the initial stage, 3-4% aluminum and 5-7% magnesium (depending on the particle size of the metal introduced into the SRP) of all of the metal introduced into the powder is oxidized. This leads to a temperature increase on the charge surface, and, consequently, an increase in the reaction rate of the decay products of the oxidizer and the binding agent. As a consequence we might expect that under the same conditions (percent of additive and particle size of the metal, pressure, binding agent, and oxidizer) the combustion rate of the SRP charge would be greater in a case where the metal reacts more in the condensed phase of the powder. This has been proven experimentally.

As apparent in Table 39, the combustion rate of compositions containing Mg(d $\approx$ 10 μm) is in all cases thigher than the combustion rate of compositions with Al(d $\approx$ 12 μm). At present it is difficult to compare the other values, first, because of the significant change in the average particle size when switching from one metal to another and, second, due to a lack of measurement data for certain metals on the thermal effect in the condensed phase.

Table 39. Effect of the nature of the metal on Z when 13.1% metal is added to stoichio-metric mixtures containing an oxidizer (10 μm) + + bitumen [283].

Oxidizer	Metal	d_M, μm	Z				
			0 atm (gage)	5 atm (gage)	10 atm (gage)	50 atm (gage)	100 atm (gage)
NH_4ClO_4	Al	0,09	1,72	1,63	1,55	1,65	—
	Al	12	1,31	—	1,29	1,11	1,11
	B	1	1,32	1,24	1,20	1,27	1,19
	Mg	10	1,97	1,72	1,58	1,30	1,20
	Ti	16	1,0	1,0	1,0	1,05	1,01
	W	2,5	0,99	0,90	0,96	1,10	1,12
	Zn	6	1,04	0,98	0,98	0,92	0,78
$KClO_4$	Al	0,2	6,45	2,72	2,31	1,65	1,09
	Al	12	1,44	1,30	1,20	1,06	1,01
	B	1	4,22	1,95	1,84	1,20	0,95
	Mg	10	3,1	1,84	1,72	1,13	0,90
	Ti	16	1,14	1,11	1,07	0,95	0,89
	W	2,5	1,12	1,10	1,09	1,07	1,01
	Zn	6	1,0	1,06	1,08	1,03	0,84

If the particle size of the oxidizer and the metal is actually small and combustion is considered to occur in a regime close to kinetic, then Z can be represented as [283]

$$Z \sim \left\{ \exp[E/R(1/T_{\mathrm{r}} - 1/T_{\mathrm{r}}')] - p^{1-2\nu_0}\frac{\Delta l'}{d_{\mathrm{M}}^2}\exp(E/RT)_{\mathrm{r}} \right\}^{0.5}, \qquad (VII.5)$$

where E is the activation energy; T_{r} and T_{r}' - combustion temperature of oxidizer-binder mixture and oxidizer-binder-metal mixture, respectively.

If T_{r}' does not depend on pressure, then expression (VII.5) can be written in the form of

$$Z \sim (A + Bp^{1-2\nu_0})^{0.5}. \qquad (VII.6)$$

from which it follows that when $\nu_0 \leq 0.5$ Z should increase with pressure, and when $\nu_0 > 0.5$, it should decrease. This is confirmed experimentally (see Table 39). From formula (VII.5), just as from (VII.6) we see that the combustion rate should increase as the particle size of the metal decreases.

Andreyev and Rogozhnikov [284] studied combustion in an ammonium perchlorate/aluminum powder system, which under certain conditions tended to shift from combustion to explosion.

The effect of the Al concentration on combustion of ammonium perchlorate was tested with medium-dispersed (63-160 μm) APC. Pure perchlorate under the conditions of a manometric bomb of 50 cm^3 burns only with an igniter consisting of gun powder (1 g), and burns slowly with a maximum pressure at 400 μs. With 27% finely dispersed (1 μm) aluminum the maximum is reached in 20 μs, at 25% it is reached sooner, and at 18, 9.5 and 5% aluminum an explosion occurs in 12 μs in the last two experiments. Thus, under the conditions of the given experiment, the lower the concentration of aluminum (within the studied limits) in the mixture, the more its combustion is inclined toward explosion.

Here the greatest increase in the danger of an explosion is observed for a concentration of aluminum (5-9%) which is considerably lower than that required for complete combustion. In other words, the maximal heat of combustion (calculated) and the tendency of the composition to shift to an explosion do not coincide. In this respect the mixture is phlegmatized, as it were, by the excess aluminum.

Experiments on the effect of the concentration of aluminum powder on the tendency of combustion to shift to an explosion were also conducted with nitroglycerin NB powder, to which the powder was mechanically admixed. The presence of moderate amounts (3% and more than 5%) aluminum noticeably intensifies combustion. A similar result - the condition of combustion intensity - was obtained when 4.8% aluminum powder was added to the composition of the powder mass. At 10% the mixture behaves just as powder without the additive.

In connection with the marked increase in the tendency of APC combustion to shift to an explosion when aluminum is added to it it is interesting to study how aluminum affects the combustion rate of APC.

The combustion rate was determined in a constant-pressure bomb at 50 atm. The ammonium perchlorate was pressed into Plexiglas tubes measuring 10 mm in diameter. As we see in Table 40, the presence of aluminum not only increases, but somewhat even decreases the combustion rate of APC.

Table 40. Effect of Al on combustion rate of ammonium perchlorate at a pressure of 50 atm.

Particle size of NH_4ClO_4, μm	Al, %	ϵ, g/cm^3	Linear combustion rate, cm/s	Mass combustion rate, g/cm$^2 \cdot$c
10	0	1.85	0.33	0.61
10	5	1.88	0.23	0.44
14	5	1.92	0.30	0.57
120-150	5	1.73	0.27	0.47

341

Experiments on the effect of aluminum on the combustion capacity of its mixtures with ammonium perchlorate, which were conducted in glass tubes and cones at a density of 1.1 g/cm^3, showed that 5% aluminum reduces the critical combustion diameter at 30 atm from 10 to 6 mm. The further increase in the concentration of aluminum in the mixture combustion capacity is somewhat increased: when the concentration of aluminum is increased from 5 to 25% the critical diameter decreases approximately 2 times.

From the result presented above we see that adding aluminum to ammonium perchlorate greatly facilitates penetration of the combustion into the depth of the charge and the transition of combustion to explosion.

One of the reasons for the effect of aluminum established by Andreyev and Rogozhnikov [284] is the increased temperature of the gaseous decomposition products of NH_4ClO_4, which results from the interaction of their oxidizing agents with the aluminum. Yet, since the aluminum reaches its greatest effectiveness not in a stoichiometric ratio corresponding to maximal combustion temperature, but at a much lower concentration, and since the combustion rate of the compressed mixture in the moderately high pressure range does not increase with the addition of aluminum, then it is possible that the main role of aluminum is not that of increasing the total combustion energy but of causing the gaseous combustion products to penetrate to a greater depth. In the presence of aluminum the gaseous combustion products of APC, which are heated to a higher temperature, are already capable of initiating combustion when they penetrate the k-phase. Here, apparently, aluminum does not affect the first conversion stages of the ammonium perchlorate, but has an active effect only on the secondary products of the conversion. Thus, aluminum has a much weaker effect on the combustion rate of a process occurring in an ordinary (nonturbulent) regime, causing virtually no increase in the combustion rate of an end-burning charge.

§ 2. Combustion Rate of Hybrid Systems

Smoot and Price [307, 308] studied the combustion rate of fuels containing metals in hybrid propellants of the composition LiH-butyl rubber-fluorine-oxygen. It was determined that the ratio between the fuel components, the composition of the oxidizer, consumption of the oxidizer, and pressure all affect the burn-out rate. The experiments were conducted on a specially designed unit, whose scheme, experimental conditions and method of determining the burn-up rate are described in detail in [309].

Table 41.   Composition of hybrid propellant.

Composition of fuel, wt. %		Pressure range, atm(abs.)	Comparison of oxidizer, wt. %		Oxidizer consumed, $g/cm^2 \cdot s$
LiH	butyl rubber		F_2	O_2	
90	10	1.62—5.93	92—100	8—0	1.26—11.2
60	40	2.32—9.35	80—100	20—0	1.12—10.5
50	50	2.46—8.86	70—100	30—0	1.76—9.83
40	60	2.32—5.93	70—100	30—0	1.12—10.5
0	100	1.58—10.97	0—100	100—0	0.98—11.2

The composition of the fuel charge varied from 100% butyl rubber to 90% lithium hydride, the composition of the oxidizer was from 100% fluorine to 100% oxygen. Table 41 presents data on the composition of the oxidizer and the fuel, the variation ranges of oxidizer consumed, and pressure in the combustion chamber   The combustion rate was measured in 5 sections along 153 cm of charges and was determined by the length of the specimen. Total expenditures of the oxidizers were also averaged with respect to time as well as the length of the specimen.

The addition of large quantities of metal or metal hydride to a hybrid fuel charge results in a substantial increase in the burn-up rate. Figure 134 in logarithmic coordinates shows graphs representing the burn-up rate as a function of the total mass expenditure of the oxidizer for fuel charges consisting of from

O to 90% LiH. The oxidizer contains the amount of O_2 necessary to oxidize the carbon in a composition burning to CO.
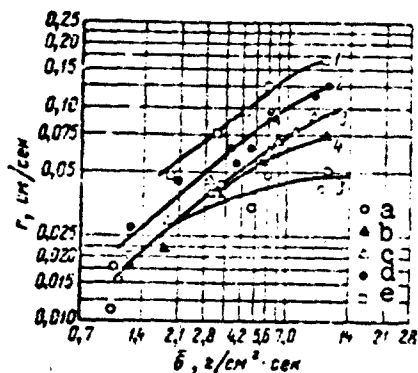

Fig. 134. Burn-up rate of LiH-butyl rubber fuel as a function of the amount of oxygen-fluorine oxidizer used at 4.2 atm. 1 - 4% O_2; 2 - 10% O_2; 3 - 30% O_2; 4 - 15% O_2.
a - 0% LiH; b - 40% LiH; c - 40% LiH; d - 60% LiH; e - 90% LiH.

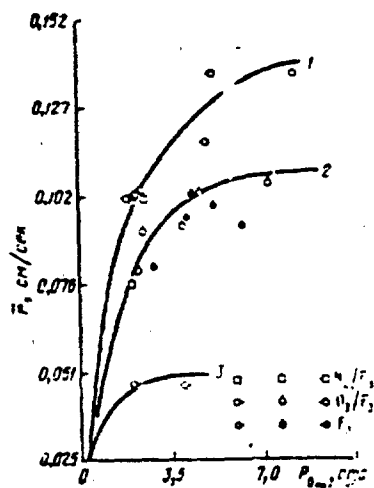Designation: $r/cm^2 \cdot сек$ = $g/cm^2 \cdot s$.

Fig. 135. Effect of total pressure and partial pressure of oxidizers on burn-up rate of LiH-butyl rubber (60/40) composition. 1 - High consumption (9.2-12.6 $g/cm^2 \cdot s$);
2 - moderate consumption (4.9-7 $g/cm^2 \cdot s$); 3 - small consumption (1.4-2.8 $g/cm^2 \cdot s$).

Designation: ата = atm(abs.).

In the range of small oxidizer consumption values (C < 2.8 $g/cm^2 \cdot s$) burn-up of a fuel charge consisting of less than 50% LiH, coincides with the burn-up rate of pure butyl rubber both for the oxygen-fluorine oxidizer as well as the fluorine oxidizer alone. Only when the concentration of LiH exceeds 50% do we observe a substantial increase in the burn-up rate. In this range (C < < 2.8 $g/cm^2 \cdot s$) the burn-up rate, as was established by the authors

344

is virtually independent of pressure and may possibly be determined
by the aerodynamics of the turbulent boundary layer which is
formed on the surface of the solid fuel, as indicated by the
power dependence of the burn-up rate on fuel consumption with
an exponent of 0.8, which is qualitatively in agreement with
the expression for the combustion rate obtained for hybrid
mixtures by Maxman and his colleagues [310]:

$$\rho_{\tau} U = 0.036 G^{0.8} (\mu/x)^{0.2} B^{0.73},$$

(VII.7)

where G is the local mass flow, $g/cm^2 \cdot s$; x — the distance from
the leading edge of the charge, cm; μ — viscosity coefficient
of main flows, $g/cm \cdot s$; ρ_{τ} — density of fuel charge, g/cm^3;
B — mass exchange parameter, equal to $(u_t/u_b)(\Delta h/h_r)(u_t/u_b)$ — ratio
of velocity of main [reference] flow to velocity in zone of
flame; Δh — enthalpy difference between flame zone and fuel
surface; h_v — effective heat of fuel gasification; U — local
linear burn-up rate, cm/s.

In the range of high values for specific oxidizer consumption
(G > 7 g/cm^2 s) the combustion rate increases with increase in
the percent of LiH for all studied compositions and has a much
weaker dependence on the consumption of the oxidizer.

Maxman [311], unlike Smoot and Price, in testing engines
under laboratory conditions at chamber pressures higher than
10.5 kg/cm^2, found that adding metal in a case where its
concentration was less than 50% in the fuel had a noticeable
effect on the burn-up rate.

Data on the effect of total and partial oxidizer pressures
are shown in Fig. 135 for a composition of 60% lithium hydride +
+ 40% butyl rubber [308].

Although the burn-up rate values in this case are higher than for the nonmetallized systems, in these systems too we observe a similar dependence of burn-up rate on both the partial pressure of the oxidizer and its mass consumption and a virtual independence of total pressure. The theoretical estimate of the burn-up rate, which was based on the assumption of turbulent heat exchange in the boundary layer, does not explain the dependence of the burn-up rate on pressure which was observed in the experiment. Thus Smoot and Price [308] supposed that one of the determining factors of the effect observed for pressure might be the process of turbulent diffusion of the active oxidizer toward the surface of the fuel and the subsequent occurrence of a heterogeneous first-order reaction between the oxidizer and the condensed fuel.

By assuming that the diffusion rate of the oxidizer and the burn-up rate of the fuel were equal

$$U\rho_\tau = k p_\theta w,$$ (VII.8)

and writing the Reynolds analogy of the Chilton-Colburn modification between mass exchange and momentum exchange for mass exchange processes, taking into account the effect of the injection on the friction coefficient,

$$k_c \, Sc^{\prime} \, U_\infty = 0.03 \lambda B_\lambda \, \mathrm{Re}^{0.2} \, [\exp(B_\lambda) - 1],$$ (VII.9)

the authors indicated above obtained a dependence for the burn-up rate, which considered the effect of pressure and the mass consumption of the oxidizer, in the form of

$$\frac{p_{0\infty}}{u\rho_\tau} = \left\{ 33 \rho_\infty \left(\frac{x}{\mu} \right)^{0.2} Sc^{\prime} \, \frac{\exp(B_\lambda) - 1}{G^{0.8} B_\lambda \lambda} \right\} + 1/k.$$ (VII.10)

where λ is the part by weight of gaseous products formed during the decomposition of the solid fuel, which is a function of the equilibrium temperature of the fuel surface [307] (coefficient λ considers the decreased effect of the injection in the case where most of the decomposition products on the fuel surface are made up by the condensed phase); $B_1 = u\rho_T(GC_{/0}/2)$ is the injection parameter; $C_{/0} = 0.03/Re^{0.2}$ is the friction coefficient in the absence of an injection; k_0 – the local mass exchange coefficient, cm/s; k – chemical reaction rate constant s^{-1}; $p_{0\infty}$ – partial pressure of oxidizer in free flow, atm; p_{0W} – partial pressure of oxidizer near fuel surface, atm; $Re = Gx/\mu$ – Reynolds number; Sc – Schmidt number; U_∞ –velocity in free flow, cm/s.

Processing of experimental data on the burn-up rates for all fuel systems with three different oxidizers studied by the authors over a wide range of oxidizer values in the form of

$$p_{0\infty}^{\,\,\,\,\prime\prime\prime}\tau - \{(p_\infty[\exp(B_1\lambda - 1)]/B_1\lambda G^{0.8}\}\qquad(VII.11)$$

gives us a line with a slope of $33\cdot(x/\mu)^{0.2}Sc^{2/3}$, which intersects the Y-axis at the point with the $1/k$ value (Fig. 136). The values of λ obtained from [307] for charges of butyl rubber, polyurethane, 60% LiH + 40% butyl rubber, and 90% LiH + 10% butyl rubber are equal to 0.5, 0.5, 0.2 and 0.05, respectively.
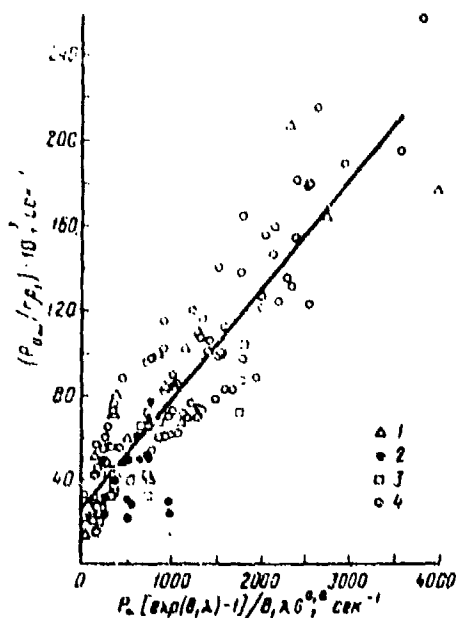

Fig. 136. Burn-up rate of hybrid fuels. 1 – Polyurethane, 2 – LiH + + butyl rubber 60/40, 3 – LiH + + butyl rubber 90/10, 4 – butyl rubber.

Designation: $сек^{-1} = s^{-1}$.

347

§ 3. Combustion Rate of Oxygen-Containing
Gas Systems with Aluminum

Cassel and his colleagues [313] measured the combustion rate
of powder aluminum in air and in various compositions of nitrogen
and oxygen. The rate was calculated by the Gauss equation based
on data obtained from the experiment: the area of the flame cone
and the velocity of the flow. From Table 42 we see that as the
concentration of aluminum particles increases the combustion
grows. This is related primarily to the growth of the maximal
combustion temperature, since all of the concentration values
presented in Table 42 are considerably lower than the stoichio-
metric composition - 315 mg/l. However, here too one might also
consider the increase in the screening effect (decrease in heat
losses resulting from radiation) with the increase in the
concentration of metal particles in the flow.

Table 42. Combustion rate values for
mixtures of powder aluminum and air.

Particle size, μ m	Concentra- tion, mg/l	Reynolds number	Combus- tion rate, cm/s
6—30	120	1420	19.2
6—30	160	1250	22.0
6—30	190	1430	23.8
30	210	1280	25.0

Although the authors do not present any data on the effect
of aluminum particle size on the combustion rate, they do note
that at the same concentration flames with finely-dispersed
aluminum have a much greater flashback tendency than with a
particle dimension of ~15 μm.

Table 43 shows measurements for flame propagation velocities
in a mixture containing 70% oxygen, 30% nitrogen, and powder
aluminum, arranged vertically in a glass tube measuring 2.5 cm
in diameter and 1.2 m in length. If we assume that the rates

348

observed are proportional to the combustion rates of mixtures in an open burner, then these results indicate an increase with a decrease in particle size. Considerable fluctuations in the flame propagation rate, reaching 50 cm/s, were noted (primarily in the second half of the tube).

Table 43. Combustion rate of a mixture 70% O_2 + 30% N_2 + aluminum.

Particle size of aluminum, μm	Al concentration, mg/l	Flame velocity, cm/s
40	100	35
	200	45
6 (80%)	150	100
6-10 (20%)	250	60

In the combustion of metallized gaseous, liquid, and solid fuels, as noted by many researchers [313, 354], a very important role is played by the heat radiation of the flame. The heat balanced equation for the heating zone with the radiation of the flame considered can be written in the form of

$$(c_p \gamma + c_d w)(T_i - T_0) V_H = \mu \left(\frac{T_{max} - T_i}{b} \right) + \frac{bw z \alpha F (T_{max}^4 - T_0^4)}{\rho_d r}, \qquad (\text{VII}.12)$$

where V_H is the combustion rate; μ – heat conductivity; T_i – ignition temperature; T_{max} and T_0 – maximal and initial temperatures of fuel mixture; σ – radiation coefficient of particle surface; c_p and ρ – specific heat capacity and density of gas; c_d, ρ_d, and w – specific heat capacity, density, and concentration of metal particles, respectively; r – average particle radius; α – coefficient which considers the radiation of the combustion products ($\alpha > 1$); F – geometric factor; b – width of combustion zone.

If we assume that the combustion time of the particles τ is determined only by the diffusion of oxygen to their surface (we ignore reactions on the surface), then

349

$$\tau = \rho_d r^2 R T_0^{*}/2 M D p T_a^{0.3}.$$ (VII.13)

where D is the coefficient of oxygen diffusion at tempertaure T_0; R - the gas, T_a - volume-averaged ambient temperature in reaction zone; p - average partial pressure of oxygen; M - oxygen equivalent of fuel expressed in grams of fuel per mole of oxygen.

Here the width of the combustion zone can be expressed

$$b = V_b \tau = V_{\text{M}} (\rho_{\text{M}}/\rho_b) \tau,$$ (VII.14)

where V_b is the rate of motion of the combustion product; ρ_{M}/ρ_b - ratio of densities of original mixture to combustion products.

Successive substitution of equation (VII.13) in (VII.14) and then in (VII.12) lets us express the combustion rate V_{M} of the gas mixture with the metal particles as parameters which can be determined from the experiment or reasonably assumed

$$V_{\text{M}}^2 = \frac{aDP}{r^2 k} \frac{T_{\max} - T_1}{T_1 - T_0 - \dfrac{r w k F \sigma a (T_{\max}^4 - T_0^4)}{\rho_d DP (c_p \rho + c_d w)}}.$$ (VII.15)

Here $a = \mu/(c_p \rho - c_d w)$ is the coefficient of the temperature conductivity of the mixture; $k = \rho_d \rho_{\text{M}} R T_{\text{M}}^{3/2}/2 M \rho_b T_a^{0.5}$.

It should, of course, be said that the obtained expression describes the change in rate as a function of certain parameters only qualitatively, since in its derivation all quantities were considered independent. However, the width of the combustion zone (equation (VII.12)), for example, is assumed for simplicity to be the same both in the case of heat transfer by radiation as well as heat conductivity. This quantity depends on r, w, and F, and they basically determine the combustion rate.

350

Expression (VII.15), as we see, predicts that the combustion rate should increase with a decrease in the particle size of the metal and should have a minimum.

§ 4. Combustion Rate of Thermite Compositions

In the 1860's the outstanding Russian scientist N. N. Beketov reacted barium oxide with aluminum and in this manner, as well as by his further studies to obtain alkali metals by subjecting their compounds to the action of metallic aluminum, founded a new branch of metallurgy - aluminothermy. Since then reactive mixtures of metal oxides with another metal, which reacts according to the system $Me_2O + Me_1 \rightarrow Me_1O + Me_2 + Q$, Cal (MeO - metal oxide and Me - metal), have been called thermites. Considering the large quantity of heat necessary to decompose a metal oxide, it becomes obvious that only fuels with a high heat capacity can be used in thermites.

Table 44 presents the properties of certain substances which characterize their use in thermites.

Table 44. Combustion heat (Cal/g) of thermite with stoichiometric ratio between components (Me/MeO ratio, %, given in parentheses).

Fuel	Oxidizer							
	B_2O_3	SiO_2	Cr_2O_3	MnO_2	Fe_2O_3	Fe_3O_4	CuO	Pb_3O_4
Al	0,73 (44/56)	0,56 (37/63)	0,60 (26/74)	1,12 (29/71)	0,93 (25/75)	0,85 (24/76)	0,94 (19/81)	0,47 (10/90)
Mg	0,91 (51/49)	0,73 (45/55)	0,74 (32/68)	1,18 (36/64)	1,05 (32/68)	0,94 (29/71)	1,0 (23/77)	0,5 (12/88)
Ca	0,81 (63/37)	0,70 (57/43)	0,67 (44/56)	1,10 (48/52)	0,93 (43/57)	0,87 (41/59)	0,94 (34/66)	0,51 (19/81)
Ti	—	—	0,29 (32/68)	0,75 (36/64)	0,57 (31/69)	0,56 (29/71)	0,70 (23/77)	0,35 (12/88)
Si	—	—	—	0,70 (24/76)	0,58 (21/79)	0,50 (19/81)	0,67 (15/85)	0,32 (7/93)
B	—	—	—	0,76 (14/86)	0,59 (12/68)	0,52 (11/89)	0,70 (8/92)	0,25 (4/96)

From the experiments of Zhemchuzhniy (cited from [2]) it follows that the amount of heat released during the combustion of thermites should be no less than 0.55 Cal/g; otherwise the combustion reaction is difficult and does not reach completion.

The oxide used to produce thermites should have a minimal heat of formation, contain oxygen (no less than 25-30%), have the greatest possible density, and be reduced into a metal which has a low melting temperature and a high boiling temperature.

It is unlikely that reactions in the gas phase will affect the combustion rate of the thermites. On the other hand, the original substances (aluminum and metal oxides) have high boiling points, which hinders the formation of the gas phase through evaporation; nevertheless, the relatively high chemical stability at high temperatures of metal oxides (as compared to the stability of organic fuels, nitrates, and chlorates) should lead to the development of high temperatures in the condensed phase, and as a result the main reaction should occur in the condensed phase without any preliminary "gasification" reaction.

The most thoroughly studied has been the combustion of the iron-aluminum thermite Fe_2O_3–Al [301-303] in a wide pressure range, beginning 10^{-2} mm Hg to 150 atm.

If we take a stoichiometric mixture of 75% Fe_2O_3 + 25% Al, then its combustion temperature with heat losses considered will be equal to 2700-3000°C (direct measurement gives us 2400°C). This is unconditionally higher than the evaporation temperature of aluminum of 2050°C, and thus the gas phase will be partially formed in this composition. In order to obtain an "absolutely" gasless combustion model, Merzhanov and his colleagues [315] diluted a mixture (25% Al + 75% Fe_2O_3) with a final combustion product - aluminum oxide - in a ratio of 70:30. In this case

calculated combustion temperature T_{max} was only ~150° higher than the boiling temperature of the most volatile component (of all original, final, and possible intermediate components) - aluminum - at atmospheric pressure. At this temperature all components (original and final) were in a molten state.

To check the calculation the combustion temperature of this composition was measured by the brightness method with the aid of an optic pyrometer in two ways: the temperature of the lateral surface - in this case the emissivity of the slag - was taken, based on tabulated data for liquid iron and aluminum oxide; the temperature in a semi-open cavity made in the specimen was measured - emissivity in this case was assumed equal to one. Error related to inaccurate emissivity, cooling of the lateral surface, and instrument error was ±100°. The temperature obtained from the experiment was 2100°C, i.e., 50° higher than the boiling point of aluminum. If we cons. 'er the rise in the boiling temperature of aluminum with pressure (even at $p \sim 50$ atm it is equal to $T_{кип} \sim 3600°C$), then we have more reason to assume that all components in the combustion process of the mixture react in the condensed phase.

Besides the iron-aluminum thermite, the combustion rate of the chromium-magnesium thermite $Cr_2O_3 + 3Mg \rightarrow 3MgO + 2Cr + 160$ Cal, the manganese-aluminum thermite $1.5MnO_2 + 2Al \rightarrow Al_2O_3 + 1.5Mn + 260$ Cal, and a mixture consisting of 80% reduced iron and 20% potassium permanganate [317] were studied.

The combustion temperature of the chromium-aluminum thermite (with heat losses considered) should be 2100-2200°C, and thus neither MgO ($T_{кип} > 3000°C$) nor Al_2O_3 ($T_{кип} > 2200°C$) should be found in a vapor state. Despite the high heat of conversion of the manganese-aluminum thermite (~1400 Cal per 1 kg of the mixture), its temperature should not be high, since it is regulated by the evaporation of the manganese ($T_{кип} \sim 1900°C$). As pressure rises

the combustion temperature should rise due to the increased
boiling temperature of the manganese. The potassium permanganate
and iron mixture should have little sensitivity to the external
atmosphere, except the forming oxides have a relatively low
dissociation pressure and the final temperature is low ($\sim 700°C$).

Figure 137 shows combustion rate values as the function of
pressure for different compositions.

As we see in Fig. 137 (curve 4), the combustion rate of
the iron-aluminum thermite increases in the entire studied
pressure range, even for the composition $Fe_2O_3 + Al + Al_2O_3$
(52.5/17.5/30) at temperatures below atmospheric; this increase
is, however, relatively slow and particularly slow at high
pressures. At a pressure of 200 mm Hg the combustion rate of
the thermite diluted by the final combustion product of Al_2O_3
is 0.85 cm/s, while at 20 atm [the thermite] consisting of
Fe_2O_3/Al (75/25) burns at a rate of 2.6 cm/s, i.e., only
about three times faster. However, its combustion rate at the
highest pressure of 140 atm is only 3 times faster than the
rate at atmospheric pressure. The nature of the change in
the combustion rate with pressure cannot be described by an
exponential law. Figure 137, curve 5, corresponds to the
chromium-magnesium thermite. The behavior of this curve is
extremely unique. At low pressures the combustion rate increases
more rapidly than it does for the iron-aluminum thermite: at
pressures of 40-50 atm it reaches a maximum combustion rate, and
as pressure continues to increase a marked decline in this rate
begins.

Figure 137, curve 6, corresponds to the thermite consisting
of $1.5 MnO_2 + 2Al$ and is similar to the curves for the iron-aluminum
thermite.
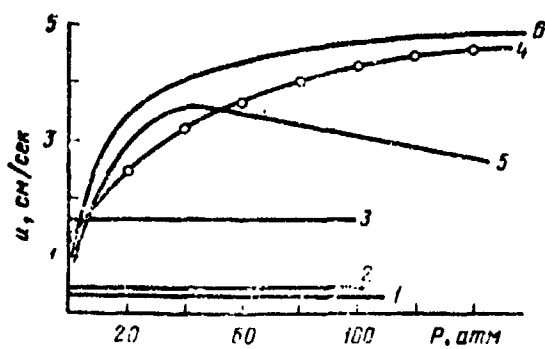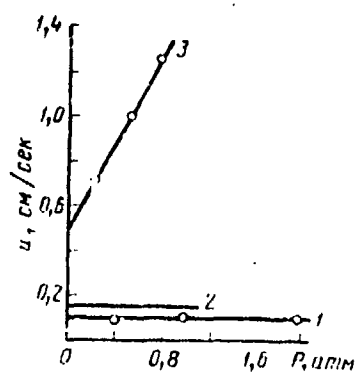
Fig. 137.   Fig. 138.

Fig. 137. Combustion rate of thermites as a function of pressure.

Fig. 138. Combustion rate of thermites in a vacuum. $1 -$ Fe + KMnO₄ (80/20);
$2-(Fe_2O_3+Al) + Al_2O_3$ (50/50); $3-(Fe_2O_3 + Al) + Al_2O_3$ (70/30) .

In the combustion of thermites of the chromium–aluminum
composition Cr_2O_3 + Al + Al_2O_3 (52.5/17.5/30) at pressures above
atmospheric (Fig. 137-1), Fe + $KMnO_4$ (80/20) in a pressure range
of 200 mm Hg - 2 atm and Fe_2O_3 + Al + Al_2O_3 (37.5/12.5/50)
(Fig. 138) in a vacuum, combustion rates are virtually independent
of pressure. We should note the difference in combustion rates
obtained by Maksimov [315] and Romodanova [316] for the thermite
Fe_2O_3 + Al + Al_2O_3 (52.5/17.5/30) (Fig. 137, curves 2 and 3,
respectively). This could possibly be related to the size of
the aluminum particles introduced into the mixture, since the
relative density of the specimens was approximately the same:
ρ/ρ_{max} = 0.65 and 0.5, respectively. In the first case aluminum
particles measuring ∿5 μm and above in diameter were used
in the preparation (particle size of iron oxide 1 μm), in the
second case - particles of less than 1 μm ($Fe_2O_3 \leq$ 100 μm).

The weight of the specimens had not changed after combustion,
and the thick slag which remained had cooled, keeping the shape
and size of the original tablet. During examination of the
structure of the slag it was noted that during combustion of the

355

thermite it had been in a liquid state. All of these facts
indicate the gasless combustion of the mixtures indicated above.
For all remaining thermites, where evaporation of the metal was
possible, combustion rate increased with pressure.

During the combustion of the composition $Fe_2O_3 + Al + Al_2O_3$
(52.5/17.5/30) in a vacuum ($P \leq 10^{-2}$ mm Hg) there is an intense
diffusion of the condensed substance - slag, particles of which
settle on the walls of the bell [sic]. The surface temperature
of this thermite, measured by means of a tungsten-rhenium thermo-
couple (7 µm), is equal to ~1200°C, while the ignition temperature
is ~880°C. Since as pressure decreases the boiling point of
aluminum also decreases, and in a vacuum (at p ~ 10^{-2} mm Hg) is
~1148°C, then obviously the forming aluminum vapors dispersed
the condensed substance of the reaction layer in the studied
specimen. As we see in Fig. 138, the combustion rate of the
composition depends on pressure.

With further dispersion of the mixture (Table 45) by the
final combustion product of Al_2O_3, the surface temperature of the
specimen drops and combustion is entirely (beginning at 40% Al_2O_3)
caused by reaction in the condensed phase, while the combustion
rate of the composition is independent of pressure.

Table 45. Surface temperature in combus-
tion of thermite $Fe_2O_3 + Al + Al_2O_3$ at
p ~ 10^{-2} mm Hg.

Composition, %			$T_{поп}$, °C
Fe_2O_3	Al	Al_2O_3	
60	20	20	1340
52,5	17,5	30	1200
45	15	40	1060
37,5	12,5	50	940

Let us examine curves 4 and 6 in Fig. 137 for iron-aluminum
and manganese-aluminum thermites. The greatest increase in rate
occurs at relatively low pressures; at high pressures there is
a saturation, as it were, and the combustion rate rises very
slowly. The total increase in the combustion rate when pressure
is increased to 150 atm is much lower than that which occurs
for powders in explosives. The increased rate with an increase
in pressure indicate that the gas phase articipates in the
reactions. In this case the gas phase is, evidently, aluminum
vapor. The relatively weak increase in the combustion rate
with pressure indicates that the role of the gas phase is in
this case limited.

Unlike the combustion of volatile explosives, where the
leading reaction occurs in the gas phase, in the combustion
of the thermites indicated above the reaction which occurs in
the condensed phase (it is to this reaction that we should
attribute the significant combustion rate component, which is
independent of pressure) is completed by the aluminum vapor
reaction in the iron oxide. If this reaction is not instantaneous,
then adsorption of the metal vapor should occur on the particle
surface of the oxide. Under this assumption the reaction rate
should depend on the amount of adsorbed aluminum. The amount
of vapor m adsorbed at different pressures p is expressed as
the Langmuir isotherm $m = abp(1 - bp)$, where a and b are certain
constants. According to the reduced ratio, at low values (bp << 1)
the amount of adsorbed vapor should increase linearly with
pressure; at high pressures (bp $\geq$ 1) this quantity should
asymptotically approach a certain limiting value (m = a). In
Fig. 137 we find the function

$$u = A + \frac{abp}{1 - bp}.$$ (VII.16)

where $A = 1.2$; $a = 36$; $b = 0.033$ at $p \geq 1$ atm; $A = 0.6$; $a = 0.04$;
$b = 0.033$ at $p < 1$ atm.

As we see, this function describes well the change in the combustion rate of iron-aluminum and manganese-aluminum thermites with the change in pressure. The presence of term A relates to reactions in the condensed phase, while $abp/(1 + bp)$ relates to adsorption of the aluminum vapor on the oxide particles with a subsequent reaction of the adsorbed aluminum.

The observed increase in the combustion rate of compositions Fe_2O_3 + Al and MnO_2 + Al can also be explained by the increased boiling temperature of aluminum (or magnesium) with pressure, which results in an increased temperature in the reaction layer of the condensed phase, and, consequently, an increase in the combustion rate; yet this is less likely. The fact is that in the studied case two substances react in the condensed phase, and the rate of this reaction is, in all probability, determined by the mixing time of the components, which may change relatively little (not exponentially) as temperature increases. If the maxwell temperature of the condensed phase were determining, then the combustion rate of thermites containing aluminum would considerably exceed the combustion rate of thermite with magnesium (because magnesium has a much lower boiling temperature); this, however, was not observed.

From the results given above (see Fig. 13δ), it is apparent that in the case of Al + Fe_2O_3; Fe_2O_3 + Al + Al_2O_3 (52.5/17.5/30 at p > 1 atm and 37.5/12.5/50 at p = 10^{-2} mm Hg) and Fe + $KMnO_4$ (80/20) in thermites in which a gas phase is absent during combustion (the evaporation of aluminum is, in particular, impossible), the chemical process also occurs exclusively in the condensed phase, the reaction rate does not depend on pressure, and in the case of extremely significant changes in the latter remains almost constant.
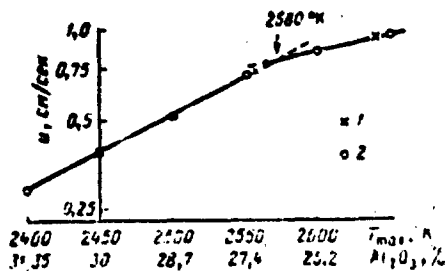
358

Fig. 139. Combustion rate of thermite $Fe_2O_3 + Al + Al_2O_3$ as a function of temperature. Density $\rho/\rho_{max} = 0.65$, 1 - combustion temperature varied by changing initial temperature, 2 - combustion temperature was varied by ammonium oxide dilution.

The temperature dependence of the combustion rate of thermite $Fe_2O_3 + Al + Al_2O_3$ (52.5/17.5/30) shows that the leading reaction occurs at temperatures close to maximal. The curve representing the dependence of $U(T_{max})$ (Fig. 139) has a break at a certain temperature $T_{max} = T'$, which is close to the boiling temperature of aluminum at atmospheric pressure. This is evidence of a breakdown under certain conditions of a gasless composition model as a result of evaporation of the more volatile component. The temperature coefficient of the combustion rate $T_{max} < T'$ is equal to $5.75 \cdot 10^{-3}$ deg^{-1} (for explosives and powders it is in a range of $3-8 \cdot 10^{-3}$ deg^{-1} [324]), at $T_{max} > T'$ $\alpha = 2.3 \cdot 10^{-3}$ deg^{-1} (from the data of Lukashenya [325] $\alpha = 2.2 \cdot 10^{-3}$ deg^{-1}).

If we assume that the diffusion is not a limiting process, which is, generally speaking, valid only for certain oxidizer particle dimensions in Fe_2O_3 and aluminum in a certain range of variation in the diffusion coefficient of liquid substances [318], then the reaction which leads the combustion process should occur in a kinetic regime. Thus, the laws governing the combustion of a gasless composition proposed in [315] can be qualitatively described if we use the thermal theory of flame propagation in homogeneous systems in which the diffusion coefficient is assumed to be equal to zero [319].

For a first-order reaction

$$u^2 = a \frac{e}{Q(1-\eta)} \frac{RT_{max}^2}{E} k \exp(-E/RT_{max}),$$

(VII.17)

359

where a is temperature conductivity, cm^2/s; R - the gas constant, Cal/mole·deg; k_0 - the preexponential factor, 1/s; E - activation energy, cal/mole; Q - thermal effect of chemical reaction of stoichiometric mixture in liquid state, cal/g; c - average heat capacity of mixture, cal/g·deg; η - percent concentration of aluminum oxide additive in mixture; T_{max} - maximal combustion temperature of composition.

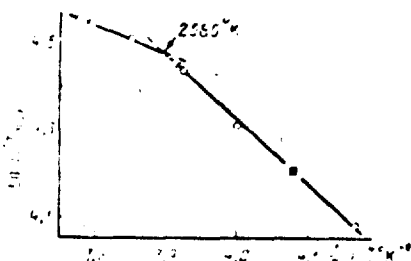Fig. 140. Combustion rate of thermite Fe_2O_3 + Al + Al_2O_3 in coordinates lg u/T_{max}-1/T.

Due to the absence of data on kinetic constants at the combustion temperature, it is difficult to compare expression (VII.17) quantitatively with the experiment. Nevertheless, the very nature of the dependence of the combustion rate on specimen density in terms of the magnitude of the temperature conductivity coefficient a = λ/cρ has been confirmed experimentally [315] (since during combustion the thermite remains a dispersion phase with ρ = const, then it might be expected that the dependence of λ(ρ) and a(ρ) is maintained over a broad temperature interval right up to temperatures observed in the flame front). In coordinates lg u/T_{max}-1/T_{max} the experimental points of the combustion rate lie well along a straight line (Fig. 140). The change in the slope of the line when T_{max} > T' is due to the beginning of noticeable evaporation in the aluminum and, as shown earlier, in this range the combustion rate changes with pressure. From the data of Fig. 140 the kinetic parameters of the reaction in the condensed phase of the thermite can be determined: E = 130 Cal/mole, k_0 = 10^{15} 1/s. The obtained value is close to the activation energy for the decomposition of ferrous oxide

360

FeO (120-129 Cal/mole) [323], which represents the intermediate decomposition product.

Data on the effect of various factors (pressure, the nature of the metal and the oxidizer, dispersion of the components, etc.) on the combustion rate of pyrotechnic compositions can be found in [1, 313].

CHAPTER VIII

EFFECT OF METALS ON MAIN PARAMETERS
EXPLOSIVE DETONATION

Many researchers [327-333] have studied the properties of explosives with various additives (aluminum, magnesium, boron, ice, sand, etc.). It was found that the addition of metals to certain explosives under certain conditions increases the high explosive effect of the blast, although the prisance of such explosives usually decline. Although the metals which are added detract some of the oxygen contained in the explosives, the energy loss resulting from incomplete combustion of the explosive is entirely compensated by the great heat of combustion of such metals as aluminum, magnesium, boron, silicon, etc., which form heat resistant oxides.

§ 1. Detonation of Metallized
Condensed Explosives

The earliest studies in this field date back to 1888-1905 with explosives, which were named ammonals, consisting of three basic components: ammonium nitrate, trinitrotoluene, and aluminum, were widely used. Table 46 shows a composition of six such mixtures.

In their presence ammonals were not comparable to such aromatic nitrocompounds as picric acid and trinitrotoluene. Nevertheless, their high explosive effect was considerably greater than that of the latter.

Table 46. Composition of ammonals (%).

Component	1 German	2 Russian	3 Russian	4 English	5 French	6 English
Ammonium nitrate	54	76,5	65	80	65	65
Trinitrotoluene	30	16,0	15	17	15	15
Aluminum	16	7,5	20	3	10	17
Carbon	—	—	—	—	10	3

Aluminum was first added to explosives in the form of a fine powder. Yet studies showed that it was not necessary to use aluminum in this form, since the desired effect could be better achieved with grain metal. The use of grain aluminum had another advantage in that it was oxidized much more slowly during storage than powder because of its much smaller effective surface (as a rule the protective film of Al_2O_3 is thicker on large particles [252]). It was assumed that its oxidation was probably the result of small quantities of free nitric acid, which is always contained in ammonium nitrate (in view of the hygroscopicity of this salt). The reason why grain aluminum can be used is, according to Kast [333], the fact that the oxidation of aluminum is a secondary process which occurs during the expansion of the explosion products, i.e., it reacts not when the explosive substance breaks down, but only with the products formed during the explosion, for example, according to the system

$$3CO_2 + 2Al \rightarrow 3CO + Al_2O_3 + 180,7 \quad Cal/mole.$$
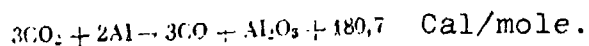
This idea by Kast, advanced on the basis of relatively little experimental material at the beginning of the century, has been only partially confirmed in more recent studies [328-331].

The detonation rate measurement for the simplest ammonal 80/20 (binary mixture of ammonium nitrate and aluminum), which were taken by Ratner and Hariton [328], showed that it was equal approximately to 4 km/s (at a charge density of 1.0 g/cm^3). This is considerably higher than the possible detonation rate of pure ammonium nitrate, which is ∿2.5 km/s.

The authors proposed that under certain conditions (a sufficient degree of grinding of the nitrate and a fine aluminum powder) that the aluminum would be oxidized practically to the point of expansion of the explosion products. However, the brisance effect of substances such as the 80/20 ammonal (and possibly other mixtures of no less caloricity) are not affected by that part of their energy which is contained in aluminum (metal) oxide vapors in the form of latent evaporation heat. During the expansion of the detonation products as a result of the drop in temperature the aluminum oxide solidifies, and this is accompanied by a release of condensation heat (120 Cal/mole), which does influence the high explosive effect. This creates (in the opinion of Ratner and Hariton [328], a disparity between the high explosives effect and the brisance effect of explosive aluminum as compared to other explosives.

In order to check this hypothesis the fugacity and brisance of ammonals of 90/10 and 95/5, less rich in aluminum, were tested. The temperature developed by these ammonals at which aluminum oxide should form in a solid state while still in the detonation wave was significantly lower. Thus, its condensation should be reflected in the brisance effect to a greater extent than for mixtures such as ammonal 80/20. These hypotheses by the authors, it would seem, have been confirmed by a comparison

of ammonals with ammotols of approximately the same caloricity (Table 47).

Table 47. Relative characteristics of ammotols and ammonals.

Trotyl or aluminum added to ammonium nitrate, %	Energy of decomposition, Cal/kg		Fugacity according to Trauzl		Brisance according to Hess (charge of 200 g, density 0.9)	
	ammotol	ammonal	ammotol	ammonal	ammotol	ammonal
20	1000	1600	1,200,400	520	20	21.8
10	700	1000	800,315	420	15.0	10.4
5	600	700	600,270	320	11.6	14.8

However, to a great extent these conclusions contradict the results obtained by Cook [335] and the literature data on the dependence of the vapor pressure of aluminum oxide on temperature [334].

Experimental results on the detonation rate D as a function of large diameter and percent concentration of aluminum (with constant density), obtained by various authors for mixtures of sodium nitrate and aluminum in a wide composition range from 100/0 to 70/30, as well as for mixtures of trotyl/Al, hexogen/ trotyl/Al, TG (trotyl and hexogen)/Al, are shown in Figs. 141 and 142, respectively. In all cases the detonation rate of the mixtures indicated above were considerably below the ideal rates calculated from the equations of state of the explosion products [336], regardless of the size of the NH_4NO_3 crystals and the aluminum particles (at least for a particle diameter of $d \geq 5$ μm), although, as we can see from Fig. 142, there is a certain tendency for the detonation rate to increase as the size of the aluminum particles decreases. The difference between the obtained detonation rate and the ideal rate is more significant for charges of

high density than of low density. As Cook notes, ratio D/D' can be less than one (D' is the ideal detonation rate), which is generally characteristic of fuels or explosives consisting of a combustible and ammonium nitrate. Nevertheless, as indicated in [337, 338], ratio D/D' for mixed charges of the oxidizer/fuel variety depends to a great extent on the diameter of the charge. Figure 143 shows dependences D = f(d) for mechanical mixtures of ammonium perchlorate and paraffin of 90/10 (grain size of NH_4ClO_4 is 10 μm) ρ_0 = 1.0 g/cm^{3} (curve 2), trotyl and colloidal boron 90/10 ρ = 0.65 g/cm^3 (curve 1), hexogen and ammonium nitrate 58/42 (grain size of NH_4NO_3 is 100 μm) (curve 4) and suspended hexogen with a particle size of 0.3-0.4 mm in tetranitromethane 30/70 (curve 3).
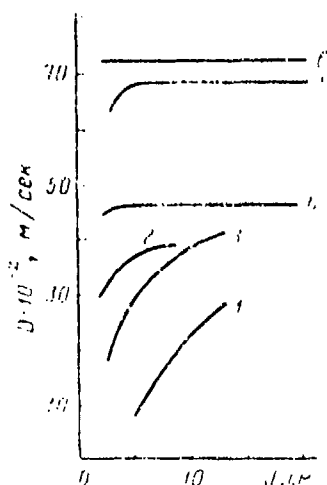

Fig. 141. Detonation rate D as function of charge diameter and concentration of aluminum. 1 – NH_4NO_3 + Al (98/2); 2 – trotyl + Al (80/20), $\rho_{зар}$ = 1.0 g/cm^3; 3 – NH_4NO_3 + Al (10/90); 4 – hexogen + + trotyl + Al (45/30/25), $\rho_{зар}$ = 1.15 g/cm^3, d_{Al} = 150-200 μm and d_{Al} < 40 μm; 5 – trotyl + Al (80/20), $\rho_{зар}$ = 1.75 g/cm^3; 6 – hexogen + trotyl + Al (45/30, 45), $\rho_{зар}$ = 1.77 g/cm^3, d_{Al} = 75-150 μm; $d_{Al} \leq$ 40 μm.

Designation: м/сек = m/s.

The main reason for the constant diameter within a certain range of charges with a nonideal detonation rate, corresponding to the decomposition energy of the oxidizer, which was observed for the indicated mixtures, is the reaction occurring in stages at the front of the detonation wave of the mixed explosives, which is caused by the decomposition kinetics of its components.
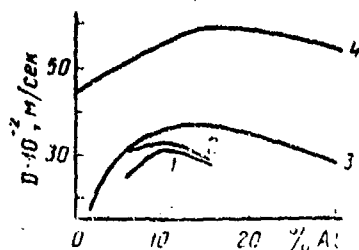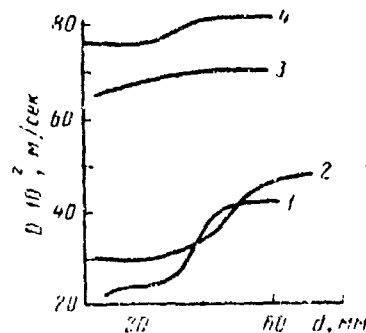
366

Fig. 142.   Fig. 143.

Fig. 142. Effect of Al particle size on detonation rate of explosives: 1 – NH_4NO_3 + Al, d_{Al} = 40-7, μm, $\rho_{зар}$ = 1.14 g/cm^3; 2 – NH_4NO_3 + Al, d_{Al} < 40 μm, $\rho_{зар}$ = 1.20 g/cm^3; 3 – NH_4NO_3 + Al, $\rho_{зар}$ = 1.05 g/cm^3; 4 – NH_4NO_3 + Al – calculated.

Fig. 143. Effect of charge diameter on detonation rate of mechanical systems.

The reaction in the wave is assumed to occur as follows: first the explosive components are completely broken down within their own volumes, then after a certain time interval (due to the difficulty of diffusion at detonation pressures of hundreds of thousands of atmospheres) the effective reaction of reaction completion between the products of their decomposition and the fuel begins. To a great extent this is confirmed by the fact that the detonation rate of the mixtures indicated above, calculated under the assumption of a reaction of only one explosive component (oxidizer) under certain conditions, are close to the nonideal detonation rate obtained experimentally at small charge diameters.

The increased detonation rate of the mixture of trotyl and colloidal boron at charge diameters greater than 40 mm indicate that metals (in particular boron) can burn in a detonation wave of condensed explosives releasing an additional quantity of heat, which increases the detonation rate (the detonation rate was

measured by ionization and optic methods, error in both cases did not exceed 50 m/s).

A great number of factors effect the rate at which energy is released in the detonation wave (reactivity of components, heat of explosion, dispersion and percent composition of mixture, charge density, etc.). The action of each of these for a specific explosive mixture is often difficult to define. However, the more the charge components vary in their dispersion, the greater will be the time difference between the decomposition of the components and the subsequent reaction completion and the greater the probability of observing a nonideal detonation rate.

The effect of the density of the explosives on the detonation rate was discovered in works [312, 326] with compositions of trotyl/Al, hexogen/trotyl/Al, and NH_4NO_3/Al (90/10), where approximately the same particle sizes were used in batches of aluminum and nitrate.

As we see in Fig. 144, the curve representing the dependence $D = D(\rho_0)$ passes through the maximal value in the charge density region of $\rho = 1.08$-1.15 g/cm^3. Cook [331] proposed that the development of this anomolous effect in $D = D(\rho_0)$ might reflect a change in the particle size of the ammonium nitrate during preparation of pressed charges. However, experiments with pressed charges and charges of bulk density prepared from nitrates which had been previously pressed and been ground (it was assumed that after this the particles would not change significantly), showed that the anomolous effect did not disappear.

We should note the higher detonation rate of explosives with a low density; this difference increases with an increase in the difference between the densities of the charges. A similar maximum was also observed on the curve representing the dependence $D = D(\rho)$ in the region of $\rho_0 = 1.08$ g/cm^3 for a mixed xplosive consisting of dinitrotoluene/ammonium nitrate (90/10) (see Fig. 144).
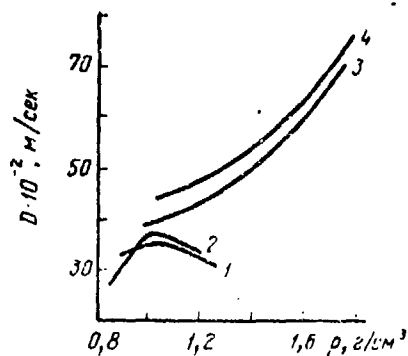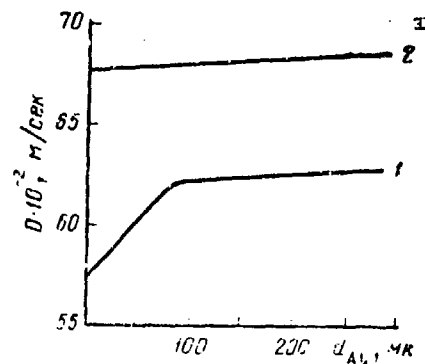
Fig. 144.   Fig. 145.

Fig. 144. Effect of density of aluminized explosives on detonation
rate: 1 - dinitrotoluene + NH_4NO, (10/90); 2 - NH_4NO_3 + Al (90/10);
3 - trotyl + Al (80/20); 4 - hexogen + trotyl + Al (45/30/25).

Fig. 145. Detonation rate of trotyl/aluminum system (85/15).
1 - ρ = 1.49 g/cm^3; 2 - ρ = 1.69 g/cm^3.

In addition to the indicated factors, the size of the
nitrate crystals also influence the detonation rate of the
NH_4NO_3/Al composition. It is difficult to vary the size of
the ammonium nitrate crystals over a wide range, and, in addition,
as noted by many authors, the reproducibility of results from
batch to batch is poor. Thus, in this problem it is not possible
to obtain results with sufficient reliability. Nevertheless, if
batches of ammonium nitrate differing greatly in their particle
size are used, then the average detonation rate will be approxi-
mately 1000 m/s lower for large NH_4NO_3 particles at the same
density and particle size in the aluminum.

In [283, 330, 331] the explosive characteristics of trotyl,
hexogen, trotyl-hexogen, and mixtures of $KClO_4$-Al, NH_4ClO_4-Al,
etc., were studied. Using a splitting-off method Dremin and
Pokhil [330, 340] measured the parameters of the detonation
wave of trotyl in the Chapman-Jouguet plane, adding aluminum
and other substances with different degrees of dispersion.
A great deal of attention in this work was given to the particle

size of the additive. The main concern of Cook in his work was to study the dependence of the detonation rate of an explosive with aluminum on the diameter of the charge, the percent of additive, and their original densities. The experimental data obtained by the authors indicated above have been reduced in Fig. 145 and in Table 48.

All charges had a length to diameter ratio L/d of 6/8. Variation in density along the axis and the radius was no more than 2%. In order to avoid the fusion of aluminum particles, charges of both densities were subjected to prolonged vibrations. For comparison Table 48 shows the detonation wave parameters for trotyl, hexogen, and an alloy of trotyl and hexogen at the densities which they would have in charges with aluminum, tungsten, and quartz sand. If the additive is inert in the detonation wave, then its effect on the detonation parameters should be determined entirely by its physical properties, such as density, heat capacity, heat conductivity, etc.

Stesik and Akimova [339], studying the effect of Al on the detonation rate and critical diameter of trotyl and hexogen, arrived at the conclusion that when the density of these explosives is high, aluminum does not have a chance to react in the chemical reaction zone of the detonation wave, while in low-density trotyl ($\rho = 1.00$ g/cm^3), where the reaction zone is greater, the aluminum begins to oxidize. This follows from the fact that adding 15% aluminum in the form of powder to trotyl reduces the critical diameter from 9 to 8 mm. One might expect a decrease in the critical diameter in this case because of the hindered dispersion of the explosion products. However, experiments with this same percent concentration of talc (oxides of $3MgO \cdot 4SiO_2 \cdot H_2O$), whose density is approximately equal to that of aluminum $\rho = 2.7$-2.8 g/cm^3, did not reveal a decrease in the critical diameter.

Table 48. Parameters of trotyl detonation wave with 15% various additives.

Additive	Particle density of additives, g/cm³	Particle size of additive, μm	Density of mixed charge ρ_1, g/cm²	Density of trotyl in charge ρ_0, g/cm³	Detonation rate D, km/s	Speed of explosion product u, km/s	Pressure $P \cdot 10^9$, bar
Al	2.70	0.2	1.49	1.38	5.75	1.27	109
Al	2.70	80	1.49	1.38	6.20	1.45	134
Al	2.70	270	1.49	1.38	6.27	1.47	137
SiO₂	2.70	Powder	1.49	1.38	5.98	1.51	135
SiO₂	2.70	270	1.49	1.38	6.27	1.53	143
W	19.1	0.4	1.49	1.28	5.68	1.33	113
Al	2.70	0.2	1.69	1.59	6.76	1.71	196
Al	2.70	270	1.69	1.59	6.84	1.73	200
SiO₂	2.70	Powder	1.69	1.59	6.45	1.60	173
SiO₂	2.70	270	1.69	1.59	6.64	1.64	183
W	19.1	0.4	1.84	1.59	6.72	1.58	196
—	—	—	—	1.28	6.00	1.56	120
—	—	—	—	1.38	6.28	1.66	144
—	—	—	—	1.59	6.94	1.83	202

Particles greater than a certain size are heated incompletely, absorb less heat, and as a result their influence is less than that of the finer particles. If we know reaction time τ and the temperature conductivity of the material of the particles added a, then we can estimate the dimensions of the particles r which will be heated [through], $r \sim (a\tau)^{0.5}$. In the reaction time interval of 10^{-6}–10^{-8} s the amount of metal particles heated through varies from 10 to 1 μm, while for oxides such as MgO, Al_2O_3, and SiO_2 it varies from 0.5–1.0 to 0.1–0.05 μm (it should be mentioned that the heat conductivity of the materials under conditions close to normal was used in the calculations).

Energy lost in compression of the additives (right up to 20–30% of the additive) is not great, and reduces the detonation wave parameters by no more than 1–5% (quartz sand with its anomolous compressibility is an exception [303]). If we maintain the idea that the particles of the additive are not able to react completely in the reaction zone of the detonation wave, then when their dimensions are increased, their influence should also decrease. It is possible that for this reason Cook [331], using aluminum particles with a rather large size in experiments with trotyl/aluminum (80/20) or hexogen/trotyl/aluminum (45/30/25), did not observe the particle size of aluminum to have any noticeable effect on critical diameter or detonation rate, and came to the conclusion that although aluminum reacts, its reaction is not the determining parameter of the detonation wave.

Thus, it is probable that additives such as SiO_2 with a particle size of d > 1 μm and aluminum with a particle size of d > 10 μm, which are shown in Table 48, are not heated [through]. This means that they do not react, i.e., they display inert behavior. Even if it is heated, tungsten, by virtue of its low heat capacity (0.035 cal/g·deg), absorbs an insignificant amount of energy and since its melting point even at atmospheric pressure equals 3370°C, then we can also consider its behavior to be inert.

The data presented in Fig. 144, as well as theoretical calculations, indicate that the dependence of the detonation rate $D = D(\rho_0)$ for a mixture of trotyl and aluminum (80/20) and trotyl/hexogen/aluminum (45/30/25) is not linear. It seems evident that this dependence is determined, as Cook believes, by the presence of lower aluminum oxides in the explosion products.

Under normal conditions (p = 1 atm, T = 293°K) aluminum oxide, as noted in the first chapter of this monograph, is a crystalline substance with a heat of formation of 400 Cal/mole . Its melting temperature is 2313°K, and its melting heat is 26 Cal/mole. So far opinion is divided concerning its boiling temperature. Experimental and theoretical calculations conducted by various authors [341-344] put this temperature value in the rather broad range of 2900-3770°K and give 120 Cal/mole as the heat of evaporation. There is reason to believe that at high temperatures Al_2O_3 is not stable and breaks down into lower oxides of AlO and Al_2O.
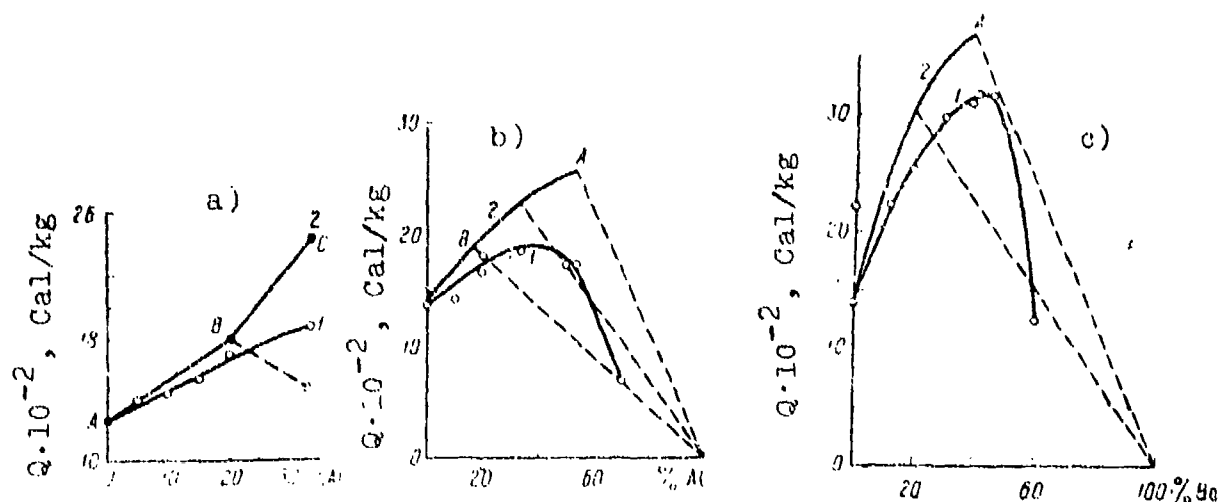

Fig. 146. Explosion heat of hexogen with additive Al (a, b) and Be (c). 1 - Experiment, 2 - theory.

373

We know that the amount of oxygen contained in most explosives (trotyl, hexogen, PETN, and others, for example) is insufficient to completely oxidize all of the carbon and hydrogen. Nevertheless, when aluminum is added up to certain limits to trotyl, hexogen, and ammonium nitrate, then as follows from the data obtained in [343], the heat of explosion per unit weight of the mixture increases: aluminum, which possesses a high combustion heat, is capable of removing oxygen from the oxides of carbon and hydrogen.

Figure 146 shows the explosion heat of hexogen with Al and Be. The upper line (curve 2, Fig. 146a) gives the numerical value of the heat released for hexogen under the assumption that initially, when less than 19.5% aluminum is added (from point A to point B) the aluminum is capable of taking oxygen only from CO_2 and H_2O, and does not take oxygen from CO. From this it follows that the most effective reaction occurs according to the system

$$C_3H_6N_6O_6 + 2Al \rightarrow Al_2O_3 + 3CO + 3H_2 + 3N_2.$$
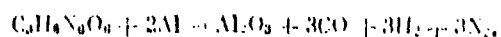
A further increase in the aluminum from this standpoint should have only a negative effect, if the aluminum is not capable of reacting with the CO. The maximal heat of explosion of the mixture of hexogen and aluminum according to the equation should be 1790 Cal/kg. We assume that the aluminum is capable of taking all of the oxygen; then from the reaction equation

$$C_3H_6N_6O_6 + 4Al \rightarrow 2Al_2O_3 + 3N_2 + 3C$$
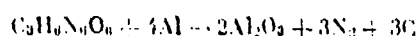
it follows that this corresponds to a heat release of 2440 Cal/mole for an aluminum concentration of 32.5-33%. The reduction of CO to carbon should for this reason give a considerable increase in the heat of explosion (curve 2 from point B to point C). Because of the low heat of formation of CO, the oxidation of aluminum by CO is advantageous from the energy standpoint. Thus, the calculated

combustion heats of compositions containing more than 20% aluminum should increase more rapidly, which is evident from Fig. 146a. In this case, where all of the oxygen and nitrogen interreact with aluminum according to the system

$$C_3H_4N_6O_6 + 8Al = 2Al_2O_3 + 6AlN + 3C + 3H_2.$$
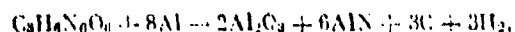
the maximum heat release corresponds to an addition of Al equal to 50-52% and itself is ~2600 Cal/kg (curve 2, Fig. 146b). The straight portion of dependence Q on the percent of aluminum, which runs down the right side from point B, indicates a decrease in heat release resulting from the fact that the excess aluminum has nothing left to interact with and plays the role of the inert constituent. It should be mentioned that in all calculation results presented above the formation of solid Al_2O_3 was assumed, which is quite natural for bomb calorimeter conditions or conditions close to them.

Now let us compare the experimental and theoretical curves. For mixtures containing less than 20% aluminum the divergence is not very great, constituting only 20-30%. This is explained, apparently, by the incomplete reaction of the aluminum under the bomb conditions.

When the concentration of aluminum is greater than 20%, the divergence between the theoretical and experimental explosion heat values begins to rise drastically (for an aluminum concentration higher than 20% water was absent). This can be attributed to the fact that although the reaction of aluminum with CO is advantageous from the energy standpoint, the process itself is difficult. The reaction of aluminum with CO can be easily seen in the diagram. The experimental value for the explosion heat of a mixture containing 67% hexogen and 33% aluminum lies midway between the value calculated under the assumption that the aluminum uses all of the oxygen and the value of 1480 Cal/kg, calculated according to the following system under the assumption

375

that oxygen is not taken from CO (dashed lines in Fig. 146b):

$$3,02C_3H_6N_6O_6 + 12.2Al \rightarrow 9,06CO + 3,04Al_2O_3 + 6,18Al + 9,06H_2 + 9,06N_2.$$
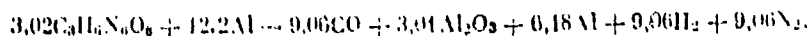
The data presented in Fig. 146a and b indicate that with the
indicated concentration of aluminum approximately half of the
CO enters into a reaction with the aluminum, as follows from
the heat calculation according to the following system:

$$3,02C_3H_6N_6O_6 + 12.2Al \rightarrow 4,53CO + 4,53C + 4,51Al_2O_3 + 3,18Al + 9,06H_2 + 9,06N_2.$$
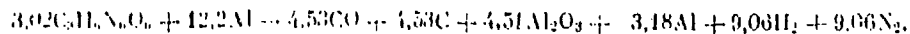
Here the "ideal" heat of 1950 Cal/kg, which is close to the
explosion heat for this mixture obtained in the experiment,
should be released.

Thus, the carbon monoxide is capable of reacting with the
aluminum, so that an increase of above 20% in the aluminum
concentration basically provides a certain increase in the
explosion heat, dispite the fact that the quantity of unused
aluminum, which represents the inert constituent, increases
significantly. In practical terms, however, the heat increase
when more than 20% aluminum is added is not great.

Region B-A (see Fig. 146b) is a region of predominately
nitride reaction. Thus, if from point B we draw a line
corresponding to the change in explosion heat of the hexogen
under the assumption that aluminum does not react with nitrogen
after all of the oxygen is used, then it will intersect the
experimental curve $Q = f(Al, \%)$. This fact points to the possible
reaction of aluminum with nitrogen and the formation of nitride.
The arrangement of points on curve 2 (see Fig. 146a, b),
corresponding to the beginning and end of certain reactions, is
conditional; actually all reactions are interconnected and,
depending on the conditions of the experiments, a certain balanced
composition of explosion products is established during the
explosion.

Experimental curve 2 (Fig. 146c) shows the change in heat release in mixtures of hexogen with powder beryllium as a function of its percent concentration in the mixture. In the given case, as we see from a comparison of curve 1 and curve 2, the nitride reactions are more marked. A considerable part of the area bounded by curve 2 is located in the nitride region of B-A.

The heat of explosion of an explosive with aluminum added increases up to a certain limit, although such detonation wave characteristics such as velocity, pressure, and velocity of explosion products, diminish. The experimental values for the rate of motion of the explosion products u for total and inert additives, as shown by Dremin and Pokhil [330], are well described by the formula

$$u = u_0 \rho_0 / \rho_1.$$ (VIII.1)

where u_0 is the velocity of explosion products of pure trotyl with a density of ρ_0 in a mixed charge and ρ_1 is the density of the mixture.

Table 49 shows velocity values for explosion of products determined experimentally and calculated according to formula (VIII.1). As we see in Table 49, the addition of aluminum to trotyl (even very fine) does not have a positive effect on this parameter of the detonation wave either.

Table 49. Rate of motion of explosion products (u, km/s) for trotyl with 15% of different additives.

Density, g/cm³	$\rho_1 = 1.0$ $(\rho_0 = 1.35)$				$\rho_1 = 1.7$ $(\rho_0 = 1.9)$					
Additive	Al			SiO$_2$	W	Al		SiO$_2$		W	—	—
Particle diameter of additive, μm	0.2	80	270	Powder	270	0.4	0.2	270	Powder	270	0.4	—	—
$u_{эксп}$, km/s	1.27	1.45	1.47	1.51	1.53	1.33	1.71	1.73	1.60	1.64	1.58	1.66	1.83
$u_{расч}$, km/s	—	—	1.54	—	—	1.34	1.72		1.59		—	—

377

From the experimental data presented above it cannot be concluded that aluminum does not react in the chemical reaction zone of the detonation wave. The addition of aluminum lowers the parameters of the detonation wave of condensed explosives more than do inert additives. This fact indicates that aluminum reacts to a different degree depending on particle size. If we take into account the heat which is spent in heating the aluminum particles (it is assumed that the temperature of the explosion products is 3000°K), then this reduces the detonation parameters by 4-5%, while experimental data for such explosives as trotyl, hexogen, and TG indicate a significantly greater change.

Basing his study on experiments to determine the work of an explosion under conditions of a lead bomb (similar to the Trauzl bomb) and under ballistic mortar conditions [344] (device for determining absolute work of explosion [345]) Belyayev was probably the first to come to the conclusion that aluminum is oxidized to the lower oxides during detonation of aluminized explosives.

The greatest expansion in a lead bomb was obtained from a mixture of hexogen and aluminum, containing 15-20% Al. If the expansion which can be produced by hexogen is taken as unity, then a mixture with 20% Al has a relative expansion of ~1.2 times. This corresponds to a work increase of approximately 25%, while the heat of explosion increases by 33%. Thus, in a mixture with 20% aluminum we observe a considerable increase in work, although this is considerably less than the increase in heat.

Another pattern is observed when experiments are conducted in a ballistic mortar: maximal work is also obtained in this case by adding 15-20% Al, although the work of the explosion of the 20% mixture is only 4% higher than that of pure hexogen. This considerable decrease in work in a mortar is characteristic not only of mixtures of hexogen and aluminum, but other aluminized

explosives. Mixtures of ammonium nitrate and aluminum in a
ballistic mortar also reduce work as compared to the data
obtained for a lead bomb, and do not differ in this respect
from mixtures of hexogen and aluminum.

Here it is important to note that explosives and mixtures
which do not contain aluminum have proportional indicators
in lead bombs and in ballistic mortars.

It can be assumed that the reason for the small work value
in the mortar is the relatively slow combustion of the aluminum.
The degree of expansion of the explosion gases in the mortar is
actually much lower than in the lead bomb: in the mortar the
degree of expansion is ~ 8, while in the lead bomb expansion is
usually 30-60 times. Thus, work in the mortar is accomplished
by high-temperature gases (the temperature of the already
"spent" exploding gases is 0.75 of the maximal temperature).
Yet the time of completing the work in the mortar is prolonged
(the time from the beginning of the explosion to the escape
of the piston-projectile is several milliseconds, and is less
than 0.5 μs for a lead bomb). Consequently, the proposal above
appears to have little foundation.

This fact is a serious argument against the explanation
for the reduced brisance effect of aluminized explosives observed
under some conditions as exclusively the reaction of the aluminum
with the explosion products, which passes into the second stage
relatively slowly (this hypothesis, as already noted at the
beginning of this chapter, was proposed by Kast [333]). Actually,
if during an air explosion the second stage (stage of reaction
of aluminum with products) is completed during the time of
expansion (which follows directly from determining the impulse
and the pressure of the shock wave at significant distances),
then there is all the more reason why under ballistic mortar
conditions this second stage should be completed in a period which
is many times greater than the case of a closed volume and higher
pressure.

379

Under certain conditions (a rather lar.,e charge diameter, careful and prolonged mixing of the components during preparation of the mixtures, submicron particle dimensions in the metal, etc.) aluminum, beryllium, boron (as shown by Apin and Voskoboynikov [329]), other metals too may react effectively with the decomposition products of one of the components of the explosive, although this circumstance cannot be the main reason for the small amount of work produced in the ballistic mortar.

The proposal by Hariton and Ratner [328] that aluminum reacts in the chemical reaction zone of the detonation wave forming Al_2O_3, which evaporates accompanied by the absorption of a significant amount of energy (which also reduces the detonation parameters), is not very probable. Brewer and Searcy [341], in analyzing gases over a boiling Al_2O_3 surface, came to the conclusion that Al_2O_3 does not exist in the gas state, but decomposes during evaporation with the formation of the lower oxide, which is unstable and in turn is transformed into Al_2O_3 [342] (the heat of formation of Al_2O_3 is approximately 3^n Cal/mole). Thus, it is probable that chemical equilibrium does not exist in a detonation wave of aluminized explosives and mixtures of aluminum with oxygen. Brewer and Searcy [341] propose that the most probable reaction for the liquid aluminum oxide is the following:

$$Al + AlO \rightarrow Al_2O_2 \ (ss),$$
$$Al_2O_2 + O \rightarrow Al_2O_3 \ (ss).$$
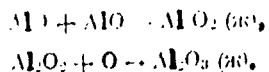
The authors of [341] registered Al_2O_3 in very small quantities in vapors over boiling aluminum oxide. However, in a spectroscopic analysis of the emission from the flame of a Bunsen burner when aluminum was burned with oxygen, Al_2O_3 was not detected [345]. For this reason the reaction probably does not play a significant role in the formation of aluminum oxide. Cook [331] thinks that in explosives mixtures Al_2O_3 is formed according to the system

380

$$Al_2O + 2CO_2 \rightleftarrows Al_2O_3 + 2CO,$$
$$Al_2O + 0.5CO_2 \rightleftarrows 0.5Al_2O_3 + 0.5CO.$$
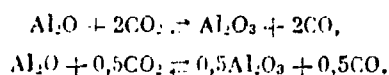
The constants of these reactions can be represented in the form of

$$K_{r_2} = 10^{21.4} \cdot 10^{-63\,000/T},$$
$$K_{r_4} = 10^{13.3} \cdot 10^{-40\,000/T}.$$

At temperatures and pressures which exist in the Chapman-Jouguet plane for mixtures of hexogen/aluminum, trotyl/aluminum, trotyl and hexogen/aluminum at low charge densities (1.0-1.5 g/cm^3), the main oxidation product of aluminum may be the lower oxide Al_2O, in the formation of which the oxygen which was formerly bound to the other product (CO_2, H_2O) is used. The heat of formation for these products, 94 and 59 Cal/mole, is accordingly much higher than the heat of formation for Al_2O (39 Cal/mole). Thus, aluminum appears to have an endothermic effect. Furthermore, when any aluminum oxides are formed the composition of gases declines (they may even decrease in quantity), which should also cause the detonation parameters to decline. Thus, Belyayev [283] showed that the work capacity of explosives with high-molecular explosion products was less than that of explosives having explosion products with a low molecular weight.

As the density of the charge increases (1.5 g/cm^3), due to a faster increase in pressure in the detonation wave than in temperature, ratio $Al_2O_{\text{газ}}/Al_2O_{3\text{тв}}$ should decrease, as assumed by Cook [331], although remaining considerable. Thus, even in this case the formation of the high-exothermic product Al_2O_3 cannot duplicate the endothermic effect of Al_2O in the Chapman-Jouguet plane of compositions such as trotyl, hexogen, and TG.

381

However, it seems to us that the most convincing view with respect to this question is held by Dremin and Pokhil [330, 340, 347], who believed that the aluminum does not react at all at the front of the detonation wave at high explosive charge densities (at least for aluminum particles greater than 0.2 μm).

Actually, when the density of the explosive is increased the width of the chemical reaction zone of the detonation wave increases, just as reaction time [347]. Thus, as shown above, no aluminum particles of any size manage to become heated in this case, and they behave as the inert additive SiO_2.

As we have seen, the detonation rate of all studied high-temperature aluminized explosives is, without exception, below that of corresponding without aluminum, despite the fact that their density is 6-8% higher (as the density of the charge is increased, the detonation rate also generally increases). It is possible, if we take charges of less density than those used in the work discussed above, that conditions may arise under which the lower aluminum oxides will be converted in the reaction zone into Al_2O_3, which should lead to higher detonation parameters.

As for composition consisting of ammonium nitrate/aluminum, an excess of oxygen when the aluminum concentration is less than 20% and rather high temperatures in the detonation wave (2600-3000°K) indicate that ratio Al_2O_{ras}/Al_2O_3 should be close to zero. However, ideal rates were not obtained in the experimental data presented above [331] for , it seems to us, two reasons: the explosive charge diameters taken were not large enough, and relatively large aluminum particle dimensions were used. Ideal detonation regimes would probably be observed only in charges of low density and high metal particle dispersion.

In ammonium nitrate/aluminum mixtures (unlike trotyl/aluminum, trotyl/hexogen/aluminum, hexogen/aluminum) mass and heat transfer in the gas phase begin to have a substantial role during detonation. The temperature of the latter compositions in the first decomposition stage of the main component is always close to the final explosion temperature, regardless of the concentration of aluminum (in the 0-15% range), while the temperature during the decomposition of ammonium nitrate alone in a mixture with aluminum does not exceed 1700°C (maximal temperature of a mixture is 2600-3000°K depending on concentration of aluminum). The sharp decline in the detonation rate as charge density increases (pressure in the chemical reaction zone grows, see Fig. 144) indicates that the limiting factor is mass transfer (diffusion is inversely proportional to pressure, heat transfer is absent).

Table 50. Effect of aluminum concentration on detonation capacity of APC/aluminum mixtures (particle size of APC 63-160 μm; ρ = 1.1-1.2 g/cm^3).

Concentration of aluminum, %	Critical detonation diameter, mm			
	conical paper tubes		cylindrical glass tubes	
	detonation	failure	detonation	failure
2.0	—	—	30	—
5.0	6	8	6,4	5,0
9,6	11	10	13,7	10,4
18,3	14	12	14,7	14,7
25,5	20	19	—	—

In [284] the detonation capacity of a mixture of ammonium perchlorate and aluminum was studied (the critical detonation diameter for charges with a density of 1.1-1.2 g/cm^3 in paper cones or cylindrical glass tubes was used as the measure of detonation capacity). It was established that when the concentration of aluminum is increased from 5 to 25%, this capacity decreases significantly.

The critical detonation diameter increased approximately 3-4 times (Table 50).

§ 2.   Detonation of Oxygen/Aluminum
System

Strauss [348] relatively recently published the result of an investigation of detonation in mixtures of aluminum powder and oxygen.

The study was performed on a device consisting of replacable tubes measuring 19.5, 26.4, 44, and 55.2 mm in diameter and 2.7 m in length. These were mounted vertically, and the other end of tube was filled with a mixture of powder and gas. This mixture then settled downward. The igniter, consisting of a pyrotechnic fuse, detonators, and explosive silver wires measuring 0.113 in diameter and 0.49 mm in length were placed at the upper end of the tube. Detonation pressures were determined in a metal tube measuring 27 mm in diameter by two diametrically opposed piezo-electric crystal sensors, mounted on the inner wall of the detonation tube at a distance of 2.5 m from the ignition point. The induction distances and propagation rates of the detonation waves were determined by mirror photographic detectors, which followed the flames being propagated in the glass tubes.

Prior to ignition the mixture was at room temperature and atmospheric pressure. In the experiment needle and spherical aluminum powders with diameters of 40 and 5 μm, respectively, were used. In order to remove water vapors and prevent the formation of powder clumps in the supply system, the aluminum was heated to 120°C prior to use. The concentration of aluminum oxide in the powder was 1.5-2.5% by weight.

The calculated Reynolds number for the oxygen flow was less than 1.00, and the presence of the powder in the gas flow decreased turbulence [349].

The distance from ignition to the point at which the velocity reached a stationary value was considered to be the induction distance. At first the flame front moved slowly. Then the movement of the flame was accelerated, possibly because the flow of the mixture in front of it became turbulent, while shock waves heated the mixture. Finally, ahead of the main flame ignition occurred, and the flame front was drastically accelerated and became smooth, emitting very strong radiation. Past the induction distance we observe thin oscillations in the flame front, whose frequency depends on tube diameter and the type of aluminum powder used (Table 51).

Table 51. Effect of diameter size of tube and powder type on frequency of spin shifts and wavelengths.

Powder	Tube diameter, mm	Wavelength, cm	Frequency, s^{-1}	λ/d
Spherical (5)	26.4	10.8	14,300	4.09
Needle (40)	26.4	9.0	16,200	3.41
Needle (40)	44.0	15.2	9,700	3.45

By applying the solution for a rotary pressure wave to the Rayleigh equation for natural vibrations in a cylindrical channel, Fey [350] showed that the step of spin shift λ, divided by the diameter of the tube, could be determined as

$$\lambda/d = \frac{\pi}{1.841} u/c.$$

(VIII.2)

where u is the detonation rate, c - the speed of sound in the gas directly behind the normal shock wave front.
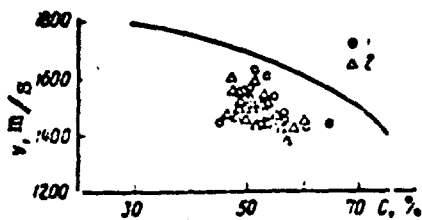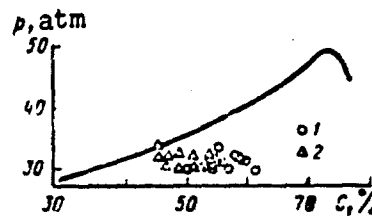
Fig. 147.   Fig. 148.

Fig. 147. Detonation rate of oxygen/aluminum mixture as a
function of aluminum concentration: —— - theory, 1 - spherical
particles, 2 - flake particles.

Fig. 148. Pressure at detonation wave front of oxygen/aluminum
mixture: —— - theory, 1 - spherical particles, 2 - flake
particles.

Figure 147 shows the established velocities of detonation
wave developing in the mixtures studied by Strausss as a function
of the percent concentration (C) by weight of aluminum. As we
see in the figure, the velocities of the waves do not depend on
tube dimensions, and are only somewhat higher toward the
spherical powder. Velocity values for the poorer mixtures are
approximately 1550 m/s and decline somewhat as the concentration
of aluminum increases.

The speed of sound in a gas in front of a normal shock wave
(at a rate of motion equal to the corresponding velocity in the
detonation mixtures of aluminum powder and oxygen) should,
according to calculations, be about 750 m/s. Then the ratio of
pitch to diameter for a rotary transverse pressure wave from
equation (VIII.2) under these conditions would be 3.5. This
quantity is close to the experimental (see Table 51).

Insignificant fluctuations, registered by two diametrically
opposed sensors, were phase shifted by 180° and, probably,
reflect the spin nature of the wave front.

The results of pressure measurements are shown in Fig. 148. The values obtained are approximately 11 atm for all mixtures containing from 45 to 60% aluminum.

From Figs. 147 and 148 we see that the measured detonation rates and pressures are respectively 9 and 14% below the theoretical quantities calculated for mixtures of aluminum powder and oxygen by the methods described in [353]. It was assumed that the following components were present in the detonation wave: gaseous O, O_2, Al, Al_2, AlO, Al_2O, Al_2O_3 and liquid Al_2O_3 oxide. The following initial conditions were taken: mass velocity of nonreacting mixture was equal to zero, temperature $298.16°K$, pressure 1 atm, and the aluminum powder contained 2% oxide.

The calculations indicate that the theoretical detonation rate values should be approximately equal to those measured for a Al_2O_3 oxide concentration of 20%. This does not correspond to the conditions of the experiment. The proposal of an adiabatic detonation process and the absence of convective losses in the calculations was entirely justified in view of the insignificant width of the front of the detonation wave and its high propagation rates. Although the radiation emitted by an aluminum frame burning in oxygen is considerable [354], nevertheless the mean free path of the radiation is not great due to the heterogeneous nature of the reagents and the combustion products. Thus, it is not possible to explain the great difference between the theoretical and experimental detonation rate for the indicated mixtures by this factor.

It is most probable that for mixtures of aluminum and oxygen, just as for metallized explosives, in the first stage the aluminum is only partially oxidized to Al_2O_3, and the main reaction products are the lower oxides AlO and Al_2O, whose heat of formation, as already noted, is much less than that of Al_2O_3.

387

BIBLIOGRAPHY

1. Сб. «Физика и химия реактивного движения». N. 1—3. М., ИЛ, 1949, стр. 65.
2. А. А. Шидловский. Основы пиротехники. М., Оборонгиз, 1964.
3. A. C. Gross, T. B. Conway. Ing. Eng. Chem., 50, 663 (1958).
4. А. П. Григорьев. Твердые ракетные топлива. М., «Химия», 1969.
5. Жидкие и твердые ракетные топлива (сб. переводов под ред. Ю. X. Шаулова). М., ИЛ, 1959.
6. Сб. «Исследование ракетных двигателей на твердом топливе». М., ИЛ, 1963, стр. 171.
7. E. Gulbransen. Rev. Sci. Instruments, 15, 201 (1944). Trans. Electrochem. Soc., 81, 327 (1942), 97, 383 (1950), 111, 103 (1964); 110, 476 (1963). J. Phys. Chem., 51, 1087 (1947).
8. Сб. «Процессы горения». М., ИЛ, 1961, стр. 375.
9. H. M. Cassel. Combustion and Flame, 6, 9 (1962).
10. J. S. Dunn. Proc. Roy. Soc., A 11, 203 (1926).
11. P. Kofstad. High temperature oxidation of metals. New York — London, Academic Press, 1966.
12. Химическая энциклопедия. М., «Советская энциклопедия», 1968.
13. N. B. Pilling, R. E. Bedworth. Inst. Metal, 29, 529 (1923).
14. Г. В. Самсонов, К. П. Портной. Сплавы на основе тугоплавких соединений. М., Оборонгиз, 1961.
15. Э. В. Бриуке, А. Ф. Капустинский. Термические константы неорганических веществ. М., Изд-во АН СССР, 1949.
16. Н. П. Герасимов, А. Н. Крестовников, А. С. Шахов. Химическая термодинамика в цветной металлургии, т. 1—4. М., Металлургиздат, 1960—1964.
17. В. К. Григорович. Периодический закон Менделеева и электронное строение металлов. М., «Наука», 1966.
18. Сб. «Исследования при высоких температурах». М., ИЛ, 1962, стр. 128.
19. J. Brewer, A. Searcy. J. Am. Chem. Soc., 22, 1793 (1954); 78, 4169 (1956).
20. R. Ackermann, R. Thorn. J. Am. Chem. Soc., 78, 4169 (1956).
21. N. Erdway, R. Siefert. J. Electrochem. Soc., 98, 83 (1951).
22. W. Chpka, J. Berkowitz, G. Grese. J. Chem. Phys., 30, 827 (1959).
23. B. Weber, W. Thompson. J. Am. Ceram. Soc, 40, 363 (1957).
24. P. Johnson. J. Am. Ceram. Soc., 23, 168 (1950).
25. E. Wilkendorf. Chem. Ing. Tech., 24, 533 (1954).
26. D. Kirby. Metallurgia, 30, 65 (1944).
27. P. Brace. J. Electrochem. Soc., 94, 170 (1948).
28. H. Wartenberg, H. Mochl. Z. Physik. Chem., 128, 439 (1937).
29. Ceramic Fabrication Processes (ed. W. D. Kingery). London; Cambridge Mass., 1958.
30. W. Kingery. J. Am. Ceram. Soc., 36, 403 (1953); 37, 107, 389 (1954); 38, 251 (1955); 39, 377 (1956).

31. *W. Kingery.* Property Measurement at High Temperatures. N. Y., Academic Press, 1959.

32. *Л. Г. Блох.* Основы теплообмена излучением. М.— Л., Госэнергоиздат, 1962.

33. *А. В. Соколов.* Оптические свойства металлов. М., Физматгиз, 1961.

34. *Л. Н. Свет.* Температурное излучение металлов и некоторых веществ. М., «Металлургия», 1964.

35. *А. И. Гордон.* Основы пирометрии. М., «Металлургия», 1964.

36. *Т. Р. Гаррисон.* Радиационная пирометрия. М., «Мир», 1964.

37. *Г. Грёбер, С. Эрк, У. Григуль.* Основы учения о теплообмене. М., ИЛ, 1958.

38. *Э. Р. Эккерт, Р. М. Дрейк.* Теория тепло- и массообмена. М.— Л., Госэнергоиздат, 1961.

39. Сб. «Техника высоких температур». М., ИЛ, 1959, стр. 157.

40. *К. С. Шифрин.* Рассеяние света в мутных средах. М., Гостехиздат, 1951.

41. *В. А. Петров.* Излучательная способность высокотемпературных материалов. М., «Наука», 1969.

42. *H. Gorton.* J. Am. Ceram. Soc., 39, 278 (1956).

43. *H. H. McMahon.* J. Opt. Soc. Am., 40, 376 (1950).

44. Таблицы по светорассеянию (под редакцией К. С. Шифрина и И. Л. Зельмановича). Л., Гидрометеорологическое издательство, 1968.

45. Handbook of thermophysical properties of solid materials. Oxford, Pergamon press, 1961.

46. *R. Seifert.* Phys. Rev., 73, 1181 (1948).

47. *W. Jost.* Diffusion in Solids, Liquids and Gases. N. Y., Academic Press, 1952.

48. *J. Roberts, C. Wheeler.* Trans. Faraday Soc., 56, 570 (1960).

49. *А. П. Гуляев.* Металловедение. М., «Металлургия», 1966.

50. *М. М. Хрущев, М. А. Бабичев.* Зав. лаб., 16, 52 (1950).

51. *Э. В. Поляк, С. В. Сергеев.* ДАН СССР, Новая серия, 30, 136 (1941).

52. *М. Л. Славинский.* Физико-химические свойства элементов. М., Изд-во черной и цветной металлургии, 1952.

53. *L. De Brouckere.* J. Inst. Met., 71, 131 (1945).

54. *H. Wilsdorf.* Nature, 168, 600 (1951).

55. *K. Thomas, M. Roberts.* J. Appl. Phys., 32, 70 (1961).

56. *М. В. Мальцев, Ю. Д. Чистяков, М. И. Цыпин.* ДАН СССР, 99, 813 (1954).

57. *Б. Ф. Ормонт.* Структуры неорганических веществ. М., Гостехтеоретиздат, 1950.

58. *D. Aylmore, S. Gregg, W. Jepson.* J. Inst. Met., 88, 205 (1960).

59. *N. Cabrera, J. Hamon.* C. R. Acad. Sci., Paris, 224, 1713 (1947).

60. *Н. Д. Данков, Л. В. Игнатов, Н. А. Шишаков.* Электронографические исследования окисных и гидроокисных пленок на металлах. М., Изд-во АН СССР, 1953.

61. *G. Preston, J. Birchenhau.* Phil. Mag., 20, 706 (1935).

62. *S. Dobinski.* Phil. Mag., 23, 397 (1937).

63. *M. Hirashima.* J. Phys. Soc. Japan, 10, 1055 (1955).

64. *W. Smeltzer.* J. Electrochem. Soc., 103, 209 (1956); 105, 67 (1958).

65. *O. Kubaschewski, H. Ebert.* Z. Metallk., 38, 232 (1947).

66. *А. В. Новоселова, Л. А. Бацанова.* Аналитическая химия бериллия. М., «Наука», 1966.

67. *Н. П. Попиров, Г. Ф. Тихинский.* Физическое металловедение бериллия. М., Атомиздат, 1958.

68. *Д. Уайт, Дж. Берк.* Бериллий. М., ИЛ, 1960.

69. *Дэв. Дарвин, Дж. Боддери.* Бериллий. М., ИЛ, 1962.

70. *В. М. Амоненко, В. Е. Иванов.* Физика металлов и металловедение, 12, 865 (1961).

71. *R. Holden, R. Speiser, H. Johnston.* J. Am. Chem. Soc., 70, 3897 (1948).

72. *D. Ginnigs, T. Douglas, A. Ball.* J. Am. Chem. Soc., 73, 1236 (1951).

73. *D. Aylmore, S. Gregg, W. Jepson.* J. Nuclear Materials, 2, 169 (1960).

74. *Р. А. Беляев.* Окись бериллия. М., Атомиздат, 1962.

75. *Я. И. Ольшанский.* ДАН СССР, 59, 1105 (1948).

76. *N. Erway, R. Seifert.* J. Electrochem. Soc., 98, 83 (1951).

77. *J. Grossweiner, R. Seifert.* J. Am. Ceram. Soc., 34, 2701 (1952).

78. *K. Kelley.* J. Am. Chem. Soc., 41, 1217 (1939).

79. *J. Brewer.* Chem. Rev., 52, 1 (1953).

80. *J. Coreman, P. Snyder.* J. Am. Chem. Soc., 75, 3102 (1953).

81. *A. Joeb.* J. Am. Ceram. Soc., 37, 96 (1954).

82. *A. Laubengayer, A. Newkirk, J. Hoard.* J. Am. Chem. Soc., 65, 1924 (1943).

83. *G. Cueilleron.* J. Ann. Chem., 19, 459 (1944).

84. *Г. А. Гальченко, А. М. Корнилов, Б. И. Тимофеев, С. М. Скуратов.* ДАН СССР, 127, 1016 (1959).

85. C. Tallen. J. Phys. Chem., 63, 311 (1959).
86. H. Johnson, H. Hersh, Kerr. J. Am. Chem. Soc., 73, 1112 (1951).
87. Г. В. Самсонов, А. Н. Марковский, А. Ф. Жигач, М. Г. Валяшко. Бор, его соединения и сплавы. Изд-во АН УССР, 1960.
88. А. А. Немодрук, З. К. Каралова. Аналитическая химия бора. М., «Наука», 1964.
89. W. Shaw, D. Hudson, G. Danielson. Phys. Rev., 89, 900 (1953).
90. F. Weintraub. Ind. Eng. Chem., 3, 2 (1911); 5, 106 (1913).
91. A. Souben, J. Margrave. J. Am. Chem. Soc., 78, 2911 (1956); 59, 132 (1935).
92. Г. Б. Бокий. Введение в кристаллохимию. М., Изд-во МГУ, 1954.
93. Г. Герцберг. Атомные спектры и строение атомов. М., ИЛ, 1948.
94. J. Cuillleron. Ann. Chem., 19, 459 (1944).
95. A. Jeunard. J. Am. Rocket. Soc., 68, 284 (1946).
96. Справочник по редким металлам (под редакцией К. А. Гемпел). М., «Мир», 1965.
97. Ю. И. Остроушко и др. Литий, его химия и технология. М., Атомиздат, 1950.
98. B. Deal, H. Svec. J. Am. Chem. Soc., 75, 6173 (1953).
99. О. А. Сонгина. Редкие металлы. М., «Металлургия», 1964.
100. А. Н. Несмеянов. Давление пара химических элементов. М., Изд-во АН СССР, 1961.
101. В. М. Гуськов. Производство магния. М., ОНТИ, 1938.
102. Н. А. Шишаков, Н. К. Андрющенко. ЖФХ, 30, 1966 (1956).
103. M. Boursion, J. Grall, R. Caillat. Rev. Metall, 54, 185 (1957).
104. T. Jeantiz, F. Rhines. Trans. AIMME, 166, 265 (1946).
105. Н. А. Маколкин. ЖПХ, 24, 460 (1951).
106. W. Fassell, J. Gesbranson, J. Jents, J. Hamilton. J. Metals, 3, 532 (1951).
107. J. Burns. Trans. ASM, 40, 144 (1948).
108. G. Siebel. Z. Metallk., 39, 97 (1948).
109. A. Keil. Z. Metallk., 42, 13 (1951).
110. О. Кубашевский, В. Гопкинс. Окисление металлов. М., «Металлургия», 1965.
111. W. Robertson, H. Uhlig. J. Electrochem. Soc., 96, 27 (1949).
112. H. Svec, D. Gibbs. J. Electrochem. Soc., 104, 434 (1957).
113. W. Campbell, V. Thomas. Trans. Electrochem. Soc., 91, 623 (1947).
114. А. И. Сарахов. Весы в физико-химических исследованиях. М., «Наука», 1968.
115. M. Dignam, W. Faucett. J. Electrochem. Soc., 113, 656 (1966).
116. Vacuum Microbalance Techniques, vol. II (ed. R. Walker). N. Y., Plenum Press, 1962, p. 153.
117. Thermal Imaging Techniques (ed. P. Glaser, R. Walker), N. Y., Plenum Press, 1964.
118. J. Boggio, R. Plumb. J. Chem. Phys., 44, 1081, 1966.
119. O. Heavens. Optical Properties of Thin Solid Films. Butterworths Scientific Publications, 1955.
120. J. Tronstad. Trans. Faraday Soc., 31, 1151 (1935).
121. A. Winterbottom. Z. Elektrochem., 62, 811 (1958).
122. W. Smeltzer. J. Elektrochem. Soc., 103, 209 (1956).
123. C. Cochran, W. Sleppy. J. Electrochem. Soc., 108, 322 (1961); Rev. Science Instr., 29, 1135 (1958).
124. A. Jenkins. J. Inst. Metals, 84, 1 (1955).
125. J. Barkowitz-Mattuck. J. Electrochem. Soc., 111, 908 (1964).
126. R. Perkins, D. Crooks. J. Metals, 13, 490 (1961).
127. R. Bartlett. Trans. AIME, 230, 1097 (1964).
128. P. Pierce. Am. Ceram. Soc. Bull., 39, 271 (1960).
129. А. Мачек, Р. Фридман, Дж. Семпл. Сб. «Гетерогенное горение». М., «Мир», 1967, стр. 21.
130. Д. Б. Сполдинг. Основы теории горения. М.— Л., Госэнергоиздат, 1959.
131. Физические измерения в газовой динамике и при горении. М., ИЛ, 1957.
132. Р. Фристом, А. А. Вестенберг. Структура пламени. М., «Металлургия», 1969.
133. R. Friedman, A. Macek. Combustion and Flame, 6, 9 (1962).
134. R. Friedman, A. Macek. 9th Symposium (Int.) on Combustion. New York—London, Academic Press, 1963, p. 703.
135. A. Macek. 11th Symposium (Int.) on Combustion. The Combustion Institute. Pittsburg, 1967, p. 203.
136. H. Cassel, I. Liebman. Combustion and Flame, 3, 467 (1959).
137. В. М. Фебел, Б. А. Напп, Л. Л. Хильденбранд, Р. Н. Серика. Сб. «Исследование ракетных двигателей на твердом топливе». М., ИЛ, 1963, стр. 175.
138. Л. А. Горбон. Сб. «Исследование ракетных двигателей на твердом топливе». М., ИЛ, 1963, стр. 181.
139. Ч. Дрю, А. Горбон, Р. Книпп. Сб. «Гетерогенное горение». М., «Мир», 1967, стр. 35.

140. «Heterogeneous combustion» (ed. by H. G. Wolfhard). New York — London, Academic Press, 1964.
141. L. DeVos. Physica, 20, 690 (1954).
142. K. P. Coffin. Burning times of magnesium ribbons in various atmospheres. NASA-TN-3332, 1954.
143. Т. Бржустовский, И. Глассмэн. Сб. «Гетерогенное горение». М., «Мир», 1967, стр. 59.
144. К. Толли. Сб. «Исследование ракетных двигателей на твердом топливе». М., ИЛ, 1963, стр. 186.
145. A. Cross, T. Conroy. Ind. Eng. Chem., 50, 663 (1958).
146. L. Nelson, I. Jundberg. J. Phys. Chem., 63, 433 (1959).
147. J. Nelson, N. Richardson. J. Phys. Chem., 68, 1268 (1964).
148. L. S. Nelson. Science, 148, 1594 (1965).
149. J. Nelson. Pyrodynamics, 3, 131 (1965).
150. J. Nelson. Nature, 207, 741 (1965).
151. J. Nelson. 11th Symposium (Int.) on Combustion. Pittsburg, The Combustion Institute, 1967, p. 409.
152. W. Parkinson, E. Reeves. Proc. Roy. Soc., A262, 409 (1961).
153. N. Kuebler, J. Nelson. J. Opt. Soc. Am., 51, 1411 (1961).
154. А. Ф. Беляев, Ю. В. Фролов, А. И. Коротков. ФГВ, 4, 323 (1968).
155. В. И. Лаврентьев, В. Г. Пелль. Скоростная киносъемка камерой СКС-2. М., «Искусство», 1963.
156. Н. Н. Бахман, А. Ф. Беляев. Горение гетерогенных конденсированных систем. М., «Наука», 1967.
157. А. С. Дубовик. Фотографическая регистрация быстропротекающих процессов. М., «Наука», 1964.
158. Л. Я. Кашпоров. 7-я Республиканская межвузовская конференция по вопросам испарения, горения и газовой динамики дисперсных систем. Одесса, Изд-во ОГУ им. И. И. Мечникова, 1967.
159. И. П. Куратов, Б. А. Гончаров. Специальные виды киносъемки. М., «Искусство», 1959.
160. J. Trostel, H. Frevert. Chem. Met. Eng., 30, 141 (1924).
161. A. Boyle, F. Lewellyn. J. Chem. Soc. Ind., 69, 843 (1950).
162. В. А. Федосеев. Труды ОГУ им. И. И. Мечникова, серия физ. наук, вып. 7. Одесса, 1960.
163. В. А. Федосеев. Физика горения. Киев, «Наукова думка», 1966, стр. 17.
164. В. А. Федосеев, С. М. Контуш, Л. В. Иванченко. Физика горения. Киев, «Наукова думка», 1966, стр. 26.
165. Б. Е. Гладков, Л. В. Федосеев. Физика горения. Киев, «Наукова думка», 1966, стр. 37.
166. Сб. «Кинетика и термодинамика химических реакций в низкотемпературной плазме» (под редакцией Л. С. Полака). М., «Наука», 1965, стр. 165.
167. М. А. Гуревич, Б. П. Сотниченко. Труды ЛПИ, № 280, 91 (1967).
168. М. А. Гуревич, А. М. Степанов. ФГВ, 2, 189 (1968).
169. М. А. Гуревич, А. М. Степанов. ФГВ, 3, 334 (1968).
170. Сб. «Прикладная магнитная гидродинамика». М., «Мир», 1965, стр. 70.
171. Ф. А. Цандер. Проблема полета при помощи реактивных аппаратов. М., Гос. авиац. и автотракт. изд-во, 1932.
172. Н. Ф. Похил, В. С. Логачев, В. М. Мальцев, В. А. Селезнев. Горение металлизированных конденсированных систем. М., ИХФ АН СССР, 1962.
173. В. С. Логачев. Кандидатская диссертация. М., ИХФ АН СССР, 1965.
174. Н. Ф. Похил, В. С. Логачев, В. М. Мальцев. ФГВ, 6, 80 (1970).
175. Н. А. Фукс. Механика аэрозолей. М., Изд-во АН СССР, 1955.
176. H. Castel, J. Lichman. Combustion and Flame, 2, 447 (1958); 6, 153 (1962).
177. А. И. Беляев. Электрометаллургия алюминия. М., Металлургиздат, 1953.
178. А. К. Бабко, И. В. Пятницкий. Количественный анализ. М., «Высшая школа», 1968.
179. З. С. Мухина. Физико-химические методы анализа металлов и сплавов. М., «Высшая школа», 1959.
180. Г. Ван-де Хюлст. Рассеяние света малыми частицами. М., ИЛ, 1961.
181. G. Mir. Ann. Physik, 25, 377 (1908).
182. M. Rayleigh. Phil. Mag., 41, 107, 274, 447 (1871); 47, 375 (1899).
183. W. Batel. Einführung in die Korngrossenmesstechnik. Springer — Verlag, 1960.
184. R. Gumprecht, C. Sliepcevich. J. Phys. Chem., 57, 90 (1953).
185. M. Prop. Chem. weekbl., 51, 489 (1961).
186. M. Beizin, K. Butler. J. Electrochem. Soc., 101, 149 (1954).
187. К. Печковская, И. Орловский, С. Силанювская. Каучук и резина, 3, 28 (1957).
188. H. Rose, B. Sullivan. Nature, 184, 4647 (1959).
189. В. П. Аксенов, К. П. Крученовий. ЖФХ, 33, 2153 (1963).

190. А. М. Бонч-Бруевич. Радиоэлектроника в экспериментальной физике. М., «Наука», 1966.
191. F. Gucker. Proceedings 11th Industrial Waste Conference, May, 1956, p. 284.
192. M. Tisher, S. Katz, A. Lieberman. Ibid., p. 268.
193. А. Г. Тихтионов. Изв. АН СССР, серия геофиз., 11, 218 (1959).
194. В. Д. Бассеич. Приборы и техн. эксперим., 6, 89 (1957).
195. П. Ф. Похил. Докторская диссертация. М., ИХФ АН СССР, 1954.
196. П. Ф. Похил. Сб. «Физика взрыва», № 2. М., Изд-во АН СССР, 1953.
197. П. Ф. Похил, А. Д. Ромоданова. ЖФХ, 39, 2757 (1965).
198. Э. И. Максимов, А. Г. Мержанов. ДАН СССР, 157, 412 (1964).
199. G. Heath, R. Hirst. 8th Symposium (Int.) on Combustion. N. Y., Williams and Wilkins, 1962, p. 711.
200. J. Vandenkerkhove. ARS — Journal, 10, 1466 (1961).
201. J. Hightower, E. Price. 11th Symposium (Int.) on Combustion. Pittsburg. The Combustion Institute, 1967, p. 463.
202. J. Watermeier, W. Aungst, S. Pfaff. 9th Symposium (Int.) on Combustion. New York — London. Academic Press, 1963, p. 316.
203. L. Pocinelly, H. Rosenstein. AJAA, 2, 10 (1962).
204. П. Ф. Похил, Л. Д. Ромоданова. Сб. «Тепло- и массоперенос», № 4. Минск, 1966, стр. 18.
205. J. Vandenkerkhove, A. Jacquotte. 8th Symposium (Int.) on Combustion. Baltimore, Williams and Wilkins, 1962, p. 650.
206. П. Ф. Похил, В. С. Толачев, В. М. Мальцев. ФГВ, 6, 143 (1970).
207. П. Ф. Похил, В. С. Толачев, В. М. Мальцев и др. ЖФХ, 39, 1281 (1965).
208. П. Ф. Похил и др. ЖФХ, 12, 2359 (1968).
209. V. A. Seleznev, P. F. Pokh l. Combustion and Flame, 13, 139 (1969).
210. J. Powling, W. Smith. Combustion and Flame, 6, 173 (1962).
211. А. И. Гордон. Основы пирометрии. М., «Металлургия», 1964.
212. А. А. Зенин. Кандидатская диссертация. М., ИХФ АН СССР, 1962.
213. О. А. Геращенко, В. Г. Федоров. Тепловые и температурные измерения. Киев, «Наукова думка», 1965.
214. А. Е. Кадышевич. Измерение температуры пламени. М., Металлургиздат, 1961.
215. И. И. Соболев. Докторская диссертация. М., ФИАН им. П.Н. Лебедева, 1953.
216. Ф. И. Баграт, Х. М. Строк. Физические измерения в газовой динамике. М., ИЛ, 1957.
217. Сб. «Температура и ее измерение». М., ИЛ, 1960, стр. 77.
218. Г. Рибо. Оптическая пирометрия. М.—Л., ГТТИ, 1934.
219. В. М. Мальцев. Кандидатская диссертация. М., ИХФ АН СССР, 1961.
220. П. Ф. Похил, В. М. Мальцев, Л. И. Гальперин. ЖФХ, 34, 1132 (1960).
221. В. М. Мальцев, П. Ф. Похил. ДАН СССР, 132, 636 (1960).
222. П. Ф. Похил, В. М. Мальцев, Г. В. Лукашеня. ЖФХ, 35, 5 (1961).
223. А. Г. Гейдон. Спектроскопия пламен. М., ИЛ, 1959.
224. А. Г. Гейдон, Х. Г. Вольфгард. Пламя, его структура, излучение и температура. М., ИЛ, 1958.
225. Сб. «Радиационные измерения температуры слабонагретых тел» (под редакцией В. Г. Вафиала). Минск, Изд-во БГУ, 1969, стр. 49.
226. А. Г. Сепридор, И. И. Соболев. ЖЭТФ, 24, 93 (1953).
227. L. Greg. Brit. J. Appl. Phys., 16, 957 (1965).
228. D. Thomas. Combustion and Flame, 12, 541 (1968).
229. H. G. Wolfhard, W. G. Parker. Proc. Phys. Soc., 62B, 523 (1949).
230. А. Л. Гейдон, И. Герл. Ударная труба в химической физике высоких температур. М., «Мир», 1966.
231. R. M. Moyerman, K. Shuler. Science, 118, 612 (1953).
232. W. Snelleman. Combustion and Flame, 11, 464 (1967).
233. H. Strong, F. Bundy, D. Larson. 3th Symposium (Int.) on Combustion. New York — London. Academic Press, 1949, p. 641.
234. A. Von Engel, J. Cozens. Proc., Phys. Soc., 82, 85 (1963).
235. A. Mellor. Pyrodynamics, 3, 65 (1965).
236. А. Меллор, Б. Глассман. Сб. «Гетерогенное горение». М., «Мир», 1967, стр. 164.
237. Т. Бржустовский, И. Глассман. Там же, стр. 126.
238. Т. Бржустовский, И. Глассман. Там же, стр. 91.
239. D. Kuehl. Pyrodynamics, 3, 65 (1965).
240. C. M. Drew, R. H. Knipe, A. S. Gordon. Pyrodynamics, 4, 325 (1966).
241. J. Crump, J. Prentice, K. Kraeutle. Combustion Science and Technology, 1, 205 (1969).
242. P. Hill, D. Adamson, D. Foland, W. Bressette. Nat. Advisory Comm. Aeron. Res. mem., 1965.
243. I. Dean. ARSJ, 31, 463 (1961).
244. R. Вуд. Сб. «Исследование ракетных двигателей на твердом топливе». М., ИЛ, 1963, стр. 191.

245. *R. Friedman, R. Nugent*, 6th Symposium (Int.) on Combustion. N. Y., Reinhold, Publishing Corp., 1957, p. 641.

246. *A. Davis*. Combustion and Flame, 7, 359 (1963).

247. *П. Ф. Похил, Л. Д. Ромоданова, В. М. Мальцев, В. С. Логачев, В. А. Селезнев*. Тезисы Первого Всесоюзного симпозиума по горению и взрыву. М., «Наука», 1968, стр. 44.

248. *А. Ф. Беляев, Б. С. Ермолаев, А. И. Коротков, Ю. Ф. Фролов*. Там же, стр. 93.

249. *R. A. Rhein*. Pyrodynamics, 3, 161 (1965).

250. *D. Smolenski, M. Severynum*. Bull. Woiskowej akademii Techn. j Dabrowskiego, 12, 37 (1963).

251. *А. Ф. Беляев, Б. С. Ермолаев, А. И. Коротков, Ю. В. Фролов*. ФГВ, 2, 207 (1969).

252. *П. Л. Данков*. ЖТФ, 12, 251 (1942).

253. *Д. Клее*. Ракетная техника и космонавтика, 12, 83 (1968).

254. *A. Macek, J. M. Semple*. 12th Symposium (Int.) on Combustion. Pitsburgh, Pennsylvania, 1968.

255. *М. А. Гуревич, И. М. Кирьянов, Е. С. Озеров*. ФГВ, 5, 217 (1969).

256. *A. Macek, J. Semple*. AIAA 5th Propulsion joint specialist Conf., Colorado, 1969.

257. *В. А. Федосеев*. Физика аэродисперсных сред, вып. 1. Киев, Изд-во Киевского университета, 1969, стр. 86.

258. *J. Prentice, C. M. Drew, H. C. Christense*. Pyrodynamics, 3, 81 (1965).

259. *Г. А. Варшавский*. Горение капли жидкого топлива (диффузионная теория). Труды НИИ НКАП, № 6. М., 1945.

260. *Л. А. Клячко*. Сб. «Горение двухфазных систем». М., Изд-во АН СССР, 1958.

261. *R. W. Bartlett, J. M. Ong, W. M. Faxsell, A. Papp*. Combustion and Flame 7, 227 (1963).

262. *A. Gordon*. 11th Symposium (Int.) on Combustion. Pittsburg, The Combustion Institute, 1967, p. 216.

263. *T. H. Rautenberg, P. D. Jonson*. J. Opt. Soc. Am., 41, 1071 (1958); 50, 602 (1960).

264. *П. Ф. Похил, В. М. Мальцев, В. М. Зайцев*. Методы исследования процессов горения и детонации. М., «Наука», 1969.

265. *P. W. Pearse, A. G. Gaydon*. The identification of molecular spectra. N. Y., J. Wiley, 1950.

266. *F. Coheur-Dehalu, B. Rosen*. Bul. Roy. Soc. Sci. de Liege, 105 (1941).

267. *E. Ryshkewitch*. Oxide Gramics. N. Y., Academic Press, 1960.

268. *В. И. Веденеев, Л. В. Гурвич, В. Н. Кондратьев, В. А. Медведев, Е. Л. Франкевич*. Справочник «Энергии разрыва химических связей, потенциалы ионизации и сродство к электронам». М., Изд-во АН СССР, 1962.

269. *L. Kirschfeld*. Metall, 14, 213 (1960); 15, 873 (1961).

270. *Д. Гиршфельдер, Ч. Кертисс, Р. Берд*. Молекулярная теория газов и жидкостей. М., ИЛ, 1961.

271. *И. Глассман*. Сб. «Исследование ракетных двигателей на твердом топливе». М., ИЛ, 1963, стр. 171.

272. *Л. Я. Клячко*. ФГВ, 5, 404 (1969).

273. *C. Christianse*. Wied. Ann., 19, 267 (1883).

274. *Д. А. Франк-Каменецкий*. Диффузия и теплопередача в химической кинетике. М., «Наука», 1967.

275. *У. Х. Доррене*. Гиперзвуковые течения вязкого газа. М., «Мир», 1966.

276. *D. K. Kuchl, M. L. Zwillenberg*. IGRPG/AIAA 3rd Solid propulsion conf. Atlantic City, New Jersey, 1968, AIAA Paper 68 — 196.

277. *M. Hoex, H. Lohnston*. J. Am. Chem. Soc., 76, 2560 (1956).

278. *Л. Н. Хитрин*. Физика взрыва и горения. М., Изд-во МГУ, 1957.

279. *T. F. Harley*. Inst. Fuel, 4, 243 (1930).

280. *A. A. Orning*. Trans. ASME, 64, 497 (1932).

281. *J. Hunger, O. Werner*. Arch. Eisenhuttenw., 23, 227 (1952).

282. *J. L. Blumental, M. J. Santy*. 11th Symposium (Int.) on Combustion. Pittsburgh, The Combustion Institute, p. 417.

283. *А. Ф. Беляев*. Горение, детонация и работа взрыва конденсированных систем. М., «Наука», 1968.

284. Сб. «Теория взрывчатых веществ». Труды МХТИ, вып. 53. М., «Высшая школа», 1967, стр. 176.

285. *П. Ф. Похил, В. С. Логачев, В. М. Мальцев*. ФГВ, 6, 407 (1970).

286. *Д. Ж. Пизелли, Т. Ф. Рейнгардт*. Сб. «Вопросы горения». М., ИЛ, 1953, стр. 241.

287. *Я. М. Паушкин*. Химия реактивных топлив. М., Изд-во АН СССР, 1962.

288. *М. Баррер, А. Жомот, Б. Ф. Вебек, Ж. Ванденкеркхове*. Ракетные двигатели. М., Оборонгиз, 1962.

289. *Я. Б. Зельдович, М. А. Ривин, Д. А. Франк-Каменецкий.* Импульс реактивной силы пороховых ракет. М., Оборонгиз, 1963.

290. *М. Барре, А. Жомотт, Б. Фрейе де Вбеке, Ж. Ванденкеркхове.* Движение ракет. М., ИЛ, 1959.

291. *Я. М. Шапиро, Г. Ю. Мазин, Н. Е. Прудников.* Теория ракетного двигателя на твердом топливе. М., Воениздат, 1966.

292. *Р. Е. Сорин.* Газотермодинамика ракетных двигателей на твердом топливе. М., «Наука», 1967.

293. *Н. Е. Алексеев.* Теория ракетных двигателей. М., Оборонгиз, 1952.

294. *Н. Е. Алексеев, А. Ф. Дрегалин, А. П. Тишин.* Теория ракетных двигателей. М., «Машиностроение», 1969.

295. *Б. В. Орлов, Г. Ю. Мазин.* Термодинамические и баллистические основы проектирования ракетных двигателей на твердом топливе. М., «Машиностроение», 1964.

296. *А. П. Соколик.* Твердые ракетные топлива. М., «Оборонгиз», 1964.

297. *Я. Б. Зельдович.* Теория горения и детонации газов. М., Изд-во АН СССР, 1944.

298. *Г. М. Кондратьев.* Тепловые измерения. М., «Наука», 1958.

299. *П. Ф. Похил, Л. Д. Ромоданова.* ЖФХ, 39, 2757 (1966).

300. *Л. Д. Ромоданова, П. Ф. Похил.* ФГВ, 6, 126 (1970).

301. *Н. Н. Бахман, В. С. Никифоров.* ЖФХ, 38, 41 (1964).

302. *О. И. Лейпунский.* ЖФХ, 34, 177 (1960).

303. *Б. В. Новожилов.* ЖФХ, 36, 1803 (1962); ДАН СССР, 131, 1400 (1960).

304. *У. Ростокер.* Металлургия бериллия. М., ИЛ, 1959.

305. *A. De S. Brisunas, N. Grant.* J. Trans. Am. Soc. Metals, 44, 117 (1952).

306. *F. C. Menkman, N. Grant.* J. Corrosion, 9, 1962 (1953).

307. *Л. Скут, К. Прайс.* Ракетная техника и космонавтика, 5, 179 (1966).

308. *Л. Скут, К. Прайс.* Ракетная техника и космонавтика, 1, 121 (1967).

309. *Л. Скут, К. Прайс.* Ракетная техника и космонавтика, 8, 44 (1965).

310. *Т. Максмен, К. Вулдриж, Р. Мэйл.* Сб. «Гетерогенное горение». М., «Мир», 1967, стр. 313.

311. *Т. Максмен.* Ракетная техника и космонавтика, 5, 244 (1966).

312. *Л. Грин.* Сб. «Гетерогенное горение». М., «Мир», 1967, стр. 282.

313. *H. M. Cassel.* Combustion and Flame, 6, 153 (1962); 3, 467 (1959); 3rd Symposium (Int.) on Combustion. Baltimore, Williams and Wilkins, 1949, p. 185.

314. *А. Ф. Беляев, Л. Д. Комкова.* ЖФХ, 24, 1302 (1950).

315. *Э. И. Максимов, А. Г. Мержанов, В. М. Шкиро.* ФГВ, 4, 24 (1965).

316. *Л. Д. Ромоданова, П. Ф. Похил.* ФГВ, 2, 277 (1969).

317. *В. Хилл, Т. Коттрелл.* IV Симпозиум «Вопросы горения и детонационных волн». М., «Оборонгиз», 1958, стр. 246.

318. Физическая энциклопедия, т. 1. «Советская энциклопедия», 1960.

319. *Я. Б. Зельдович.* ЖЭТФ, 12, 1948 (1942).

320. *Y. B. Zeldovich, G. I. Barenblatt.* Combustion and Flame, 3, 61 (1959).

321. *Б. В. Новожилов.* ДАН СССР, 141, 151 (1961).

322. *S. F. Boys, J. Corner.* Proc. Roy. Soc., 197A, 90 (1949).

323. *О. А. Есин, П. В. Гельд.* Физическая химия пирометаллургических процессов. М., Металлургиздат, 1962.

324. *А. Ф. Беляев, Г. В. Лукашеня.* ЖФХ, 36, 1050 (1962).

325. *Г. В. Лукашеня, А. П. Погребенков.* ЖФХ, 36, 2784 (1962).

326. *В. В. Горбунов* и др. ФГВ, 2, 271 (1969); 4, 2 (1968).

327. *Г. Каст.* Взрывчатые вещества и средства воспламенения. М.—Л., ОНТИ, 1932.

328. *С. Б. Ратнер, Ю. Б. Харитон.* ЖФХ, 20, 221 (1946).

329. *И. М. Воскобойников.* ПМТФ, 5, 115 (1963).

330. *А. Н. Дремин, П. Ф. Похил, М. И. Арифов.* ДАН СССР, 131, 1140 (1960).

331. *H. A. Cook.* J. Phys. Chem., 61, 2 (1957).

332. *J. Taylor.* Detonation in Condensed Explosives. Oxford, Clarendon press, 1952.

333. *G. Kast.* Z. Sch. u. Sprest., 5, 251 (1901).

334. Сб. «Термодинамические свойства индивидуальных веществ», т. II. М., Изд-во АН СССР, 1962.

335. *M. A. Cook.* Science of high explosives. N. Y., 1958; *M. P. Murgai.* J. Chem. Phys., 21, 1403 (1953).

336. *Я. Б. Зельдович, А. С. Компанеец.* Теория детонации. М., Гостехтеориздат, 1955.

337. *А. Я. Апин, И. М. Воскобойников.* ПМТФ, 4, 55 (1960).

338. *А. Я. Апин, И. М. Воскобойников, Г. С. Соснова.* ПМТФ, 5, 115 (1963).

339. *Л. Н. Акимова, Л. Н. Стесик, А. Я. Апин.* Оценка времени реакции алюминия в детонационной волне. М., ИХФ АН СССР, 1957.

340. *А. Н. Дремин, П. Ф. Похил*. ДАН СССР, 128, 989 (1959).
341. *I. Brewer, A. W. Searcy*. J. Am. Chem. Soc., 73, 5308 (1951).
342. *M. A. Cook, G. S. Horsley*. J. Appl. Phys., 27, 269 (1956).
343. *А. Я. Апин, Ю. А. Лебедев*. Сб. «Физика взрыва». М., Изд-во АН СССР, 1953, стр. 3, 90, 125.
344. *R. Edse* et al. J. Opt. Soc. Am., 53, 436 (1963).
345. *H. A. Cook* et al. J. Phys. Chem., 58, 1114 (1954).
346. *M. A. Cook*. J. Chem. Phys. 16, 1081 (1948).
347. *А. Н. Дремин, П. Ф. Похил*. ДАН СССР, 127, 1245 (1959).
348. *В. Страусс*. Ракетная техника и космонавтика, 6, 159 (1968).
349. *I. D. Doig, G. H. Roper*. Energy Requirements in Pneumatic Conveying. Australian Chemical Engineering, Feb., 1963.
350. *J. Fry*. J. Chem. Phys., 20, 942 (1952).
351. *О. Д. Дмитриевски*. Оптико-механическая промышленность, 2, 55 (1967).
352. *С. Г. Гренишин, Ю. П. Щепеткин*. Оптико-механическая промышленность, 1, 1 (1961).
353. *R. Edse, E. Fishburne*. Aerothermochemistry. N. Y., Wiley, 1968.
354. *R. Edse*. J. Opt. Soc. Am., 53, 436 (1963).
355. *Б. И. Хайкин, В. Н. Блошенко, А. Г. Мержанов*, ФГВ, 5, 474 (1970).
356. *М. А. Гуревич, К. И. Лапкина, Е. С. Озеров*. ФГВ, 6, 172 (1970).